# Einfluss von Herz-Kreislauf-Parametern auf das Nah-Infrarot-Spektroskopie (NIRS) Signal

Projekt A3-22.N-13/2009-8




**Förderungsnehmer:**

Technische Universität Graz
Institut für Semantische Datenanalyse/Knowledge Discovery
Laboratory of Brain-Computer Interfaces
Krenngasse 37/IV
8010 Graz

**Förderungsgeber:**

Land Steiermark
p.A. Amt der Stmk. Landesregierung
A3 - Wissenschaft und Forschung
Trauttmansdorfgasse 2
8010 Graz

# Inhaltsverzeichnis

# Beteiligte Personen

**Univ.-Prof. Dr.phil. Christa Neuper, (Projektleitung)**

Technische Universität Graz
Institut für Semantische Datenanalyse/Knowledge Discovery
Laboratory of Brain-Computer Interfaces
Krenngasse 37/IV, 8010 Graz

Karl-Franzens-Universität Graz
Büro der Rektorin
Universitätsplatz 3/I, 8010 Graz

**Dipl.-Ing. BSc. Günther Bauernfeind**

Technische Universität Graz
Institut für Semantische Datenanalyse/Knowledge Discovery
Laboratory of Brain-Computer Interfaces
Krenngasse 37/III, 8010 Graz

**Ao.Univ.-Prof. Dipl.-Ing. Dr.techn. Hermann Scharfetter**

Technische Universität Graz
Institut für Medizintechnik
Kronesgasse 5/II, 8010 Graz

**Univ.-Prof.i.R. Dipl.-Ing. Dr.techn. Gert Pfurtscheller**

Technische Universität Graz
Institut für Semantische Datenanalyse/Knowledge Discovery
Laboratory of Brain-Computer Interfaces
Krenngasse 37/IV, 8010 Graz

# Tabellenverzeichnis

# Abbildungsverzeichnis

# Kurzdarstellung des Projektinhaltes und der Indikatoren für den Nachweis der Realisierung

Seit einigen Jahren gewinnen moderne Ansätze des Neurofeedbacks immer stärker an Bedeutung. Die möglichen Anwendungsfelder reichen dabei von der Behandlung hyperaktiver Kinder [20, 31] über Epilepsie-Prävention [17, 44] und Schlaganfall-Therapie [8, 9, 47] bis hin zur Kommunikations- bzw. Ansteuerungshilfe für schwerst gelähmte Patienten [12, 33, 34, 38].

In Forschungsarbeiten der letzten 20 Jahre konnte gezeigt werden, dass nach einer entsprechenden Trainingsphase mit Feedback, sowohl bei Gesunden als auch bei schwerstbehinderten Patienten eine bemerkenswerte Beeinflussung der eigenen Hirntätigkeit erzielt werden kann[11, 41]. Die dazu notwendigen Methoden der Brain-Computer Interface (BCI)-Technologie basieren dabei üblicherweise auf der Detektion unterschiedlicher kognitiver Prozesse aus mittels Elektroenzephalografie (EEG) gemessenen Signalen [32, 42]. Neben der Verwendung des EEG ist jedoch auch eine Realisierung solcher Systeme auf Basis der funktionellen Magnetresonanztomographie (fMRI) [45, 46] oder der Magnetoenzephalographie (MEG) [12] möglich. Neben diesen bereits gut etablierten Methoden bietet sich zusätzlich die Nah-Infrarot Spektroskopie (NIRS) als eine weitere, viel versprechende Methode an [15].

Als Anwendung in der Neurowissenschaft ist die NIRS relativ jung. Sie ist eine nichtinvasive optische Technik, welche die Erfassung funktioneller Aktivitäten im menschlichen Gehirn ermöglicht. Gegenüber EEG, fMRI und MEG bietet die NIRS den Vorteil einer einfacheren Applikation. Weitere Vorteile gegenüber fMRI und MEG bestehen in einer kostengünstigeren Anschaffung sowie der Mobilität des Messgerätes. Die Verwendbarkeit der NIRS für die Feedbackgabe hängt maßgeblich von der eindeutigen und korrekten

Detektion kognitiver Prozesse ab. In den letzten Jahren wurde eine Vielzahl von Studien durchgeführt, welche die neuronale Aktivierung unter anderem bei visuellen [13, 23, 24], kognitiven [6, 22, 26, 27, 43] und motorischen Aufgaben [21, 25, 48, 49] mit NIRS untersuchen. Dabei wurde jedoch wenig bis kaum Augenmerk auf den Einfluss physiologischer Rhythmen, wie Herzraten- (HR) und Blutdruck- (BP) Schwankungen oder Schwankungen in der Atemfrequenz, gelegt. Diese Rhythmen können die gemessenen Aktivierungsmuster teilweise überlagern [18, 30] und somit zu einer Falschdetektion führen [5, 6, 14].

Das Ziel dieses Projekts ist die Untersuchung von systemischen Einfüssen auf mittels NIRS gemessenen Aktivierungsmuster. Darber hinaus sollen geeignete Signalverarbeitungsansätze entwickelt werden, welche eine Elimination dieser Einflüsse ermöglichen. Damit wird die Qualität der Feedbackgabe für zukünftige auf NIRS basierende Systeme entscheidend verbessert.

**Indikatoren für Realisierungsnachweis:**

- Entwicklung verschiedener Signalverarbeitungsansäze zur Elimination systemischer Einflüsse
- Veröffentlichung der Ansätze in der Open-Soure Software-Bibliothek "BioSig"(`http://biosig.sourceforge.net/`)
- Veröffentlichungen in Form von Konferenzbeiträgen und Artikeln

# Kapitel 1

# Einleitung

Die Erforschung des Gehirns mit modernen Untersuchungsverfahren wie der Nah-Infrarot Spektroskopie (NIRS), einer vielversprechenden, nichtinvasiven, optischen Methode der Neurowissenschaft, ermöglicht Einblicke in die neurophysiologischen Vorgänge der Informationsverarbeitung im Menschen. Im Zuge dieses Projekts wurde der Einfluss physiologischer Rhythmen, wie Herzraten- (HR) und Blutdruck- (BP) Schwankungen oder Schwankungen in der Atemfrequenz auf funktionelle, mittels NIRS gemessen,e Aktivitäten im menschlichen Gehirn untersucht. Darüber hinaus wurden geeignete Signalverarbeitungsansätze entwickelt, welche eine Elimination dieser Einflüsse sowohl Offline als auch Online ermöglichen. Dies ist vor allem hinsichtlich der Verwendung von NIRS für optische Brain-Computer-Interface (oBCI) Systeme von großer Relevanz.

Das Projekt umfasste eine zweijährige Grundlagenstudie zur Untersuchung von systemischen Einflüssen auf mittels NIRS gemessene Aktivierungsmuster. Zu diesem Zweck wurde der Studienablauf in vier Arbeitspakete (working package, WP) unterteilt:

**WP1: Multimodale NIRS-Messungen und Analyse:** Im Zuge dieses WPs wurden multimodale Messungen (Ein- und Multikanal NIRS-Messungen sowie systemische Signale wie Atmung, BP, EKG und Puls teilweise in Kombination mit EEG) analysiert bzw. durchgeführt. Das Ziel dieses WPs war es, das Ausmaß der verschiedenen systemischen Einflüsse auf das NIRS-Signal genauer bestimmen zu können.

**WP2: Entwicklung geeigneter Signalverarbeitungsmethoden:** In diesem WP wurden geeignete Signalverarbeitungsansätze zur Elimination dieser Einflüsse entwickelt und untersucht.

**WP3: Realtime-Applikationen:** In diesem WP wurden Möglichkeiten von

Realtime-Applikation verschieder Signalverarbeitungsansätze untersucht.

**WP4: Endbericht, Veröffentlichungen:** Dieses WP beinhaltet die Veröffentlichung der Ergebnisse in Form von Journalpublikationen, Proceedings und Poster sowie die Erstellung eines Endberichts.

## 1.1 Verwendete Systeme zur Signalaufzeichnung

In diesem Teil des Berichts erfolgt eine Auflistung der zur Signalaufzeichnung verwendeten Systeme, Geräte und Sensoren und kurze technische Erklärungen.

### 1.1.1 NIRS-Systeme

Für die Aufzeichnung der im Rahmen des Prokjekts verwendeten NIRS-Daten wurden zwei verschiedene NIRS-Systeme verwendet. Bei den Systemen handelt es sich um:

#### Einkanal NIRS System

Beim Einkanal NIRS-System handelt es sich um ein im Rahmen einer Diplomarbeit [1, 2] am Institut für Semantische Datenanalyse entwickeltes, Eigenbausystem (Abbildung 1.1). Das System basiert auf dem "Continuous Wave"-Prinzip und verwendet LEDs als Lichtquelle. Die LEDs werden dabei in direkten Kontakt mit der Kopfhaut gebracht. Zur Detektion des am Kopf abgenommene Lichtes wird ein Lawinendiodenmodul, welches durch eine Fiberglasleitung mit dem Aufnehmer am Kopf verbunden ist, verwendet. Der Abstand zwischen Quelle und Detektor beträgt 3 cm und korrespondiert mit einer Eindringtiefe des Lichts von ca. 2.5 cm. Somit sind hemodynamische Untersuchungen der Kortexoberfläche bzw. auch von Gewebebereichen einige mm unterhalb der Oberfläche möglich. Abbildung 1.3A zeigt die Anordnung der Quellen und des Detektors.

#### Multikanal NIRS System

Beim Multikanal NIRS-System (Abbildung 1.2) handelt es sich um ein ETG-4000 der Firma Hitachi (Hitachi Medical Co., Japan), welches vom Arbeitsbereich Neuropsychologie am Institut für Psychologie der Karl-Franzens Universität Graz (Kooperationspartner) für Messungen zur Verfügung gestellt

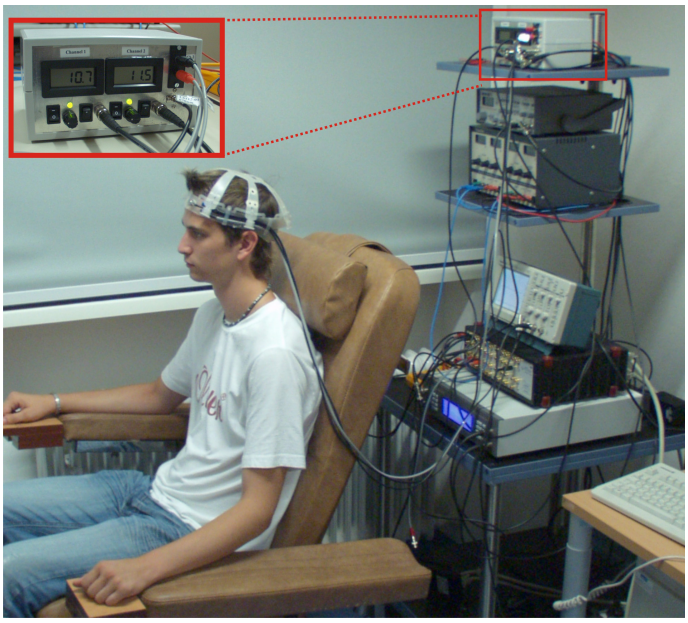

**Abbildung 1.1:** Bild des Einkanal NIRS-Systems. Die kleine Darstellung in der linken oberen Ecke zeigt das Hauptmodul des NIRS-Systems. Der Hardware-Turm zeigt die Zusammenstellung des gesamten Systems (externer Signalgenerator, Spannungsversorgung, Oszilloskop sowie Biosignalverstärker zur Aufzeichnung der Systemischen Signale). Der Proband trägt eine Halterung, welche für Messungen über dem präfrontal Kortex verwendet wird. (Modifiziert aus [2])

wurde. Das System basiert ebenfalls auf dem "Continuous Wave"-Prinzip, verwendet jedoch im Gegensatz zum Einkanal NIRS System Laserdioden anstelle der LEDs als Signalquelle. Mit diesem System ist es möglich, verschiedene Messsets zu verwenden welche Messungen mit bis zu 52 Kanälen erlauben. Der Quelle-Detektor Abstand beträgt bei diesem System ebenfalls 3 cm (Abbildung 1.3B) und erlaubt somit, mit dem Einkanal NIRS-System vergleichbare Messungen durchzuführen.

Sowohl das Multikanal als auch das Einkanal NIRS-System messen relative Konzentrationsschwankungen von oxygeniertem (oxy-Hb) und deoxygeniertem Hämoglobin (deoxy-Hb)[1] in mM mm (Millimolar Millimeter, ein Molar entspricht einem Mol pro Liter).

[1]Im weiteren Verlauf dieses Berichts wird die Konzentration von oxy-Hb und deoxy-Hb mit [oxy-Hb] bzw. [deoxy-Hb] bezeichnet.

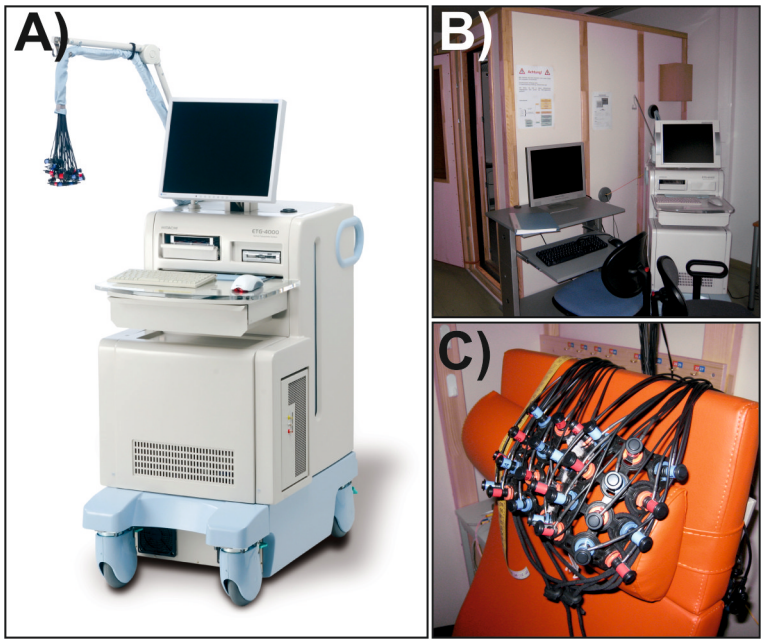


**Abbildung 1.2:** A) Darstellung des Multikanal NIRS-Systems ETG-4000 (Hitachi Medical Co., Japan). B) Messumgebung. C) Beispiel eines Probesets.

### 1.1.2 Systemische Signale

Um die Unteruchung der physiologischen Einflüsse zu ermöglichen, ist es notwendig, diese zeitgleich mit dem NIRS-Signal aufzuzeichnen. Die Folgenden systemischen Signale wurden daher unter Verwendung eines Mehrkanal-Biosignalverstärkers der Firma Guger Technologies OEG, Graz, wie folgt aufgezeichnet.

#### Blutdruck (BP)

Für die Aufzeichnung des kontinuierlichen Blutdruck (BP)-Signals wurde ein Blutdruckmonitor (CNAP$^{TM}$ Monitor 500) der Firma CNSystems Medizintechnik AG, Graz, verwendet. Der Monitor ermöglicht die nicht-invasive, kontinuierliche Messung des Blutdrucksignals, welches über den Biosignalverstärker zeitgleich mit dem NIRS-Signal aufgezeichnet werden kann. Aus dem kontinuierlichen Signal kann in weiterer Folge auch der diastolische (BPdia) und der systolische (BPsys) Blutdruckverlauf(**calcBPlin.m, sysdetect.m, diadetect.m**, siehe Anhang B) berechnet werden. Abbildung 1.4 zeigt den CNAP$^{TM}$ Monitor 500 sowie ein damit gemessenes BP Signal und die daraus berechneten BPdia und BPsys Verläufe.

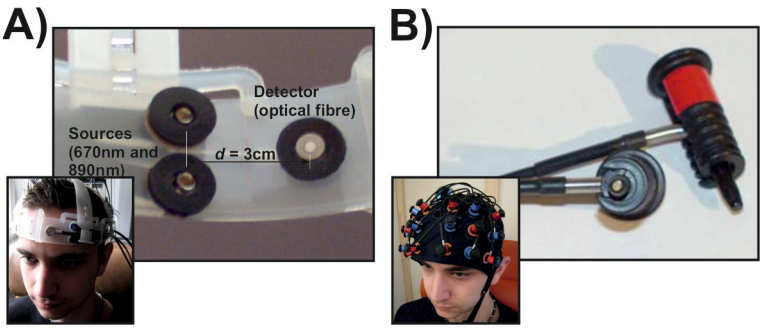


**Abbildung 1.3:** A) Optoden des Einkanal NIRS-Systems und B) des Multikanal NIRS-System. Beide Systeme weisen einen Quelle-Detektorabstand von 3 cm auf welcher mit einer Eindringtiefe in den Kortex von ca. 2.5 mm korrespondiert. Für weiter Details siehe [1, 2].

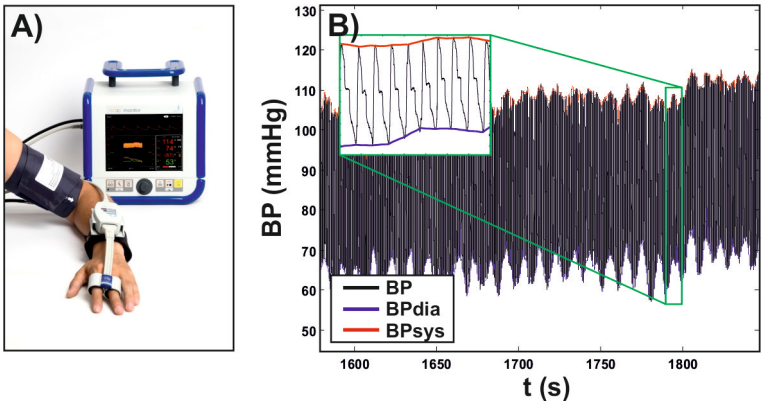


**Abbildung 1.4:** A) Blutdruckmonitor CNAP$^{TM}$ Monitor 500 B) Kontinuierliches Bluddrucksignal und die daraus berechneten BPdia und BPsys Verläufe.

### Atmung (RESP)

Die Atmung wurde unter Verwendung eines Brustgurtes mit Dehnungsmessstreifen (Respiratory Effort Sensor, Pro-Tech Services Inc.) gemessen und unter Verwendung des Biosignalverstärkers aufgezeichnet (Abbildung 1.5A).

### Elektrokardiogramm (EKG)

Das Elektrokardiogramm (EKG) wurde bipolar mit Hilfe von Elektroden, welche am Thorax montiert wurden, aufgezeichnet. Aus dem EKG wurden die QRS-Komplexe mit Hilfer eines automatischen Verfahrens detektiert und daraus der Herzraten (HR)-Verlauf berechnet (Abbildung 1.5B).

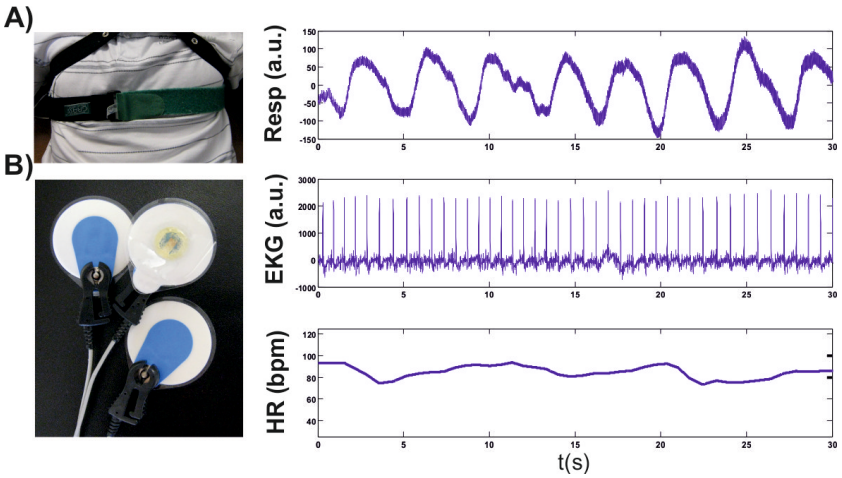


**Abbildung 1.5:** A) Brustgurt sowie gemessenes Atmungssignal B) EKG Elektroden sowie aufgezeichnetes EKG-Signal und daraus berechneter HR-Verlauf.

# Kapitel 2

# WP1: Multimodale NIRS-Messungen und Analyse

Im Rahmen dieses WPs wurden im Verlauf multimodaler Messungen verschiedene systemische Signale wie Atmung, Blutdruck, EKG, Puls und HR gleichzeitig mit NIRS sowie teilweise in Kombination mit EEG, gemessen. Das Ziel dieses WPs war es, das Ausmaß der verschiedenen systemischen Einflüsse auf das NIRS-Signal genauer bestimmen zukönnen.

Meilensteine dieses WPs waren:

- **Erstellung der Messparadigmen**
  Entsprechende Messparadigmen wurden entwickelt und von der Ethikkommission der Medizinischen Universität Graz bewilligt (Votum 21-317 ex 09/10).
- **Hard- und softwaretechnische Implementation der Messungen**
  Entsprechende Hard- und softwaretechnische Implementationen der Messungen wurde durchgeführt und von der Ethikkommission der Medizinischen Universität Graz bewilligt (Votum 21-317 ex 09/10).
- **Analyse von Daten und Definition der systemischen Einflüsse**
  Die Ergebnisse dieses Meilensteins sind nachfolgend aufgeführt.

## 2.1 Definition und Analyse der systemischen Einflüsse

Physiologische Störungen wie Puls, Atmung und Blutdruckschwankungen im NIRS-Signal sind nicht zu verhindern. Als plakatives Beispiel dient dazu

das in Abbildung 2.1A dargestellte Leistungsspektrum eines NIRS-Signals (Räpresentativer Proband, Kanal 48 (FP1), Ruhemessung) welches relevante Störanteile im Bereich um 1.3 Hz (Puls, 80 bpm), 0.27 Hz (Atmung, 16 Atemzüge pro Minute) und 0.1 Hz (Mayer Wave) aufweist (siehe dazu auch Abbildung 2.1B). Diese Anteile überlagern bei Messungen teilweise die gesuchten hämodynamischen Veränderungen kognitiver Tasks und erschweren somit deren Detektion [5, 6, 15, 18].

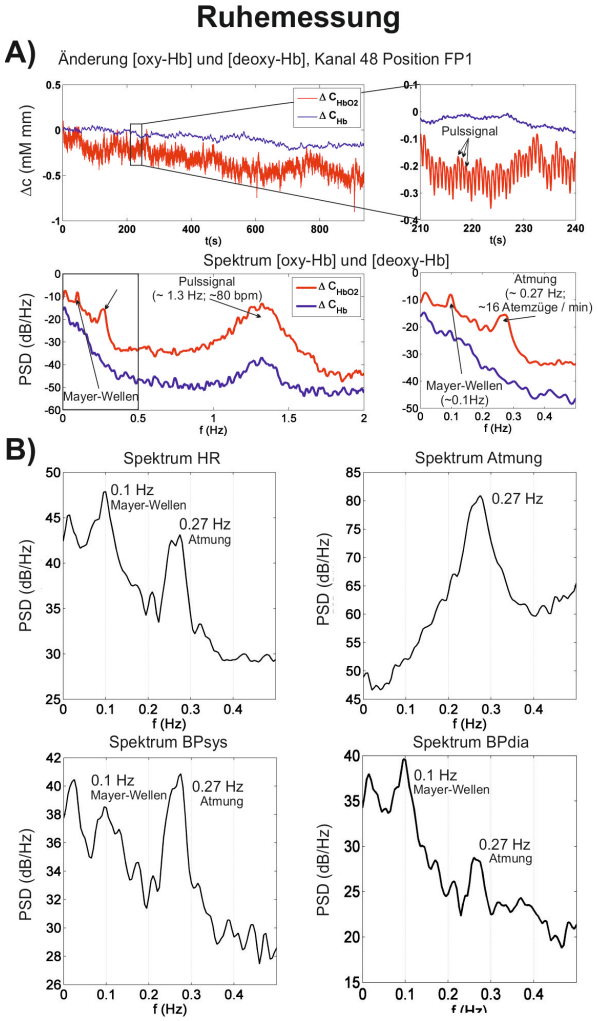


**Abbildung 2.1:** A) Konzentrationsänderungen von oxy-Hb und deoxy-Hb sowie die aus diesen Signalen berechneten Spektren mit Peaks bei 0.1 Hz (Mayer-Wellen), 0.27 Hz (Atmung) und 1.3 Hz (Puls). B) Spektren der zeitgleich Aufgezeichneten HR-, Atmungs- und Blutdrucksignale.

Um nun diese Einflüsse aus dem Signal eliminieren zu können, ist es notwendig, die Zusammenhänge der einzelnen Parameter im kardiovaskulären System und deren Einfluss auf das NIRS-Signal genauer zu untersuchen, wobei das Hauptaugenmerk auf Oszillationen im Bereich von 0.1 Hz (Mayer-Wellen, Resonanz- bzw. Eigenfrequenz der Baroreflex Regelschleife) liegt. Diese Oszillationen beeinflussen das Signal hinsichtlich einer Single-Trial Klassifikation (siehe dazu auch Kapitel 4.3) kognitiver Prozesse in oBCI-Systemen am stärksten [16].

Für die nachfolgenden Untersuchungen der systemischen Einflüsse wurden die Daten von unterschiedlichen Messparadigmen analysiert. Folgende Pardigmen wurden verwendet: Zuerst wurde eine Ruhemessung mit einer Dauer von 5 Min. durchgeführt, um die probandentypische Eigenfrequenz der Baroreflex-Regelschleife bestimmen zu können. Danach wurden die Probanden aufgefordert kurze Fingerbewegung (Drücken eines Schalters) in selbst gewählten Abständen durchzuführe. Anschließend mussten die Probanden in zwei weiteren Messungen periodisch vorgegebene und zufällig vorgegeben Druckbewegungen ausführen. Für die Messungen wurde das Einkanal NIRS-System (Kapitel 1.1.1) verwendet. Die bei der Analyse gefundenen Ergebnisse [36, 39, 40] wurden in folgenden Publikationen (nachfolgend kurz zusammengefasst) veröffentlicht:

**G. Pfurtscheller, D. Klobassa, G. Bauernfeind and C. Neuper. Cardiovascular responses after brisk finger movement and their dependency on the eigenfrequency of the baroreflex loop. *Neurosci Lett*, 490(1):31-35, 2011.**

**Zusammenfassung:** Der Baroreflex, vorwiegend beteiligt an der kurzzeitigen Blutdruckregulation, wird stark durch Aktivierungen medullarer Zirkulationszentren des Hirnstamms und höher Hirnzentren beeinflusst. Ein wichtiges Merkmal des Baroreflexes ist dabei seine starke Präferenz für Oszillationen im Bereich von 0.1 Hz, welche auch als Resonanz- oder "Eigenfrequenz" (EF) der Regelschleife (die sogenannten Mayer Wave) bezeichnet werden. Die Studie [40] untersuchte den Zusammenhang der "Eigenfrequenz" mit Änderungen in beat-to-beat Herzratenintervallen (RRI) und Schwankungen im arteriellen Blutdruck (BP) in Ruhe (Abbildung 2.2) und nach der Ausführung kurzer Fingerbewegungen an einer Gruppe von 17 Versuchspersonen. Die durchgeführten Analysen offenbarten dabei signifikante Zusammenhänge zwischen BP- ($r = 0.63$, $p < 0.01$) bzw. RRI-Änderungen ($r = 0.59$, $p < 0.05$) und der Eigenfrequenz der Baroreflex-Regelschleife (Abbil-

dung 2.3).

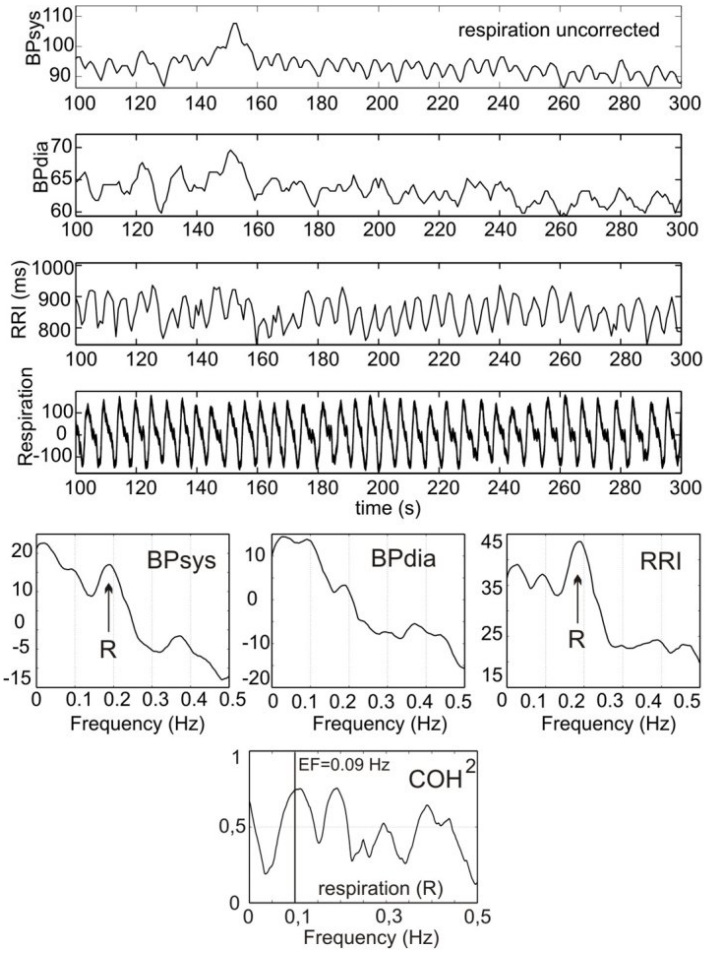


**Abbildung 2.2:** Oberer Abschnitt: Verlauf des systolischen (BPsys) und diastolischen (BPdia) Blutdruck sowie der RRI Verlauf und das aufgezeichnete Atmungssignal während der Ruhemessung an einem repräsentativen Probanden. Unterer Abschnitt: BPdia, BPsys und RRI Spektrum sowie berechnete Koheränzspektrum zwischen RRI und BPdia. (Modifiziert aus [40])

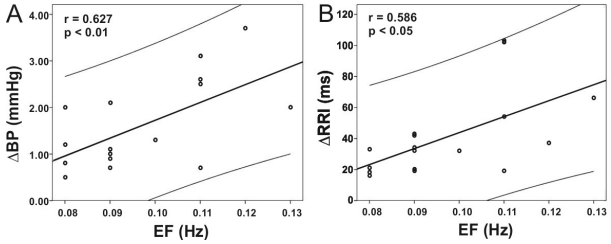


**Abbildung 2.3:** Signifikanter Zusammenhang zwischen A) Bludruckänderungen ($\Delta$BP) und B) beat-to-beat Herzratenintervalländerungen($\Delta$RRI) und der Eigenfrequenz (EF). (Modifiziert aus [40])

**G. Pfurtscheller, D. Klobassa, C. Altstätter, G. Bauernfeind and C. Neuper. About the stability of phase-shifts between slow oscillations around 0.1 Hz in cardiovascular and cerebral systems. *IEEE Trans Biomed Eng*, 58(7):2064-2071, 2011.**

**Zusammenfassung:** Ein wichtiges Merkmal des Baroreflexes ist seine starke Präferenz für Oszillationen im Bereich von 0.1 Hz. Diese Studie [39] untersuchte den Zusammenhang zwischen Änderungen des Herzratenintervalls (RRI) und Schwankungen im arteriellen Blutdruck (BP) sowie Änderungen der prefrontalen Hämoglobinkozentration ([oxy-Hb] und [deoxy-Hb]) an 19 Versuchspersonen während einer 5-minütigen Ruhemessung bzw. während der Ausführung kurzer Fingerbewegungen. Es wurden dabei die Phasenkopplungen zwischen kardiovaskulären und [(de)oxy-Hb] Oszillationen im Bereich der Eigenfrequenz (ca. 0.1 Hz) untersucht (Abbildung 2.5). Die Analyse ergab Phasenverschiebungen zwischen RRI und BP im Bereich von -10° bis zu -118° (BP ist dabei immer voreilend). Diese Phasenverschiebungen veränderten sich signifikant ($p < 0.01$) durch die Ausführung der Fingerbewegungen (Abbildung 2.4). Die Koppelung zwischen den kardiovaskulären und [(de)oxy-Hb] Oszillationen war im Gegensatz dazu weniger klar ausgeprägt. Nur 12 der 19 Versuchspersonen wiesen dabei eine Phasenkopplung zwischen [oxy-Hb] und BP-Oszillationen auf. Diese Ergebnisse könnten durch einen vorwiegend nichtlinearen Zusammenhang zwischen dem kardiovaskulären und hämodynamischen System erklärt werden.

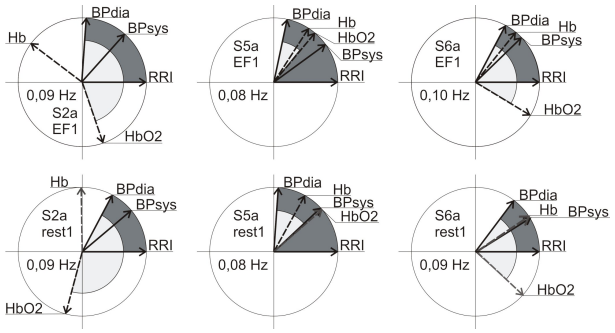


**Abbildung 2.4:** Beispiele für die Phasenverschiebung zwischen kardiovaskulären und [(de)oxy-Hb] Oszillationen im Bereich der Eigenfrequenz in drei repräsentativen Probanden während Ruhe (obere Reihe) und während Bewegungsausführung (untere Reihe). Der BPdia ist dabei immer voreilend zum RRI. Des Weiteren ist [deoxy-Hb] immer voreilend zu [oxy-Hb]. (Modifiziert aus [39])

**G. Pfurtscheller, G. Bauernfeind, C. Neuper and F. H. Lopes da Silva. Does conscious intention to perform a motor act depend on slow prefrontal (de)oxyhemoglobin oscillations in the resting brain? *Neurosci Lett*, 508(2):89-94, 2012.**

**Zusammenfassung:** Basierend auf den in [39, 40] gefundenen Ergebnissen stellte sich die Frage, ob langsame Oszillationen im Bereich von 0.1 Hz zur Intention einer Bewegungsausführung in Verbindung stehen. Um diese Frage genauer beantworten zu können wurde in dieser Studie [36] der Zusammenhang zwischen kontinuierlichen Bludruckschwankungen, der Herzrate, präfrontalen [oxy-Hb] und [deoxy-Hb] Schwankungen sowie Änderungen des EEG Signals über sensorimotorischen Arealen an 10 Versuchspersonen genauer untersucht. Dazu wurden Daten während einer Ruhemessung von 5 Min. und einer Messung, bei der die Versuchspersonen in selbstgewählten Zeitabständen eine Bewegung durchführen, analysiert. Die Analyse der Ruhemessung ergab einen Zusammenhang zwischen präfrontalen [oxy-Hb]- und [deoxy-Hb]-Schwankungen im Bereich der Eigenfrequenz und Änderungen der Leistung im $\alpha$ und/oder $\beta$ Frequenzbereich von $3.6 \pm 0.9$ s. Ein ähnlicher Zusammenhang konnte ebenfalls für die Bewegungsausführung festgestellt werden (Abbildung 2.6). In dieser Arbeit konnte zum ersten Mal festgestellt werden, dass die Intention einer Bewegungsausführung möglicherweise zeitlich mit langsamen Oszillationnen des [oxy-Hb]-Signals im Bereich von 0.1 Hz zusammenhängt.

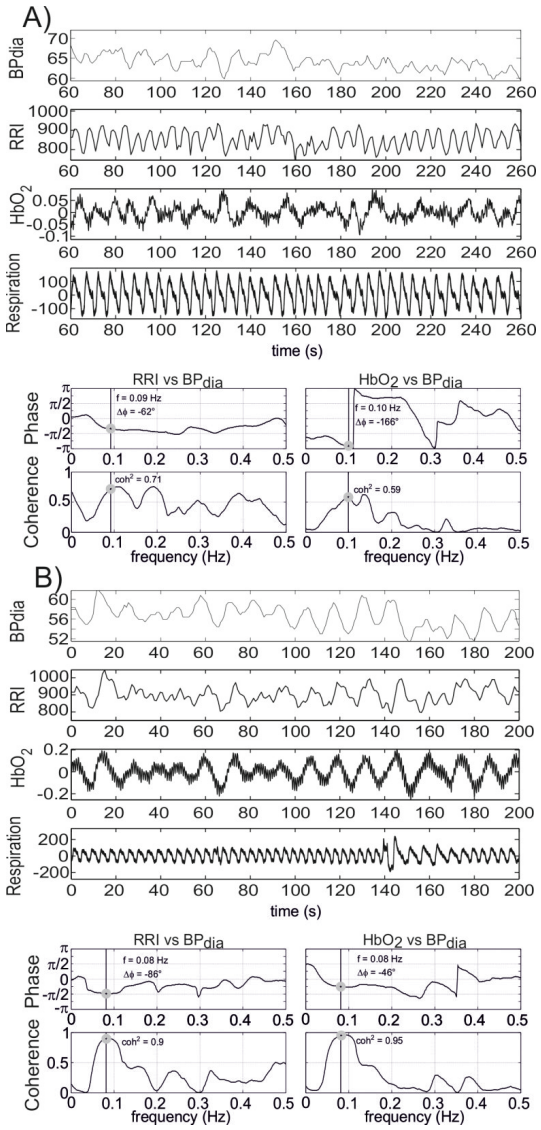


**Abbildung 2.5:** Beat-to-beat Zeitserie (200 s) sowie die zugehörigen Spektren von zwei repräsentativen Versuchspersonen (mit großer Phasenverschiebungen zwischen BP und [oxy-Hb] A) und mit kleiner B)). Oberer Teil: Zeitsignal BPdia (mm Hg), RRI, [oxy-Hb] (mM mm) und Atmung. Unterer Teil Links: Phasen- und Kohärenzspektrum (RRI und BPdia) Rechts: [oxy-Hb] und BPdia. Automatisch detektierte Frequenz-, Kohärenz-und Phasenwerte sind mittels vertikalen Linien markiert. (Modifiziert aus [39])

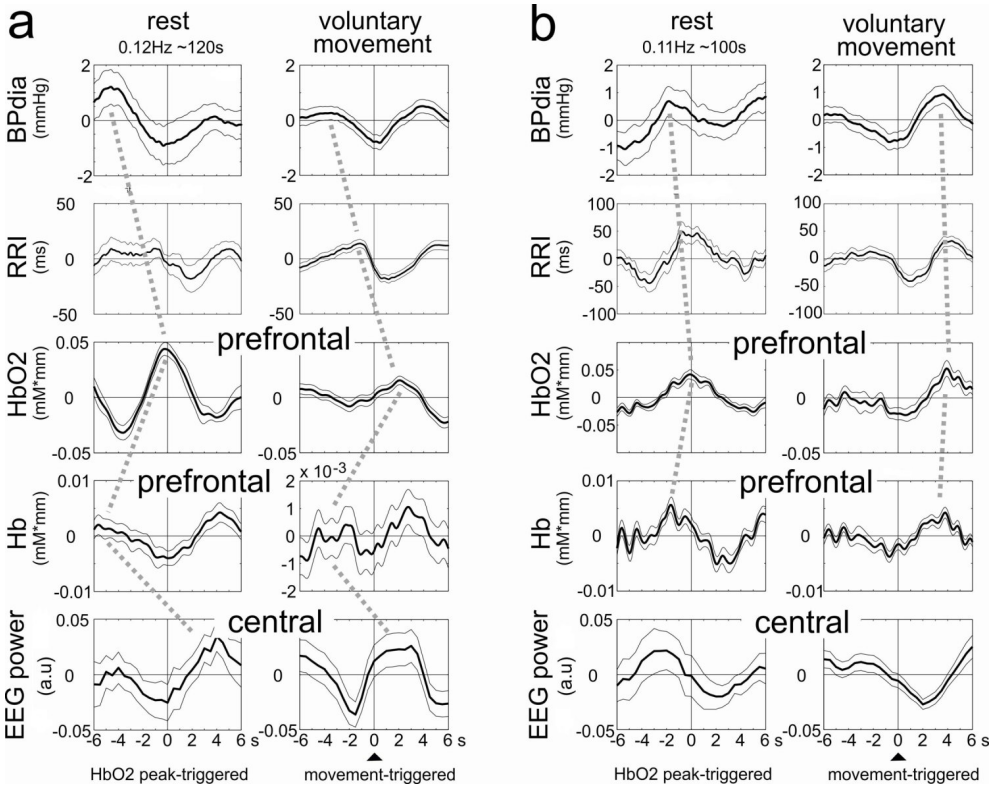


**Abbildung 2.6:** Mittelungen (mean $\pm$ SE) von verschiedenen physiologischen Signalen während Ruhemessung und Bewegungsausführung am Beispiel von zwei charakteristischen Versuchspersonen. Die Phasenverschiebungen zwischen den einzelnen Signalen ist dabei als punktierte Linie dargestellt. (Modifiziert aus [36])

## 2.2 Durchführung von multimodalen Messungen unter Verwendung des Multikanalsystems

Dieser Abschnitt beschreibt kurz die durchgeführten multimodalen Messungen unter Verwendung des Multikanal NIRS-Systems (Kapitel 1.1.1), welche in weiterer Folge für die in Kapitel 3 durchgeführten Entwicklung und Analyse geeigneter Signalverarbeitungsmethoden herangezogen wurden.

Die Messungen wurden im Zuge einer Studie [4, 29] zur Untersuchung kortikaler Trainingseffekte bei der Verwendung eines 2-Klassen, auf Bewegungsvorstellung basierenden BCI-Systems an 10 Versuchspersonen durchgeführt. Die Versuchspersonen mussten dabei an einer Serie von zehn experimentellen Messungen (eine Screening, sechs Feedback (EEG) sowie drei NIRS Sessions) teilnehmen (Abbildung 2.7A). Nach dem Screening wurde bei allen Versuchspersonen die erste NIRS Session, gefolgt von einem Block aus drei Feedbackmessungen, durchgeführt. Anschließend folgten erneut eine NIRS Session und ein Block mit drei weiteren Feedbackmessungen, welche wiederum von einer letzten NIRS Session abgeschlossen wurden. Zwischen den einzelnen Sessions lag dabei eine Zeitspanne von minimal drei, maximal sechs Tagen. Während den NIRS Sessions mussten die Versuchpersonen Hand- und Fussbewegungen in einem fixen, sich wiederholenden Schema, vorstellen (Abbildung 2.7B). Neben der Bewegungsvorstellung wurde in einem zusätzlichen Durchgang (nach Abschluss der Studie) auch die jeweiligen Bewegungsausführungen gemessen.

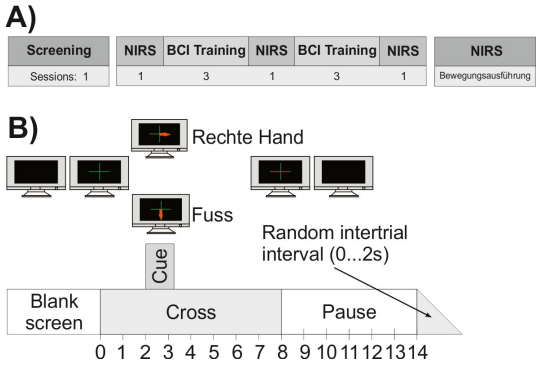


**Abbildung 2.7:** A) Zeitlicher Verlauf der Studie und B) Timing des Paradigmas. (Modifiziert aus [4])

Für die NIRS Messung wurde das in Kapitel 1.1.1 beschriebene Multikanalsystem verwendet, um die durch den Task induzierten hämodynamischen Responses zu detektieren. Die Messkanäle, angeordnet in einem Gitter (3x11) bestehend aus 16 Detektoren und 17 Quellen, wurden dazu über dem motorischen Kortex platziert (Abbildung 2.8).

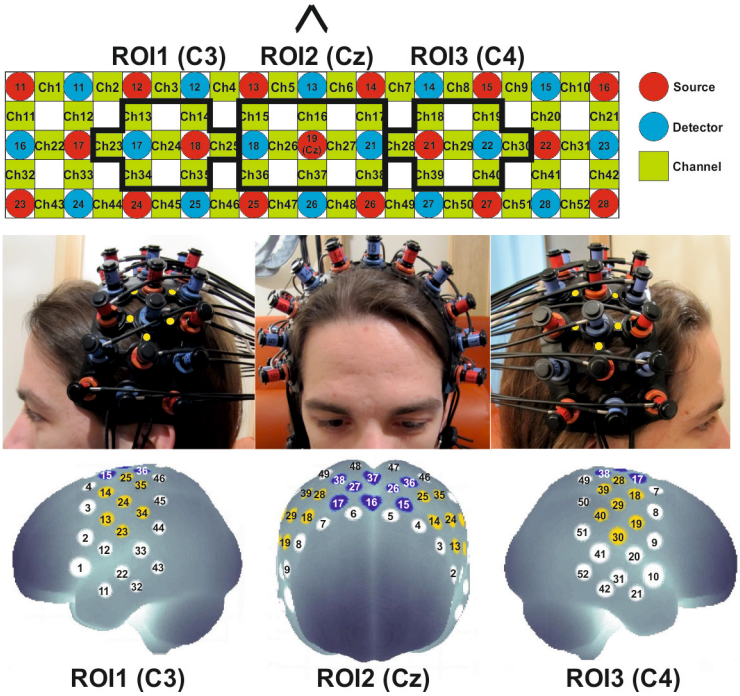


**Abbildung 2.8:** Schematische Darstellung der Messpositionen des 3x11 Messgitters. (Modifiziert aus [4])

Neben den NIRS Signalen wurden in allen Sessions das EKG und die Atmung aufgezeichnet. In der ersten NIRS Session wurde zusätzlich der Puls (über einen Fingerpulssensor) und in der zweiten und dritten Session der kontinuierliche Blutdruck (CNAP$^{TM}$ Monitor 500, Kapitel 1.1.2) aufgezeichnet.

# Kapitel 3

# WP2: Entwicklung geeigneter Signalverarbeitungsmethoden

Wie bereits erwähnt, sind biologische Störungen wie Puls, Atmung und Blutdruckschwankungen im NIRS-Signal nicht zu verhindern. Es ist daher notwendig, geeignete Signalverarbeitungsmethoden zu entwickeln, welche eine einfache Elimination dieser Einflüsse (Offline sowie, bedeutend schwieriger, Online) ermöglichen.

Meilensteine dieses WPs waren:

- **Entwicklung von Signalverarbeitungsansätzen zur Elimination der systemischen Einflüsse**
  Diverse Signalverarbeitungsansätze wurden entwickelt/untersucht und implementiert.

- **Softwaretechnische Implementation und Analyse**
  Die Ergebnisse dieses Meilensteins sind nachfolgend aufgeführt.

## 3.1 Puls

Das Frequenzspektrum des Pulses liegt je nach Versuchsperson im Allgemeinen in einem Bereich von ca. 0.8 - 2 Hz (48 - 120 bpm). Wie in Abbildung 3.1A klar zu erkennen, beeinflusst der Puls die gemessenen [(de)oxy-Hb] Signale entsprechend. Neben der erschwerten Offline-Analyse kognitiver Tasks erweist sich der Einfluss des Pulses vor allem für eine kontinuierliche Feedbackgabe in Online-Systemen als entsprechend störend (Kapitel 4). Der Grund dafür liegt darin begründet, dass sich dieser Parameter direkt auf

das präsentierte Feedback auswirkt und hier ebenfalls Schwankungen verursacht. Im Zuge dieses WPs wurden verschiedene Signalverarbeitungsansätze für eine Elimination des Pulses untersucht und implementiert.

- Der einfachste Ansatz, um diesen Einfluss zu eliminieren, ist die Verwendung eines Tiefpassfilters (Abbildung 3.1B).
- Als weitere Methode bietet es sich an die Mittelwerte der Pulsschwankungen zu berechnen und diese zu interpolieren (Pulse Remove), um ein von den Pulsschwankungen befreites Signal zu erhalten (Abbildung 3.1C). Die Implementierung dieser Methode basiert auf dem in der Arbeit von Coyle et al. [14] angedachten "cardiac pulse removal algorithm".

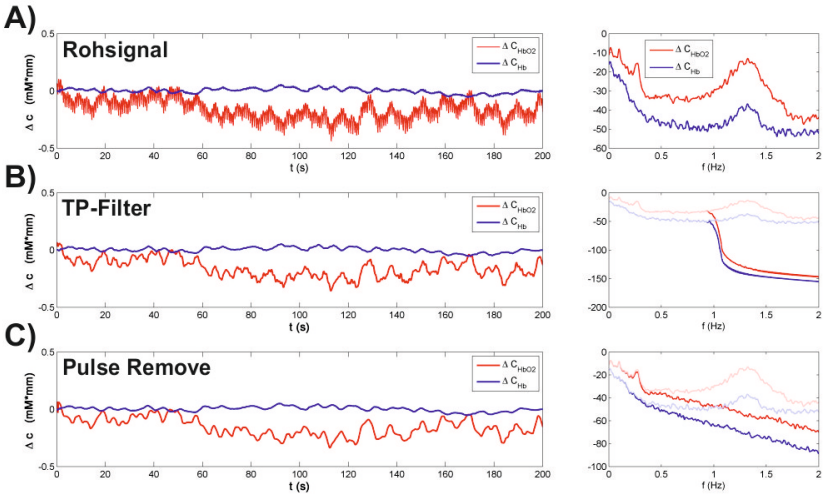


**Abbildung 3.1:** Zeitserie eines [oxy-Hb] und [deoxy-Hb] Signals (200s) als Rohsignal A) mit Elimination des Pulses durch TP-Filterung B) und mit Elimination durch Pulse Remove Algorithmus C) sowie die dazugehörigen Spektren: B) und C) enthalten zum Vergleich auch das Spektrum des Rohsignals.

Die beiden beschrieben Methoden haben jedoch den Nachteil, dass dabei für eine Analyse kortikaler Tasks möglicherweise relevante Signalkomponenten des NIRS-Signals ebenfalls teilweise eliminiert werden können. Es wurde daher eine weitere Methode, die adaptive Filterung, zur Elimination der Pulsschwankungen untersucht.

Adaptive Filter sind Filter deren Parameter sich den Eigenschaften des Signals bzw. der Störung automatisch anpassen. Im Folgenden wurde die Elimination der Pulsschwankungen mit Hilfe eines adaptiven Algorithmus, basierend auf dem Least-Mean-Squares (LMS)-Verfahren untersucht (**adaptPulsremove.m**, Anhang B). Der Puls beeinflusst über eine unbekannte Übertragungsfunktion die von einer kortikalen Aktivierung verursachten [oxy-Hb] und [deoxy-Hb]-Signale. Die mit dem NIRS-System gemessenen Signale sind somit eine Summe aus der kortikalen Aktivierung und einer nicht messbaren Störung (Abbildung 3.2A). Zur Definition des Störsignals wurde das kontinuierliche Blutdrucksignal (Bandpass-gefiltert zwischen 0.8 und 1.8 Hz) herangezogen (Abbildung 3.2B). Der verwendete Algorithmus bildet nun die unbekannte Übertragungsfunktion unter Verwedung des definierten Störsignals nach, so dass der Ausgang gleich der nicht messbaren Störung wird (Abbildung 3.2C). Es ist nun möglich, durch Subtraktion der so berechneten "unbekannten" Störung vom gemessenen Signal ein vom Puls bereinigtes Ausgangssignal, zu erhalten (Abbildung 3.2D).

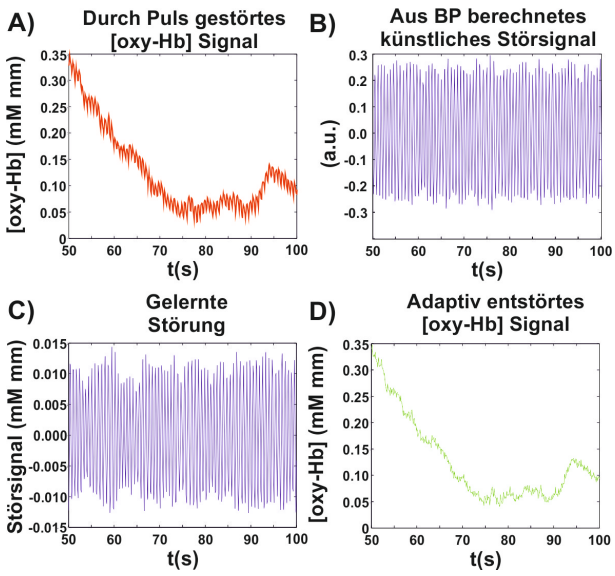


**Abbildung 3.2:** Signale der adaptiven Filterung. A) Durch Puls gestörtes [oxy-Hb] Signal. B) Aus BP gebildetes künstliches Störsignal. C) Gelernte Störung. D) Adaptiv entstörtes [oxy-Hb] Signal.

Um die Qualität dieser Methode genau abschätzen zu können wurde in weiterer Folge der Ansatz an in Kapitel 2.2 aufgezeichneten Daten der zweiten und dritten Session getestet. Dazu wurden der Pulseinfluss aus allen über dem motorischen Kortex gelegenen Messkanälen (34 Kanäle) entfernt.

Anschließend wurde die Leitungsreduktion im Bereich von 0.8 bis 1.8 Hz berechnet und über alle verwendeten Kanäle gemittelt. Zusätzlich wurde die Qualität des Ansatzes überprüft, indem auch die Leistungsredukton in den nicht von der Filterung betroffenen Frequenzbereichen (0 bis 0.79 Hz und 1.81 bis 2 Hz) berechnet wurde (in weiterer folge als Stabilität bezeichent). Je näher der Wert der Stabilität bei Null und je höher die Leistungsreduktion im Pulsbereich ist, desto genauer funktioniert die Pulselimination.

Tabelle 3.1 zeigt die Ergebnisse zur Qualitätsuntersuchung am [oxy-Hb] Signal an zehn Versuchspersonen (Daten aus 2.2; Session 2 und 3). Im Mittel (über beide Sessions) wurde eine Reduktion von 76.9 % im Frequenzbereich von 0.8 bis 1.8 Hz und eine Stabilität von 0.2 % (im Frequenzbereichen von 0 bis 0.79 Hz und 1.81 bis 2 Hz) erzielt. Eine graphische Darstellung der erzielten Reduktion ist in Abbildung 3.3 anhand einer repräsentativen Versuchsperson (M1, Session 2) dargestellt.

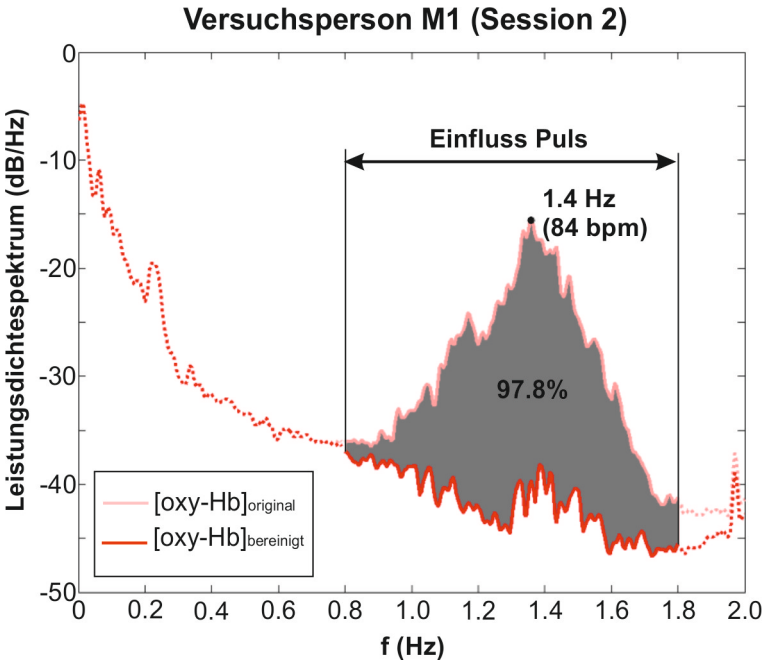


**Abbildung 3.3:** Reduktion des Pulseinflusses mittels adaptiver Filterung anhand einer repräsentativen Versuchsperson (M1, Session 2). Mittelung über 34 Kanäle.

**Tabelle 3.1:** Peakfrequenz des Pulses in (Hz), Leistungsreduktion im Bereich von 0.8 bis 1.8 Hz und Stabilität im Frequenzbereichen von 0 bis 0.79 Hz und 1.81 bis 2 Hz in (%) beim Einsatz des adaptiven Filters an [oxy-Hb] Signalen. Für die Untersuchung wurden Daten aus 2.2 (Session 2 und 3) herangezogen.

| Subj. | Session 2 | | | Session 3 | | |
|---|---|---|---|---|---|---|
| | Puls Peak (Hz) | Leistungsreduktion (%) | Stabilität (%) | Puls Peak (Hz) | Leistungsreduktion (%) | Stabilität (%) |
| M1 | 1.4 | 97.8 | 0.0 | 1.1 | 84.0 | 0.0 |
| M2 | 1.4 | 88.0 | 0.0 | 1.4 | 60.1 | 0.0 |
| M3 | 0.9 | 82.5 | -0.1 | 0.8 | 53.0 | 0.1 |
| M4 | 1.4 | 90.3 | 0.2 | 1.5 | 93.2 | 0.1 |
| M5 | 1.2 | 92.6 | 0.7 | 1.2 | 84.2 | -0.1 |
| M6 | 1.0 | 96.5 | -0.1 | 1.2 | 97.1 | 0.0 |
| M7 | 1.7 | 46.8 | 0.0 | 1.5 | 31.7 | 0.0 |
| M8 | 1.4 | 88.6 | 0.6 | 1.4 | 61.2 | -0.1 |
| M9 | 1.3 | 66.6 | 1.7 | 1.4 | 94.6 | 0.5 |
| M10 | 1.4 | 85.5 | 0.0 | 1.8 | 43.5 | 0.4 |
| Mean | 1.3 | 83.5 | 0.3 | 1.3 | 70.3 | 0.1 |
| STD | 0.2 | 15.6 | 0.6 | 0.3 | 23.3 | 0.2 |

| | Mittelung über beide Sessions | | |
|---|---|---|---|
| | Puls Peak (Hz) | Leistungsreduktion (%) | Stabilität (%) |
| Mean | 1.3 | 76.9 | 0.2 |
| STD | 0.2 | 20.9 | 0.4 |

## 3.2 Atmung- und Blutdruckschwankungen

Das Frequenzspektrum der Atmung liegt im Allgemeinen in einem Bereich von ca. 0.2 - 0.3 Hz (12 - 18 Atemzüge pro Minute), das der störenden Blutdruckschwankungen (Mayer Wave) um 0.1 Hz. Wie in Abbildung 3.4 zu erkennen, beeinflussen beide Störungen die gemessenen [(de)oxy-Hb] Signale entsprechend. Da für die Elimination der beiden Störungen die selben Signalverarbeitungsansätze verwendet werden können folgt nachfolgend eine Zusammenfassung derselben.

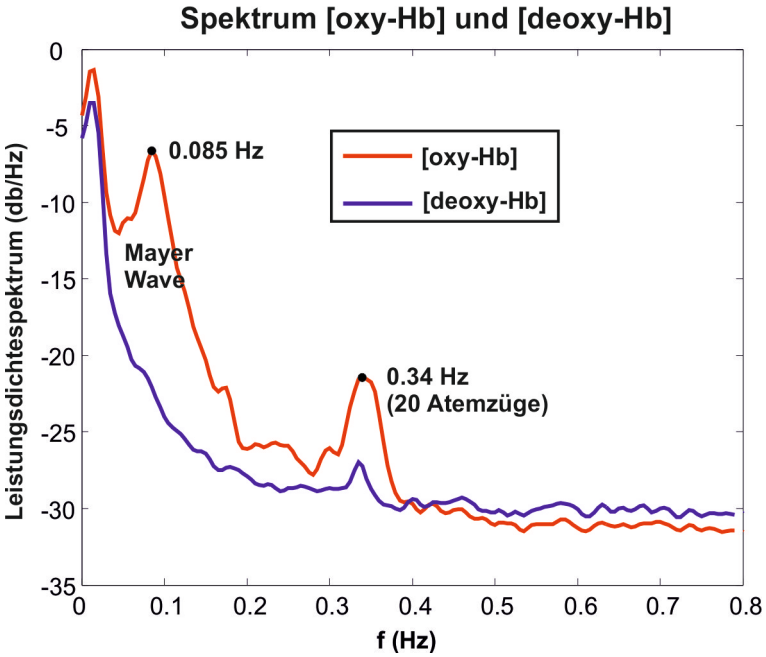


**Abbildung 3.4:** Leistungsdichtespektrum des [oxy-Hb] und [deoxy-Hb] Signals am Beispiel einer repräsentativen Versuchsperson (M2, Session 3) mit deutlichem Einfluss der Mayer Wave (hier im Bereich um 0.085 Hz) sowie der Atmung (im Bereich um 0.34 Hz).

### 3.2.1 Transfer-Funktions (TF) Modell

Als erster Ansatz wurde ein Transfer-Funktion-Modell (Gleichung 3.1, [5, 19]) für den Einsatz an NIRS-Signalen adaptiert und untersucht [3] (**remNoise-TF.m**, Anhang B).

Das Modell besitzt folgende Form:

$$\mathrm{X}[n] = \sum_{u=0}^{m} g_u \mathrm{Y}[n-u] + \mathrm{N}[n] \tag{3.1}$$

$X$ (n=1,2,3,...) steht dabei für das gestörte NIRS Signal, und $Y$ für das Störsignal (Atmungs- oder Blutdruckstörung). Der Ausdruck 3.2

$$\sum_{u=0}^{m} g_u \mathrm{Y}[n-u] \tag{3.2}$$

entspricht dem zu eliminierenden Einfluss der Störung im NIRS-Signal und $N$ dem NIRS-Signal ohne Störung. Durch Minimierung des Mittleren Quadratischen Fehlers $\mathrm{E}(\mathrm{N}^2[n])$ kann der Parameter $g_u$ (u=1,2,3, ... , m) der TF über

$$\gamma_{xy}(-j) = \sum_{u=0}^{m} g_u \gamma_{yy}(u-j) \tag{3.3}$$

mit $j = 0, 1, 2, ..., m$, wobei $\gamma_{xy}$ die Autokovarianzfunktion von $\mathrm{Y}[n]$ ist und $\gamma_{xy}$ der Kreuzkovarianzfunktion zwischen $\mathrm{X}[n]$ und $\mathrm{Y}[n]$ entspricht, abgeschätzt werden.

Dafür wird jedoch der optimale Wert für $m$ in Gleichung (2.2) benötigt. Entsprechend [19] muss hierfür ein Wert zwischen $m = 5$ und 15 gewählt werden. Mit den somit berechneten Parametern von $g_u$ ist es nun möglich, das gewünschte Signal ohne Störung wie folgt zu berechnen.

$$\mathrm{N}[n] = \mathrm{X}[n] - \sum_{u=0}^{m} g_u \mathrm{Y}[n-u] \tag{3.4}$$

Für genaue Informationen zum TF Algorithmus wird in weiterer Folge auf [19] verwiesen.

Diese Methode bietet sich vor allem für den Einsatz bei Einkanalmessungen an, wobei sie auch für Multikanalmessungen ohne Probleme verwendet werden kann. Zur Verwendung dieser Methode ist jedoch die zeitgleiche Aufzeichnung der Störsignale (Atmung, Blutdruck oder EKG) notwendig.

### 3.2.2 Independent Component Analyse (ICA)

Als weitere Methode wurde die Verwendung der ICA untersucht [3] (**remNoiseICA.m**, Anhang B). Kurz zusammengefasst, wird in diesem Ansatz

das gestörte NIRS Signal in unabhängige Komponenten (indipendent components, ICs) mit Hilfe der SOBI ICA [10] zerlegt. Anschließend wird die Koheränz zwischen jeder IC und den Störsignalen berechnet. ICs, für welche die Koheränz mit einem Störsignal größer als der Mittelwert aller Koheränzen plus eine Standardabweichung ist, werden eliminiert. Die verbleibenden ICs werden anschließend benutzt, um das entstörte Signal zu rekonstruieren. Zur Verwendung dieser Methode ist ebenfalls die zeitgleiche Aufzeichnung der Störsignale (Atmung, Blutdruck oder EKG) notwendig.

### 3.2.3 Vergleich ICA und TF

Um die Qualität der Methoden genau abschätzen zu können, wurden die Ansätze an in Kapitel 2.2 aufgezeichneten Daten der zweiten und dritten Session getestet. Dazu wurden sowohl der Atmungs- als auch der Mayer Wave-Einfluss aus allen über dem motorischen Kortex gelegenen Messkanälen (34 Kanäle) entfernt. Zur Definition der Störsignale wurden in beiden Methoden die gleichen Signale verwendet. Für die Definition des Atmungseinflusses wurde das Signal des Atmungssensors im Bereich von 0.2 bis 0.4 Bandpassgefiltert und für die Blutdruckschwankungen wurde das zwischen 0.07 und 0.13 Hz gefilterte BPdia Signal verwendet (Kapitel 2.2). Anschließend wurde die Leitungsreduktion in den Bereichen von 0.07 bis 0.13 Hz (Mayer Wave) und 0.2 bis 0.4 Hz (Atmung) berechnet und über alle verwendeten Kanäle gemittelt. Zusätzlich wurde die Qualität des Ansatzes überprüft, indem auch die Stabilität in den nicht von der Filterung betroffenen Frequenzbereichen (0 bis 0.6, 0.14 bis 0.19 und 0.41 bis 0.8 Hz) berechnet wurde.

Tabelle 3.2 zeigt die Ergebnisse zur Qualitätsuntersuchung des ICA und TF Ansatzes am [oxy-Hb] Signal an zehn Versuchspersonen (Daten aus 2.2; Session 2 und 3). Im Mittel (über beide Sessions) wurde für die TF Methode eine Reduktion von 54 % (Mayer Wave) bzw. 28 % (Atmung) erziehlt. Es trat zusätzlich kein signifikanter Unterschie zur ICA Methode (43 % (Mayer Wave) bzw. 16 % (Atmung)) auf (Abbildung 3.5B). Bei der Untersuchung der Stabilität wies jedoch die TF Methode eine signifikant ($p < 0.01$) besser Performance auf (ICA (25 %) zu TF (3 %)). Eine graphische Darstellung der erzielten Reduktion für den TF-Ansatz ist in Abbildung 3.5A anhand einer repräsentativen Versuchsperson (M1, Session 2) dargestellt. Da der ICA-Ansatz neben einer guten Elimination der Störsignale leider auch die Amplitude des Nutzsignals abschwächt, ist für eine Elimination des Atmungs- und Mayer Wave-Einflusses die TF-Methode zu empfehlen.

**Tabelle 3.2:** Prozentuelle Reduktion der Störeinflüsse (Mayer Wave (Mayer) und Atmung (Resp.)) sowie Stabilität (Stab.) in den nicht beeinflussten Frequenzbereichen bei Verwendung der TF und ICA Methode [3]

| | Transfer-Funktion | | | | | | ICA | | | | | |
|---|---|---|---|---|---|---|---|---|---|---|---|---|
| | Session 2 | | | Session 3 | | | Session 2 | | | Session 3 | | |
| Subj. | Mayer % | Resp. % | Stab. % | Mayer % | Resp. % | Stab. % | Mayer % | Resp. % | Stab. % | Mayer % | Resp. % | Stab. % |
| M1 | 55.6 | 45.4 | 5.9 | 33.1 | 45.0 | 8.5 | 34.6 | 31.9 | 6.9 | 31.1 | 26.8 | 29.5 |
| M2 | 77.1 | 31.2 | 8.6 | 71.3 | 40.9 | 4.5 | 11.5 | 15.7 | 18.8 | 90.4 | 33.1 | 43.7 |
| M3 | 56.8 | 32.4 | 2.5 | 14.4 | 9.4 | 0.4 | 66.3 | 16.7 | 25.7 | -0.4 | -32.2 | 5.4 |
| M4 | 87.7 | 10.1 | 6.3 | 80.6 | 24.7 | 2.7 | 90.0 | 25.7 | 35.1 | 91.0 | 30.6 | 20.7 |
| M5 | 20.0 | -0.5 | 2.0 | 21.9 | 3.8 | 1.4 | 10.6 | 8.3 | 17.0 | 33.7 | 14.2 | 19.2 |
| M6 | 77.1 | 17.6 | 9.4 | 69.9 | 12.9 | 3.5 | 27.4 | 30.4 | 34.8 | 71.0 | 18.5 | 22.3 |
| M7 | 43.3 | 45.7 | 3.1 | 54.5 | 48.4 | 5.9 | 29.6 | -27.3 | 51.6 | -12.7 | -5.8 | -12.9 |
| M8 | 80.0 | 47.1 | 1.5 | 26.1 | 37.5 | 0.1 | 53.9 | -36.3 | 22.0 | 40.0 | 27.7 | 30.3 |
| M9 | 39.4 | 45.7 | 3.4 | 63.3 | 56.0 | 3.9 | 47.9 | 45.4 | 39.8 | 30.4 | 54.2 | 11.7 |
| M10 | 74.3 | 13.7 | 1.9 | 31.8 | -0.4 | -9.2 | 82.4 | 27.6 | 23.8 | 30.9 | 16.5 | 51.8 |
| mean | 61.1 | 28.8 | 4.5 | 46.7 | 27.8 | 2.2 | 45.4 | 13.8 | 27.5 | 40.6 | 18.4 | 22.2 |
| SD | 21.8 | 17.5 | 2.9 | 23.8 | 20.3 | 4.7 | 27.7 | 26.2 | 12.9 | 34.6 | 23.5 | 18.6 |

| | Mittelung über beide Sessions | | | | | |
|---|---|---|---|---|---|---|
| | Mayer % | Resp. % | Stab. % | Mayer % | Resp. % | Stab. % |
| mean | 53.9 | 28.3 | 3.3 | 43.0 | 16.1 | 24.9 |
| SD | 23.4 | 18.5 | 4.0 | 30.6 | 24.3 | 15.8 |

Die Ergebnisse zu dieser Untersuchung wurden bereits in

**G. Bauernfeind, I. Daly and G.R. Müller-Putz. On the removal of physiolgical artifacts from fNIRS. *Proceedings of the 3rd TOBI Workshop 2012*, 2012.**

publiziert, des Weitern ist eine zusätzliche Publikation zu diesem Thema in Arbeit.

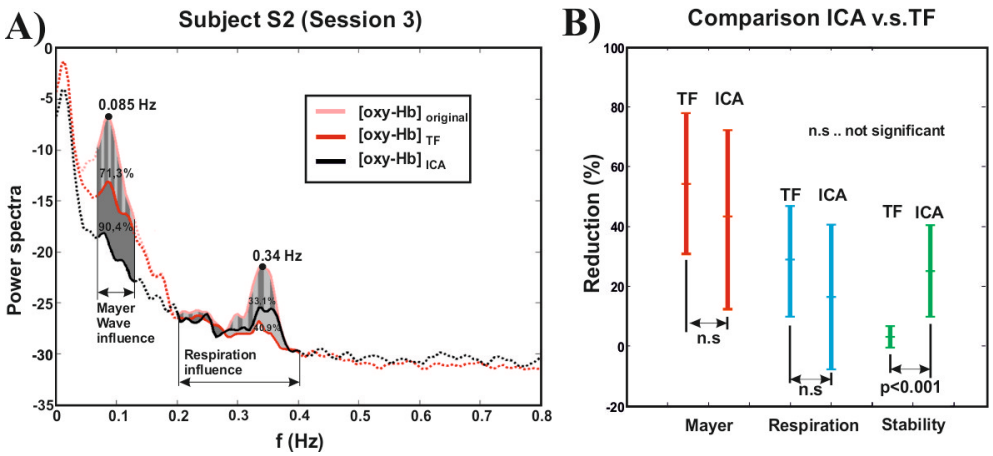


**Abbildung 3.5:** A) Reduktion des Mayer Wave- und Atmungseinflusses mittels ICA und TF Methode anhand einer repräsentativen Versuchsperson (M2, Session 2). Mittelung über 34 Kanäle. B) Allgemeiner Vergleich ICA und TF. Bild aus [3] entnommen.

Abbildung 3.6 zeigt am Beispiel von kortikalen Aktivierungsmustern, welche durch eine Fußbewegungsvorstellung entstehen, die Reduktion der Störungen durch den Einsatz der TF Methode. In Abbildung 3.6A ist das gemessene Muster vor der Anwendung der TF Methode dargestellt. Deutlich ist sowohl im gemittelten Verlauf als auch in der topographischen Verteilung eine großflächige Abnahme in [oxy-Hb] über dem motorischen Kortex zu erkennen. Nach dem Einsatz der TF Methode ist diese Abnahme nur noch auf die Areale für die linke und rechte Hand (C3, C4) begrenzt und es ist eine deutliche Zunahme im Areal für die Füße (Cz) zu erkennen (Abbildung 3.6B).

Da es jedoch nicht immer möglich ist, den Blutdruck mit aufzuzeichnen, wurde, basierend auf den Erkenntnissen in [40], der Einsatz des HR-Signals anstelle des diastolischen Blutdrucks untersucht. Dazu wurde aus dem EKG das kontinuierliche HR-Signal berechnet und ebenfalls wie das BPdia Signal

**Tabelle 3.3:** Vergleich zwischen der prozentuelle Reduktion des Störeinflüsses der Mayer Wave unter Verwendung des BPdia und der HR für die TF Methode. Für die Untersuchung wurden ebenfalls die Daten aus 2.2 (Session 2 und 3) herangezogen.

| Subj. | Session 2 | | Session 3 | |
|---|---|---|---|---|
| | BPdia (%) | HR (%) | BPdia (%) | HR (%) |
| M1 | 55.6 | 35.4 | 33.1 | 13.2 |
| M2 | 77.1 | 53.0 | 73.1 | 73.7 |
| M3 | 56.8 | 38.3 | 14.4 | 23.4 |
| M4 | 87.7 | 73.6 | 80.6 | 69.5 |
| M5 | 20.0 | 18.5 | 21.9 | 24.0 |
| M6 | 77.1 | 53.6 | 69.9 | 59.1 |
| M7 | 43.3 | 33.6 | 54.5 | 44.7 |
| M8 | 80.0 | 68.1 | 26.1 | 49.6 |
| M9 | 39.4 | 35.3 | 63.3 | 43.1 |
| M10 | 74.3 | 63.5 | 31.8 | 56.6 |
| Mean | 61.1 | 47.3 | 46.7 | 45.7 |
| STD | 21.8 | 17.8 | 23.8 | 20.3 |

| | Mittelung über beide Sessions | |
|---|---|---|
| | BPdia (%) | HR (%) |
| Mean | 53.9 | 46.5 |
| STD | 24.2 | 17.5 |

zwischen 0.07 und 0.13 Hz gefiltert. Tabelle 3.3 vergleicht die Ergebnisse der Reduktion des Mayer Wave Einflusses bei Verwendung des BPdia und der HR. Im Mittel (über beide Sessions) wurde für die auf dem BPdia basierende TF Methode eine Reduktion von 54 % erreicht (siehe dazu auch Tabelle 3.2). Im Vergleich konnte kein signifikater Unterschied zur Verwendung der HR (46.5 %) gefunden werden, wobei jedoch eine Tendenz in Richtung leicht verringerter Reduktionsergebnisse auftrat.

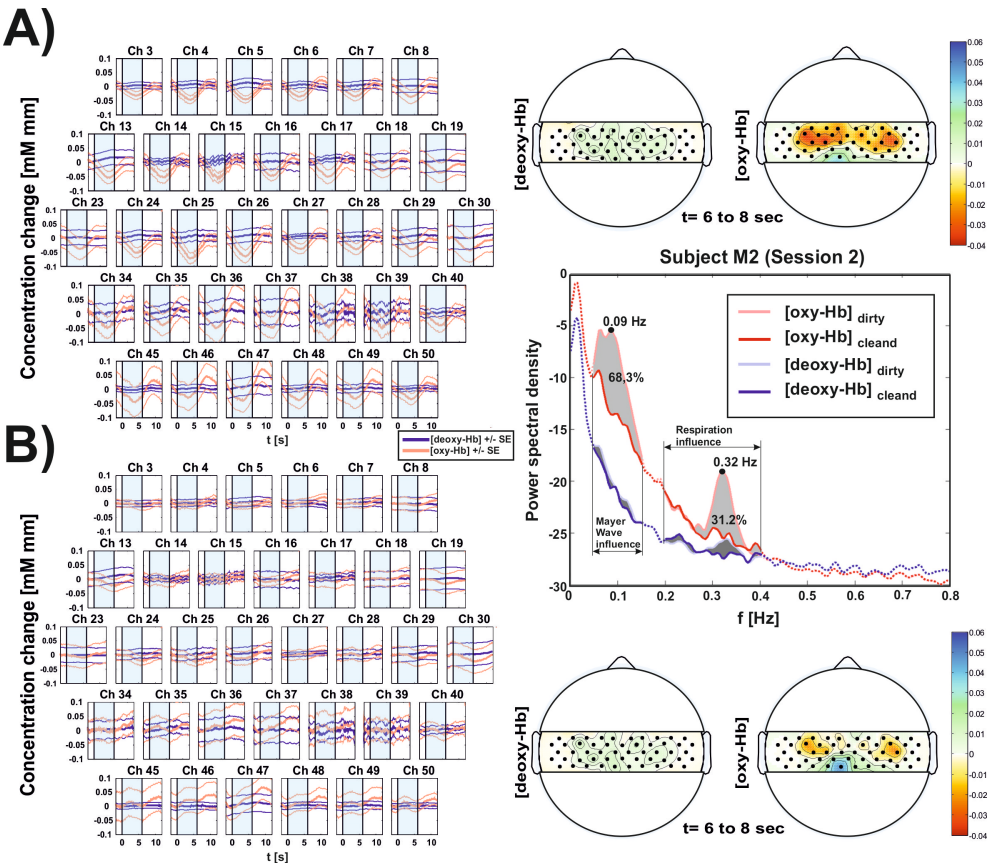


**Abbildung 3.6:** Repräsentatives Beispiel für die Anwendung der TF Methode zur Reduktion des Mayer Wave und Atmungseinflusses. A) Gemittelte Konzentrationsänderung (Mean $\pm$ STD) sowie topographischer Verlauf von [oxy-Hb] und [deoxy-Hb] während der Ausführung einer Fußbewegungsvorstellung (Sekunde 0 bis 6) vor und B) nach Anwendung der TF Methode. Zusätzlich ist das Leistungsdichtespektrum (gemittelt über alle Kanäle) zur Verdeutlichung der Reduktion in [oxy-Hb] und [deoxy-Hb] inkludiert.

## 3.3 Räumliche Filterung

Für Multikanalmessungen wurde die Verwendung eines Common Average Referenz-Filters (CAR, Räumliches Filters) implementiert (**remNoiseCAR.m**, Anhang B) und bereits in diversen Studien, unter Referenzierung dieses Projektes (siehe dazu die unten angeführten Referenzen), verwendet. Bei diesem Ansatz wird zu jedem Zeitpunkt von jedem Messkanal der Mittelwert aller Kanäle abgezogen. Somit ist es möglich, Störungen (Puls-, Atmungs- und Blutdruckschwankungen sowie Bewegungsartefakte), die sich auf alle Kanäle annähernd gleich auswirken, teilweise bzw. vollständig aus den Messsignalen zu eliminieren. Ein Vorteil dieser Methode ist, dass keine zusätzliche Aufzeichnung der physiologischen Signale notwendig ist, weiters ist sie sehr einfach zu implementieren. Ein Nachteil dieser Methode ist jedoch, dass zusätzlich zu der Elimination der Störsignale, auch das Nutzsignal (ähnlich dem ICA Ansatz) leicht abgeschwächt wird. Diese Abschwächung wirkt sich jedoch nicht auf die topographische Verteilung der hämodynamischen Signale, sondern nur auf deren Amplitude aus.

Tabelle 3.4 zeigt die Ergebnisse der Reduktion des Mayer Wave-, des Atmungs- und des Puls-Einflusses bei Verwendung eines CAR-Filters. Im Mittel (über beide Sessions) wurde eine Reduktion von 71.6 % (Mayer Wave), 41.4 % (Atmung) und 69.1 % (Puls) erreicht. Eine graphische Darstellung der erzielten Reduktion für den CAR-Ansatz ist in Abbildung 3.7 anhand einer repräsentativen Versuchsperson (M4, Session 3) dargestellt.

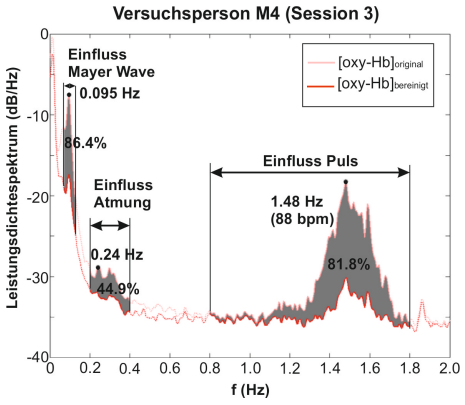


**Abbildung 3.7:** Reduktion des Mayer Wave-, Atmungs- und Puls-Einflusses mittels CAR-Methode anhand einer repräsentativen Versuchsperson (M4, Session 3). Mittelung über 34 Kanäle.

**Tabelle 3.4:** Prozentuelle Reduktion der Störeinflüsse (Mayer Wave (Mayer), Atmung (Resp.)) und Puls) bei Verwendung der CAR Methode.

| | Common Average Referenz (CAR)-Ansatz | | | | | |
|---|---|---|---|---|---|---|
| | Session 2 | | | Session 3 | | |
| Subj. | Mayer (%) | Resp. (%) | Puls (%) | Mayer (%) | Resp. (%) | Puls (%) |
| M1 | 76.7 | 68.9 | 90.5 | 73.1 | 69.3 | 93.0 |
| M2 | 82.2 | 42.6 | 75.2 | 87.8 | 58.9 | 77.0 |
| M3 | 64.7 | 29.6 | 71.9 | 65.4 | 34.3 | 63.7 |
| M4 | 89.2 | 22.4 | 67.5 | 86.4 | 44.9 | 81.1 |
| M5 | 39.3 | 25.0 | 79.1 | 37.8 | 8.7 | 67.1 |
| M6 | 86.0 | 36.4 | 86.1 | 86.5 | 73.3 | 82.0 |
| M7 | 51.6 | 42.7 | 34.8 | 60.5 | 47.1 | 27.6 |
| M8 | 87.7 | 34.6 | 59.7 | 72.9 | 30.4 | 59.7 |
| M9 | 63.5 | 60.4 | 62.8 | 63.7 | 59.9 | 63.3 |
| M10 | 81.0 | 39.4 | 73.9 | 82.2 | 29.4 | 65.2 |
| Mean | 71.6 | 40.2 | 70.1 | 71.6 | 42.6 | 68.0 |
| STD | 16.3 | 14.7 | 15.7 | 15.6 | 17.8 | 17.7 |

| | Mittelung über beide Sessions | | |
|---|---|---|---|
| | Mayer (%) | Resp. (%) | Puls (%) |
| Mean | 71.6 | 41.4 | 69.1 |
| STD | 15.5 | 15.9 | 16.3 |

Abbildung 3.8 zeigt den Einsatz eines CAR-Filters für die Untersuchung einer Handbewegungsdurchführung (siehe dazu Kapitel 2.2). Abbildung 2.8 zeigt die prinzipielle Anordnung der Messkanäle über den relevanten Regionen C3 (Areal für rechte Handbewegung), Cz (Areal für Fubewegung) und C4 (Areal für eine linke Handbewegung) sowie die Positionierung an einer Versuchsperson. Abbildung 3.8A zeigt das gemittelte Muster einer rechtsseitigen Handbewegung mit einer genaueren Darstellung der Messkanäle 23 (Region C3) und 30 (Region C4). In dieser Darstellung ist deutlich ein starker Anstieg in der [oxy-Hb] Konzentration über alle Messkanäle zu erkennen, welcher auf den Blutdruckeinfluss (kleine Darstellung) während der Aufgabenausführung zurückzuführen ist und das eigentliche kortikale Aktivierungsmuster der Aufgabe überlagert. Durch die Verwendung des CAR-Filters ist es nun möglich, diesen globalen Blutdruckeinfluss zu eliminieren (Abbildung 3.8B) und das eigentliche Aktivierungsmuster (Aktivierung über C3) klar darzustellen. Die topographische Darstellung stellt dieses klar abgegrenzte Muster nochmals deutlich dar.

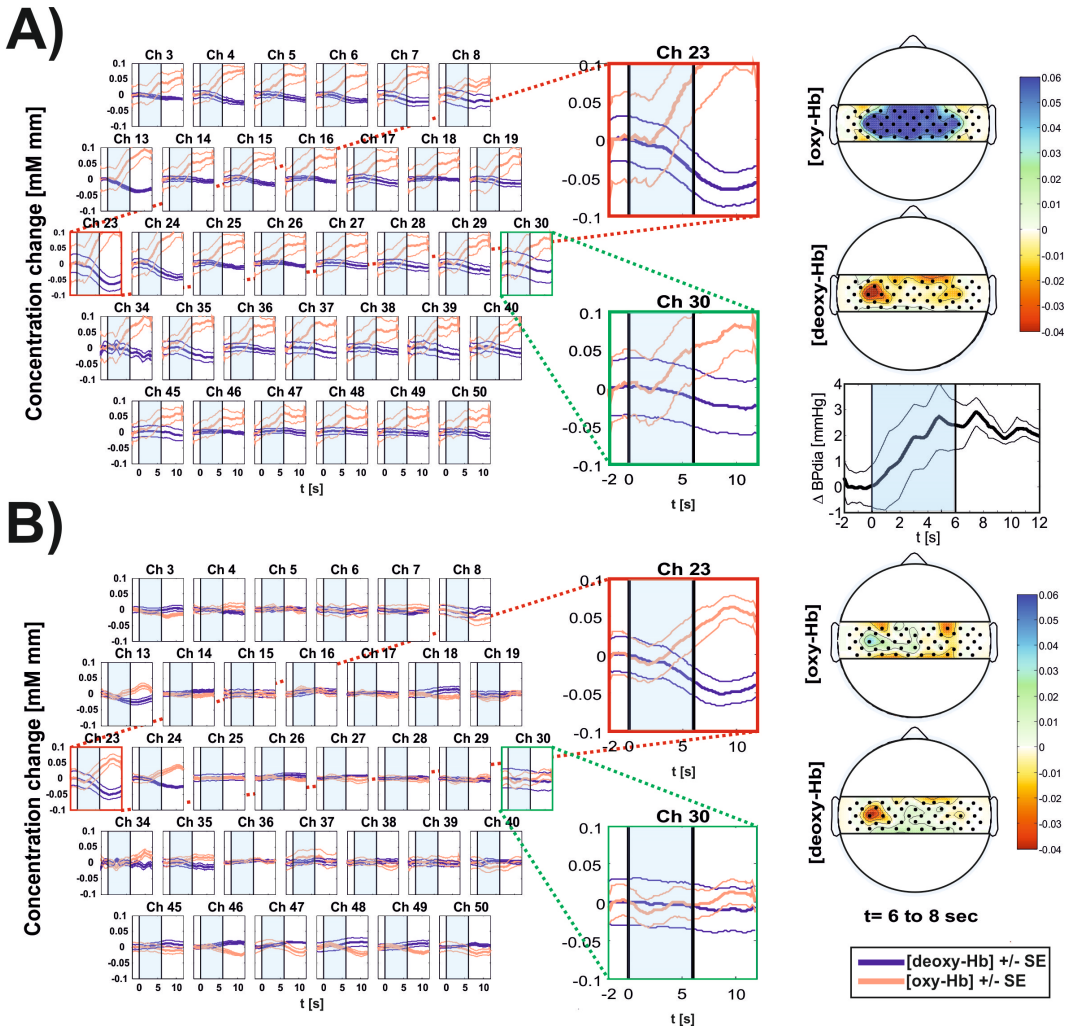


**Abbildung 3.8:** Repräsentatives Beispiel für die Anwendung de rCAR Methode zur Reduktion des Mayer Wave, Atmungs- und Puls-Einflusses. A) Gemittelte Konzentrationsänderung (Mean $\pm$ STD) sowie topographischer Verlauf von [oxy-Hb] und [deoxy-Hb] während der Ausführung eines Handbewegungstasks (rechte Hand, Sekunde 0 bis 6) vor und B) nach Anwendung der CAR Methode. Zusätzlich sind der globale Blutdruckeinfluss und die topographische Darstellung der [oxy-Hb] und [deoxy-Hb] inkludiert.

### 3.3.1 Publikationen unter Verwendung der CAR Methode

**G. Pfurtscheller, G. Bauernfeind, S. Wriessnegger and C. Neuper. Focal frontal (de)oxyhemoglobin responses during simple arithmetic. *Int J Psychophysiol*, 76(3):186-192, 2010.**

**G. Bauernfeind, S. C. Wriessnegger, G. Pfurtscheller and C. Neuper. Investigation of hemodynamic responses during simple arithmetic. Annotations for the use as control signal for optical brain-computer interface (oBCI) applications. *Proceedings of the 4$^{th}$ International BCI Meeting 2010*, 2010.**

**G. Bauernfeind, S. C. Wriessnegger, G. Pfurtscheller and C. Neuper. Fokale frontale (De)oxyhämoglobinänderung während einfacher arithmetischer Aufgaben: Anmerkungen zur Verwendung als Steuersignale für optische Gehirn-Computer-Interface (oBCI)-Anwendungen. *Kongress 5 Jahre INGE St.*, 30-30, 2010.**

**Zusammenfassung:** Im Zuge dieser Studie [37], wurden kortikale Aktivierungsmuster (Änderungen von [oxy-Hb] und [deoxy-Hb]) über dem präfrontalen Kortex während der Ausführung einfacher arithmetischer Aufgaben an 10 Versuchspersonen untersucht. Um eine genaue Lokalisation dieser Muster zu ermöglichen wurde dabei der CAR-Ansatz verwendet. Bei acht der zehn Versuchspersonen konnte dabei Folgendes festgestellt werden: Die Versuchspersonen zeigten eine fokale bilaterale Zunahme der [oxy-Hb] Konzentration im dorsolateralen präfrontalen Cortex (DLPFC) bei gleichzeitiger Abnahme der [oxy-Hb] im anterior präfrontalen Cortex (APFC). Die Zunahme der [oxy-Hb] Konzentration im linken DLPC sowie die Abnahme im APFC waren dabei signifikant, während die [deoxy-Hb] Änderung keine signifikanten Änderungen aufwies. Diese Erkenntnisse wurden in weiter Folge im Kontext einer "fokalen Aktivierung/ umgebenden Deaktivierungërläutert und diskutiert.

**S. C. Wriessnegger, G. Bauernfeind, K. Schweizer, S. Kober, C. Neuper and G.R. Müller-Putz. Prefrontal activation during inhibitory motor control of learned hand and foot movements: An fNIRS study. *Front Neurosci*, (under review).**

**G. Bauernfeind, K. Schweizer, S. C. Wriessnegger, S. Kober, G. Pfurtscheller and C. Neuper. Neural correlates of the execution**

**and inhibition of well learned foot and finger movements: an NIRS study. *Proceedings of the 1st TOBI Workshop 2010*, 38-38, 2010.**

**Zusammenfassung:** Inspiriert durch die fMRI- Forschungsarbeit von Hummel et al. [28] zum kontextuellen Abruf gelernter Verhaltensweisen wurde in dieser Studie die adäquate Kontrolle von erlernten motorischen Mustern mit Hilfe der NIRS an 16 Versuchspersonen untersucht, wobei auch hier die Methode der CAR-Filterung zur Auswertung herangezogen wurde.

**G. Bauernfeind and V. Kaiser and T. Kaufmann and A. Kreilinger and A. Kübler and C. Neuper. Cortical effects of BCI training measured with fNIRS. *Int J Bioelect*, 13(2), 66-67, 2011.**

**Zusammenfassung:** Diese Studie [4] umfasste die Untersuchung kortikaler Trainingseffekte bei der Verwendung eines 2-Klassen, auf Bewegungsvorstellung basierenden BCI-Systems [29]. Zwölf Versuchspersonen wurden Trainiert, mittels Hand- oder Fußvorstellung einen Cursor auf einem Bildschirm zu steuern. Das Steuersignal wurde dazu aus dem EEG extrahiert. Mit Hilfe der NIRS wurde dabei nun untersucht welche kortikalen Areale bei diesem Training involviert sind und wie sich die Aktivität dieser Areale im Laufe des Trainings verändern. Um auch hier eine genaue Lokalisation der Aktivierungsmuster zu erhalten, wurde die Methode der CAR-Filterung der hämodynamischen Signale angewandt. Gleichzeitig wurden auch systemische Signale wie Atmung, Blutdruck und EKG gleichzeitig mit NIRS-Signal aufgezeichnet (Kapitel 2.1). Die statistische Auswertung der NIRS-Signale im Kontext des Trainings wurde jedoch bereits durchgeführt [4], wobei signifikante Aktivitätsänderungen während des Trainings entsprechend der Trainingsaufgabe gefunden wurden. Eine weitere Analyse unter Verwendung der TF-Methode ist in Vorbereitung.

# Kapitel 4

# WP3: Realtime-Applikationen

In diesem WP wurden Möglichkeiten von Realtime-Applikationen verschieder Signalverarbeitungsansätze untersucht. Dieses WP inkludiert die Implementation der Ansätze sowie die Datenanalyse und Auswertung.

Meilensteine dieses WPs waren:

- **Implementation von Signalverarbeitungsansätzen zur Elimination der systemischen Einflüsse**
  Diverse Signalverarbeitungsansätze wurden implementiert.
- **Analyse und Auswertung**
  Die Ergebnisse dieses Meilensteins sind nachfolgend aufgeführt.

## 4.1 Puls

### 4.1.1 Tiefpassfilter

Der einfachste Ansatz, um diesen Einfluss des Pulses zu eliminieren, ist die Verwendung eines Tiefpassfilters (Abbildung 3.1B). Eine onlinefähige Implementation für die Elimination von Pulsschwankungen, welche das Feedback beeinflussen, wurde durchgeführt. Dazu wurde ein sogenannter "Moving Average-Filter" verwendet, welche die störenden Anteile des Pulses aus dem Signal eliminiert. Abbildung 4.2 zeigt das dazu verwendete Simulink-Modell, in welchem ein solches Filter eingesetzt wurde.

Diese Implementation wurde bereits in einer Studie zur Realisierung eines asynchronen hybriden BCI-Systems verwendet [35]:

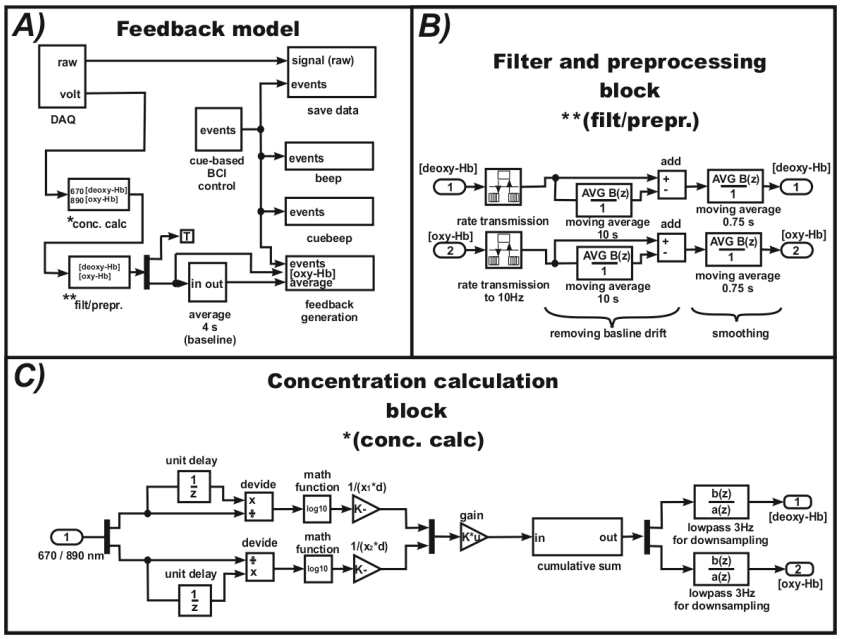


**Abbildung 4.1:** A) Simulink Modell mit Blöcken für C) Konzentrationsberechung und B) Preprocessing (Elimination des Pulses und Basline-Drifts).

**G. Pfurtscheller, B. Z. Allison, G. Bauernfeind, C. Brunner, S. Solis Escalante, R. Scherer, T. O. Zander, G. R. Müller-Putz, C. Neuper and N. Birbaumer. The hybrid BCI *Front Neurosci*, 4:42, 2010.**

**Zusammenfassung:** In der Studie [35] wurde ein asynchrones, hybrides BCI-System entwickelt, welches ein oBCI mit einer auf SSVEP basierten Orthesenkontrolle kombiniert (Abbildung 4.2). Die Untersuchung wurde an einer Versuchsperson durchgeführt, wobei die Orthesenkontrolle unter Verwendung des oBCI-System ein- bzw. ausgeschalten werden musste. Der Versuchsperson wurde die relative oxy-Hb Konzentration (gemessen über dem präfrontalen Kortex) als Feedbacksignal rückgemeldet. An dieser Stelle kam der "Moving-Average-Filterßum Einsatz, um die aufgrund des Pulses bedingten Schwankungen des Feedbacksignals zu unterdrücken. Die Versuchsperson konnte nun durch willentliche Veränderung der Konzentration nach überschreiten eines Schwellwerts die SSVEP-Kontrolle ein- bzw. ausschalten (sogenannter "Brain Switch", siehe Abbildung 4.2).

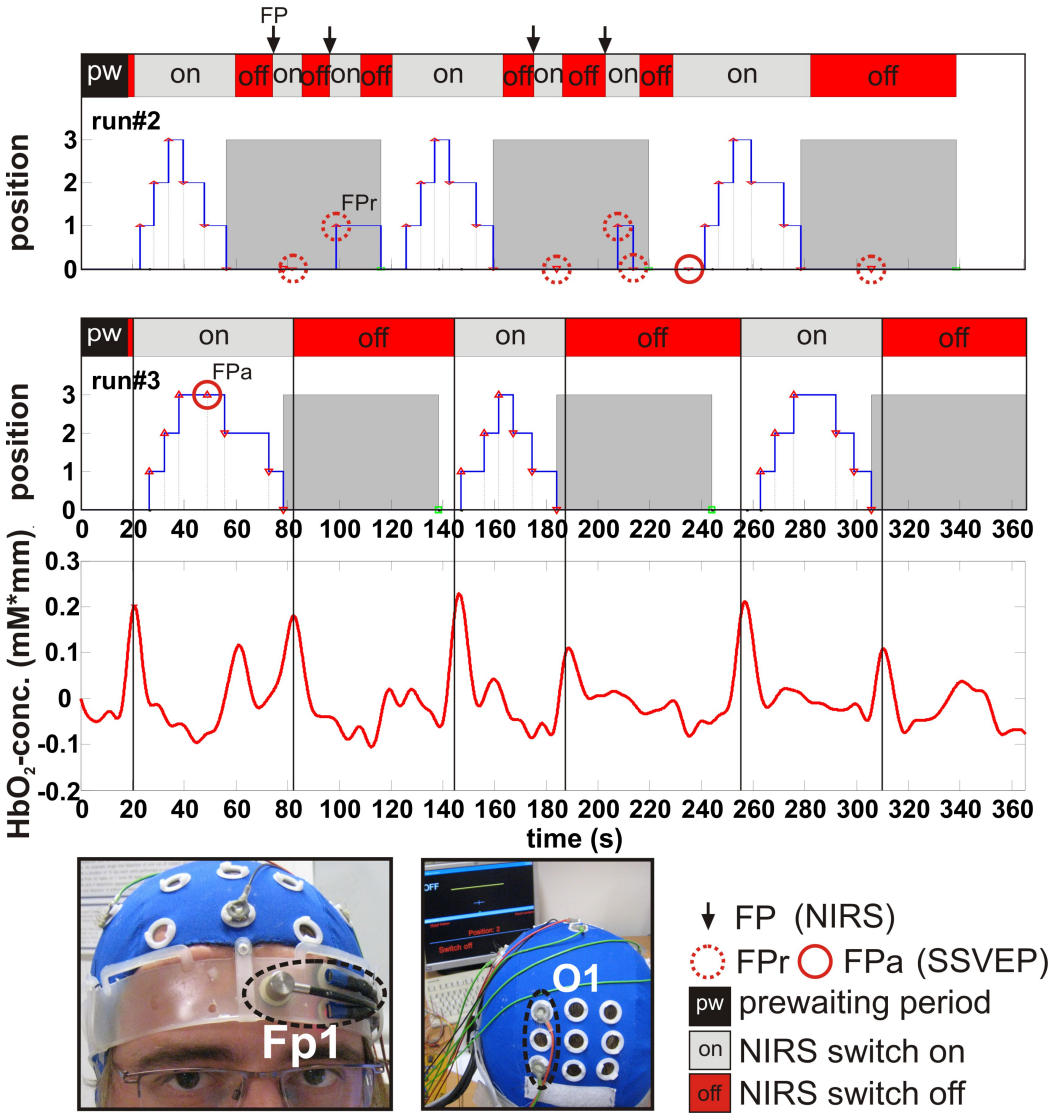


**Abbildung 4.2:** Von oben nach unten: Position des "Brain-Switch" (grau markierte Bereiche kennzeichnen die geschlossene Position) sowie die Position des SSVEP-Orthese (grau markierte Bereiche kennzeichnen vorgegebene Ruhezeiten) für die zweite bzw. dritte Messung an der Versuchsperson. Darunter dargestellt, der Verlauf der oxy-Hb Konzentration sowie die Messposition für die präfrontale NIRS Messung und die Elektrodenmontage zur Steuerung der SSVEP Orthese. (Bild aus [35] übernommen)

### 4.1.2 Adaptive Störunterdrückung des Pulses

Dieser Abschnitt behandelt die Realtime-Implementation des in Kapitel 3 beschriebenen Verfahrens zur adaptiven Störunterdrückung des Pulssignals. Abbildung 4.3A zeigt das Modell zur adaptiven Filterung mittels LMS Filter (adaptiver FIR-Filter dessen Koeffizienten mittels LMS-Verfahren angepasst werden) eines einzelnen Kanals. Zusätzlich zeigt Abbildung 4.3B die Signale der adaptiven Filterung. Der dabei verwendete LMS Filter stammt aus dem Signal Processing Blockset (MATLAB$^{TM}$, MathWorks®, Natick, Massachusetts (USA)). Als Input wird das gestörte [oxy-Hb] oder [deoxy-Hb]-Signal verwendet. Zur Definition des Störsignals kann das zwischen 0.8 und 1.8 Hz gefilterte BPdia oder ein Fingerpulssignal verwendet werden. Der Faktor $f$ dient lediglich dazu, das künstliche Störsignal amplitudenmäßig ungefähr an die unbekannte Störung anzupassen und kann aus einer kurzen Testmessung eruiert werden.

Zur Analyse wurden die in Kapitel 2.2 gemessen Daten herangezogen und die Methode wurde in einer Realtime-Simulation getestet. Tabelle 4.1 vergleicht die in der Offline-Implementierung (Kapitel 3) gewonnenen Leistungsreduktionen mit den Ergebnissen der Realtime-Simulation. Für die Realtime-Simulation wurde im Mittel eine Reduktion des Pulseinflusses von 64.6% erzielt. Die Stabilität beträgt -0.8 %. Im Vergleich mit der Offline-Implementierung (mittlere Leistungsreduktion 76.9 %, Stabilität 0.2 %, Tabelle 3.1) wurde sowohl für die Leistungsreduktion ($p < 0.01$) als auch für die Stabilität ($p < 0.01$) ein signifikant niedrigeres Ergebniss erziehlt. Diesem Ergebnis liegt jedoch zugrunde, dass für das in Kapitel 3 beschriebene Verfahren alle Datenpunkte der Messung (auch "zukünftige") verwendet wurden, während die Anpassung der Filterkoeffizienten für die Realtime-Implementation nur auf bereits vorhandene Datenpunkte basiert.

**Tabelle 4.1:** Leistungsreduktion im Bereich von 0.8 bis 1.8 Hz und Stabilität im Frequenzbereichen von 0 bis 0.79 Hz und 1.81 bis 2 Hz in (%) bei der Realtime-Simulation des adaptiven Filters an [oxy-Hb] Signalen. Für die Untersuchung wurden Daten aus 2.1 (Session 2 und 3) herangezogen. Die Ergebnisse der Versuchsperson M10, Session 3 wurden aufgrund einer Störung nicht für die abschließende Mittelwert- und STD-Berechnung herangezogen.

| Subj. | Session 2 | | Session 3 | |
|---|---|---|---|---|
| | Leistungsreduktion (%) | Stabilität (%) | Leistungsreduktion (%) | Stabilität (%) |
| M1 | 78.4 | -1.0 | 79.9 | -1.0 |
| M2 | 75.3 | -1.0 | 57.6 | -1.0 |
| M3 | 75.7 | -0.9 | 38.8 | -0.7 |
| M4 | 64.8 | -1.0 | 79.1 | -1.0 |
| M5 | 77.7 | -0.3 | 66.1 | -1.1 |
| M6 | 87.4 | -0.9 | 89.5 | -0.9 |
| M7 | 40.4 | -1.0 | 31.2 | -1.0 |
| M8 | 61.6 | -0.9 | 53.2 | -1.0 |
| M9 | 63.5 | 0.8 | 75.3 | -1.0 |
| M10 | 31.7 | -1.1 | (-176.5) | (-0.6) |
| Mean | 65.6 | -0.7 | 63.4 | -1.0 |
| STD | 17.6 | 0.6 | 78.1 | 0.2 |

| | Mittelung über beide Sessions | |
|---|---|---|
| | Leistungsreduktion (%) | Stabilität (%) |
| Mean | 64.6 | -0.8 |
| STD | 18.2 | 0.4 |

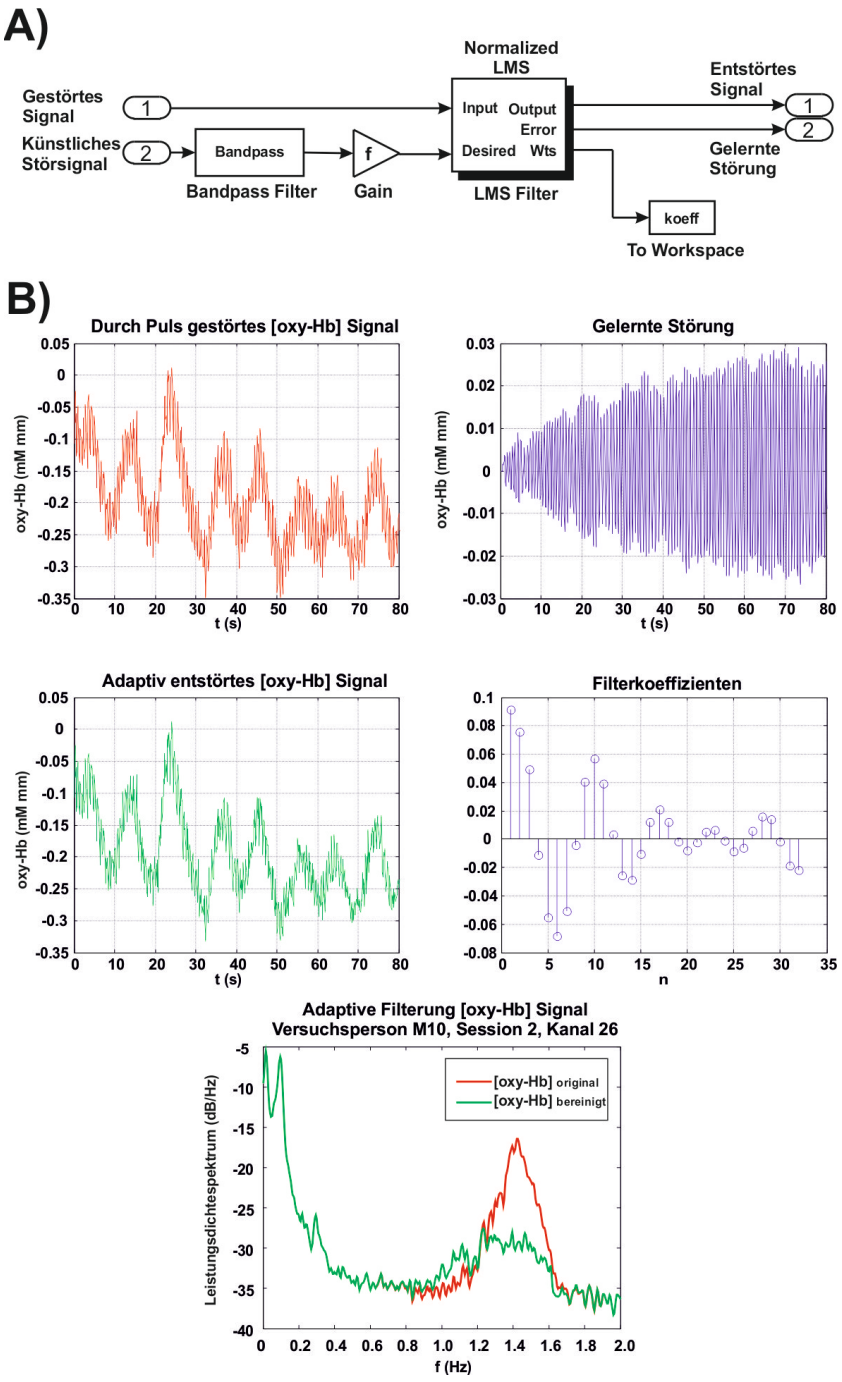


**Abbildung 4.3:** A) Simulink Modell der adaptiven Filterung eines Kanals B) Signale (ersten 200s der Daten dargestellt) der Filterung sowie die Filterkoeffizienten und die Darstellung der Leistungsreduktion im Bereich des Pulses (M10, Session 2, Kanal 26).

## 4.2 Atmung und Blutdruckschwankungen

Für Multikanalmessungen bietet sich vor allem die in Kapitel 3.3 beschriebene Verwendung eines Common Average Referenz-Filters (CAR, Räumliches Filters) an. Der Vorteil dieser Methode liegt in der einfachen Implementierung sowie in der Vergleichbarkeit der Ergebnisse. Die Implementation liefert sowohl Offline als auch in Realtime die selben Reduktionsergebnisse (Tabelle 3.4). Bei der Implementierung muss jedoch darauf geachtet werden, Kanäle mit schlechter Signalqualität aus der räumlichen Filterung auszuschließen, da diese sonst durch die CAR-Filterung auch alle anderen Kanäle negativ beinflussen würden. Dazu ist es notwendig, vor der eigentlichen Messung einen kurzen Signalcheck durchzuführen, um die entsprechenden Kanäle zu eruieren. Abbildung 4.4A zeigt den entwickelten CAR-Block zur räumlichen Filterung. Die Funktionsweise (Abbildung 4.4B) basiert auf einer einfachen Matrixmultiplikation $u * k$, wobei die Matrix entsprechend der Kanalanzahl und der exkludierten Kanäle zu berechnen ist. Abbildung 4.4C zeigt das Beispiel einer solchen Filtermatrix für zehn Kanäle, wobei hier zu Anschauungszwecken zwei Kanäle (Kanal 3 und 5) mit schlechter Signalqualität angenommen wurden.

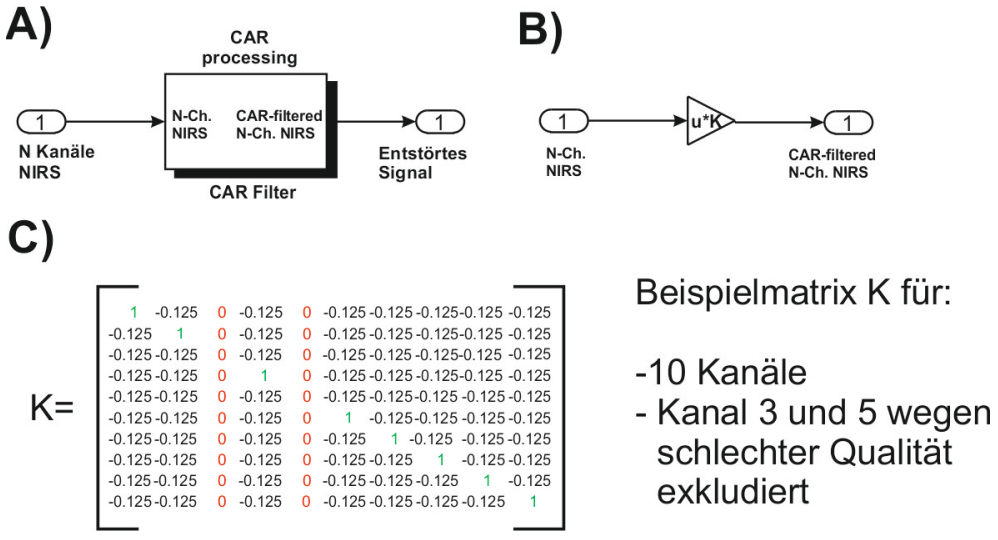


**Abbildung 4.4:** A) Simulink Modell der CAR Filterung basierend auf einer B) Matrixmultiplikation $u * k$. C) Beispielmatrix, zehn Kanäle (Kanal 3 und 5 exkludiert).

## 4.3 Single-trial Klassifikation Antagonistischer Muster

Zusätzlich zur Elimination der Einflüsse wurde auch eine robuste Single-trial Klassifkation von hämodynamischen Mustern untersucht [7]. Ein kurze Zusammenfassung der erzielten Ergebnisse der Studien

**G. Bauernfeind, R. Scherer, G. Pfurtscheller and C. Neuper. Single-trial classification of antagonistic oxyhemoglobin responses during mental arithmetic. *Med Biol Eng Comput*, 49(9):979-984, 2011.**

**G. Bauernfeind, R. Scherer, G. Pfurtscheller and C. Neuper. Classication of Focal Frontal Oxyhemoglobin Responses During Mental Arithmetic. *Proceedings of the 5$^{th}$ International Brain-Computer Interface Conference 2011*, 264-267, 2011.**

**G. Bauernfeind, S. C. Wriessnegger, G. Pfurtscheller and C. Neuper. Fokale frontale (De)oxyhämoglobinänderung während einfacher arithmetischer Aufgaben: Anmerkungen zur Verwendung als Steuersignale für optische Gehirn-Computer-Interface (oBCI)-Anwendungen. *Kongress 5 Jahre INGE St.*, 30-30, 2010.**

ist nachfolgend angefügt.

**Zusammenfassung:** Verschiedene Forschungsgruppen haben im Laufe der letzten Jahrzehnte ihren Schwerpunkt auf Kommunikations- bzw. Ansteuerungshilfe für schwerst gelähmte PatientInnen gelegt. Als Steuersignale können dabei die sensomotorischen Aktivierungsmuster während einer Bewegungsvorstellung herangezogen werden. Neben diesen ist auch eine Verwendung von Aktivierungsmustern während kognitiven Aufgaben, hier im speziellen bei Durchführung einer einfachen arithmetischen Aufgabe, möglich. In den letzten Jahren konnte in vielen NIRS-Studien eine starke Beteiligung des präfrontalen Cortex (PFC) gezeigt werden. Dabei wurden jedoch nur wenige Messpositionen (meist eine oder zwei) für die NIRS-Messung herangezogen. Um einen genaueren Einblick in Bildung und Verteilung der Aktivierungsmuster zu erhalten, wurde in einer Vorabstudie [37] ein Multikanal NIRS-Systems verwendet. Die Untersuchungen wurden an einer Gruppe von zehn gesunden ProbandInnen durchgeführt. Bei acht der zehn Personen konnte

über dem dorsolateralen PFC ein fokaler bilateraler Anstieg in [oxy-Hb], begleitet von einem Abfall des [deoxy-Hb], gemessen werden. Parallel zu dieser dorsolateralen Aktivierung war auch ein Anstieg in [deoxy-Hb] bei gleichzeitigem Abfall des [oxy-Hb] über dem mittleren Bereich des anterior PFC, messbar (siehe dazu auch [37] sowie die Zusammenfassung der Studie in Kapitel 3.3.1). Bei diesem Verlauf handelt es sich um ein sogenanntes antagonistisches Muster (e.g. Zunahme [oxy-Hb] dorsolateral, Abnahme [oxy-Hb] präfrontal). Ausgehend von diesen Ergebnissen wurde spekuliert, dass die Verwendung dieses antagonistischen Musters von großem Nutzen ist, da sich eventuelle Störeinflüsse des Pulses, der Atmung und der Mayer Wave annähernd gleich auf beide Signale auswirken und somit die Trennschärfe der Muster nicht beeinflussen. In [7] wurde daher die oben genannte Hypothese unter Verwendung einer BCI Offline-Simulation untersucht. Dazu wurden die in [37] gewonnen Daten herangezogen. Es wurde festgestellt, dass die Verwendung antagonistischer Kanäle/Verläufe die Klassifikationsgenauigkeit signifikant verbessert. Abbildung 4.5 zeigt den Vergleich zur Klassifizierung mit einzelner Kanälen. Diese werden entsprechend stärker von Störsignalen beeinflusst, wodurch die Klassifikationsgenauigkeit signifikant schlechter ($p < 0.01$) als im Fall der Verwendung von antagonistischen Kanälen/Verläufen ist.

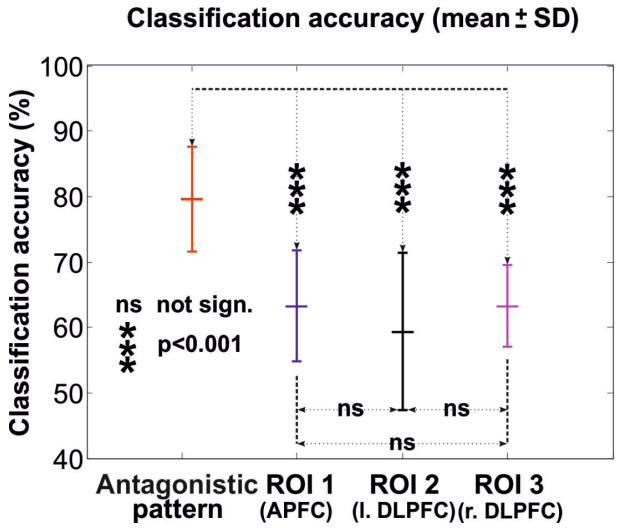


**Abbildung 4.5:** Klassifikationsergebnisse bei Verwendung von antagonistischen Kanälen/Verläufen und einzelnen Kanälen/Verläufen. (Abbildung aus [7] übernommen)

# Kapitel 5

# Zusammenfassung sowie Veröffentlichungen im Rahmen des Projektes

## 5.1 Zusammenfassung

Das Ziel dieses Projekts war die Untersuchung von systemischen Einfüssen auf mittels NIRS gemessenen Aktivierungsmuster. Darüber hinaus sollten geeignete Signalverarbeitungsansätze entwickelt werden, welche eine Elimination dieser Einflüsse ermöglichen.

Die Untersuchung der systemischen Einfüssen wurden durchgeführt und in drei Veröffentlichungen publiziert [36, 39, 40]. Grundsätzlich können drei Haupteinflussfaktoren festgelegt werden: Puls, Atmung und Blutdruckschwankungen (Mayer Wave).

### 5.1.1 Offline

Für eine Offline-Elimination dieser Einflüsse, z.B. in neurowissenschaftlichen Studien, wurden die in Kapitel 3 präsentierten Ansätze entwickelt bzw. untersucht. Die softwaretechnische Implementation der Ansätze sind in Anhang B angefügt und können auch über die Open-Soure Software-Bibliothek "BioSig" (`http://biosig.sourceforge.net/`) bezogen werden.

**Puls:** Das Frequenzspektrum des Pulses liegt im Allgemeinen in einem Bereich von ca. 0.8  2 Hz (48 - 120 bpm). Zur Elimination wurden drei verschiedene Ansätze präsentiert:

- Verwendung eines Tiefpassfilters
- "Pulse Remove" Algorithmus
- Adaptive Filterung **(adaptPulsremove.m)**

Die ersten beiden Ansätze haben den Nachteil, dass dabei, für eine Analyse kortikaler Tasks möglicherweise relevante, Signalkomponenten des NIRS-Signals ebenfalls teilweise eliminiert werden. Es wird daher für zukünftige Messungen die Verwendung der Methode der adaptive Filterung zur Elimination der Pulsschwankungen empfohlen.

**Atmungs- und Blutdruckschwankungen:** Das Frequenzspektrum der Atmung liegt im Allgemeinen in einem Bereich von ca. 0.2 - 0.3 Hz (12 - 18 Atemzüge pro Minute), das der störenden Blutdruckschwankungen (Mayer Wave) um 0.1 Hz. Da für die Elimination der beiden Störungen die selben Signalverarbeitungsansätze verwendet werden können, wurden zur Elimination folgende Ansätze implementiert:

- Transfer-Funktions (TF) Modell **(remNoiseTF.m)**
- Independent Component Analyse (ICA) **(remNoiseICA.m)**
- Common Average Referenz-Filter (CAR) **(remNoiseCAR.m)**

Alle drei Methoden weisen eine gute Reduktion der Störeinflüsse auf, wobei jedoch sowohl beim ICA- als auch beim CAR-Ansatz zusätzlich zur Elimination der Störsignale auch das Nutzsignal leicht abgeschwächt wird. Es wird daher für Offline-Analysen die Verwendung der TF-Ansatzes zur Elimination der Atmungs- und Blutdruckschwankungen empfohlen.

### 5.1.2 Online

Für eine Realtime-Elimination der Einflüsse, für auf NIRS basierende BCI-Systeme, wurden die in Kapitel 4 präsentierten Ansätze entwickelt bzw. untersucht.

**Puls:** Zur Realtime-Elimination des Pulses wurden zwei verschiedene Ansätze präsentiert:

- Verwendung eines Tiefpassfilters ("Moving Average-Filter")
- Störunterdrückung des Pulses mittels adaptiven FIR-Filter

Wie bereits erwähnt, hat die Verwendung eines TP-Filters den Nachteil, dass dabei möglicherweise relevante Signalkomponenten des NIRS-Signals ebenfalls teilweise eliminiert werden. Dieser Nachteil wird durch die Verwendung der adaptiven Störunterdrückung vermieden, womit diese Methode für zukünftige Anwendungen in oBCI-Systemen zu bevorzugen ist.

**Atmungs- und Blutdruckschwankungen:** Für die Elimination der beiden Störungen können die selben Signalverarbeitungsansätze verwendet werden.

- Verwendung antagonistischer Muster
- Common Average Referenz-Filter (CAR)

Wie in Kapitel 4.3 beschrieben, bringt die Verwendung von antagonistischen Mustern den Vorteil, dass eine Elimination der Störeinflüsse nicht notwendig ist. Leider treten diese Verläufe nicht bei allen Task-spezifischen hämodynamischen Aktivierungen auf. Grundsätzlich wird daher für die Realtime-Elimination der Einflüsse die Implementierung eines CAR-Filters empfohlen.

## 5.2 Veröffentlichungen im Rahmen des Projektes

Auf die Unterstützung durch das Land Steiermark wurde in folgenden Arbeiten und Präsentationen hingewiesen:

# Journal Artikel

### 2012

G. Pfurtscheller, G. Bauernfeind, C. Neuper and F. H. Lopes da Silva. Does conscious intention to perform a motor act depend on slow prefrontal (de)oxyhemoglobin oscillations in the resting brain? *Neurosci Lett*, 508(2):89-94, 2012.

### 2011

G. Bauernfeind, R. Scherer, G. Pfurtscheller and C. Neuper. Single-trial classification of antagonistic oxyhemoglobin responses during mental arithmetic. *Med Biol Eng Comput*, 49(9):979-984, 2011.

G. Bauernfeind,V. Kaiser, T. Kaufmann, A. Kreilinger, A. Kübler and C. Neuper. Cortical effects of BCI training measured with fNIRS. *Int J Bioelectromag*, 13:66-67, 2011.

G. Pfurtscheller, D. Klobassa, C. Altstätter,G. Bauernfeind and C. Neuper. About the stability of phase-shifts between slow oscillations around 0.1 Hz in cardiovascular and cerebral systems. *IEEE Trans Biomed Eng*, 58(7):2064-2071, 2011.

G. Pfurtscheller, D. Klobassa, G. Bauernfeind and C. Neuper. Cardiovascular responses after brisk finger movement and their dependency on the "eigenfrequency" of the baroreflex loop. *Neurosci Lett*, 490(1):31-35, 2011.

### 2010

G. Pfurtscheller, G. Bauernfeind, S. C. Wriessnegger and C. Neuper C. Focal frontal (de)oxyhemoglobin responses during simple arithmetic. *Int J Psychophysiol*, 76(3):186-92, 2010.

G. Pfurtscheller, B. Z. Allison, G. Bauernfeind, C. Brunner, S. Solis Escalante, R. Scherer, T. O. Zander, G. R. Müller-Putz, C. Neuper and N. Birbaumer. The hybrid BCI *Front Neurosci*, 4:42, 2010.

## Proceedings

### 2012

G. Bauernfeind, I. Daly and G.R. Müller-Putz. On the removal of physiolgical artifacts from fNIRS. *Proceedings of the 3$^{rd}$ TOBI Workshop 2012*, 2012.

### 2011

G. Bauernfeind, R. Scherer, G. Pfurtscheller and C. Neuper. Classication of Focal Frontal Oxyhemoglobin Responses During Mental Arithmetic. *Proceedings of the 5$^{th}$ International Brain-Computer Interface Conference 2011*, 264-267, 2011.

G. Pfurtscheller, G. Bauernfeind and C. Neuper. Slow Phase-related Oscillations of Prefrontal (De)oxyhemoglobin and Central EEG Alpha and Beta Power in the Resting Brain. *Proceedings of the 5$^{th}$ International Brain-Computer Interface Conference 2011*, 340-342, 2011.

### 2010

G. Bauernfeind, S. C. Wriessnegger, G. Pfurtscheller and C. Neuper. Fokale frontale (De)oxyhämoglobin-änderung während einfacher arithmetischer Aufgaben: Anmerkungen zur Verwendung als Steuersignale für optische Gehirn-Computer-Interface (oBCI)-Anwendungen. *Kongress 5 Jahre INGE St.*, 30-30, 2010.

G. Bauernfeind, K. Schweizer, S. C. Wriessnegger, S. Kober, G. Pfurtscheller and C. Neuper. Neural correlates of the execution and inhibition of well learned foot and finger movements: an NIRS study. *Proceedings of the 1$^{st}$ TOBI Workshop 2010*, 38-38, 2010.

## Poster und Vorträge

### 2012

G. Bauernfeind, I. Daly and G.R. Müller-Putz. On the removal of physiolgical artifacts from fNIRS. *3$^{rd}$ TOBI Workshop 2012*. Würzburg, 21.03.2012 [Vortrag]

### 2011

G. Bauernfeind, R. Scherer, G. Pfurtscheller and C. Neuper. Classication of Focal Frontal Oxyhemoglobin Responses During Mental Arithmetic. *5$^{th}$ International Brain-Computer Interface Conference 2011*. Graz, 23.09.2011

[Poster]

G. Pfurtscheller, G. Bauernfeind and C. Neuper. Slow Phase-related Oscillations of Prefrontal (De)oxyhemoglobin and Central EEG Alpha and Beta Power in the Resting Brain. *5th International Brain-Computer Interface Conference 2011*. Graz, 23.09.2011 [Vortrag]

## 2010

G. Bauernfeind, V. Kaiser, T. Kaufmann, A. Kreilinger, A. Kübler and C. Neuper. Cortical effects of BCI training measured with fNIRS. *2nd TOBI Workshop 2010*. Rom, 02.12.2010 [Poster]

G. Bauernfeind, R. Scherer, S. C. Wriessnegger, G. Pfurtscheller and C. Neuper. Single trial classification of focal frontal (de)oxyhemoglobin responses during simple arithmetic. *Kongress 5 Jahre INGE St.* Graz, 07.10.2010 [Poster]

G. Bauernfeind. Hybrid BCIs (NIRS and SSVEP) and BCIs based on other non-motor tasks. *4th International BCI Meeting: Workshop for Novel BCI Designs*. Asilomar CA, 02.06.2010 [Vortrag]

G. Bauernfeind, S. C. Wriessnegger, G. Pfurtscheller and C. Neuper. Investigation of hemodynamic responses during simple arithmetic. Annotations for the use as control signal for optical brain-computer interface (oBCI) applications. *4th International BCI Meeting 2010*. Asilomar CA, 31.05.2010 [Vortrag]

G. Bauernfeind, K. Schweizer, S. C. Wriessnegger, S. Kober, G. Pfurtscheller and C. Neuper. Neural correlates of the execution and inhibition of well learned foot and finger movements: an NIRS study. *1st TOBI Workshop 2010*. Graz, 03.02.2010 [Poster]

Der Förderungswerber erklärt sich mit einer Begutachtung des Antrags - bzw. bei Genehmigung in weiterer Folge der vorzulegenden Berichte - durch einen externen Experten einverstanden.

Der Förderungswerber bestätigt mit seiner Unterschrift die Richtigkeit und Vollständigkeit sämtlicher Angaben.

Graz, 19.03.2012
Ort, Datum

Technische Universität Graz
Institut für Semantische Datenanalyse
Kopernikusgasse 37
A-8010 Graz

Stampiglie und Unterschrift der Projektleitung

# Literaturverzeichnis


[1] G. Bauernfeind. *Entwicklung eines Nah-Infrarot-Spektroskopie-Systems für die Verwendung als optisches Brain-Computer Interface*. PhD thesis, Graz University of Technology, Austria, 2006.

[2] G. Bauernfeind. *Nah-Infrarot-Spektroskopie am Menschen*. VDM Verlag, 2008.

[3] G. Bauernfeind, I. Daly, and G. R. Müller-Putz. On the removal of physiolgical artifacts from fnirs. *Proceedings of the 3rd TOBI Workshop 2012*, 2012 (in press).

[4] G. Bauernfeind, V. Kaiser, T. Kaufmann, A. Kreilinger, A. Kübler, and C. Neuper. Cortical effects of bci training measured with fnirs. *Int J Bioelect*, 13(2):66–67, 2011.

[5] G. Bauernfeind, R. Leeb, C. Neuper, and G. Pfurtscheller. Reducing the blood pressure influence on characteristic hemodynamic responses: a preliminary NIRS study. *Proceedings of the 4th International Brain-Computer Interface Workshop and Training Course*, pages 309–314, 2008.

[6] G. Bauernfeind, R. Leeb, S. Wriessnegger, and G. Pfurtscheller. Development, set-up and first results of a one-channel near-infrared spectroscopy system. *Biomed Tech (Berl)*, 53(1):36–43, 2008.

[7] G. Bauernfeind, R. Scherer, G. Pfurtscheller, and C. Neuper. Single trial classification of antagonistic oxyhemoglobin responses during mental arithmetic. *Med Biol Eng Comput*, 49(9):979–984, 2011.

[8] T. S. Bearden, J. E. Cassisi, and M. Pineda. Neurofeedback training for a patient with thalamic and cortical infarctions. *Appl Psychophysiol Biofeedback*, 28(3):241–253, 2003.

[9] J. Belda-Lois, S. M. Horno, I. Bermejo-Bosch, J. C. Moreno, J. L. Pons, D. Farina, M. Iosa, M. Molinari, F. Tamburella, A. Ramos, A. Caria, T. Solis-Escalante, C. Brunner, and M. Rea. Rehabilitation of gait after stroke: a review towards a top-down approach. *J NeuroEng Rehab*, 8(66), 2011.

[10] A. Belouchrani, K. Abed-Meraim, J. Cardoso, and E. Moulines. A blind source seperation technique using second-order statistics. *IEEE Trans Sig Proc*, 45(2):434–444, 1997.

[11] N. Birbaumer. Breaking the silence: brain-computer interfaces (BCI) for communication and motor control. *Psychophysiology*, 43(6):517–532, 2006.

[12] N. Birbaumer, C. Weber, C. Neuper, E. Buch, K. Haapen, and L. Cohen. Physiological regulation of thinking: brain-computer interface (BCI) research. *Prog Brain Res*, 159:369–391, 2006.

[13] W. N. Colier, V. Quaresima, R. Wenzel, M. C. van der Sluijs, B. Oeseburg, M. Ferrari, and A. Villringer. Simultaneous near-infrared spectroscopy monitoring of left and right occipital areas reveals contralateral hemodynamic changes upon hemi-field paradigm. *Vision Res*, 41(1):97–102, 2001.

[14] S. Coyle, T. Ward, and C. Markham. Physiological noise in near-infrared spectroscopy: implications for optical brain computer interfacing. *Engineering in Medicine and Biology Society, 2004. IEMBS '04. 26th Annual International Conference of the IEEE*, 6:4540–4543, 2004.

[15] S. Coyle, T. E. Ward, C. Markham, and G. McDarby. On the suitability of near-infrared (NIR) systems for next-generation brain-computer interfaces. *Physiol Meas*, 25(4):815–822, 2004.

[16] S. Coyle, T. E. Ward, and C. M. Markham. Brain-computer interface using a simplified functional near-infrared spectroscopy system. *J Neural Eng*, 4(3):219–226, 2007.

[17] T. Egner and M. B. Sterman. Neurofeedback treatment of epilepsy: from basic rationale to practical application. *Expert Rev Neurother*, 6(2):247–257, 2006.

[18] C. E. Elwell, R. Springett, and E. Hillman. Oscillations in cerebral haemodynamics - Implications for functional activation studies. *Adv Exp Med Biol*, 471:57–65, 1999.

[19] G. Florian, A. Stancak, and G. Pfurtscheller. Cardiac response induced by voluntary self-paced finger movement. *Int J Psychophysiol*, 28(3):273–283, 1998.

[20] D. J. Fox, D. F. Tharp, and L. C. Fox. Neurofeedback: an alternative and efficacious treatment for Attention Deficit Hyperactivity Disorder. *Appl Psychophysiol Biofeedback*, 30(4):365–373, 2005.

[21] M. A. Franceschini, S. Fantini, J.H. Thompson, J.P. Culver, and D.A. Boas. Hemodynamic evoked response of the sensorimotor cortex measured noninvasively with near-infrared optical imaging. *Psychophysiology*, 40(4):548–560, 2003.

[22] M. J. Herrmann, A. C. Ehlis, P. Scheuerpflug, and A. J. Fallgatter. Optical topography with near-infrared spectroscopy during a verbal-fluency task. *Psychophysiology*, 19(2):100–105, 2005.

[23] M. J. Herrmann, A. C. Ehlis, A. Wagener, C. P. Jacob, and A. J. Fallgatter. Near-infrared optical topography to assess activation of the parietal cortex during a visuo-spatial task. *Neuropsychologia*, 43(12):51713–1720, 2005.

[24] M. J. Herrmann, T. Huter, M. M. Plichta, A. C. Ehlis, G. W. Alpers, A. Mhlberger, and A. J. Fallgatter. Enhancement of activity of the primary visual cortex during processing of emotional stimuli as measured with event-related functional near-infrared spectroscopy and event-related potentials. *Hum Brain Mapp*, 29(1):28–35, 2008.

[25] C. Hirth, H. Obrigand K. Villringer, A. Thiel, J. Bernarding, W. Muhlnickel, H. Flor, U. Dirnagl, and A. Villringer. Non-invasive functional mapping of the human motor cortex using near-infrared spectroscopy. *Neuroreport*, 7(12):1977–1981, 1996.

[26] M. J. Hofmann, M. J. Herrmann, I. Dan, H. Obrig, M. Conrad, L. Kuchinke, A. M. Jacobs, and A. J. Fallgatter. Differential activation of frontal and parietal regions during visual word recognition: an optical topography study. *Neuroimage*, 40(3):1340–1349, 2008.

[27] Y. Hoshi and M. Tamura. Detection of dynamic changes in cerebral oxygenation coupled to neuronal function during mental work in man. *Neurosci Lett*, 150(1):5–8, 1993.

[28] F. Hummel, R. Saur, S. Lasogga, C. Plewnia, M. Erb, D. Wildgruber, W. Grodd, and C. Gerloff. To act or not to act. Neural correlates of

executive control of learned motor behavior. *Neuroimage*, 23(4):1391–1401, 2004.

[29] V. Kaiser, G. Bauernfeind, T. Kaufmann, A. Kreilinger, A. Kbler, and C. Neuper. Cortical effects of user learning in a motor-imagery bci training. *Int J Bioelect*, 13(2):60–61, 2011.

[30] H. P. Koepchen. Physiology of rhythms and control systems: An integrative approach. In H. Haken and H.P. Koepchen, editors, *Rhythms in physiological systems: In integrative approach*, pages 3–20. Springer, 1991.

[31] U. Leins, G. Goth, T. Hinterberger, C. Klinger, N. Rumpf, and U. Strehl. Neurofeedback for children with ADHD: a comparison of SCP and Theta/Beta protocols. *Appl Psychophysiol Biofeedback*, 32(2):73–88, 2007.

[32] W. Lutzenberger, T. Elbert, B. Rockstroh, and N. Birbaumer. Biofeedback of slow cortical potentials. II. Analysis of single event-related slow potentials by time series analysis. *Electroencephalogr Clin Neurophysiol*, 48(3):302–311, 1980.

[33] C. Neuper, G. R. Müller-Putz, R. Scherer, and G. Pfurtscheller. Motor imagery and EEG-based control of spelling devices and neuroprostheses. In C. Neuper and W. Klimesch, editors, *Event-related dynamics of brain oscillations*. Elsevier, 2006.

[34] G. Pfurtscheller, , C. Neuper, G. R. Müller, B. Obermaier, G. Krausz, A. Schlögl, R. Scherer, B. Graimann, C. Keinrath, D. Skliris, M Wörtz, G. Supp, and C. Schrank. Graz-BCI: state of the art and clinical applications. *IEEE Trans Neural Syst Rehabil Eng*, 11(2):177–180, 2003.

[35] G. Pfurtscheller, B. Z. Allison, G. Bauernfeind, C. Brunner, S. Solis Escalante, R. Scherer, T. O. Zander, G. R. Müller-Putz, C. Neuper, and N. Birbaumer. The hybrid BCI. *Front Neurosci*, 4:42, 2010.

[36] G. Pfurtscheller, G. Bauernfeind, C. Neuper, and F. H. Lopes da Silva. Does conscious intention to perform a motor act depend on slow prefrontal (de)oxyhemoglobin oscillations in the resting brain? *Neurosci Lett*, 508(2):89–94, 2012.

[37] G. Pfurtscheller, G. Bauernfeind, S. C. Wriessnegger, and C. Neuper. Focal frontal (de)oxyhemoglobin responses during simple arithmetic. *Int J Psychophysiol*, 76(3):186–192, 2010.

[38] G. Pfurtscheller, C. Guger, G. Müller, G. Krausz, and C. Neuper. Brain oscillations control hand orthosis in a tetraplegic. *Neurosci Lett*, 292(3):211–214, 2000.

[39] G. Pfurtscheller, D. Klobassa, C. Altstätter, G. Bauernfeind, and C. Neuper. About the stability of phase-shifts between slow oscillations around 0.1 hz in cardiovascular and cerebral systems. *IEEE Trans Biomed Eng*, 58(7):2064–2071, 2011.

[40] G. Pfurtscheller, D. Klobassa, G. Bauernfeind, and C. Neuper. Cardiovascular responses after brisk finger movement and their dependency on the "eigenfrequency" of the baroreflex loop. *Neurosci Lett*, 490(1):31–35, 2011.

[41] G. Pfurtscheller, G. R. Müller-Putz, A. Schlögl, B. Graimann, R. Scherer, R. Leeb, C. Brunner, C. Keinrath, F. Y. Lee, G. Townsend, C. Vidaurre, and C. Neuper. 15 years of BCI research at Graz University of Technology: current trends. *IEEE Trans Neural Syst Rehabil Eng*, 14:205–210, 2006.

[42] J. P. Rosenfeld, A. P. Rudell, and S. S. Fox. Operant control of neural events in humans. *Science*, 165(895):821–823, 1969.

[43] M. L. Schroeter, S. Zysset, T. Kupka, F. Kruggel, and D. Yves von Cramon. Near-infrared spectroscopy can detect brain activity during a colorword matching Stroop task in an event-related design. *Human Brain Map*, 17:61–71, 2002.

[44] J. E. Walker and G. P. Kozlowski. Neurofeedback treatment of epilepsy. *Child Adolesc Psychiatr Clin N Am*, 14(1):163–176, 2005.

[45] N. Weiskopf. Real-time fMRI and its application to neurofeedback. *Neuroimage*, 2011 (in press).

[46] N. Weiskopf, R. Veit, M. Erb, K. Mathiak, W. Grodd, R. Goebel, and N. Birbaumer. Physiological self-regulation of regional brain activity using real-time functional magnetic resonance imaging (fMRI): methodology and exemplary data. *Neuroimage*, 19(3):577–586, 2003.

[47] K. Wing. Effect of neurofeedback on motor recovery of a patient with brain injury: a case study and its implications for stroke rehabilitation. *Top Stroke Rehabil*, 8(3):45–53, 2001.

[48] M. Wolf, U. Wolf, V. Toronov, A. Michalos, A. L. Paunescu, J. Choi, and E. Gratton. Different time evaluation of oxyhämoglobin and deoxyhämoglobin concentration changes in visual and motor cortices during functional stimulation: A near-infrared spectroscopy study. *Neuroimage*, 16:704–712, 2002.

[49] S. C. Wriessnegger, J. Kurzmann, and C. Neuper. Spatio-temporal differences in brain oxygenation between movement execution and imagery: a multichannel near-infrared spectroscopy study. *Int J Psychophysiol*, 67(1):54–63, 2008.

# Anhang A

## Journal Artikel

## Proceedings

## Poster

Neuroscience Letters 508 (2012) 89–94

Contents lists available at SciVerse ScienceDirect

Neuroscience Letters

journal homepage: www.elsevier.com/locate/neulet

# Does conscious intention to perform a motor act depend on slow prefrontal (de)oxyhemoglobin oscillations in the resting brain?

Gert Pfurtscheller[a,*], Günther Bauernfeind[a], Christa Neuper[a,b], Fernando H. Lopes da Silva[c]

[a] Laboratory of Brain-Computer Interfaces, Institute for Knowledge Discovery, Graz University of Technology, A-8010 Graz, Austria
[b] Department of Psychology, University of Graz, A-8010 Graz, Austria
[c] Center for NeuroScience, Swammerdam Institute for Life Sciences, University of Amsterdam, 1098 SM Amsterdam, The Netherlands

ARTICLE INFO

*Article history:*
Received 10 October 2011
Received in revised form 5 December 2011
Accepted 14 December 2011

*Keywords:*
Blood pressure oscillations
(De)oxyhemoglobin oscillations
EEG oscillations
Resting brain
Voluntary movement

ABSTRACT

Characteristically within the resting brain there are slow fluctuations (around 0.1 Hz) of EEG and NIRS-(de)oxyhemoglobin ([deoxy-Hb], [oxy-Hb]) signals. An interesting question is whether such slow oscillations can be related to the intention to perform a motor act. To obtain an answer we analyzed continuous blood pressure (BP), heart rate (HR), prefrontal [oxy-Hb], [deoxy-Hb] and EEG signals over sensorimotor areas in 10 healthy subjects during 5 min of rest and during 10 min of voluntary finger movements. Analyses of prefrontal [oxy-Hb]/[deoxy-Hb] oscillations around 0.1 Hz and central EEG band power changes in the beta (alpha) band revealed that the positive [oxy-Hb] peaks preceded the central EEG beta (alpha) power peak by $3.6 \pm 0.9$ s in the majority of subjects. A similar relationship between prefrontal [oxy-Hb] and central EEG beta power was found during voluntary movements whereby the post movement beta power increase (beta rebound) is known to coexist with a decreased excitability of cortico-spinal neurons. Therefore, we speculate that the beta power increase ~3 s after slow fluctuating [oxy-Hb] peaks during rest is indicative for a slow excitability change of central motor cortex neurons. This work provides the first evidence that initiation of finger movements at free will in relatively constant intervals around 10 s could be temporally related to slow oscillations of prefrontal [oxy-Hb] and autonomic blood pressure in the resting brain.



## 1. Introduction

Large-scale infra-slow oscillations at frequencies ranging from 0.02 to 0.2 Hz were detected in electrocorticogram measures of cat [27] and human [1,28] EEG, using full-band recordings. In addition, oscillations around 0.1 Hz were also observed in cerebral (de)oxyhemoglobin ([deoxy-Hb], [oxy-Hb]) and cerebral blood flow velocity [10,19,31]. These slow oscillations may be related to the fluctuations observed in the time course of other physiological signals, such as in fMRI BOLD signals [13,14] and appear to condition neuronal responses evoked by external stimuli and can account for the variability of the latter [2,3]. The intriguing possibility that these slow oscillations may influence brain responses and other brain activities seems increasingly likely. Monto et al. [16] showed that the ability of a subject to detect somatosensory stimuli was correlated with the phase, but not with the amplitude, of slow EEG oscillations. From these experimental observations, it may be hypothesized that these slow oscillations reflect the excitability dynamics of cortical networks.

Recently we tried to give an answer to the question: "Does conscious intention to perform a motor act depend on slow cardiovascular rhythms?" [21]. In detail the onset of brisk, self-paced finger movement was studied in relationship to the slope of slow oscillations around 0.1 Hz in blood pressure (BP) and heart rate (HR) intervals. Nine out of 22 healthy subjects performed self-paced movements in relatively periodic intervals of around 10 s at the decreasing slope of the slow 0.1-Hz BP oscillation. In the other subjects the intervals between movements were either random or strongly synchronized with their respiration. To search further for the reason for these periodic initiations of movements at free will in intervals of around 10 s, we studied the phase-coupling between slow prefrontal [deoxy-Hb] and [oxy-Hb] oscillations in the resting brain and their coupling to slow Rolandic EEG fluctuations. Such a phase-coupling between prefrontal [deoxy-Hb] and [oxy-Hb] (squared coherence >0.4) was found in 10 subjects. We therefore hypothesized that slow hemodynamic oscillations in the prefrontal cortex during rest can be related to slow EEG fluctuations recorded from cortical motor areas. The latter may be apparent through changes in the power of central EEG alpha and/or beta rhythms.

* Corresponding author at: Laboratory of Brain-Computer Interfaces, Institute for Knowledge Discovery, Graz University of Technology, Krenngasse 37, A-8010 Graz, Austria. Tel.: +43 316 873 5301; fax: +43 316 873 5349.
*E-mail address:* pfurtscheller@tugraz.at (G. Pfurtscheller).

0304-3940/$ – see front matter © 2012 Elsevier Ireland Ltd. All rights reserved.
doi:10.1016/j.neulet.2011.12.025

## 2. Material and methods

We measured prefrontal [oxy-Hb] and [deoxy-Hb] with a custom made one-channel, continuous wave method-based NIRS system (for details see [4]) during 5 min of rest and 10 min of voluntary finger movements along with general physiological variables such as BP, respiration and HR. Subjects were instructed to perform voluntary, brisk finger movements (self-paced at free will) within a period of 10 min. No other instruction was given. Each subject's right index finger rested on a micro switch with a defined pressure point. A sloping edge in the recorded signal corresponded to a movement onset; similarly a rising edge was synchronous to the offset. The sources and the detector for the NIRS-recording were placed over the frontal cortex 1.5 cm to the left and right of position FP1 according to the international 10/20 system for EEG recording (for details see [21]). A fifth-order Butterworth filter with a cut-off frequency of 0.9 Hz was used to remove variability due to the cardiac cycle. In addition we recoded three EEG signals (0.5–100 Hz) bipolarly over the sensorimotor cortex (electrodes were placed 2.5 cm anterior and posterior to C3, Cz and C4) using a biosignal amplifier (g.BSamp, g.tec medical engineering GmbH, Austria). All of signals were sampled at a frequency of 500 Hz. Ten healthy subjects (seven male, three female) aged 20–31 years ($M$ = 23.9, SD = 3.2) were investigated, all of whom had slow oscillations around 0.1 Hz in [oxy-Hb] and [deoxy-Hb] signals in the resting brain.

Beat-to-beat intervals (RRI) in the ECG signal and the intervals of diastolic BP (BPdia), were linearly interpolated, resampled at 2 Hz, and displayed as a time series. Cross-spectra were calculated for [oxy-Hb] and [deoxy-Hb] signals resampled at 2 Hz. The spectral values of 1024 samples were smoothed using a 31-point triangular window (for details see [21]). After an automatic search for the largest peak (dominant frequency (DF)) in the cross-spectrum in the range 0.07–0.13 Hz, the corresponding coherence ($COH^2$) and phase-shift (PHA) values were determined.

### 2.1. EEG processing and calculation of time-frequency maps during movement

Time-frequency maps were calculated from the voluntary movement session. Trials of 12 s duration (6 s before and 6 s after movement onset) were analyzed and the event-related desynchronisation (ERD) and event-related synchronization (ERS) quantified [20]. The reference interval was chosen from −1.5 to −0.5 s before movement onset. These maps were used to search for subject-specific, most reactive frequency bands of alpha or beta oscillations in the movement task. Two patterns are apparent. In the alpha band the power starts to decrease (ERD) ∼2 s prior to movement onset; in the beta band, the power displays a short-lasting increase (beta rebound, beta ERS) after termination of movement. The EEG channel with the most reactive frequency band (either alpha or beta band) found in the movement session was used for the calculation of the EEG band power time course during rest (see Table 1) and movement. The recorded EEG signals were band pass filtered (fourth-order Butterworth filter) using the most-reactive frequency bands (see Table 1) and, the samples squared and averaged over epochs of 5 s. The epochs were overlapped by 0.5 s. This resulted in an alpha (beta) power time series sampled at 2 Hz.

### 2.2. [Oxy-Hb] peak-triggered averaging during rest

For the physiological signals recorded during rest no triggers were available. Fortunately in many subjects the [oxy-Hb] signal displayed clear oscillations through some seconds with peaks at intervals of ∼10 s. Therefore we introduced the following procedure to search for [oxy-Hb] peaks and generate triggers for the data processing during rest. This included the following processing steps:

1) Searching for a segment with stable [oxy-Hb] oscillations and at least 10 clear [oxy-Hb] peaks with inter-peak-intervals of >7 s and <13 s.
2) Marking each positive [oxy-Hb] peak in the selected segment (trigger setting). Examples are shown in Fig. 1.
3) Calculating averages of [oxy-Hb], [deoxy-Hb], EEG band power, BP and RRI by using [oxy-Hb]-triggerred 12 s epochs with 6 s prior to the trigger. Before averaging, the mean of each trial was subtracted from the individual samples.
4) Searching for the minimum and maximum in the averaged EEG power curve and the maximum of the averaged [deoxy-Hb] that were temporally closest to the [oxy-Hb] peak. The time shift of the EEG power minimum close to the [oxy-Hb] peak was named "Es", the time shift of the EEG power maximum and [oxy-Hb] peak "Fs" and the time shift between consecutive [oxy-Hb] and [deoxy-Hb] peaks "Hs" (for an example, see Fig. 2).
5) Determining the mean period of the oscillations around 0.1-Hz (DFp) out of the cross spectrum: DFp = 1/DF.
6) Estimating the *prefrontal activity time* (PAT) in seconds: PAT = DFp/2 + Es–Hs (see Table 1; last column). This is the time between the prefrontal [deoxy-Hb] wave minimum and the following minimum in the EEG band power time course (this corresponds to a maximal ERD) in sensorimotor areas.

## 3. Results

During 5 min of rest the [oxy-Hb]/[deoxy-Hb] exhibited slow oscillations which were not stationary in all subjects. In most of the subjects relatively stable patterns were present for periods of only ∼100 s, whereby the frequency of the oscillations could differ between [oxy-Hb] and [deoxy-Hb] during a given period. Examples of 2 such characteristic subjects with non-stationary patterns are shown in Fig. 1. In one subject [oxy-Hb] displayed oscillations at ∼0.12 Hz, in the first 100 s, while [deoxy-Hb] within the same time period displayed irregular fluctuations around 0.05 Hz. Later, both [oxy-Hb] and [deoxy-Hb] oscillated at ∼0.09 Hz (Fig. 1a). In another subject (Fig. 1b), in-phase [oxy-Hb]/[deoxy-Hb] oscillations at 0.12 Hz were present for ∼100 s. The mean phase shifts calculated over 5 min during rest, together with the dominant frequencies from all 10 subjects, are summarized in Table 1.

The phase shifts between [oxy-Hb] and [deoxy-Hb] oscillations during rest and during voluntary movement were very similar but revealed a trend to smaller phase shifts (mean ± SD over all subjects; rest: $-60.30^\circ \pm 62.47$; voluntary movement: $-45.20^\circ \pm 63.26$) in the movement condition. This may be explained by the superposition of spontaneous and induced [oxy-Hb]/[deoxy-Hb] changes in the movement task. The latter are the result of afferent activity through muscle activation that travels to the brain and generates not only HR and BP but also [oxy-Hb]/[deoxy-Hb] responses.

### 3.1. [Oxy-Hb] peak-triggered averages of hemodynamic and EEG signals

Ten to fourteen consecutive positive [oxy-Hb] peaks were found in all subjects. We selected these peaks (marked by small circles in Fig. 1) as triggers in order to compute triggered-averages of all physiological variables. The results of [oxy-Hb]-triggered averages of [oxy-Hb], [deoxy-Hb] and EEG band power are displayed in Fig. 2. The [oxy-Hb] peak-triggered-averages revealed a significant ($p < 0.05$, paired $t$-test) central EEG band power change in 7 subjects (the EEG frequency bands analyzed are indicated in Table 1). The

**Table 1**
EEG electrode location, frequency band, dominant frequency, phase-shift and squared coherence of [oxy-Hb]/[deoxy-Hb] oscillations (left side) and characteristic features obtained from [oxy-Hb] peak-triggered [deoxy-Hb] and EEG power averages (right side) during 5 min of rest.

| N10 | EEG | | Coupling [oxy-Hb] vs [deoxy-Hb] during 5 min rest | | | | | [Oxy-Hb] triggered averages during rest | | | | | |
|---|---|---|---|---|---|---|---|---|---|---|---|---|---|
| | Electrode/ frequency | | DF | Period DFp | Phase shift | | $COH^2$ | No peaks/segment | | EEG min Es | EEG max FS | Deoxy Hs | PAT |
| | | Hz | Hz | s | grad | s | | | s | s | s | s | s |
| S1 | c3 | 16–28 | 0.125 | 8.00 | −201 | −4.47 | 0.63 | 13 | 0–120 | 0.00 | 4.00 | −4.00 | 8.00 |
| S2 | c3 | 15–25 | 0.098 | 10.20 | −101 | −2.86 | 0.64 | 10 | 150–250 | −1.50 | 3.00 | −3.00 | 6.60 |
| S3 | c3 | 13–20 | 0.109 | 9.17 | −95 | −2.42 | 0.40 | 13 | 50–150 | 0.50 | 3.50 | −1.50 | 6.59 |
| S4 | c3 | 18–29 | 0.088 | 11.36 | −80 | −2.53 | 0.69 | 13 | 150–300 | −2.50 | 2.50 | −2.00 | 5.18 |
| S5 | cz | 10–15 | 0.109 | 9.17 | −67 | −1.71 | 0.55 | 12 | 50–150 | 2.50 | – | −2.00 | 9.09 |
| S6 | c4 | 9–11 | 0.082 | 12.20 | −20 | −0.68 | 0.87 | 11 | 150–290 | – | – | −1.00 | – |
| S7 | cz | 10–14 | 0.084 | 11.90 | −18 | −0.60 | 0.70 | 13 | 130–280 | −1.50 | 3.50 | −1.00 | 5.45 |
| S8 | c3 | 8–13 | 0.113 | 8.85 | −14 | −0.34 | 0.83 | 11 | 100–200 | – | – | 0 | – |
| S9 | cz | 9–13 | 0.121 | 8.26 | −7 | −0.16 | 0.76 | 14 | 120–260 | – | – | 0 | – |
| S10 | c4 | 9–11 | 0.082 | 12.20 | 0 | 0.00 | 0.66 | 14 | 0–150 | 0.5 | 5.00 | 0 | – |
| Mean | | | 0.10 | 10.13 | −60.30 | −1.58 | 0.67 | 12 | | −0.29 | 3.58 | −1.45 | 6.82 |
| SD | | | 0.02 | 1.66 | 62.47 | 1.47 | 0.14 | 1 | | 1.68 | 0.86 | 1.34 | 1.50 |

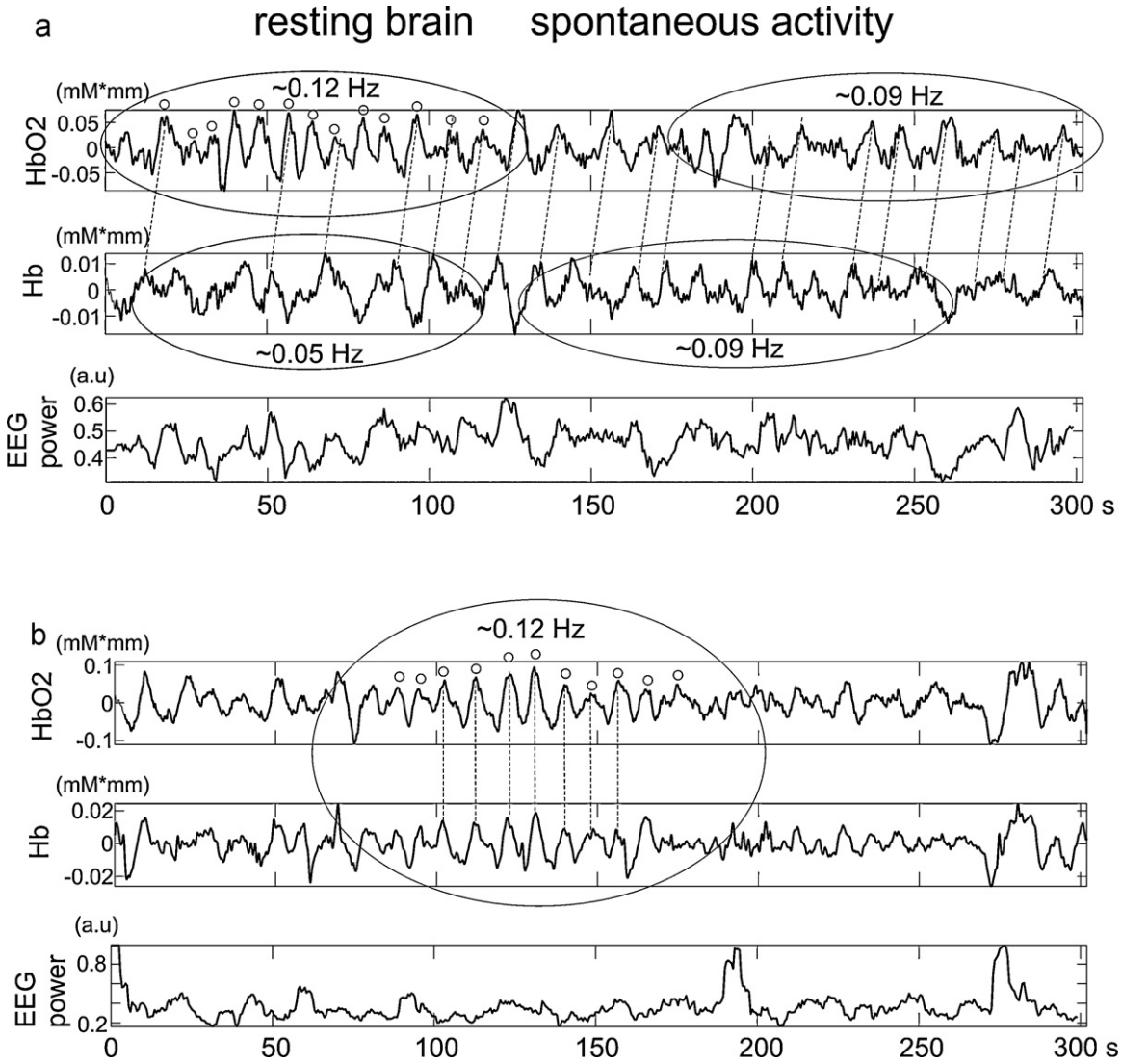


**Fig. 1.** Data from 2 subjects one with a large phase shift (201°) between [oxy-Hb] and [deoxy-Hb] oscillations (a) and one with a small phase shift (14°) (b). [Oxy-Hb] and [deoxy-Hb] changes (in mM mm) and EEG band power recorded during 5 min of rest. The [oxy-Hb] peaks used for averaging are indicated by small circles, and periods of relatively regular [oxy-Hb] ([deoxy-Hb]) oscillations are marked by ellipses.

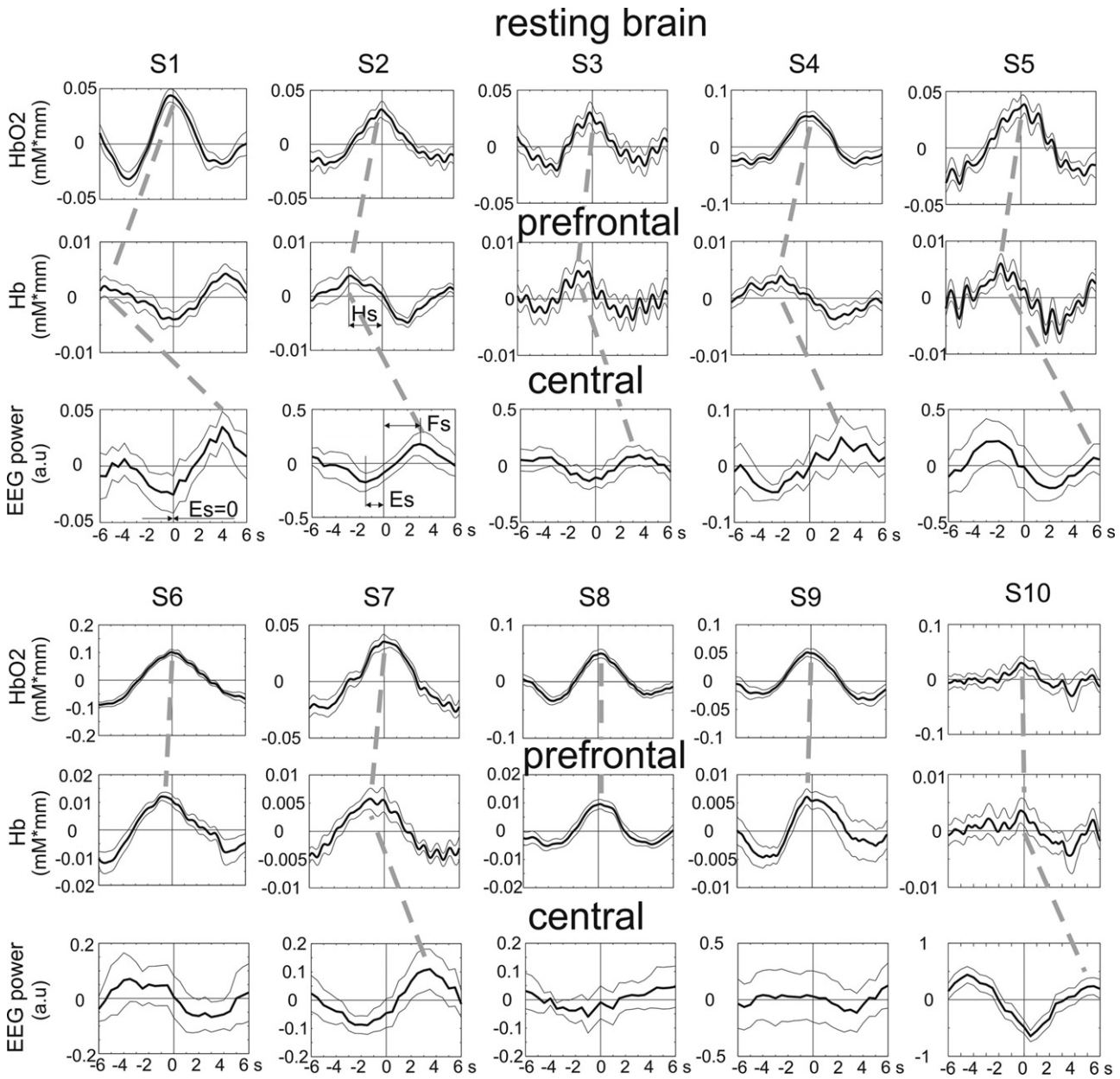


**Fig. 2.** Left side: [oxy-Hb] peak-triggered [oxy-Hb], [deoxy-Hb] and EEG band power changes (mean ± SE) starting 6 s before and ending 6 s after the trigger. Data from 10 subjects. The approximate time relationships (phase shifts) between the [oxy-Hb], [deoxy-Hb] and EEG power peaks in the individual averages are indicated by broken lines. Parameters in (s) extracted from the averaged [oxy-Hb], [deoxy-Hb] and EEG power epochs are indicated.

EEG power maximum occurred at 3.6 ± 0.9 s relative to the [oxy-Hb] peak. The time delay estimated between prefrontal [deoxy-Hb] decrease and following central EEG band power minimum (prefrontal activity time, PAT) was 6.8 ± 1.5 s. In one subject (S10), averaging was performed synchronous to the EEG power minima because no [oxy-Hb] peaks could be detected; in the other 3, no significant, averaged EEG power changes were found. Details about the number of trials used for averaging and the parameters extracted from the averaged [oxy-Hb], [deoxy-Hb] and EEG power epochs are summarized in Table 1.

From the 7 subjects with coupled [oxy-Hb]/[deoxy-Hb] and EEG power oscillations during rest, 5 performed their voluntary movement with relatively constant intervals of ~10 s. In these 5 subjects, the time courses of the averaged EEG band power displayed a great similarity in the case of the [oxy-Hb] peaks-triggered EEG during rest and the movement-triggered EEG. In 4 subjects, the beta power increased after the trigger (for a characteristic example see Fig. 3a) and in one subject, the alpha power decreased after the trigger (see Fig. 3b). Of interest are also the similarities in the averaged BP and [oxy-Hb] time courses during rest and movement (examples see Fig. 3a and b). These similarities can be explained by the similar phase coupling between slow cardiovascular and cerebral hemodynamic oscillations observed during rest and in movement session [19].

## 4. Discussion

The coupling between slow prefrontal [oxy-Hb] and central beta (alpha) band power fluctuations can be studied either by averaging of EEG band power epochs synchronous to consecutive [oxy-Hb] peaks and search for the delay between [oxy-Hb] and EEG power peaks or, for example, by using of cross wavelet transform [8], or phase-locking values [25]. We first used the fast and simple averaging method and found in 7 subjects a clear relationship between the

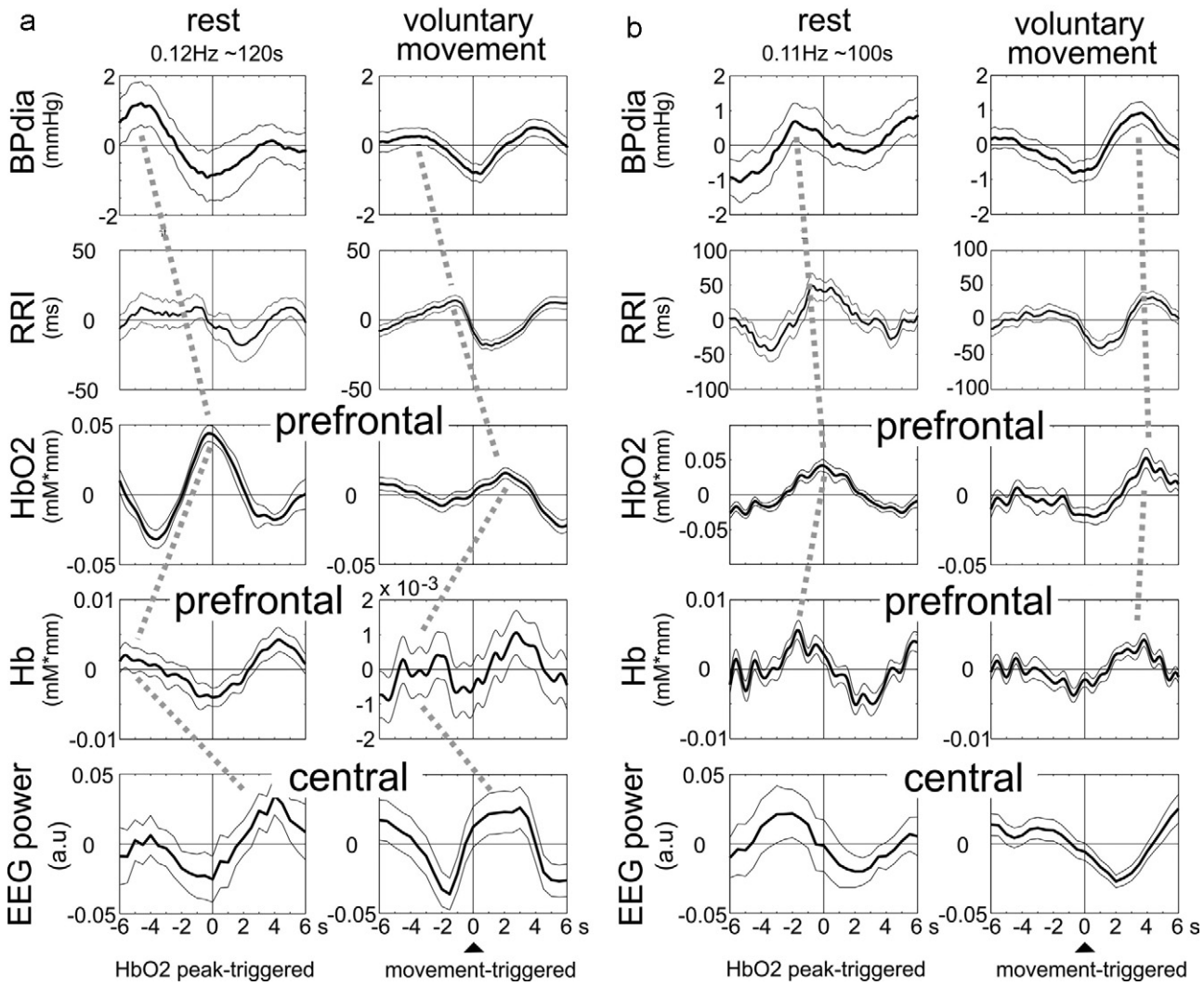


**Fig. 3.** Averages (mean ± SE) of different physiological signals obtained during 5 min of rest and 10 min of voluntary finger movements in 2 characteristic subjects one with changes in beta power (a) and one with changes in alpha power (b). [Oxy-Hb]-triggered averages are displayed (left panels in (a and b)) and movement-triggered averages (right panels). The phase shifts between slow oscillations in BP, RRI, [oxy-Hb] and [deoxy-Hb] are indicated by a stippled line connecting the corresponding peaks. Note the similar phase shifts in the resting brain and during movement.

positive [oxy-Hb] peak and central beta (alpha) power changes in the resting state. In the majority of subjects, a central beta (alpha) power increase was found 3.6 ± 0.9 s (mean ± SD) after the [oxy-Hb] peak during rest. A similar short-lasting beta power increase, known as beta rebound or post movement beta ERS, is characteristic for the termination of a motor act [12,17,18] and was also observed in subjects who initiated voluntary movements in relatively constant intervals of ~10 s (see example in Fig. 3a) For the interpretation of these transient, either beta (alpha) power increase or alpha power decreases, respectively, ~3 s after the [oxy-Hb] peak we have to remember the behavior of mu and central beta oscillations in a movement task. The temporal coexistence of a post-movement beta power increase and an alpha (mu) power decrease is characteristic for the dynamics of different sensorimotor oscillations in a movement task [9,22]. It is therefore not surprising that during rest the [oxy-Hb] peak is related in most subjects to a beta power maximum and in some to an alpha power minimum ~3 s after the [oxy-Hb] peak.

It is generally accepted that the beta rebound reflects a state of active immobilisation [23], or selective deactivation of networks in motor areas [20]. In other words, the change of a large population of neurons in the motor cortex from a state of increased excitability to a state of decreased excitability can be accompanied by the generation of a beta burst. This is confirmed by a transcranial magnetic stimulation (TMS) study showing that during the time period shortly before and during movement the excitability of corticospinal neurons was increased, while it was significantly reduced during the first second after movement-offset [6]. We can speculate therefore, that the cyclic beta power increase ~3 s after slow fluctuating [oxy-Hb] peaks during rest is indicative for a cyclic excitability change of motor cortex neurons.

When we accepted that a decrease in [deoxy-Hb] and an increase in fMRI BOLD signal correlate rather well [5,26] and any prefrontal activation in a motor task precedes the motor cortex activation by some seconds [24], than the latter in form of a mu and/or central beta ERD has to be preceded by a prefrontal [deoxy-Hb] decrease during rest. The estimated PAT of 6.8 ± 1.5 s is comparable with the findings of Soon et al. [24] showing, that the prefrontal fMRI BOLD signal encodes a subject's decision to perform a motor act up to 7 s ahead of time.

Further research is needed into the finding that the phase shift between prefrontal [deoxy-Hb] and [oxy-Hb] oscillations can vary in a broad range from subject to subject, namely between 0° and about 180°. It is not completely clear what the relationship is

between cerebral vasomotion around 0.1 Hz [15] and neurovascular coupling, and the role of cerebral blood volume and cerebral blood flow [30], respectively in the resting brain. Other important future directions include studying longer periods of resting activity and EEG analysis in fixed (e.g. 9–13 Hz and 15–25 Hz) frequency bands. The use of subject-specific bands was a first step to study EEG and (de)oxyhemoglobin fluctuations during rest because data from a movement session were also available.

## 5. Conclusion

The phase coupling between slow BP oscillations (Mayer waves) and prefrontal [oxy-Hb] oscillations [19] and the temporary relationship between prefrontal [oxy-Hb] waves and central EEG beta (alpha) power changes in the resting brain provides the first evidence, that the initiation of a motor act (e.g. voluntary movement, motor imagery) can be related, at least in some subjects under certain circumstances, to slow BP changes. The relationship between cerebral and cardiovascular activities are highly non-stationary [7,11,29] and its therefore understandable that not all subjects can display a coupling between slow changing cerebral and cardiovascular signals during 5 min of rest.

## Acknowledgments

This work was supported by the EU project PRESENCCIA (IST-27731), "Land Steiermark" (project A3-22.N-13/2009-8), the Neuro Center Styria (NCS) and the "Allgemeine Unfallversicherungsanstalt" in Austria. We would like to thank C. Altstätter for help with data processing and I. Daly and B. Allison for proof reading.

## References

[1] P. Achermann, A.A. Borbély, Low-frequency (<1 Hz) oscillations in the human sleep electroencephalogram, Neuroscience 81 (1) (1997) 213–222.
[2] A. Arieli, A. Sterkin, A. Grinvald, A. Aertsen, Dynamics of ongoing activity: explanation of the large variability in evoked cortical responses, Science 273 (5283) (1996) 1868–1871.
[3] R. Azouz, C.M. Gray, Cellular mechanisms contributing to response variability of cortical neurons in vivo, J. Neurosci. 19 (6) (1999) 2209–2223.
[4] G. Bauernfeind, R. Leeb, S.C. Wriessnegger, G. Pfurtscheller, Development, set-up and first results of a one-channel near-infrared spectroscopy system, Biomed. Techn. (Berl.) 53 (1) (2008) 36–43.
[5] R.B. Buxton, K. Uludağ, D.J. Dubowitz, T.T. Liu, Modeling the hemodynamic response to brain activation, Neuroimage 23 (Suppl. 1) (2004) 220–233.
[6] R. Chen, Z. Yaseen, L.G. Cohen, M. Hallett, The time course of corticospinal excitability in reaction time and self-paced movements, Ann. Neurol. 44 (1998) 317–325.
[7] C.A. Giller, M. Mueller, Linearity and non-linearity in cerebral hemodynamics, Med. Eng. Phys. 25 (2003) 633–646.
[8] A. Grinsted, J.C. Moore, S. Jevrejeva, Application of the cross wavelet transform and wavelet coherence to geophysical time series, Nonlinear Proc. Geophys. 11 (2004) 561–566.
[9] J.D. Guieu, J.L. Bourriez, P. Derambure, L. Defebvre, F. Cassim, Temporal and spatial aspects of event-related desynchronization and movement-related cortical potentials, in: G. Pfurtscheller, F.H. Lopes Da Silva (Eds.), Handbook of Electroencephalography and Clinical Neurophysiology, Revised Series 6, Elsevier, Amsterdam, 1999, pp. 279–290.
[10] Y. Hoshi, M. Tamura, Fluctuations in the cerebral oxygenation state during the resting period in functional mapping studies of the human brain, Med. Biol. Eng. Comput. 35 (4) (1997) 328–330.
[11] X. Hu, V. Nenov, T.C. Glenn, L.A. Steiner, M. Czosnyka, M. Bergsneider, N. Martin, Nonlinear analysis of cerebral hemodynamic and intracranial pressure signals for characterization of autoregulation, IEEE Trans. Biomed. Eng. 53 (2) (2006) 195–209.
[12] M.T. Jurkiewicz, W.C. Gaetz, A.C. Bostan, D. Cheyne, Post-movement beta rebound is generated in motor cortex: evidence from neuromagnetic recordings, Neuroimage 32 (3) (2006) 1281–1289.
[13] D.A. Leopold, Y. Murayama, N.K. Logothetis, Very slow activity fluctuations in monkey visual cortex: implications for functional brain imaging, Cereb. Cortex 13 (4) (2003) 422–433.
[14] D. Mantini, M.G. Perrucci, C. Del Gratta, G.L. Romani, M. Corbetta, Electrophysiological signatures of resting state networks in the human brain, Proc. Natl. Acad. Sci. U.S.A. 104 (32) (2007) 13170–13175.
[15] J.E. Mayhew, S. Askew, Y. Zheng, J. Porrill, G.W. Westby, P. Redgrave, D.M. Rector, R.M. Harper, Cerebral vasomotion: a 0. 1-Hz oscillation in reflected light imaging of neural activity, Neuroimage 4 (3 Pt. 1) (1996) 183–193.
[16] S. Monto, S. Palva, J. Voipio, J.M. Palva, Very slow EEG fluctuations predict the dynamics of stimulus detection and oscillation amplitudes in humans, J. Neurosci. 28 (33) (2008) 8268–8272.
[17] C. Neuper, G. Pfurtscheller, Post-movement synchronization of beta rhythms in the EEG over the cortical foot area in man, Neurosci. Lett. 216 (1) (1996) 17–20.
[18] G. Pfurtscheller, A. Stancák Jr., G. Edlinger, On the existence of different types of central beta rhythms below 30 Hz, Electroencephalogr. Clin. Neurophysiol. 102 (4) (1997) 316–325.
[19] G. Pfurtscheller, D.S. Klobassa, C. Altstätter, G. Bauernfeind, C. Neuper, About the stability of phase-shifts between slow oscillations around 0.1 Hz in cardiovascular and cerebral systems, IEEE Trans. Biomed. Eng. 58 (7) (2011) 2064–2071.
[20] G. Pfurtscheller, F. Lopes da Silva, Event-related EEG/MEG synchronization and desynchronization: basic principles, Clin. Neurophys. 110 (1999) 1842–1857.
[21] G. Pfurtscheller, R. Ortner, G. Bauernfeind, P. Linortner, C. Neuper, Does conscious intention to perform a motor act depend on slow cardiovascular rhythms? Neurosci. Lett. 468 (2010) 46–50.
[22] G. Pfurtscheller, A. Stancák Jr., C. Neuper, Post movement beta synchronization: a correlate of an idling motor area? Electroencephalogr. Clin. Neurophys. 98 (1996) 281–293.
[23] R. Salmelin, M. Hämäläinen, M. Kajola, R. Hari, Functional segregation of movement-related rhythmic activity in the human brain, Neuroimage 2 (4) (1995) 237–243.
[24] C.S. Soon, M. Brass, H.J. Heinze, J.D. Haynes, Unconscious determinants of free decisions in the human brain, Nat. Neurosci. 11 (5) (2008) 543–545.
[25] A. Spiegler, B. Graimann, G. Pfurtscheller, Phase coupling between different motor areas during tongue-movement imagery, Neurosci. Lett. 369 (1) (2004) 50–54.
[26] J. Steinbrink, A. Villringer, F. Kempf, D. Haux, S. Boden, H. Obrig, Illuminating the BOLD signal: combined fMRI-fNIRS studies, Magn. Reson. Imaging 24 (4) (2006) 495–505.
[27] M. Steriade, D.A. McCormick, T.J. Sejnowski, Thalamocortical oscillations in the sleeping and aroused brain, Science 262 (5134) (1993) 679–685.
[28] S. Vanhatalo, J.M. Palva, M.D. Holmes, J.W. Miller, J. Voipio, K. Kaila, Infraslow oscillations modulate excitability and interictal epileptic activity in the human cortex during sleep, Proc. Natl. Acad. Sci. U.S.A. 101 (14) (2004) 5053–5057.
[29] C.D. Wagner, P.B. Persson, Chaos in the cardiovascular system: an update, Cardiovasc. Res. 40 (2) (1998) 257–264.
[30] M. Wolf, U. Wolf, V. Toronov, A. Michalos, L.A. Paunescu, J.H. Choi, E. Gratton, Different time evolution of oxyhemoglobin and deoxyhemoglobin concentration changes in the visual and motor cortices during functional stimulation: a near-infrared spectroscopy study, Neuroimage 16 (3 Pt. 1) (2002) 704–712.
[31] R. Zhang, J. Zuckerman, C. Giller, B. Levine, Transfer function analysis of dynamic cerebral autoregulation in humans, Am. J. Physiol. 274 (1 Pt. 2) (1998) H233–H241.

Med Biol Eng Comput
DOI 10.1007/s11517-011-0792-5

ORIGINAL PAPER

# Single-trial classification of antagonistic oxyhemoglobin responses during mental arithmetic

**Günther Bauernfeind · Reinhold Scherer · Gert Pfurtscheller · Christa Neuper**

Received: 22 February 2011 / Accepted: 14 June 2011


**Abstract** Near-infrared spectroscopy (NIRS) is a non-invasive optical technique that can be used for brain–computer interfaces (BCIs) systems. A common challenge for BCIs is a stable and reliable classification of single-trial data, especially for cognitive (mental) tasks. With antagonistic activation pattern, recently found for mental arithmetic (MA) tasks, an improved online classification for optical BCIs using MA should become possible. For this investigation, we used the data of a previous study where we found antagonistic activation patterns (focal bilateral increase of [oxy-Hb] in the dorsolateral prefrontal cortex in parallel with a [oxy-Hb] decrease in the medial area of the anterior prefrontal cortex) in eight subjects. We used the [oxy-Hb] responses to search for the best antagonistic feature combination and compared it to individual features from the same regions. In addition, we investigated the use of antagonistic [deoxy-Hb], total hemoglobin [Hbtot] and pairs of [oxy-Hb] and [deoxy-Hb] features as well as the existence of a group-related feature set. Our results indicate that the use of the antagonistic [oxy-Hb] features significantly increases the classification accuracy from 63.3 to 79.7%. These results support the hypothesis that antagonistic hemodynamic response patterns are a suitable control strategy for optical BCI, and that only two prefrontal NIRS channels are needed for good performance.

G. Bauernfeind (✉) · R. Scherer · G. Pfurtscheller · C. Neuper
Laboratory of Brain-Computer Interfaces, Institute for Knowledge Discovery, Graz University of Technology, Krenngasse 37, 8010 Graz, Austria
e-mail: g.bauernfeind@tugraz.at

C. Neuper
Department of Psychology, University of Graz, Universitätsplatz 2/III, 8010 Graz, Austria

**Keywords** Near-infrared spectroscopy (NIRS) · Single-trial classification · Antagonistic oxyhemoglobin responses · Mental arithmetic · Brain–computer interface (BCI)

## 1 Introduction

Near-infrared spectroscopy (NIRS) is a non-invasive optical technique for the assessment of functional brain activity during cognitive, visual, visuo-motor, and motor tasks (e.g., [5, 7, 8, 10, 17, 25]). Resulting task-specific changes in the metabolic response, i.e., concentration changes of oxy- and deoxyhemoglobin ([oxy-Hb], [deoxy-Hb]), can be used alternatively to [2, 15, 22] or in combination with EEG [16] for brain–computer interfaces systems (optical and hybrid BCIs). The temporal resolution of the hemodynamic response—in the range of several seconds—limits the information transfer rates achievable for BCI-based communication. This can be seen as the major drawback of NIRS-based BCIs. There are, however, several advantages when using NIRS as input signal for non-invasive BCIs compared to the use of the electroencephalogram (EEG). These include no conductive gel required, no influence of electrooculographic artifacts, and most important the sensor placement is more practical and user-friendly and thus better suited for daily applications [3].

The robust single-trial detection of brain activity is one relevant issue for all types of BCIs that are based on classification. The identification of brain patterns that naïve user can reliably generate and that are stable over time may significantly contribute to more accurate discrimination. Previously we investigated changes of [oxy-Hb] and [deoxy-Hb] during a mental arithmetic (MA) task [17]. We found antagonistic activation patterns in eight out of ten

Published online: 24 June 2011

subjects, i.e., a focal bilateral increase of [oxy-Hb] in the dorsolateral prefrontal cortex (DLPFC) and simultaneously a [oxy-Hb] decrease in the medial area of the anterior prefrontal cortex (APFC). A Bonferroni post-test showed that the mean (over all eight subjects) [oxy-Hb] responses in left DLPFC and APFC displayed a statistically significant difference compared to a baseline period prior to the task; the mean response in the right DLPFC was not significant (for more details see [17]) but a few individuals showed additionally strong responses in this area (e.g., Fig. 3 in [17]). These findings are in line with results from fMRI and EEG studies where such antagonistic activation patterns ("focal activation/surround deactivation") have been already described (e.g., [4, 19]) during the performance of motor tasks. Given the results, we hypothesized that the focal antagonistic hemodynamic response pattern during MA may be reliably detected by recording only two NIRS channels over the prefrontal cortex.

In this article, we evaluate the above hypothesis by means of cue-based BCI off-line simulations using the data of eight subjects of a previous study [17] and show for the first time that antagonistic [oxy-Hb] responses from left or right DLPFC in combination with APFC significantly increase the discrimination of MA from rest compared to the standard way of using individual features only from one single region (e.g., [15]). One can certainly expect that the use of two features results in an increase of the discriminatory power. Our results, based on eight subjects, however, may be relevant for practical BCI systems because sensor location and instructions for subjects are known a-priori and well defined.

## 2 Materials and methods

### 2.1 Subjects, experimental paradigm, and data collection

In [17], the investigations were carried out on a group of Ten paid University students (five males and five females, all right-handed aged $26.1 \pm 2.7$ years. The study was approved by the Medical University of Graz Institutional Review Board. Subjects were without medical conditions, compensated for participation, and gave written informed consent after the aim of the study was explained to them. For the investigations presented in this article, we used the data of eight subjects (three male, five female, aged $26.0 \pm 2.8$ years) which showed a relative focal bilateral increase of [oxy-Hb] in the DLPFC in parallel with a decrease in the medial area of the APFC. Participants were asked to perform cue-guided mental subtraction. More precisely, prior each task a 10-s baseline interval was recorded. During the task, they had to sequentially subtract a one-digit number from a two-digit number (e.g., $97 - 4 = 93$, $93 - 4 = 89$, ...; the initial subtraction was presented visually on a monitor) as quickly as possible for 12 s, afterward a 28-s resting period was given. Subjects performed 3 or 4 runs (six trials per class and run) resulting in 18 or 24 trials per class, respectively.

A continuous wave system (ETG-4000, Hitachi Medical Co., Japan) was used to record brain oxygenation. The multi-channel system measures the change of [oxy-Hb] and [deoxy-Hb] in the unit of millimolar millimeter (mM × mm) and consists of 16 photo-detectors and 17 light emitters ($3 \times 11$ grid), resulting in a total of 52 channels (Fig. 1a). The lowest line of channels was arranged along the FP1-FP2 line according to the international EEG 10-20 system. For further details on the channel placement, see [17].

### 2.2 Data analysis

After removing baseline drifts by using a 0.01 Hz high pass filter, the task-related concentration changes of [oxy-Hb] referred to a 10-s baseline interval prior to the task (seconds −10 to 0) were calculated (For further details see [1] and [17]). To capture the antagonistic [oxy-Hb] patterns, we defined three regions of interest (ROI): $ROI_1$ consisted of channels 46, 47, and 48 over APFC, $ROI_2$ of channels 18, 28, and 29 over left DLPFC and $ROI_3$ of channels 13, 23, and 24 over right DLPFC (Fig. 1a).

For classification, Fisher's linear discriminant analysis (LDA) classifier was used. To evaluate the LDA generalization, data recorded from each subject was split into a training and evaluation set. The former, consisting of 10 or 16 trials respectively, was used to train and test the discriminative power of [oxy- Hb] feature combinations selected from the different ROIs. The best performing features were selected and used to train the LDA. The evaluation set, composed of the last eight trials, was then used to assess the performance of the trained LDA.

Concentration changes of the [oxy-Hb] response at second $tm_j = 10, 11, 12, 13$, and 14 (±2 s around the end of the MA task, to cover also delayed task-related parts of the response) were labeled as class MA. Samples at second $tr_k = 26, 27, 28, 29$, and 30 (lying in between two MA tasks) were labeled as class REST. Features consist of an individual [oxy-Hb] value of one channel at a fixed time (tm or tr). In Tables 1 and 2, the positions of the channels (channel number as well as underlying Brodmann and anatomical areas) and the corresponding time points are indicated. For each subject, independent LDAs were trained and validated (leave-one-out cross validation) with individual [oxy-Hb] responses for each possible

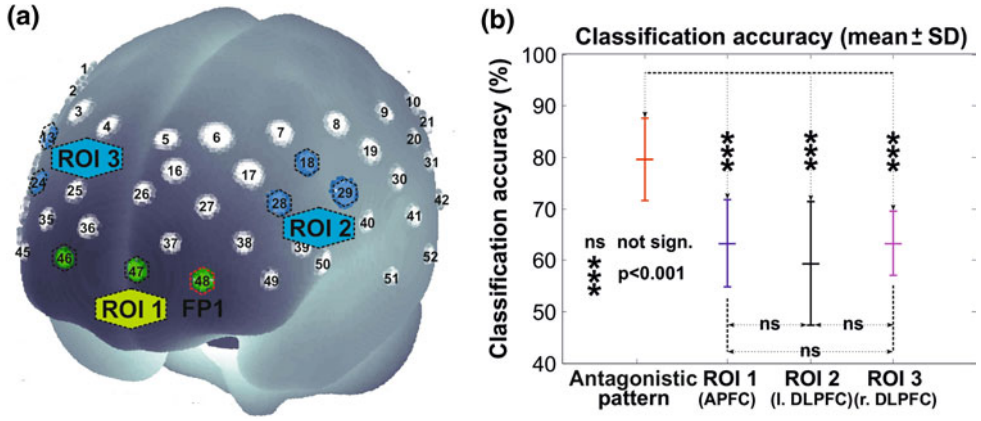


**Fig. 1** **a** Projections of the 52 NIRS channel positions (3 × 11 grid) on the cortical surface. Positions are overlaid on a MNI-152 compatible canonical brain which is optimized for NIRS analysis [21]. Also indicated are the ROI. **b** Significant contrasts of the classification accuracy between the antagonistic and individual features

combination ($ROI_i$, $tm_j$, $tr_k$) with $i = 1,2,3$; $j = 1,2, \ldots, 5$, $k = 1, 2, \ldots, 5$. Exhaustive Search, i.e., all possible feature combinations were evaluated, was used in the above procedure to identify the best performing antagonistic feature combination ($ROI_1$, $ROI_2$, $tm_j$, $tr_k$) or ($ROI_1$, $ROI_3$, $tm_j$, $tr_k$) with $j = 1,2, \ldots, 5$ and $k = 1,2, \ldots, 5$.

The same procedure was applied also to the antagonistic [deoxy-Hb], antagonistic total hemoglobin [Hbtot] = [oxy-HB] + [deoxy-Hb] and to tuples of ([oxy-Hb], [deoxy-Hb]) concentrations. In addition, antagonistic [oxy-Hb] changes that perform best over all subjects were researched (group-related [oxy-Hb] pattern). In the latter, we identified the most commonly selected features over all subjects at the averaged time points of tm and tr.

## 3 Results

### 3.1 Off-line simulation

We used the best performing classifiers calculated from the training set and computed an off-line simulation with the evaluation set (eight trials per class, summarized in Tables 1, 2). Six out of the eight subjects (75%) performed better than the chance level (71.9% ($\alpha = 0.05$) for eight trials [14]) when antagonistic patterns are used (Table 1). Only one subject performed better than random when using individual features from $ROI_1$, $ROI_2$, or $ROI_3$, respectively (see Table 2). An analysis of variance (ANOVA) and a Newman–Keuls post-test revealed that antagonistic

**Table 1** Classification accuracies (Acc.; bold numbers indicate classification accuracies above the chance level (71.9% for eight trials)) and used features (Pos.$_i$, indicating the underlying Brodmann and anatomical areas; tm and tr, corresponding time points) for the antagonistic [oxy-Hb] patterns for all subjects

| Sub. | Antagonistic [oxy-Hb] pattern | | | | | | | | |
|---|---|---|---|---|---|---|---|---|---|
| | Acc. (%) | Pos.$_1$ | | | Pos.$_2$ | | | tm (s) | tr (s) |
| | | Ch. | BA | Anat. | Ch. | BA | Anat. | | |
| S1 | 68.75 | 46[a] | 10 | SFG | 24[b] | 46 | MFG | 10 | 29 |
| S2 | **87.50** | 47[a] | 10 | MeFG | 24[b] | 46 | MFG | 13 | 30 |
| S3 | **75.00** | 48[a] | 10 | MFG | 29[c] | 9 | IFG | 12 | 29 |
| S4 | **87.50** | 48[a] | 10 | MFG | 29[c] | 9 | IFG | 14 | 28 |
| S5 | **81.25** | 47[a] | 10 | MeFG | 28[c] | 46 | MFG | 13 | 26 |
| S6 | 68.75 | 46[a] | 10 | SFG | 28[c] | 46 | MFG | 10 | 26 |
| S7 | **87.50** | 47[a] | 10 | MeFG | 18[c] | 9 | MFG | 10 | 29 |
| S8 | **81.25** | 47[a] | 10 | MeFG | 28[c] | 46 | MFG | 12 | 26 |
| Mean | 79.69 | | | | | | | 11.75 | 27.88 |
| SD | 8.01 | | | | | | | 1.58 | 1.64 |

[a] APFC, [b] r. DLPFC, [c] l. DLPFC

*BA* Brodmann area, *SFG* superior frontal gyrus, *MFG* middle frontal gyrus, *IFG* inferior frontal gyrus, *MeFG* medial frontal gyrus

**Table 2** Classification accuracies (in %) for individual [oxy-Hb] features for all subjects

| Sub. | $ROI_1$ [oxy-Hb] | | | | | | $ROI_2$ [oxy-Hb] | | | | | | $ROI_3$ [oxy-Hb] | | | | | |
|---|---|---|---|---|---|---|---|---|---|---|---|---|---|---|---|---|---|---|
| | Acc. (%) | Pos. | | | tm (s) | tr (s) | Acc. (%) | Pos. | | | tm (s) | tr (s) | Acc. (%) | Pos. | | | tm (s) | tr (s) |
| | | Ch. | BA | Anat. | | | | Ch. | BA | Anat. | | | | Ch. | BA | Anat. | | |
| S1 | 62.50 | 46[a] | 10 | SFG | 11 | 29 | 56.25 | 18[c] | 9 | MFG | 10 | 26 | 56.25 | 24[b] | 46 | MFG | 10 | 30 |
| S2 | 62.50 | 47[a] | 10 | MeFG | 10 | 26 | 50.00 | 28[c] | 46 | MFG | 11 | 30 | 62.50 | 24[b] | 46 | MFG | 14 | 26 |
| S3 | 62.50 | 46[a] | 10 | SFG | 11 | 27 | 50.00 | 29[c] | 9 | IFG | 11 | 26 | 68.75 | 24[b] | 46 | MFG | 12 | 27 |
| S4 | **81.25** | 48[a] | 10 | MFG | 13 | 29 | 50.00 | 29[c] | 9 | IFG | 10 | 27 | 62.50 | 24[b] | 46 | MFG | 13 | 26 |
| S5 | 50.00 | 47[a] | 10 | MeFG | 12 | 26 | 68.75 | 28[c] | 46 | MFG | 11 | 27 | 56.25 | 24[b] | 46 | MFG | 11 | 30 |
| S6 | 62.50 | 46[a] | 10 | SFG | 10 | 26 | 50.00 | 28[c] | 46 | MFG | 10 | 26 | 62.50 | 24[b] | 46 | MFG | 10 | 26 |
| S7 | 62.50 | 46[a] | 10 | SFG | 13 | 28 | **81.25** | 18[c] | 9 | MFG | 10 | 29 | 62.50 | 23[b] | 46 | MFG | 12 | 28 |
| S8 | 62.50 | 48[a] | 10 | MFG | 10 | 26 | 68.75 | 28[c] | 46 | MFG | 12 | 26 | **75.00** | 23[b] | 46 | MFG | 14 | 27 |
| Mean | 63.28 | | | | 11.25 | 27.13 | 59.38 | | | | 10.63 | 27.13 | 63.28 | | | | 12.00 | 27.50 |
| SD | 8.48 | | | | 1.28 | 1.36 | 12.05 | | | | 0.74 | 1.55 | 6.19 | | | | 1.6 | 1.69 |

Bold numbers indicate classification accuracies above the chance level of 71.9%

[a] APFC, [b] r. DLPFC, [c] l. DLPFC

*BA* Brodmann area, *SFG* superior frontal gyrus, *MFG* middle frontal gyrus, *IFG* inferior frontal gyrus, *MeFG* medial frontal gyrus

features perform significantly better than individual features ($F_{(3/21)} = 8.74$; $p < 0.001$; Fig. 1b). Figure 1b depicts the significant contrasts of the classification accuracy between the antagonistic and individual features. The *Y*-axis indicates the mean classification accuracy over all subjects for the use of antagonistic feature combinations and individual features from $ROI_1$, $ROI_2$, or $ROI_3$ (see also Tables 1, 2).

### 3.2 Comparison of antagonistic [oxy-Hb], [deoxy-Hb], [Hbtot], and ([oxy-Hb], [deoxy-Hb]) features

We computed an off-line simulation with the evaluation set using the best performing antagonistic [deoxy-Hb], [Hbtot], and ([oxy-Hb], [deoxy-Hb]) features (Table 3). By using antagonistic [deoxy-Hb], only two subjects performed better than random. An ANOVA and a Newman–Keuls post-test revealed that antagonistic [oxy-Hb] features perform significantly better than antagonistic [deoxy-Hb] features ($F_{(4/28)} = 2.81$; $p < 0.05$). No significant differences between antagonistic [oxy-Hb], antagonistic [Hbtot] as well as ([oxy-Hb], [deoxy-Hb]) tuples were found. In the case of [Hbtot] four and in the case of ([oxy-Hb], [deoxy-Hb]) three out of the eight subjects, respectively, performed significantly better than random.

### 3.3 Stability of antagonistic [oxy-Hb] features

According to the findings of the feature selection and off-line simulation, we used the most commonly selected features of all subjects (Ch. 47, APFC and Ch. 28, l. DLPFC at the averaged time points of tm and tr (tm = 12 s, tr = 28 s; Table 1)). The group-related [oxy-Hb] features set achieved in average a classification accuracy of 70.3% over all subjects (Table 3). No significant differences were found between the use of subject-specific antagonistic features and the above group-related feature set. Four out of the eight subjects performed better than the chance level (mean 78.1%).

## 4 Discussion

The aim of the study was to investigate the usefulness of antagonistic [oxy-Hb] patterns in the context of single-trial classification for brain-computer interfacing. The results show that two NIRS channels placed over predefined brain areas, i.e., left or right DLPFC and APFC, respectively, may significantly increase the performance of optical BCIs compared to the more common approach to use only one channel (e.g., [15, 20]).

In the feature selection process, we looked for best performing antagonistic and individual features, respectively. To account for the low number of trials available for evaluating the performance, we adapted the chance level of classification to guarantee the correct comparison [14]. By using the best antagonistic [oxy-Hb] features performing an off-line simulation mean classification accuracy (%) of $79.69 \pm 8.01$ (mean $\pm$ SD, Table 1) was computed. Individual features performed worse (classification accuracies (%) of $63.28 \pm 8.48$ ($ROI_1$), $59.38 \pm 12.05$ ($ROI_2$), and $63.28 \pm 6.19$ ($ROI_3$), Table 2). In each case, only one

**Table 3** Classification accuracies (in %) for antagonistic [deoxy-Hb], [Hbtot], and tuples of [oxy-Hb] and [deoxy-Hb] features for all subjects

In addition, the classification accuracies (bold numbers indicate accuracies above the chance level of 71.9%) using a group-related set of antagonistic [oxy-Hb] features are shown

| Subj. | Antagonistic pattern | | | | |
|---|---|---|---|---|---|
| | [oxy-Hb] | [deoxy-Hb] | [Hbtot] | [deoxy-Hb] and [oxy-Hb] | Group-related |
| S1 | 68.75 | 68.75 | 50.00 | 68.75 | 68.75 |
| S2 | **87.50** | 62.50 | **81.25** | 68.75 | **75.00** |
| S3 | **75.00** | 62.50 | 56.30 | **75.00** | 68.75 |
| S4 | **87.50** | **81.25** | **93.75** | **81.25** | **87.50** |
| S5 | **81.25** | 50.00 | 68.75 | 68.75 | 62.50 |
| S6 | 68.75 | 56.25 | 56.25 | 62.50 | 50.00 |
| S7 | **87.50** | 62.25 | **93.75** | 68.75 | **75.00** |
| S8 | **81.25** | **87.50** | **81.25** | **93.75** | **75.00** |
| Mean | 79.69 | 66.38 | 72.66 | 73.44 | 70.31 |
| SD | 8.01 | 12.48 | 17.33 | 9.88 | 10.95 |

subject reached accuracies above the chance level. In contrast, with the antagonistic features 6 of the eight subjects (75%) performed accuracies (mean 83.3%) above the chance level. So the use of antagonistic [oxy-Hb] features, compared to individual [oxy-Hb] features from $ROI_1$, $ROI_2$, and $ROI_3$, significantly increased the classification accuracy (Tables 1 and 2; Fig. 1b).

In addition, we compared antagonistic [oxy-Hb] with antagonistic [deoxy-Hb], [Hbtot], and ([oxy-Hb], [deoxy-Hb]) tuples features. [deoxy-Hb], [Hbtot], and [(de)oxy-Hb] performed worse (classification accuracies (%) of $63.38 \pm 12.48$ ([deoxy-Hb]), $72.66 \pm 17.33$ ([Hbtot]), and $73.44 \pm 9.88$ ([oxy-Hb] and [deoxy-Hb]), Table 3) whereby only [deoxy-Hb] exhibits significant difference to the use of [oxy-Hb]. These lower classification accuracies may be simply explained by the fact that [deoxy-Hb] changes are smaller in amplitude, usually by a factor two or more (e.g., [9, 13]), and higher in variance than [oxy-Hb] changes, more susceptible by noise and therefore less suitable as feature for single-trial classification.

The performance comparison between the use of subject-specific versus group-related features surprisingly revealed no significant differences. This supports the hypothesis that MA generates focal and rather well defined metabolic response patterns. For the realization of optical BCIs, this means that the considered features are spatially focused, task-related and valid for several users. Antagonistic activation patterns known as "focal activation/surround deactivation" have been described in different studies. So, e.g., "focal ERD / surround ERS" was reported during hand and foot movement execution or imagination in EEG [19, 23] and "positive BOLD/negative BOLD" in fMRI ([4, 11]. The usability of this phenomenon for classification in motor imagery based BCI systems (ERD/ERS) is well documented [18]. Novel is however that this phenomenon is also present in NIRS data [17], and in this study, we showed the first time the usefulness of this phenomenon for NIRS data classification. Although the study revealed significant results, some limitations should also be mentioned. First of all, the number of subjects is low. However, concerning the significant increase of the classification accuracy using antagonistic [oxy-Hb] changes instead of individual features only from one single region, our findings suggest that the use of antagonistic patterns may be a suitable control strategy for optical BCIs. However, to clarify this in more detail, especially in an online study, a bigger sample is needed. Another limitation is the temporal resolution of the hemodynamic response—in the range of several seconds—which limits the information transfer rates achievable for BCI-based communication. In [17], we found a delay of the onset and a peak latency of the hemodynamic responses in the order of 2–3 s. With the paradigm, classification approach and analysis windows used for this study in mind, around 12 s (MA) to 16 s (REST) (Table 1) would be needed to classify the task reasonable well. By shortening the baseline interval prior to the task to 5 s, this might lead to a maximal achievable information transfer rate of around 3–3.5 bits/min (comparable with results in [2]). To increase this transfer rate further basic research is necessary, e.g., investigating the use of fast optical signals [6, 12, 24].

In summary, this study suggests that the use of antagonistic [oxy-Hb] features may significantly increase the classification accuracy. The off-line simulation results confirmed our hypothesis that two prefrontal NIRS channels can capture antagonistic hemodynamic patterns during a MA task that can be detected reasonably well without the need of time consuming user-adaptation. In combination with the self paced paradigm, the use of antagonistic pattern may be an important contribution for simple and cheap optical BCI systems which are currently in development.

**Acknowledgment** The authors' BCI research has been supported by the EU project PRESENCCIA (IST-2006-27731), "Land Steiermark" (project A3-22. N-13/2009-8), and the Neuro Center Styria (NCS) in Graz, Austria.

## References


1. Bauernfeind G, Leeb R, Wriessnegger SC, Pfurtscheller G (2008) Development, set-up and first results for a one-channel near-infrared spectroscopy system. Biomed Technol 53:36–43
2. Coyle SM, Ward TE, Markham CM (2007) Brain–computer interface using a simplified functional near-infrared spectroscopy system. J Neural Eng 4:219–226
3. Coyle SM, Ward T, Markham CM, McDarby G (2004) On the suitability of near-infrared systems for next generation brain computer interfaces. Physiol Meas 25:815–822
4. Ehrsson HH, Geyer S, Naito E (2003) Imagery of voluntary movement of fingers, toes, and tongue activates corresponding body-part-specific motor representations. J Neurophysiol 90: 3304–3316
5. Franceschini MA, Fantini S, Thompson JH, Culver JP, Boas DA (2003) Hemodynamic evoked response of the sensorimotor cortex measured noninvasively with near-infrared optical imaging. Psychophysiol 40:548–560
6. Gratton G, Fabiani M (2001) Shedding light on brain function: the event-related optical signal. Trends Cogn Sci 5(8):357–363
7. Herrmann MJ, Ehlis AC, Wagener A, Jacob CP, Fallgatter AJ (2005) Near-infrared optical topography to assess activation of the parietal cortex during a visuo-spatial task. Neuropsychologia 43:1713–20
8. Herrmann MJ, Huter T, Plichta MM, Ehlis AC, Alpers GW, Mühlberger A, Fallgatter AJ (2008) Enhancement of activity of the primary visual cortex during processing of emotional stimuli as measured with event-related functional near-infrared spectroscopy and event-related potentials. Hum Brain Mapp 29:28–35
9. Hock C, Müller-Spahn F, Schuh-Hofer S, Hofmann M, Dirnagl U, Villringer A (1995) Age dependency of changes in cerebral hemoglobin oxygenation during brain activation: a near-infrared spectroscopy study. J Cereb Blood Flow Metab 15(6):1103–1108
10. Hofmann MJ, Herrmann MJ, Dan I, Obrig H, Conrad M, Kuchinke L, Jacobs AM, Fallgatter AJ (2008) Differential activation of frontal and parietal regions during visual word recognition: an optical topography study. Neuroimage 40:1340–1349
11. Hummel F, Saur R, Lasogga S, Plewnia C, Erb M, Wildgruber D, Grodd W, Gerloff C (2004) To act or not to act. Neural correlates of executive control of learned motor behavior. Neuroimage 23(4):1391–1401
12. Kato T (2004) Principle and technique of NIRS-Imaging for human brain FORCE: fast-oxygen response in capillary event. Int Cong Ser 1270:85–90
13. Maki A, Yamashita Y, Ito Y, Watanabe E, Mayanagi Y, Koizumi H (1995) Spatial and temporal analysis of human motor activity using noninvasive NIR topography. Med Phys 22(12):1997–2005
14. Müller-Putz GR, Scherer R, Brunner C, Leeb R, Pfurtscheller G (2008) Better than random? A closer look on BCI results. Int J Bioelectromagn 10:52–55
15. Naito M, Michioka Y, Ozawa K, Ito Y, Kiguchi M, Kanazawa T (2007) A communication means for totally locked-in ALS patients based on changes in cerebral blood volume measured with near-infrared light. IEICE Trans Inf Syst E 90(D): 1028–1037
16. Pfurtscheller G, Allison BZ, Bauernfeind G, Brunner C, Solis Escalante T, Scherer R, Zander TO, Mueller-Putz G, Neuper C, Birbaumer N (2010) The hybrid BCI. Front Neurosci 4:42
17. Pfurtscheller G, Bauernfeind G, Wriessnegger SC, Neuper C (2010) Focal frontal (de)oxyhemoglobin responses during simple arithmetic. Int J Psychophysiol 76:186–192
18. Pfurtscheller G, Brunner C, Schlögl A, Lopes da Silva FH (2006) Mu rhythm (de)synchronization and EEG single-trial classification of different motor imagery tasks. Neuroimage 31:153–159
19. Pfurtscheller G, Neuper C (1994) Event-related synchronization of mu rhythmin the EEG over the cortical hand area in man. Neurosci Lett 174:93–96
20. Sagara K, Kido , Ozawa K (2009) Portable single-channel NIRS-based BMI system for motor disabilities' communication tools. Conf Proc IEEE Eng Med Biol Soc 602–605
21. Singh A K, Okamoto M, Dan H, Jurcak V, Dan I (2005) Spatial registration of multichannel multi-subject fNIRS data to MNI space without MRI. Neuroimage 27:842–841
22. Sitaram R, Zhang H, Guan C, Thulasidas M, Hoshi Y, Ishikawa A, Shimizu K, Birbaumer N (2007) Temporal classification of multichannel near-infrared spectroscopy signals of motor imagery for developing a brain-computer interface. Neuroimage 34: 1416–1427
23. Suffczynski P, Pijn JP, Pfurtscheller G, Lopes da Silva FH (1999) Event-related dynamics of alpha band rhythm: a neuronal network model of focal ERD/surrounded ERS. In: Pfurtscheller G, Lopes da Silva FH (eds) Handbook of electroencephalography and clinical neurophysiology, revised edition vol VI, Elsevier, Amsterdam, pp 67–85
24. Wolf M, Wolf U, Choi JH, Gupta R, Safonova LP, Paunescu LA, Michalos A, Gratton E (2002) Functional frequency-domain near-infrared spectroscopy detects fast neuronal signal in the motor cortex. Neuroimage 17(4):1868–1875
25. Wriessnegger SC, Kurzmann J, Neuper C (2008) Spatio-temporal differences in brain oxygenation between movement execution and imagery: a multichannel nearinfrared spectroscopy study. Int J Psychophysiol 67:54–63

International Journal of Bioelectromagnetism
Vol. 13, No. 2, pp. 66 - 67, 2011
www.ijbem.org

# Cortical effects of BCI training measured with fNIRS

**Günther Bauernfeind[a], Vera Kaiser[a], Tobias Kaufmann[b], Alex Kreilinger[a], Andrea Kübler[b], Christa Neuper[a,c]**

[a]*Institute for Knowledge Discovery, Graz University of Technology, Graz, Austria*
[b]*Department of Psychology I, Biological Psychology, Clinical Psychology and Psychotherapy, University of Würzburg, Würzburg, Germany*
[c]*Department of Psychology, University of Graz, Graz, Austria*

Correspondence: G Bauernfeind, Institute for Knowledge Discovery, Graz University of Technology, Krenngasse 37, 8010 Graz, Austria. E-mail: g.bauernfeind@tugraz.at, phone +43 316 873 5312, fax +43 316 873 5349

***Abstract.*** This study investigates the cortical training effects using a 2-class motor imagery (MI) based BCI. Twelve subjects were trained to use right hand or feet MI to control a cursor on a screen. The feedback was calculated by using features based on the EEG. To assess which areas are involved in the training, and how activity in these areas changes over time, three fNIRS measurements were applied before, in between and after the training. The statistical analysis of the measurement revealed that significant activity changes in the involved areas during the training can be found and that they occur accordingly to the task.

*Keywords:* BCI training, motor imagery (MI), fNIRS, cortical trainings effects

## 1. Introduction

The research work of the past decades showed that various parameters of brain activity, in particular EEG patterns, can be brought under voluntary control (e.g. [Birbaumer, 2006]). To contrive such intentional control of activity, it is essential to perform training sessions with feedback [McFarland 1998] [Pineda 2003]. As a result of feedback training, for example motor imagery (MI) based BCI training, and non-stationarity of the measured EEG signals, relevant EEG patterns usually change and require the adjustment of classifier and feedback [Neuper 2006] [Vidaurre2007]. To evaluate which areas are involved in such changes, and how the activity of these areas changes over time, the present study investigates cortical effects of BCI training with multichannel fNIRS measurements.

## 2. Material and Methods

### 2.1. Subjects and experimental procedure

The investigations were carried out on a group of 15 subjects (8 male, 7 female, all right-handed, aged 24±2.3). Each subject participated in a series of ten experimental sessions: one screening, six feedback and three fNIRS sessions without feedback (min 3, max 6 days between the sessions; Fig 1A). Three participants did not complete the training and the data of two subjects were excluded from analysis due to bad data quality. After the screening, the subjects performed an initial fNIRS measurement followed by a first block of three feedback sessions and the second fNIRS session. The final fNIRS measurement was performed after the second block of feedback sessions. In the fNIRS sessions the participants had to imagine cue-guided right hand (RH) or feet (FE) MI in a fixed repetitive time scheme (Fig 1B). Between 20 to 60 RH/FE trials were collected during one fNIRS session. In the trainings sessions (each consisting of 160 RH and 160 FE trials) the subjects received an additional feedback in form of a cursor on a computer screen.

### 2.2. Data acquisition and processing

The EEG was recorded bipolarly from electrodes placed over C3, Cz and C4. For fNIRS recording a multichannel continuous wave system was used. The system measures the change of [oxy-Hb] and [deoxy-Hb] in mM mm and consists of 16 detectors and 17 emitters (3×11 grid, 52 Ch.). The grid was arranged above the motor cortex (Fig 1C). For the subsequent analysis only the [oxy-Hb] data of

channels covering functional involved areas were used. After removing baseline drifts, a common average reference spatial filter was used. Subsequent the task-related concentration changes referred to a 2 s baseline interval prior to the task were calculated. Afterwards the averages of three regions of interest (ROI; $ROI_1$ over C3; $ROI_2$ over Cz and $ROI_3$ over C4; Fig 1C) were computed. For statistical analysis the subjects were split into two equal groups (n=5) according to their mean classification accuracy of the EEG sessions (accuracy < or > 70%), afterwards a 2x2x3x3 analysis of variance (ANOVA) with the factors "GROUP" (good vs. worse performer), "CLASS" (hand vs. feet), "CHANNEL" (C3, Cz, C4) and "SESSION" (S1, S2 and S3) was performed.

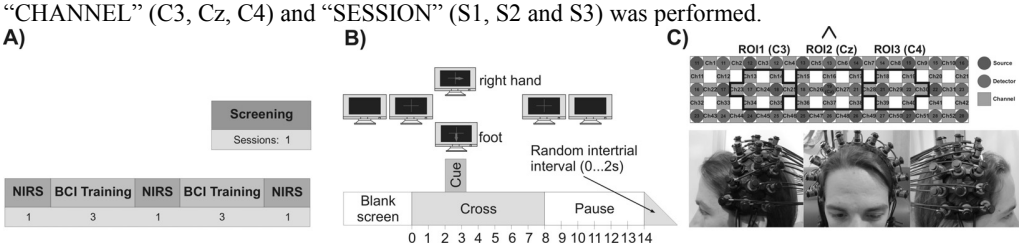


***Figure 1.*** *A) Experimental sessions B)Timing of the fNIRS paradigm C) Schematic illustration of the multi-channel array, array mounted on a subjects.*

## 3. Results

The results of the ANOVA revealed a significant interaction "GROUP" x "CHANNEL" x "SESSION" ($F_{(4, 32)} = 3.68$, $p<0.05$). A Newman-Keuls post-test showed that for worse performer (<70% accuracy) significant differences between C3 and C4 during session one (.0063±0.0039; -.0058±.0044) and two (.0001±.0062; -.0082±.0048) and between Cz and C4 during session two (.0021±.0042; -.0082±.0048) and three (.0035±.0032; -.0056±.0044) can be found. For the good performer (>70% accuracy) significant differences between C3 (.0044±.0077) and Cz (-.0048±.0032) can be found in session three.

## 4. Discussion

According to the group membership, significant differences in the course of the BCI training can be found. The subjects below 70% accuracy showed significant cortical activation differences between C3 and C4 (strong lateralization effect) as well as between Cz and C4, but no significant difference between C3 and Cz in the course of the training. These findings could be interpreted as a co-activation of C3 and Cz during both tasks, which may explain that these subjects performed worse in the EEG sessions (mean classification accuracies below 70%). In contrast the subjects above 70% showed no significant differences between C3 and C4 as well as between Cz and C4 in the course of the training, but according to the trainings task (hand vs. feet MI) significant differences between C3 and Cz at the end of the feedback training.

In summary, the study demonstrates that significant activity changes in functionally involved areas in the course of the training can be found and that these changes occur accordingly to the trainings task.


### Acknowledgements

This work is supported by the European ICT Program Project FP7-224631, the "Land Steiermark" (project A3-22. N-13/2009-8) and the Neuro Center Styria (NCS) in Graz, Austria.


### References


Birbaumer N, Weber C, Neuper C, Buch E, Haapen K, Cohen, L. Physiological regulation of thinking: brain-computer interface (BCI) research. Prog Brain Res, 159: 369–391, 2006.

McFarland DJ, McCane LM, Wolpaw JR. EEG-based communication and control: short-term role of feedback. IEEE Trans Rehabil Eng, 6(1): 7-11 1998.

Neuper C, Müller-Putz GR, Scherer R, Pfurtscheller G. Motor imagery and EEG-based control of spelling devices and neuroprostheses. Prog Brain Res, 159: 393-409, 2006.

Pineda JA, Silverman DS, Vankov A, Hestenes J. Learning to control brain rhythms: making a brain-computer interface possible. *IEEE Trans Neural Syst Rehabil Eng*, 11(2): 181-184, 2003.

Vidaurre C, Schlögl A, Scherer R, Cabeza R, Pfurtscheller G. Study of on-line adaptive discriminant analysis for EEG-based brain computer interfaces. *IEEE Trans on Biomed Eng,* 54:550-556, 2007.

# About the Stability of Phase Shifts Between Slow Oscillations Around 0.1 Hz in Cardiovascular and Cerebral Systems

Gert Pfurtscheller*, *Member, IEEE*, Daniela S. Klobassa, Christof Altstätter, Günther Bauernfeind, and Christa Neuper

***Abstract*—One important feature of the baroreflex loop is its strong preference for oscillations around 0.1 Hz. In this study, we investigated heart rate intervals, arterial blood pressure (BP), and prefrontal oxyhemoglobin changes during 5 min rest and during brisk finger movements in 19 healthy subjects. We analyzed the phase coupling around 0.1 Hz between cardiovascular and (de)oxyhemoglobin oscillations, using the cross-spectral method. The analyses revealed phase shifts for slow oscillations in BP and heart rate intervals between $-10^\circ$ and $-118^\circ$ (BP always leading). These phase shifts increased significantly ($p < 0.01$) in the movement session. The coupling between cardiovascular and oxyhemoglobin oscillations was less clear. Only 12 subjects demonstrated a phase coupling ($COH^2 \geq 0.5$) between oxyhemoglobin and BP oscillations. This may be explained by an overwhelming proportion of nonlinearity in cardiovascular and hemodynamic systems. The phase shifts between slow cardiovascular and hemodynamic oscillations are relatively stable subject-specific biometric features and could be of interest for person identification in addition to other biometric data. Slow BP-coupled oscillations in prefrontal oxyhemoglobin changes can seriously impair the detection of mentally induced hemodynamic changes in an optical brain–computer interface, a novel nonmuscular communication system.**

***Index Terms*—Blood pressure (BP), cardiovascular oscillations, heart rate (HR), near-infrared spectroscopy (NIRS), oxyhemoglobin oscillations.**

## I. Introduction

SLOW arterial blood pressure (BP) and heart rate (HR) oscillations have been addressed in many studies. Rhythmic fluctuations in the HR were described, for the first time, by von Haller [1]. Mayer [2] was the first who reported on slow waves in human BP around 0.1 Hz (so-called Mayer waves; for review see Julien [3]). The involvement of the baroreceptor reflex in the genesis of slow oscillations around 0.1 Hz was proposed by Guyton and Harris in [4]. Important components of the baroreflex loop are the baroreceptors, the cardiopulmonary receptors, the cardiovascular nuclei in the brain stem, and the heart. Several simulation studies predicting Mayer waves have been described [5]–[9] and showed that one important feature of the baroreflex loop is its strong preference for oscillations around 0.1 Hz, which can be seen as "resonance" or "eigenfrequency" of the loop, and another feature is the lead of BP oscillations before beat-to-beat interval (inverse of HR) oscillations.

Slow 0.1-Hz oscillations have been reported not only in the BP and HR [3], [7], [9]–[11] but also in different cerebral signals, such as oxygen availability of cortical tissue, cerebral blood-flow velocity (CBFV), oxyhemoglobin changes, full-band EEG, and cerebrospinal fluid [12]–[21]. The relationship between intrinsic 0.1-Hz oscillations in the resting brain and in the cardiovascular system deserves special attention, because the identification of the mechanism underlying the generation of these slow oscillations in central and autonomous systems is still elusive. Two theories have been proposed to explain the generation of 0.1-Hz oscillations: first, the generation of slow oscillations as a resonance phenomenon of the baroreflex loop [7], [9], [10] and second, the independence of baroreceptor influences probably as result of central oscillators. From a series of observations in anesthetized animals, we know that central oscillators may contribute to the generations of oscillations around 0.1-Hz (pacemaker theory; for details see [3]).

Of interest is the mutual interaction between brain and heart. Recently, Thayer and Lane [22] made a review starting with the work of Claude Bernard over 150 years ago about the physiology of heart–brain connections and discussing the pathways via which the prefrontal cortex can control cardiac activity. From nonhuman animal research, we have evidence that cortical systems, especially including the medial-prefrontal cortex, act as a network together with subcortical systems (known as "central autonomic network") to initiate and represent cardiac autonomic adjustments [23], [24]. Further insight in the brain–heart connections may be obtained by studying the phase coupling between slow fluctuations in cardiovascular and central autonomic networks through analysing BP time series and (de)oxyhemoglobin (Hb, $HbO_2$) recordings at optodes placed over the prefrontal cortex.

We hypothesized that cyclic finger movements at the resonance frequency of the baroreflex loop ($\sim$0.1 Hz) would have

Manuscript received October 27, 2010; revised January 26, 2011 and March 10, 2011; accepted March 14, 2011. Date of publication April 5, 2011; date of current version June 17, 2011. This work was supported in part by the EU Project PRESENCCIA (IST-27731), "Land Steiermark" (Project A3-22.N-13/2009-8), in part by the Neuro Center Styria (NCS), and in part by the "Allgemeine Unfallversicherungsanstalt" (AUVA). *Asterisk indicates corresponding author.*

*G. Pfurtscheller is with the Laboratory of Brain–Computer Interfaces, Institute for Knowledge Discovery, Graz University of Technology, Graz 8010, Austria (e-mail: pfurtscheller@tugraz.at).

D. S. Klobassa and C. Neuper are with the Department of Psychology and the Laboratory of Brain–Computer Interfaces, Institute for Knowledge Discovery, Graz University of Technology, Graz 8010, Austria (e-mail: daniela.klobassa@tugraz.at; neuper@tugraz.at).

C. Altstätter and G. Bauernfeind are with the Laboratory of Brain–Computer Interfaces, Institute for Knowledge Discovery, Graz University of Technology, Graz 8010, Austria (e-mail: altstaet@sbox.tugraz.at; g.bauernfeind@tugraz.at).

Digital Object Identifier 10.1109/TBME.2011.2134851

an impact on the strength of phase coupling between slow oscillations in cardiovascular (BP, beat-to-beat intervals) and hemodynamic ($HbO_2$) systems and involve linear or nonlinear system components. In the former case, the coherence may have a large value as a measure of linearity; the opposite would be true in the latter case [8], [17], [25]–[27].

Cyclic brisk finger movements are accompanied by two responses, the HR response and the BP response. First, "central commands" [22], [28], which impinge upon brainstem cardiovascular nuclei induce cardiac slowing [29], [30], and efferences from motor cortex innervate the somatic musculature. Second, the reafferent input from kinaesthetic receptors evoked by the movement elicits changes in BP known as "exercise pressure response" [31] and accounts for a cardiac acceleration. Finger movements are also accompanied by changes in motor cortex excitability associated to premovement negative potential shifts [32] and premovement EEG desynchronization [33], both of frontal cortex origin.

Knowledge about the incidence of slow fluctuations in cerebral oxy- and deoxyhemoglobin changes is very important for developing a near-infrared spectroscopy (NIRS)-based brain–computer interface (BCI) [34]–[36]. Such an optical BCI is a new nonmuscular communication and control system that directly measures (de)oxyhemoglobin changes associated with the user's intent and transforms the recorded signal into a control signal [37], [38]. Mentally elicited (de)oxyhemoglobin changes (e.g., through mental arithmetic or motor imagery [39], [40]) have a small magnitude and are often hidden in slow spontaneous (de)oxyhemoglobin fluctuations. For classification approaches, it is essential to improve the SNR and to decrement false classifications that occur primarily due to misclassification of physiological noise [41]. Regardless of the improvement of the SNR, it is of general interest to know how the couplings are distributed in a normal population.

The most common biometric method of person identification is through fingerprints. This method is, however, not always secured enough and therefore it becomes important to find other biometric methods to replace or augment the fingerprint technology as, e.g., by recording and analyzing signals from the brain (EEG) and heart. While bioelectric signals from the brain have already been used as biometric measures for person identification [42]–[47], the use of cardiovascular features is relatively novel. It has already been shown that electrocardiogram (ECG) traces exhibit features that are unique to an individual and may be suitable as biometric measure [48]–[50]. While these identification methods rely only on the ECG signal, it is of interest whether the common analyses of ECG and BP signals also reveal biometric information, especially when phase shifts of slow oscillations are considered. Reproducible and stable phase-shift measures could be one additional feature in a battery of biometric measures from brain and heart signals.

This study aims to answer the following questions.

1) Does a difference exist in the strength of phase coupling between beat-to-beat fluctuations of arterial BP and HR intervals during rest and cyclic finger movements?
2) How many subjects display slow arterial BP-coupled prefrontal (de)oxyhemoglobin fluctuations around 0.1 Hz?
3) Are phase shifts measures between 0.1-Hz oscillations in beat-to-beat HR intervals, BP, and (de)oxyhemoglobin suitable as biometric measures?

TABLE I
HR AND BP DATA

| | HR (bpm) | $BP_{sys}$ (mmHg) | $BP_{dia}$ (mmHg) |
|---|---|---|---|
| Rest | 71.9 ± 4.8 | 111.5 ± 4.3 | 70.2 ± 2.6 |
| EF1 | 70.1 ± 4.4 | 112.5 ± 4.2 | 71.3 ± 3.1 |
| EF2 | 70.2 ± 4.3 | 111.6 ± 4.5 | 70.1 ± 2.9 |

Mean Values (± SD) of HR (bpm), BPsys (mmHg) and BPdia (mmHg) of 19 Subjects for Rest, Periodic (EF1) and Randomized Movements (EF2).

## II. METHODS

### A. Sample

Twenty-six naive subjects (12 males and 14 females) aged 19 to 31 years (23 ± 2.8, mean ± SD) participated voluntarily in this study. All subjects were right-handed (Edinburgh-Handedness-Inventory (EHI) [51]), had normal or corrected to normal vision and were seated in a comfortable armchair for the experiments. All experiments were in compliance with the World Medical Association Declaration of Helsinki. The protocol was approved by the Ethics Committee of the Medical University of Graz and the subjects gave informed written consent before the experiments.

### B. Experimental Paradigm

The study consisted of different sessions, namely data recording during rest, during self-paced brisk finger movements, periodic cued finger movements, and cued finger movements in random intervals. Part of the data about self-paced movements has been published recently [52]. Here, we report data from initial 5-min recording periods during rest (labeled "rest") and two sessions with 40 cued brisk finger movements, one with periodically presented cues (labeled "EF1") and one with randomly presented cues (labeled "EF2"). From the 5-min BP recording during rest, the power spectrum was estimated. When one dominant peak was found in the power spectrum between 0.07 and 0.13 Hz, it was interpreted as the "eigenfrequency" of the cardiovascular system. In the case of periodical stimulation (EF1), the interstimulus was equivalent to the subject-specific peak frequency. The intervals between randomly presented cues (EF2) varied between 9 and 23 s. For further details see [52].

After inspecting the data, five subjects were eliminated due to high BP, irregular respiration, extraventricular contractions, or recording artifacts. Two of the remaining 21 subjects were eliminated because of optode problems during the NIRS recordings. The data from 19 subjects (aged 23 ± 2.9 years; mean ± SD) are reported. HR and BP data are summarized in Table I.

### C. Data Recording and Processing

For this study, we analyzed the ECG recorded bipolarly at electrodes placed on the thorax (filter setup: 0.5–100 Hz), the BP, and the respiration. All of these signals were sampled at a frequency of 500 Hz. For BP recording, a continuous noninvasive monitoring system (CNAP Monitor 500, CNSystems, Austria) was used. Data were recorded from the proximal limb of the index or middle finger. The respiration patterns were obtained by using a respiratory sensor (Respiratory Effort Sensor, Pro-Tech Services, Inc., filter setup: 0.1–100 Hz). (De)oxyhemoglobin fluctuations were recorded with a custom made one-channel, continuous wave method-based NIRS system (for details see [34]). The sources and the detector were placed over the frontal cortex 1.5 cm to the left and right of position FP1 according to the international 10/20 system for EEG recording [53]. A fifth-order Butterworth filter with a cutoff frequency of 0.9 Hz was used to remove variability due to the cardiac cycle. After detection of the beat-to-beat intervals (RRI) in the ECG signal (based on an algorithm using a filter bank to decompose the ECG signal into various subbands), the intervals were linearly interpolated, resampled at 2 Hz, and displayed as RRI time series. From the arterial BP recording, the systolic (BPsys) and diastolic (BPdia) pulse pressure amplitudes were extracted, linearly interpolated, resampled at 2 Hz, and displayed as BPsys and BPdia time series. Power spectra were estimated for all signals after subtraction of the mean over all samples. Recording time of all variables varied, depending on the task between 5 min (rest), 8 min (EF1, cyclic movements), and 15 min (EF2, randomized movements). For all spectra calculations, 1024 samples were used. The spectral values were smoothed using a 31-point triangular window, and cross spectra were calculated between all variables ([54]; for details see De Boer *et al.* [10], [11]). After an automatic search for the largest peak in the cross spectrum in the range 0.07–0.13 Hz, the corresponding coherence ($COH^2$) and phase shift (PHA) values were determined. When no peak was found in the indicated range, the frequency was set to 0.1 Hz. Examples of time series and cross spectra (coherence and phase) from two representative subjects are displayed in Fig. 1.

### D. Statistics

Statistical analysis contained a Shapiro–Wilk test for testing normal distribution of the data and paired sample *t*-tests for evaluating differences in phase shifts and time delays. All relevant data were normally distributed. Because of multiple comparisons, the Holm–Bonferroni method was used for alpha adjustment to reduce the probability of a Type I error. Pearson's product moment correlation was used for evaluating possible relations between phase shifts in the different conditions.

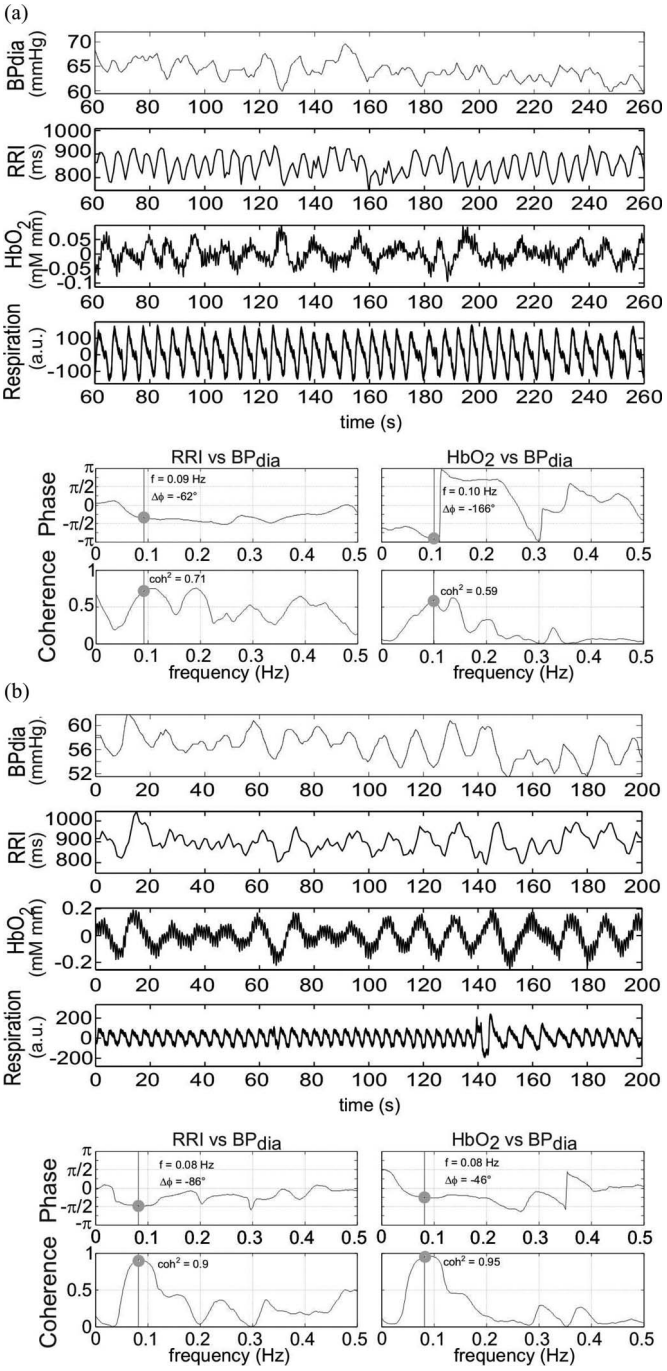


Fig. 1. Beat-to-beat time series (200 s) and spectra from two representative subjects [(a) one with a large phase shift between BP and $HbO_2$ and (b) one with a small phase shift (b)]. *Upper panels:* Time series of BPdia (mmHg), RRI (ms), $HbO_2$ (mM*mm) and respiration (a.u.) during rest. *Lower panels:* Phase- and coherence spectra from RRI and BPdia time series (left side) and from $HbO_2$ and BPdia time series (right side). The automatically determined frequency, phase, and coherence values are indicated by vertical lines.

## III. Results

### A. Phase Shifts Between Slow BP and RRI Oscillations Around 0.1 Hz

Fig. 1 shows two representative examples of BPdia, RRI, $HbO_2$ and respiration signals recorded during rest (upper panels) and the corresponding phase and coherence spectra between RRI versus BPdia and $HbO_2$ versus BPdia (lower panels). One subject [see Fig. 1(a)] displayed oscillations at 0.09 Hz with a large phase shift between $HbO_2$ and BPdia, while the other subject [see Fig. 1(b)] displayed oscillations with a frequency at 0.08 Hz and a small phase shift between $HbO_2$ and BPdia.

TABLE II
PHASE COUPLING BETWEEN RRI, ARTERIAL BP, AND $HbO_2$

| | RRI-$BP_{sys}$ | RRI-$BP_{dia}$ | $HbO_2$-$BP_{dia}$ |
|---|---|---|---|
| | *(N = 19)* | | *(N = 12)* |
| **Rest** | | | |
| Frequency (Hz) | 0.10 ± 0.01 | 0.10 ± 0.02 | 0.10 ± 0.02 |
| $COH^2$ | 0.68 ± 0.18 | 0.69 ± 0.17 | 0.66 ± 0.15 |
| Time delay (s) | -0.99 ± 0.51 | -2.35 ± 0.81 | -1.49 ± 1.31 |
| Phase shift (°) | -35 ± 18 | -81 ± 21 | -55 ± 46 |
| **EF1** | | | |
| Frequency (Hz) | 0.10 ± 0.01 | 0.10 ± 0.01 | 0.09 ± 0.01 |
| $COH^2$ | 0.68 ± 0.23 | 0.75 ± 0.15 | 0.54 ± 0.25 |
| Time delay (s) | -1.54 ± 0.88 | -2.77 ± 0.92 | -1.66 ± 1.37 |
| Phase shift (°) | -51 ± 24 | -93 ± 23 | -56 ± 47 |
| **EF2** | | | |
| Frequency (Hz) | 0.10 ± 0.01 | 0.09 ± 0.02 | 0.10 ± 0.01 |
| $COH^2$ | 0.64 ± 0.19 | 0.69 ± 0.16 | 0.52 ± 0.20 |
| Time delay (s) | -1.51 ± 0.96 | -2.88 ± 1.04 | -1.62 ± 1.12 |
| Phase shift (°) | -49 ± 25 | -92 ± 22 | -56 ± 36 |

*Left:* Frequency (Hz), coherence ($COH^2$), time delays (s), and phase shift (°) (mean ± SD) calculated for RRI and BPsys, and RRI and BPdia oscillations around 0.1 Hz for rest, EF1 and EF2.

*Right:* Frequency (Hz), coherence ($COH^2$), time delays (s) and phase shift (°) (mean ± SD) between $HbO_2$ and BPdia oscillations around 0.1 Hz for 12 selected subjects ($COH^2 \geq 0.5$) during rest.

Remarkable in Fig. 1 are the relatively similar phase shifts for cardiovascular oscillations in both subjects (between RRI and BPdia: $-62°$ and $-86°$) and the quite different phase shifts ($-166°$ and $-46°$) between $HbO_2$ and BPdia oscillations. The mean ± SD values for phase coupling between arterial BP and RRI oscillations at ~0.1 Hz for all three sessions are summarized in Table II. For example, a strong phase coupling ($COH^2 = 0.69 \pm 0.17$; mean ± SD) was found during rest, not only for slow oscillations in BPdia and RRI (PHA $= -82° \pm 21°$), but also for oscillations in BPsys and RRI ($COH^2 = 0.68 \pm 0.18$; PHA $= -35° \pm 18°$). Only one subject displayed a weak coupling ($COH^2 < 0.5$).

The analysis of phase shifts between slow BP and RRI oscillations revealed not the expected significantly stronger, but only a tendency to a slightly stronger (p = 0.051) phase coupling during cyclic finger movements ($COH^2 = 0.75$) when compared to rest ($COH^2 = 0.69$). The phase shifts between RRI and BPdia, and between RRI and BPsys oscillations were significantly larger ($p < 0.01$) in the cyclic movement session compared to rest ($-93°$ to $-81°$ and $-51°$ to $-35°$, respectively). The phase shift variations over all subjects are visualized in Fig. 2. Also, the time delays between RRI and BPsys oscillations were significantly longer ($p < 0.05$) during cyclic movement ($-1.54$ s) compared to the rest ($-0.99$ s). The correlation values across subjects between the different phase shifts and sessions (rest, cyclic movement) are indicated in Fig. 3.

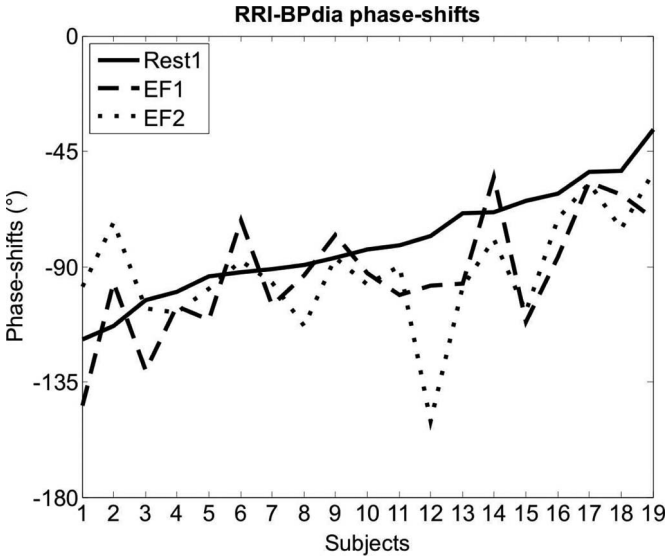


Fig. 2. Display of phase shifts between slow RRI and BPdia oscillations (0° to $-180°$) for all 19 subjects for the sessions rest, cyclic (EF1) and randomized movements (EF2). Subjects are ordered according to the size of phase shifts during rest.

### *B. Phase Shifts Between Slow BP and Prefrontal (De)Oxyhemoglobin Oscillations Around 0.1 Hz*

In detail, the phase coupling between following time series were estimated for the sessions rest, cyclic and randomized movements (in parenthesis, following the names of the two time series, the number of subjects with a $COH^2 \geq 0.5$ during rest are indicated): $HbO_2$ versus BPdia (12 subjects), $HbO_2$ versus RRI (6), $HbO_2$ versus BPsys (5) $HbO_2$ versus Hb (10), Hb versus BPdia (6), Hb versus RRI (7), and Hb versus BPsys (5). The best results involved $HbO_2$ and BPdia: 12 out of 19 subjects showed a $COH^2 \geq 0.5$ during rest with $COH^2 = 0.66 \pm 0.15$ (mean ± SD) and a relative variable phase shift of PHA $= -55° \pm 46°$ documenting that the phase shift between $HbO_2$ and BPdia (with BP leading) was varying between $-1°$ and $-167°$ (see also Fig. 4). These phase shifts were reproduced in the movement tasks. The following correlations were obtained: $r = 0.85$ ($p < 0.01$) for phase shifts between rest and cyclic movements (see Fig. 3) and $r = 0.91$ ($p < 0.01$) between rest and randomized movements. These findings of the great intersubject variability of phase shifts and the high correlation between recordings during rest and finger movement suggest that the phase coupling between $HbO_2$ and BPdia may be one suitable feature for biometric identification. Of interest is also that 12 out of 19 subjects displayed a $COH^2 \geq 0.5$ for coupling between $HbO_2$ and BPdia time series, but only five subjects for coupling between $HbO_2$ and BPsys time series.

### *C. Visualization of Phase Shifts in Form of Subject-Specific Vector Diagrams*

Vector diagrams were constructed for a better visualization of the individual phase differences in the resting state and during cyclic finger movements. The vector diagrams of three different subjects are displayed in Fig. 5. Of interest are the different

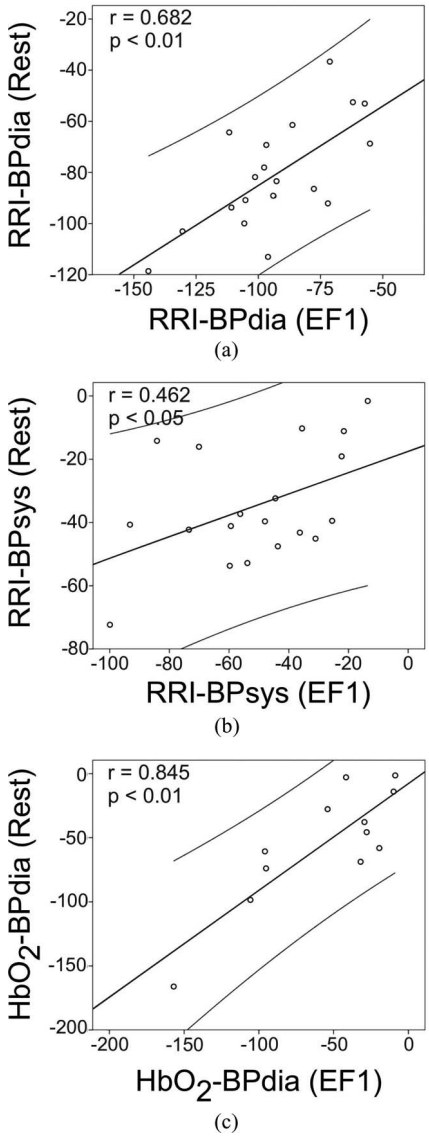


Fig. 3. Scatter plots displaying significant correlations between phase shifts during rest and during cyclic movements (EF1). The larger the phase shift between (a) RRI and BPdia respectively, (b) RRI and BPsys, and (c) RRI and $HbO_2$ during rest, the larger the phase shift during cyclic movement, and vice versa. In addition, the line of best fit and a 95% confidence interval are plotted in the diagrams.

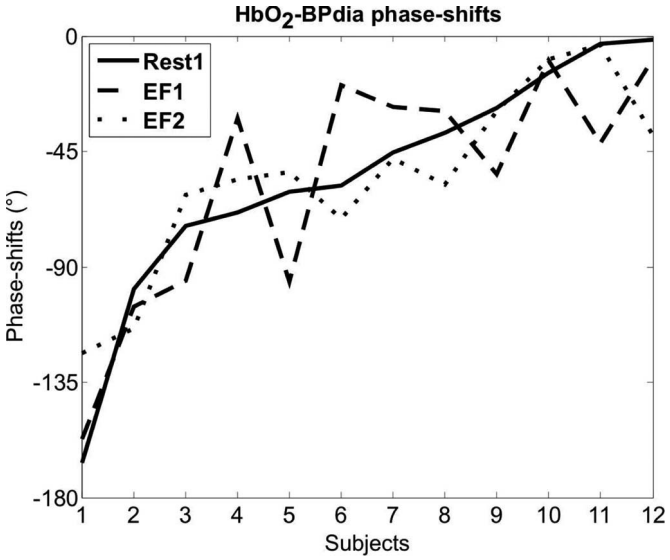


Fig. 4. Display of phase shifts between $HbO_2$ and BPdia oscillations (0° to −180°) for 12 selected subjects ($COH^2 \geq 0.5$ during rest) for the sessions rest, EF1 and EF2. Subjects are ordered according to the size of phase shifts during rest.

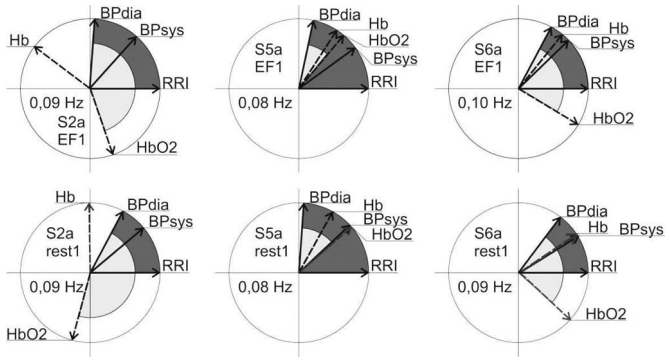


Fig. 5. Examples of vector diagrams from rest (lower diagrams) and movement sessions (upper diagrams) from three characteristic subjects. One with a large phase shift between BPdia and $HbO_2$ (left vector diagrams), one with a medium phase shift (right diagrams) and one with a small phase shift (middle diagrams). Phase differences between BPdia and RRI are indicated by "dark gray" and between $HbO_2$ and BPdia by "bright gray." BPdia leads always RRI and Hb leads always $HbO_2$ oscillations around 0.1 Hz.

"resonance" frequencies between 0.08 and 0.10 Hz, the difference in phase shifts between subjects and the relative similarity of the phase shift differences in the rest and movement sessions in all three subjects.

## IV. Discussion

### *A. Phase Coupling Between Slow Arterial BP and RRI Oscillations Around 0.1 Hz*

Abrupt decreases and increases in systolic arterial BP produce baroreflex-mediated shortening and lengthening, respectively, of the beat-to-beat interval [55] and slow fluctuations in arterial pressure result in subsequent changes in beat-to-beat intervals in the same direction. The phase shifts found during rest were $-35° \pm 18°$ between RRI and BPsys oscillations and $-81° \pm 21°$ between RRI and BPdia oscillations around 0.1 Hz. Relationships between slow BP and RRI oscillations have been reported by cross-spectral analyses [10], [11], [56]. The former reported a phase shift of 60° for the lead of systolic BP to RRI fluctuations and a phase shift of 90° for the lead of diastolic BP fluctuations and the latter a phase shift between −30° and −50° for BPsys and RRI oscillations in the range 0.07–0.13 Hz.

The expected higher phase coupling in all subjects during cyclic movement was not fulfilled. There was only a trend to a higher phase coupling but the increase of coherence reached not significance. In the case of a dominantly linear process, a coherence value close to 1.0 can be expected. Notably, during rest, no subject displayed a $COH^2 > 0.9$, while during cyclic movement, four subjects reached a $COH^2 > 0.9$. In some subjects, however, the coherence (actually $COH^2$) was also close

to 0.5 during cyclic movement. This gives support to the notion that some components in the cardiovascular system are not linear [25], and these components vary from subject to subject. In contrast to the strength of phase coupling, the phase shift was significantly larger between slow oscillations in BPdia and RRI as well as BPsys and RRI during cyclic movement compared to rest. It is well known that under such circumstances (cyclic movements), physiological oscillations may be entrained to behavioral responses and due to the latency (delay) of the BP response in the range of up to 6 s [57] and the premovement cardiac slowing [30], [52], [58] an additional time delay is introduced and the phase shift is enlarged.

### *B. Slow BP-Coupled Oscillations Around 0.1 Hz in Prefrontal (De)Oxyhemoglobin*

This study has used cross-correlation technique in normal subjects to investigate whether slow $HbO_2$ oscillations around 0.1 Hz are related (phase-coupled) to arterial BP oscillations. In only 64% of the subjects, phase-coupled $HbO_2$ and BP oscillations were found. The mean coherence during rest was $0.66 \pm 0.15$ (mean $\pm$ SD), and the mean phase shift was $-55^\circ \pm 46^\circ$. Similar numbers were found during movement (see Table II). The high standard deviation around $40^\circ$ in all sessions can be explained by the phase shifts varying between $\sim$zero [slow $HbO_2$ and BP oscillations are in-phase; for example, see Figs. 1(b) and 5 (middle panel)] and $\sim 180^\circ$ [slow oscillations are out-of-phase; for example, see Figs. 1(a) and 5 (left panel)] during rest but also in movement sessions. This is a novel finding and can be interpreted that in each subject a specific "wiring" exists within and between baroreflex loop and central autonomic networks. No significant phase shift changes were observed during cyclic or randomized movement compared to rest.

The reason for this relatively small number of phase-coupled $HbO_2$ and BP oscillations could be the overwhelming proportion of nonlinearity in cardiovascular and hemodynamic systems [8], [17], [25]–[27]. In all cases, the BP oscillations lead $HbO_2$ oscillations. These results suggest that, at least in some subjects, in addition to intrinsic hemodynamic oscillations, BP-coupled oscillations can also be found in the brain. Besides the NIRS technique, the transcranial Doppler (TCD) sonography technique can help to study the relationship between slow oscillations in the cerebral and cardiovascular systems. It is widely accepted that CBFV as measured by TCD is proportional to the blood flow through insonated vessels and suitable to provide information about cerebral autoregulation [14]. Diehl *et al.* [59] reported a phase shift between arterial BP and CBFV of $71^\circ \pm 30^\circ$ (mean $\pm$ SD) in normal subjects. At this time, it is not clear which relationship does exist between slow BP-coupled $HbO_2$ and CBFV oscillations. TCD measures the velocity (CBFV) of blood flow in the middle cerebral artery, whereas NIRS measures an averaged tissue concentration ($HbO_2$) in the illuminated region that consists of arterial, arteriolar, capillary, and venous flow. An isolated increase of cerebral blood flow will lead to an increase in $HbO_2$ and a decrease in Hb, while an isolated increase in cerebral blood volume leads to an increase in both $HbO_2$ and Hb [60].

The stronger phase coupling between $HbO_2$ and BPdia on the one side, and the weaker coupling between $HbO_2$ and BPsys on the other, is unexpected and needs explanation. One reason could be that slow BPdia changes are clearly leading BPsys changes (see Table II and Fig. 5) and therefore the BPdia may also be seen as the driving force for slow $HbO_2$ oscillations. Another reason could be the physiologically plausible relationship between successive BP values and RR intervals and respiratory variations: the diastolic pressure values depend mainly on the preceding diastolic pressure values and are minimally influenced by respiration; the BPsys is linearly related to RR intervals and strongly modulated by respiration (see models for the baroreflex loop [7], [11]). The more stable behavior of diastolic pressure values could be also a reason for the stronger coupling between $HbO_2$ and BPdia compared to $HbO_2$ and BPsys.

## V. Conclusion

Two points are of interest. First, in about 60% of the subjects, clear BP-coupled $HbO_2$ oscillations around 0.1 Hz were observed in the NIRS signal recorded over the prefrontal cortex. These oscillations can be seen as physiological noise [41] when an optical BCI is realized. They can be removed, e.g., by the use of a transfer function model [61]. The prefrontal cortex is of special interest because the optodes can be easily attached there [34], [35] and because the user's intent is accompanied by the activation of prefrontal networks [62]. Such optical BCIs with optodes placed over the prefrontal cortex might be suitable for use at home or work and can be realized as brain switch either alone or in combination with an EEG-based BCI [34], [35], [63], [64]. Second, phase shifts between slow arterial BP, HR beat-to-beat intervals and oxyhemoglobin oscillations are relatively stable, subject-specific and similar during rest and movement. This is an interesting observation, but it is still unclear if measures of the "eigenfrequency" of slow cardiovascular oscillations and phase shifts between cardiovascular and cerebral oscillations around 0.1 Hz are suitable biometric features for person identification (even in combination with other biometric data). Further research is needed, especially to investigate the reproducibility and long-term stability of these parameters.

## Appendix

### List of Abbreviations

| | |
|---|---|
| BCI | Brain–computer interface |
| BP | Blood pressure (noninvasive recorded continuous signal) |
| BPsys | Systolic BP amplitude |
| BPdia | Diastolic BP amplitude |
| CBFV | Cerebral blood flow velocity |
| $COH^2$ | Coherence squared |
| ECG | Electrocardiogram |
| EF1 | Session with periodically presented cues |
| EF2 | Session with randomly presented cues |
| EHI | Edinburgh-Handedness-Inventory |
| HR | Heart rate |
| Hb | Deoxyhemoglobin |
| $HbO_2$ | Oxyhemoglobin |

| | |
|---|---|
| NIRS | Near-infrared spectroscopy |
| PHA | Phase shift |
| RRI | Beat-to-beat interval |
| TCD | Transcranial Doppler sonography |

## ACKNOWLEDGMENT

The authors are grateful to P. Linortner and R. Ortner for their support in data collection, and B. Allison for English correction.

## REFERENCES

[1] A. von Haller, *Elementa Physiologiae Corporis Humani*. vol II. Lausanne, Swiss: Sumptibus M. M. Bousquet et Sociorum, 1760.

[2] S. Mayer, "Studien zur Physiologie des Herzens und der Blutgefässe. 6. Abhandlung: Über spontane Blutdruckschwankungen," in *Proc. Sitzungsberichte Akademie der Wissenschaften in Wien. Mathematisch-naturwissenschaftliche Klasse, Anatomie*, Wien, Austria, 1876, vol. 74, pp. 281–294.

[3] C. Julien, "The enigma of Mayer waves: Facts and models," *Cardiovasc. Res.*, vol. 70, no. 1, pp. 12–21, Apr. 2006.

[4] A. C. Guyton and J. W. Harris, "Pressoreceptor-autonomic oscillation; a probable cause of vasomotor waves," *Am. J. Physiol.*, vol. 165, no. 1, pp. 158–166, Apr. 1951.

[5] R. DeBoer, J. Karemaker, and J. Strackee, "Hemodynamic fluctuations and baroreflex sensitivity in humans: A beat-to-beat model," *Am. J. Physiol.*, vol. 253, pp. H680–H689, 1987.

[6] J. Madwed, P. Albrecht, R. Mark, and R. Cohen, "Low-frequency oscillations in arterial pressure and heart rate: A simple computer model," *Am. J. Physiol.*, vol. 256, no. 6, pp. H1573–H1579, Jun. 1989.

[7] A. M. VanRoon, L. J. Mulder, M. Althaus, and G. Mulder, "Introducing a baroreflex model for studying cardiovascular effects of mental workload," *Psychophysiology*, vol. 41, no. 6, pp. 961–981, Nov. 2004.

[8] H. Seidel and H. Herzel, "Bifurcations in a nonlinear model of the baroreceptorcardiac reflex," *Phys. D.*, vol. 115, no. 1–2, pp. 145–160, Apr. 1998.

[9] K. Wesseling and J. Settels, "Baromodulation explains short-term blood pressure variability," in *The Psychophysiology of Cardiovascular Control*, J. Orlebeke, G. Mulder, and L. VanDoornen, Eds. New York: Plenum Press, 1985, pp. 69–97.

[10] R. DeBoer, J. Karemaker, and J. Strackee, "Relationships between short-term blood-pressure fluctuations and heart-rate variability in resting subjects. I: A spectral analysis approach," *Med. Biol. Eng. Comput.*, vol. 23, no. 4, pp. 352–358, Jul. 1985.

[11] R. DeBoer, J. Karemaker, and J. Strackee, "Relationships between short-term blood-pressure fluctuations and heart-rate variability in resting subjects. II: A simple model," *Med. Biol. Eng. Comput.*, vol. 23, no. 4, pp. 359–364, Jul. 1985.

[12] S. Vanhatalo, J. Palva, M. Holmes, J. Miller, J. Voipio, and K. Kaila, "Infraslow oscillations modulate excitability and interictal epileptic activity in the human cortex during sleep," *Proc. Natl. Acad. Sci. U.S.A.*, vol. 101, no. 14, pp. 5053–5057, Apr. 2004.

[13] R. Cooper, H. C. W. Walter, and A. Winter, "Regional control of cerebral vascular reactivity and oxygen supply in man," *Brain Res.*, vol. 3, no. 2, pp. 174–191, Dec. 1966.

[14] R. Diehl, D. Linden, and D. Lücke, P. Berlit, "Spontaneous blood pressure oscillations and cerebral autoregulation," *Clin. Auton. Res.*, vol. 8, no. 1, pp. 7–12, Dec. 1998.

[15] N. Lundberg, "Continuous recording and control of ventricular fluid pressure in neurosurgical practice," *Acta Psychiatr. Scand. Suppl.*, vol. 36, no. 149, pp. 1–193, 1960.

[16] M. Schroeter, M. Bücheler, C. Preul, R. Scheid, O. Schmiedel, T. Guthke, and D. Y. von Cramonet, "Spontaneous slow hemodynamic oscillations are impaired in cerebral microangiopathy," *J. Cereb. Blood Flow Metab.*, vol. 25, no. 12, pp. 1675–1684, Dec. 2005.

[17] G. Taga, Y. Konishi, A. Maki, T. Tachibana, M. Fujiwara, and H. Koizumi, "Spontaneous oscillation of oxy- and deoxy- hemoglobin changes with a phase difference throughout the occipital cortex of newborn infants observed using non-invasive optical topography," *Neurosci. Lett.*, vol. 282, no. 1–2, pp. 101–104, Mar. 2000.

[18] V. Toronov, M. Franceschini, M. Filiaci, S. Fantini, M. Wolf, A. Michalos, and E. Gratton, "Near-infrared study of fluctuations in cerebral hemodynamics during rest and motor stimulation: Temporal analysis and spatial mapping," *Med. Phys.*, vol. 27, no. 4, pp. 801–815, Apr. 2000.

[19] Y. Tzeng, S. Lucas, G. Atkinson, C. Willie, and P. Ainslie, "Fundamental relationships between arterial baroreflex sensitivity and dynamic cerebral autoregulation in humans," *J. Appl. Physiol.*, vol. 108, no. 5, pp. 1162–1168, May 2010.

[20] R. Zhang, J. Zuckerman, C. Giller, and B. Levine, "Transfer function analysis of dynamic cerebral autoregulation in humans," *Am. J. Physiol.*, vol. 274, no. 1 pt 2, pp. H233–241, Jan. 1998.

[21] F. Zheng, A. Sassaroli, and S. P. Fantini, "Phasor representation of oxy- and deoxyhemoglobin concentrations: What is the meaning of out-of-phase oscillations as measured by near-infrared spectroscopy?," *J. Biomed. Opt.*, vol. 15, no. 4, pp. 040512-1–040512-3, Jul./Aug. 2010.

[22] J. F. Thayer and R. D. Lane, "Claude bernard and the heart-brain connection: Further elaboration of a model of neurovisceral integration," *Neurosci. Biobehav. Rev.*, vol. 33, no. 2, pp. 81–88, Aug. 2008.

[23] E. Benarroch, "The central autonomic network: Functional organization, dysfunction, and perspective," *Mayo Clin. Proc.*, vol. 68, no. 10, pp. 988–1001, Oct. 1993.

[24] L. Resstel and F. M. Correa, "Involvement of the medial prefrontal cortex in central cardiovascular modulation in the rat," *Auton. Neurosci.*, vol. 126–127, pp. 130–138, Jun. 2006.

[25] C. Wagner and P. Persson, "Chaos in the cardiovascular system: An update," *Cardiovasc. Res.*, vol. 40, no. 2, pp. 257–264, Nov. 1998.

[26] X. Hu, V. Nenov, T. Glenn, L. Steiner, M. Czosnyka, M. Bergsneider, and N. Martin, "Nonlinear analysis of cerebral hemodynamics and intercranial pressure signals for characterization of autoregulation," *IEEE Trans. Biomed. Eng.*, vol. 53, pp. 195–209, 2006.

[27] C. A. Giller and M. Müller, "Linearity and non-linearity in cerebral hemodynamics," *Med. Eng. Phys.*, vol. 25, pp. 633–646, 2003.

[28] A. Verberne and N. Owens, "Cortical modulation of the cardiovascular system," *Prog. Neurobiol.*, vol. 54, no. 2, pp. 149–168, Feb. 1998.

[29] E. Damen and C. Brunia, "Changes in heart rate and slow brain potentials related to motor preparation and stimulus anticipation in a time estimation task," *Psychophysiology*, vol. 24, no. 6, pp. 700–713, Nov. 1987.

[30] D. Papakostopoulos, N. Banerji, and P. Pocock, "Performance, EMG, brain electrical potentials and heart rate change during a self-paced skilled motor task in parkinson's disease," *J. Psychophysiol.*, vol. 4, pp. 163–183, 1990.

[31] B. Yates and S. Stocker, "Integration of somatic and visceral inputs by the brainstem: Functional considerations," *Exp. Brain Res.*, vol. 119, no. 3, pp. 269–275, Apr. 1998.

[32] L. Deecke, B. Grözinger, and H. Kornhuber, "Voluntary finger movement in man: Cerebral potentials and theory," *Biol. Cybern.*, vol. 23, no. 2, pp. 99–119, Apr. 1976.

[33] G. Pfurtscheller and F. L. da Silva, "Event-related EEG/MEG synchronization and desynchronization: Basic principles," *Clin. Neurophysiol.*, vol. 110, no. 11, pp. 1842–1857, Nov. 1999.

[34] G. Bauernfeind, R. Leeb, S. Wriessnegger, and G. Pfurtscheller, "Development, set-up and first results of a one-channel near-infrared spectroscopy system," *Biomed. Tech. (Berl).*, vol. 53, no. 1, pp. 36–43, 2008.

[35] S. Coyle, T. Ward, and M. C., G. McDarby, "On the suitability of near-infrared systems for next generation brain-computer interfaces," *Physiol. Meas.*, vol. 25, pp. 815–822, Aug. 2004.

[36] F. Matthews, P. Pearlmutter, T. Ward, C. Soraghan, and C. Markham, "Hemodynamics for brain-computer interfaces: Optical correlates of control signals," *IEEE Signal Process. Mag.*, vol. 25, no. 1, pp. 87–94, 2008.

[37] S. M. Coyle, T. Ward, and C. Markham, "Brain-computer interface using a simplified functional near-infrared spectroscopy system," *J. Neural Eng.*, vol. 4, no. 3, pp. 219–226, Apr. 2007.

[38] S. Luu and T. Chau, "Decoding subjective preference from single-trial near-infrared spectroscopy signals," *J. Neural Eng.*, vol. 6, no. 1, p. 016003, Apr. 2009.

[39] S. Wriessnegger, J. Kurzmann, and C. Neuper, "Spatio-temporal differences in brain oxygenation between movement execution and imagery: A multichannel near-infrared spectroscopy study," *Int. J. Psychophysiol.*, vol. 67, no. 1, pp. 54–63, Jan. 2010.

[40] G. Pfurtscheller, G. Bauernfeind, S. Wriessnegger, and C. Neuper, "Focal frontal (de)oxyhemoglobin responses during simple arithmetic," *Int. J. Psychophysiol.*, vol. 76, no. 3, pp. 186–192, Jun. 2010.

[41] S. Coyle, T. Ward, and C. Markham, "Physiological noise in near-infrared spectroscopy: Implications for optical brain computer interfacing," in *Proc. IEEE Eng. Med. Biol. Soc. Conf.*, 2004, vol. 6, pp. 4540–4543.

[42] S. Marcel and J. R. Millán, "Person authentication using brainwaves (EEG) and maximum a posteriori model adaptation," *IEEE Trans. Pattern Anal. Mach. Intell.*, vol. 29, no. 4, pp. 743–752, Apr. 2007.

[43] M. Näpflin, M. Wildi, and J. Sarnthein, "Test-retest reliability of resting EEG spectra validates a statistical signature of persons," *Clin. Neurophysiol.*, vol. 118, no. 11, pp. 2519–2524, Nov. 2007.
[44] R. Palaniappan and D. P. Mandic, "Biometrics from brain electrical activity: A machine learning approach," *IEEE Trans. Pattern Anal. Mach. Intell.*, vol. 29, no. 4, pp. 738–742, Apr. 2007.
[45] R. Palaniappan and K. Ravi, "Improving visual evoked potential feature classification for person recognition using PCA and normalization," *Pattern Recog. Lett.*, vol. 27, no. 7, pp. 726–733, May. 2006.
[46] M. Poulos, M. Rangoussi, N. Alexandris, and A. Evangelou, "On the use of EEG features towards person identification via neural networks," *Med. Inform. Internet Med.*, vol. 26, pp. 35–48, Jan. 2001.
[47] L. Thie and E. Fried, "Acclairism: Questioning biometric technology through an airport security clearance system," in *Conf. Human Factors Comput. Syst., CHI'05 Extended Abstracts Human Factors Computing Systems*, Portland, OR, pp. 1148–1149.
[48] S. C. Fang and H. L. Chan, "Human identification by quantifying similarity and dissimilarity in electrocardiogram phase space," *Pattern Recog.*, vol. 42, no. 9, pp. 1824–1831, Sep. 2009.
[49] S. A. Israel, J. M. Irvine, A. Cheng, M. D. Wiederhold, and B. K. Wiederhold, "ECG to identify individuals," *Pattern Recog.*, vol. 38, pp. 133–142, Jan. 2005.
[50] F. Sufi and I. Khalil, "Faster person identification using compressed ECG in time critical wireless telecardiology applications," *J. Netw. Comput. Appl.*, vol. 34, no. 1, pp. 282–293, Jan. 2011.
[51] R. Oldfield, "The assessment and analysis of handedness: The Edinburgh inventory," *Neuropsychologia*, vol. 9, pp. 97–113, 1971.
[52] G. Pfurtscheller, R. Ortner, G. Bauernfeind, P. Linortner, and C. Neuper, "Does conscious intention to perform a motor act depend on slow cardiovascular rhythms?," *Neurosci. Lett.*, vol. 468, pp. 46–50, Jan. 2010.
[53] H. Jasper, "The ten-twenty electrode system of the international federation," *Electroencephalogr. Clin. Neurophysiol.*, vol. 10, pp. 371–375, 1958.
[54] G. Jenkins and D. G. Watts, *Spectral Analysis and Its Applications*. San Francisco, CA: Holden-Day, 1986.
[55] A. Steptoe and C. Vögele, "Cardiac baroreflex function during postural change assessed using non-invasive spontaneous sequence analysis in young men," *Cardiovasc. Res.*, vol. 24, no. 8, pp. 627–632, Aug. 1990.
[56] T. Kuusela, T. Kaila, and M. Kähönen, "Fine structure of the low-frequency spectra of heart rate and blood pressure," *BMC Physiol.*, vol. 13, pp. 3–11, Oct. 2003.
[57] G. Pfurtscheller, D. S. Klobassa, G. Bauernfeind, and C. Neuper, "Cardiovascular responses after brisk finger movement and their dependency on the "eigenfrequency" of the baroreflex loop," *Neurosci. Lett.*, vol. 490, pp. 31–35, 2011.
[58] J. Jennings, M. V. der Molen, R. Somsen, and C. Terezis, "On the shift from anticipatory heart rate deceleration to acceleratory recovery: Revisiting the role of response factors," *Psychophysiology*, vol. 27, pp. 385–395, 1990.
[59] R. Diehl, D. Linden, D. Lücke, and P. Berlit, "Phase relationship between cerebral blood flow velocity and blood pressure. a clinical test of autoregulation.," *Stroke*, vol. 3, pp. 1801–1804, Oct. 1995.
[60] M. Wolf, U. Wolf, V. Toronov, A. Michalos, A. L. Paunescu, J. Choi, and E. Gratton, "Different time evaluation of oxyhämoglobin and deoxyhämoglobin concentration changes in visual and motor cortices during functional stimulation: A near-infrared spectroscopy study," *Neuroimage*, vol. 16, pp. 704–712, 2002.
[61] G. Florian, A. Stancak, and G. Pfurtscheller, "Cardiac responses induced by voluntary selfpaced finger movements," *Int. J. Psychophys.*, vol. 28, pp. 273–283, 1998.
[62] P. Haggard, "Conscious intention and motor cognition," *Trends Cogn. Sci.*, vol. 9, pp. 290–295, Jun. 2005.
[63] M. Naito, Y. Michioka, K. Ozawa, Y. Ito, M. Kiguchi, and T. Kanazawa, "Hemodynamics for brain-computer interfaces: Optical correlates of control signals," *IEEE Signal Process. Mag.*, vol. 25, no. 1, pp. 87–94, 2008.
[64] G. Pfurtscheller, B. Allison, C. Brunner, G. Bauernfeind, T. Solis-Escalante, R. Scherer, T. Zander, G. Müller-Putz, C. Neuper, and N. Birbaumer, "The hybrid BCI," *Front Neurosci.*, vol. 4, pp. 1–11, Apr. 2010, doi: 10.3389/fnpro.2010.00003.

**Gert Pfurtscheller** (M'00) received the M.S. and Ph.D. degrees in electrical engineering from the Graz University of Technology, Graz, Austria.

He was a Full Professor of Medical Informatics and a Professor of Brain–Computer Interfaces at the Graz University of Technology (TUG), a Visiting Professor at Cape Town University and Vancouver University and is an Emeritus Professor at TUG since October 2009. He was the Head of the Institute of Biomedical Engineering, the Director of the Ludwig Boltzmann Institute for Medical Informatics and Neuroinformatics and is the Founding Director of the Brain–Computer Interface Laboratory (BCI-Lab), TUG. He has authored more than 300 publications in peer-reviewed journals and published four books. He was honored by election as a member of the Austrian Academy of Science.

**Daniela S. Klobassa** received the M.S. degree in psychology from the Karl Franzens University of Graz, Graz, Austria. She is currently working toward the M.D. degree from the Medical University of Graz, Graz.

She is a Research Associate at the Institute of Knowledge Discovery, University of Technology, Graz. Her research interests include brain–computer interface and neurophysiology.

**Christof Altstätter** received the M.S. degree in electrical and biomedical engineering from the Graz University of Technology, Graz, Austria.

He is currently at the Laboratory of Brain–Computer Interfaces, Institute for Knowledge Discovery, Graz University of Technology. He is a Research Associate at the Institute for Knowledge Discovery.

**Günther Bauernfeind** received the M.S. degree in electrical and biomedical engineering from the Graz University of Technology, Graz, Austria, where he is currently working toward the Ph.D. degree.

He is a Research Associate at the Institute for Knowledge Discovery. His research interests include optical brain–computer communication systems and biosignal processing.

**Christa Neuper** received the Ph.D. degree in psychology from the University of Graz, Graz, Austria.

She is the Head of the Institute for Knowledge Discovery, which hosts the Brain-Computer Interface Laboratory at the Graz University of Technology, and a Full Professor of Neuropsychology at the University of Graz. Her research interests include development and basic research for brain–computer communication, neurorehabilitation, and neuronal correlates of cognitive processes.

Neuroscience Letters 490 (2011) 31–35

Contents lists available at ScienceDirect

Neuroscience Letters

journal homepage: www.elsevier.com/locate/neulet

# Cardiovascular responses after brisk finger movement and their dependency on the "eigenfrequency" of the baroreflex loop

Gert Pfurtscheller[a,*], Daniela S. Klobassa[a,b], Günther Bauernfeind[a], Christa Neuper[a,b]

[a] Laboratory of Brain-Computer Interfaces, Institute for Knowledge Discovery, Graz University of Technology, Krenngasse 37, A-8010 Graz, Austria
[b] Department of Psychology, University of Graz, A-8010 Graz, Austria

ARTICLE INFO

*Article history:*
Received 18 October 2010
Received in revised form 7 December 2010
Accepted 8 December 2010

*Keywords:*
Slow arterial blood pressure oscillations
Mayer waves
Finger movement
Heart rate response
Blood pressure response
Baroreflex loop

ABSTRACT

The baroreflex is mainly involved in short-term blood pressure regulation and strongly influenced by activations of medullary circulation centres in the brain stem and higher brain centres. One important feature of the baroreflex is its strong preference for oscillations around 0.1 Hz, which can be seen as resonance or "eigenfrequency" (EF) of the control loop (so-called Mayer waves). In the present study we investigated beat-to-beat heart rate intervals (RRI) and arterial blood pressure (BP) changes after brisk finger movement and their relationship to the "eigenfrequency" determined by cross spectral analysis between RRI and arterial blood pressure time series of 17 healthy subjects. The analyses revealed significant correlations between BP response magnitude ($r = 0.63$, $p < 0.01$) respectively RRI response magnitude ($r = 0.59$, $p < 0.05$) and EF. This can be interpreted in such a way that subjects with a "high" EF (>0.10 Hz) elicit larger BP responses as well as larger RRI responses when compared to subjects with a "low" EF (<0.10 Hz).



The baroreflex is mainly involved in short-term blood pressure (BP) regulation and strongly influenced by activations of medullary circulation centres in the brain stem and higher brain centres. Important components of the baroreflex loop are the baroreceptors converting BP changes to neural activity, the cardiopulmonary receptors, the cardiovascular nuclei in the brain stem and the heart with circulation (for review see Seidel and Herzel [21] and Van Roon et al. [25]). The various effector systems are controlled via vagal and sympathetic efferents, whereby the most important effector is the vagally controlled heart rate (HR) via the sino-atrial (SA) node. The SA node lying near the right atrium is the driving force of the heart's rhythm. The SA node responds very quickly to vagal (~150 ms latency) in contrast to sympathetic (~1–2 s) influence [23].

One important feature of the baroreflex loop is its strong preference for oscillations around 0.1 Hz, which can be seen as resonance or "eigenfrequency" (EF, so-called Mayer waves) of the loop [10,25,26]). Such 0.1 Hz oscillations have been reported not only in the BP and HR but also in different physiological signals. So Cooper et al. [3] reported irregular rhythmical changes in the oxygen availability of cortical tissue of about six waves per minute and Lundberg [13] found intracranial pressure fluctuations at a rate of 4–8/min. Schroeter et al. [20] reported on spontaneous low-frequency oscillations of oxyhemoglobin ($HbO_2$) at optodes placed over the occipital cortex, and Witte et al. [27] described the occurrence of EEG bursts in full-term newborns ("tracé alternant" EEG pattern) in intervals of approximately 10 s. Of interest are also spontaneous oscillations in cerebral blood flow velocity (CBFV) measured with Doppler ultrasound probes around 0.1 Hz (see e.g. [8,24,29]). Recently, common fluctuations around 0.1 Hz have been reported in BP, HR and prefrontal recorded $HbO_2$ signals [18].

The objective of the present study was to investigate the relationship between BP and beat-to-beat heart rate intervals (RRI) responses after cued brisk finger movement and the EF of the baroreflex loop. Brisk finger movements are often used to investigate cardiac responses [9,14,18]. In brisk movements, motor commands are prepared in unity and sent off in one package. In contrast, slow movement motor commands undergo continual feedback control from higher centres, which adaptively shape the movement regarding direction and force [7]. Cued movements allow a controlled investigation of the response patterns, in comparison to self-paced (at free will) movements, which are triggered by the subject's internal strategies. Knowledge of the magnitude of HR (inverse of RRI) responses in individual subjects can be useful in the case of a hybrid brain–computer interface (BCI) system based on simultaneous EEG and HR processing. It has been suggested that the performance of a BCI may be enhanced when both EEG and ECG are simultaneously analyzed and classified during mental simulation of movement [19].

Twenty-six naive subjects (12 male, 14 female) aged 19–31 years ($M = 23$, SD = 2.8) participated voluntarily in the present study. All subjects were right-handed (Edinburgh-Handedness-Inventory

* Corresponding author. Tel.: +43 316 873 5301; fax: +43 316 873 5349.
*E-mail address:* pfurtscheller@tugraz.at (G. Pfurtscheller).

0304-3940/$ – see front matter © 2010 Elsevier Ireland Ltd. All rights reserved.
doi:10.1016/j.neulet.2010.12.020

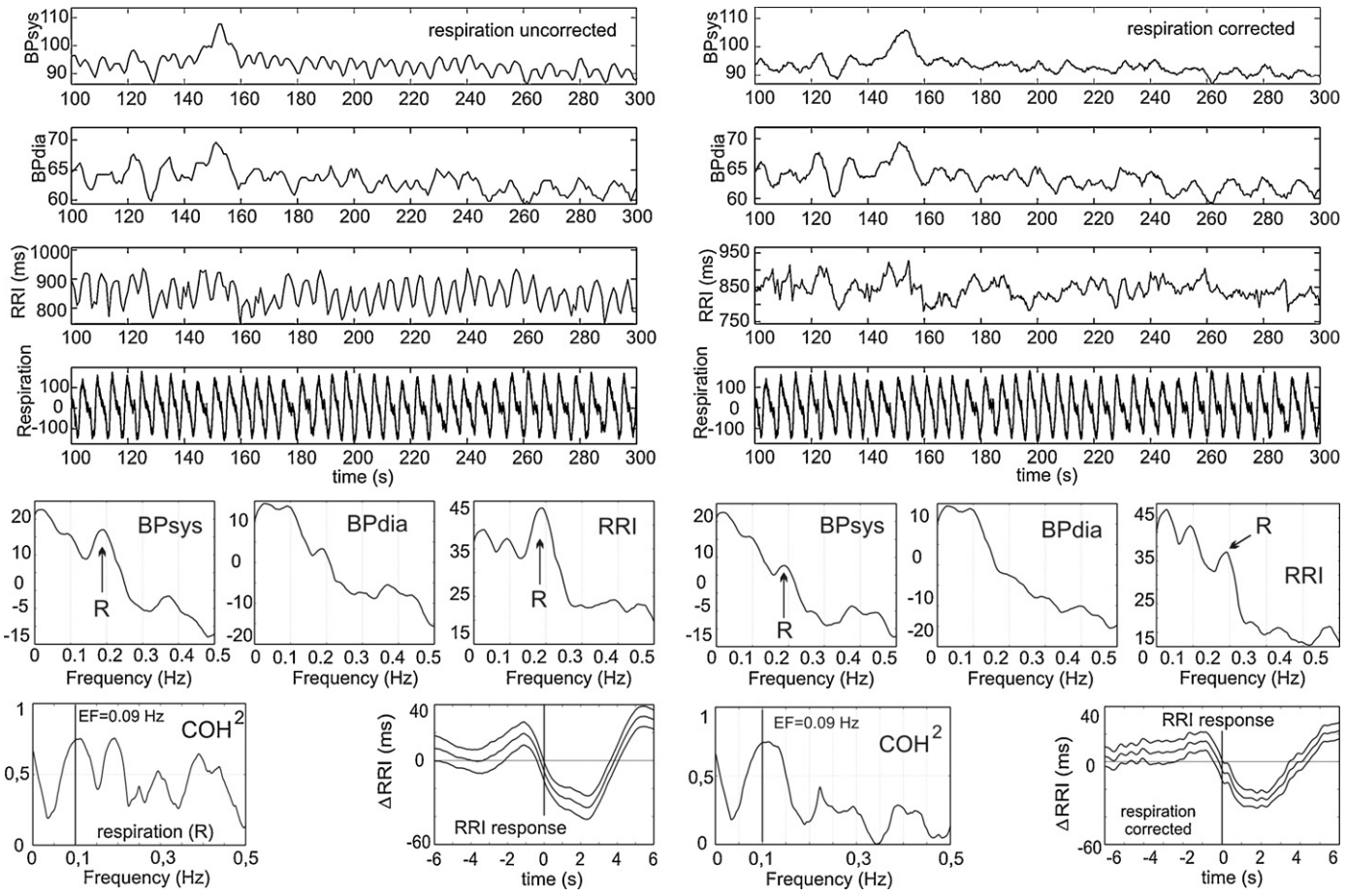


**Fig. 1.** Upper part: examples of systolic blood pressure (mm Hg), diastolic blood pressure (mm Hg), RR interval (ms) time series and respiration signal (a.u.) recorded during rest (200 s) in subject AS2. Respiration-corrected data (right side) and uncorrected data (left side) are presented. Lower part: power spectra for BP and RRI time series, coherence spectra for RRI and BPdia ($COH^2$) and averaged RRI responses for respiration-corrected (right side) and uncorrected signals (left side). The respiration peak in the spectra is indicated ("R").

(EHI) [15]), sitting in a comfortable chair, and gave their written informed consent for the study, which was approved by the ethics committee of the Medical University of Graz. The study consisted of different sessions, namely data recording during rest, during self-paced brisk finger movements, periodic cued finger movements and cue-paced finger movements in random intervals. Part of the data about self-paced movements has been published recently [18]. Here we report on data from 5-min recordings during rest and brisk finger movements in cued randomized intervals; the intervals varied between 9 and 23 s and the total recording time was ~11 min.

After inspection of the data, four subjects were eliminated due to high blood pressure, irregular respiration, extra ventricular contractions, and/or recording artefacts. Missing of heart or BP beats or triggering to another event, such as an extrasystole, may have large effects on the evoked responses and the power spectra, respectively [1]. Therefore, the detection process and the averaged data were both visually inspected. Five additional subjects were thus excluded, leaving 17 subjects for further data analysis.

For this study, we analyzed the ECG recorded bipolarly at electrodes placed on the thorax (filter setup: 0.5–100 Hz). For BP recording, a continuous non-invasive monitoring system (CNAP™ Monitor 500, CNSystems, Austria) was used. Data were recorded from the proximal limb of the index or middle finger. The respiration patterns were obtained by using a respiratory sensor (Respiratory Effort Sensor, Pro-Tech Services Inc., filter setup: 0.1–100 Hz). ECG, blood pressure (BP) and the respiration were sampled at a frequency of 500 Hz.

The first step in ECG processing was to detect the QRS complexes in the electrocardiogram (ECG). Afterwards, RR intervals were linearly interpolated and displayed as RRI time series. From the arterial BP recording, the beat-to-beat systolic (BPsys) and diastolic (BPdia) pulse pressures were extracted, linearly interpolated and also time series generated. A transfer function model [9] was used to remove respiratory-related variability from instantaneous RRI- and BP-time series. Examples of time series with and without respiration correction are displayed in Fig. 1. Fig. 1 shows also the respiratory variability, especially in the RRI and BPsys time series (Fig. 1, left side). After respiration correction, the respiration-related variability is clearly reduced (Fig. 1, right side).

The EF can be determined from various signals as RRI or BP-time series through auto spectra calculations and spectral peak termination, as well as from the complex cross spectrum (coherence and phase spectra) between RRI and BP time series. When one dominant peak was found in the cross spectrum between 0.07 and 0.13 Hz it was interpreted as the "eigenfrequency" of the baroreflex loop (examples of coherence spectrum, see Fig. 1). When no peak was found, the frequency was set to 0.1 Hz. Cross spectra were calculated from the RRI, and the BP beat-to-beat time series resampled at 2 Hz (for details on the used procedure, see DeBoer et al. [5,6]).

Respiration corrected BP- and RRI-time series were averaged across trials starting 6 s prior and ending 6 s after movement onset. RRI responses were standardized by expressing the responses as difference scores in (ms) between the positive peak immediately before movement-onset and the following negative peak in a 4-s window after movement. In the case of BP responses, the dif-

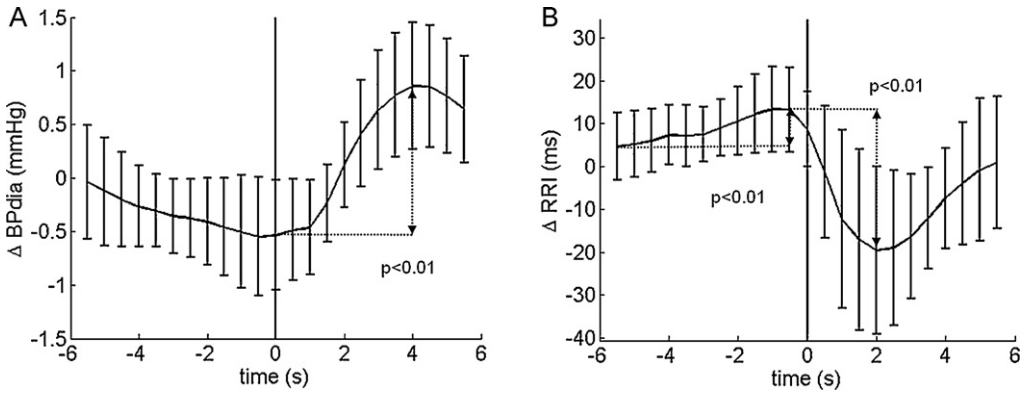


**Fig. 2.** Grand average time courses of diastolic blood pressure changes (A) and RRI changes (B) for the time period 6 s before and 6 s after brisk finger movement. Error bars indicate ±SD of the mean calculated for 500 ms intervals. Significant RRI changes (between 5.5 s and 0.5 s prior to movement and between 0.5 s prior to 2 s after movement) and blood pressure changes (between 0 s and 4 s after movement) are indicated. Zero indicates the onset of cue presentation (movement began ~250 ms afterwards).

ferences in (mm Hg) are reported between a 1-s interval during movement-onset (baseline) and the following positive peak within a 8-s window. In this paper, we focus exclusively on the analysis of BPdia responses. The averaged BPdia response displayed in the majority of subjects a smaller intertrial variance when compared with the systolic pressure. This suggests that BPdia responses display a small intertrial variability and/or fewer disturbances, caused perhaps through the automated respiration correction. BPdia responses are also less influenced by exercise, effort and respiration than systolic BP responses [12].

Statistical analysis contained a paired sample *t*-test for evaluating BP changes before and after movement, an ANOVA with repeated measures and a Tukey's HSD post hoc test for evaluating RRI changes at three time-points before and after movement. Pearson's product moment correlation was used for evaluating possible relations between EF and BP responses, respectively, RRI responses. Important assumptions for these methods like normal distribution and variance homogeneity of the data were met.

Grand average RRI and BPdia responses (mean ± SD) are displayed in Fig. 2 and the characteristic features are summarized in Table 1. The heart rate shows a biphasic response starting with a deceleration before movement, followed by a fast acceleration after movement. In contrast, the BPdia response is monophasic, with a maximum at 4.4 s ± 1.1 (mean ± SD) after movement onset. In both cases, statistical analysis revealed significant changes in RRI and BP responses. On average, all 17 subjects showed a highly significant increase (5.28 ms) in RRI (cardiac slowing) prior to movement onset (95% confidence interval (CI) 19.83–41.02; $p = 0.000$), a highly significant decrease (30.43 ms) in RRI (cardiac acceleration) after movement (95% CI −35.73 to −14.55; $p = 0.000$), and a highly significant increase (1.42 mm Hg) in BP after movement (95% CI −1.91 to 0.93; $p = 0.000$).

Correlation analysis revealed not only a significant correlation ($r = 0.627$; $p < 0.01$) between the BPdia responses defined by its magnitude (ΔBP in mm Hg) and the EF (Fig. 3A), but also a significant correlation ($r = 0.586$; $p < 0.05$) between the RRI responses in ms (Fig. 3B) and the EF, as well as between the BPdia delay in s and the EF (Fig. 3C). The higher the EF the higher the BP and RRI response magnitudes and the longer the BPdia delay and vice versa. In addition there is a significant relationship between RRI changes and BP changes (Fig. 3D). The higher the BP response magnitude, the longer the RRI and vice versa.

The estimation of the EF of the baroreflex loop revealed subject-specific values whereby either one dominant spectral peak or multiple peaks of various magnitudes were detected in the range 0.07–0.13 Hz. The multiple peaks can be caused either by a slightly changing EF as function of time or by the simultaneous existence of two or more slow oscillations around 0.1 Hz. Support for the latter gives a paper reporting on the fine structure of low-frequency RRI and BP spectra [11]. They found two principal frequency com-

**Table 1**
Basic data of the group, RRI, HR and BP response characteristics, and "eigenfrequencies". The mean and SD are also indicated for each feature.

| Cue-paced movement | | | | | | | | | Rest |
|---|---|---|---|---|---|---|---|---|---|
| Subj. | Sex | Age (years) | HR (bpm) | ΔRRI (ms) | RRI delay (s) | BPdia (mm Hg) | ΔBPdia (mm Hg) | BPdia delay (s) | EF (Hz) |
| AS2 | m | 26 | 63 | 43 | 2.3 | 71 | 2.1 | 4.5 | 0.09 |
| AS4 | f | 23 | 76 | 21 | 4.4 | 72 | 1.2 | 6.8 | 0.08 |
| AS6 | m | 23 | 89 | 33 | 2.7 | 72 | 2.0 | 5.2 | 0.08 |
| AS7 | m | 20 | 68 | 102 | 2.2 | 61 | 2.6 | 3.9 | 0.11 |
| AS8 | f | 20 | 70 | 42 | 4.8 | 59 | 1.1 | 6.2 | 0.09 |
| AU2 | m | 27 | 64 | 19 | 1.2 | 67 | 0.9 | 3.3 | 0.09 |
| AU3 | m | 23 | 61 | 66 | 0.9 | 69 | 2.0 | 3.0 | 0.13 |
| AT7 | m | 23 | 65 | 103 | 1.4 | 77 | 2.5 | 3.0 | 0.11 |
| AQ9 | m | 26 | 70 | 18 | 1.5 | 79 | 1.2 | 3.5 | 0.08 |
| AS3 | f | 22 | 61 | 19 | 2.0 | 71 | 0.7 | 4.5 | 0.11 |
| AS5 | m | 31 | 68 | 16 | 4.0 | 61 | 0.5 | 5.8 | 0.08 |
| AU4 | f | 20 | 63 | 34 | 2.4 | 60 | 1.1 | 3.6 | 0.09 |
| AU5 | f | 24 | 66 | 54 | 3.0 | 73 | 3.1 | 3.8 | 0.11 |
| AT6 | m | 27 | 63 | 32 | 2.0 | 78 | 1.3 | 4.0 | 0.10 |
| AT9 | m | 21 | 60 | 32 | 2.5 | 65 | 0.7 | 5.5 | 0.09 |
| AU6 | f | 21 | 74 | 20 | 1.5 | 67 | 1.0 | 4.0 | 0.09 |
| AS9 | f | 21 | 84 | 37 | 3.5 | 78 | 3.7 | 4.5 | 0.12 |
| Mean | | 23.41 | 68.53 | 40.65 | 2.49 | 69.41 | 1.60 | 4.42 | 0.10 |
| SD | | 3.08 | 8.16 | 26.74 | 1.13 | 6.61 | 0.94 | 1.13 | 0.02 |

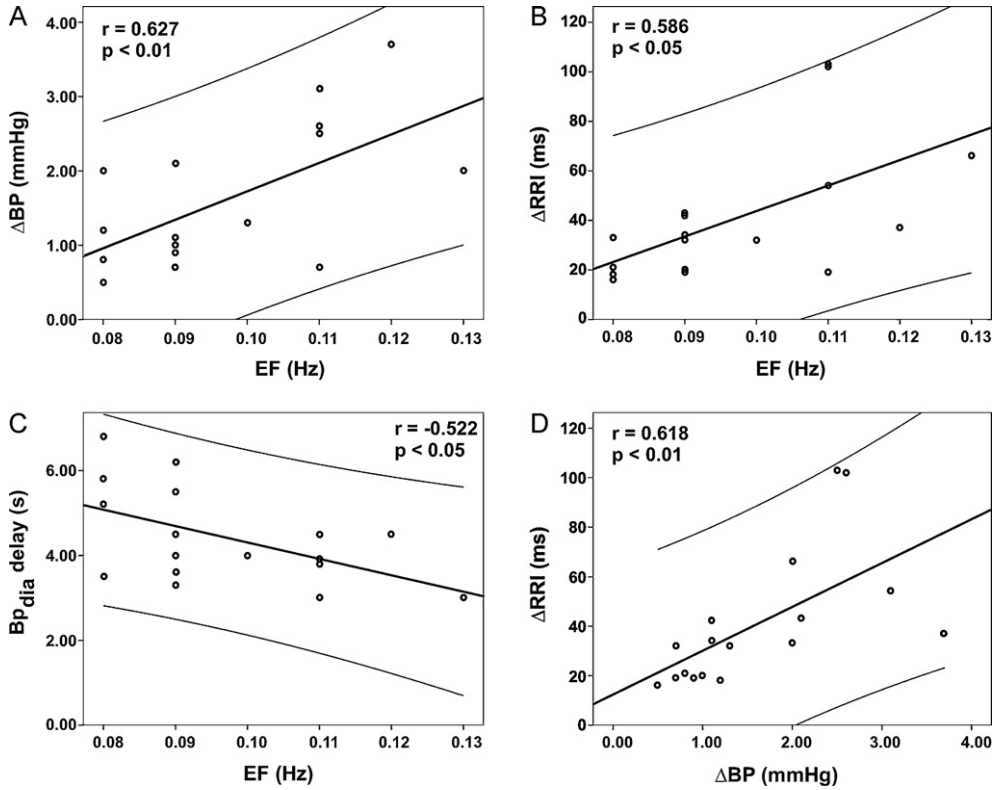


**Fig. 3.** Scatter plots displaying relationships between blood pressure change (A), RRI change (B), BPdia delay (C) and "eigenfrequency". In addition, the relationship between RRI and BP changes is indicated (D). The line of best fit and a 95% confidence interval are plotted in the diagrams.

ponents, one at $0.076 \pm 0.012$ Hz and another at $0.117 \pm 0.016$ Hz both with only slight variations over a recording time of 12 min. This is of interest because we frequently found peaks at similar frequencies in only 5 min of data.

One limitation of the spectral techniques used is that they can only cope with linear systems. The cardiovascular system constituting of two basic oscillators: the cardiac pacemaker, which generates the heartbeat with a period of about 1 s; the baroreflex loop, which causes BP and HR oscillations around 10 s and is non-linear [21]. However, RRI and BP changes were small so that the calculation via cross spectrum might not have been biased by non-linearity. In this relationship, it is also important to note that there was a significant linear correlation between RRI and BPdia changes (see Fig. 3D).

The EF can be determined not only from BP spectra [18] but also from cross spectral analysis of BP and RRI time series. We think the latter is more suitable because of the strong link between BP and HR regulation within the baroreceptor loop. Decreases and increases in arterial BP produce baroreflex-mediated shortening and lengthening, respectively, of the RR intervals [22].

Concerning the RRI and BP responses elicited through brisk finger movement two mechanisms have to be considered: first, "central commands" are relayed to cardiovascular nuclei in the brain stem that control the heart rate. Furthermore, somatic musculature is innervated via efferences from motor cortex. Second, the reafferent input from kinaesthetic receptors evoked by the movement elicits changes in blood pressure known as "exercise pressure response" [28]. The RRI response starts with a significant cardiac deceleration more than 2 s prior to stimulus presentation and movement onset. It is generally accepted that both attention directed toward an external stimulus (cue) and motor preparation are accompanied by a cardiac slowing [2,4]. The muscular contraction accounts for the cardiac acceleration (RRI decrease) after a latency of ~0.5 s due to abrupt suppression of vagal neural afferents. Both cardiovascular responses show a great inter-subject variability whereby large responses in the BP are also manifest in RRI time series, documented by a significant correlation ($r = 0.618$, $p < 0.01$) between both responses.

Although the cardiovascular system is highly non-linear, some linearity can be assumed because of the small RRI and BPdia changes observed in the order of ~100 ms and ~5 mm Hg close to the resting values. When a linear system generates spontaneous oscillations with frequencies of e.g. 0.1 Hz, the response function should consist of a type of damped sinusoidal response with the same frequency [21]. Therefore, it is not unexpected that "fast" oscillations (EF > 0.1 Hz) are accompanied by a short-latency (short delay) response and "slow" oscillations (EF < 0.1 Hz) by a long-latency response. This relationship is documented by significant correlations between EF and RRI response ($r = 0.586$, $p < 0.05$) and EF and BP response magnitude ($r = 0.627$, $p < 0.01$). The correlation between BP responses and EF was slightly stronger than the correlation between RRI responses and EF. This is not surprising because the primary goal of the baroreflex loop with its characteristic EF is to regulate the blood pressure and not the heart rate. The novel result is that subjects with a higher EF of the baroreflex loop share larger BP and RRI responses with short delays.

Recently, a new type of hybrid brain–computer interface (BCI) was introduced based on simultaneous EEG and HR processing [19]. It has been suggested that the performance of a BCI can be enhanced when motor imagery related changes are simultaneously processed and classified not only in the EEG but also in the ECG. Such motor imagery elicited HR changes in the order of several beats-per-minute have been reported during BCI experiments in a highly immersive virtual environment [16,17]. Such a hybrid BCI may work best for users with a large cardiac response. The determination of the "eigenfrequency" can help identify such users. Subjects with a higher EF may be more suitable for such a hybrid BCI than subjects with a low EF.

## Acknowledgements

The work was supported by the EU project PRESENCCIA (IST-27731), "Land Steiermark" (project A3-22.N-13/2009-8), the Neuro Center Styria (NCS) and the "Allgemeine Unfallversicherungsanstalt" (AUVA). The authors are grateful to P. Linortner and R. Ortner for their support in data collection, C. Altstätter for software support and B. Allison for English correction.

## References

[1] G.G. Berntson, J.R. Stowell, ECG artifacts and heart period variability: don't miss a beat!, Psychophysiology 35 (1998) 127–132.
[2] G. Bohlin, A. Kjellberg, Orienting activity in two-stimulus paradigms as reflected in heart rate, in: H. Kimmel, E. Van Olst, J.F. Orlebeke (Eds.), The Orienting Reflex in Humans, Erlbaum, Hillsdale, NJ, 1979, pp. 169–198.
[3] R. Cooper, H.J. Crow, W.G. Walter, A.L. Winter, Regional control of cerebral vascular reactivity and oxygen supply in man, Brain Res. 3 (1966) 174–191.
[4] E.J.P. Damen, C.H.M. Brunia, Changes in heart rate and slow brain potentials related to motor preparation and stimulus anticipation in a time estimation task, Psychophysiology 24 (1987) 700–713.
[5] R.W. DeBoer, J.M. Karemaker, J. Strackee, Relationships between short-term blood-pressure fluctuations and heart-rate variability in resting subjects. I. A spectral analysis approach, Med. Biol. Eng. Comput. 23 (1985) 352–358.
[6] R.W. DeBoer, J.M. Karemaker, J. Strackee, Hemodynamic fluctuations and baroreflex sensitivity in humans: a beat-to-beat model, Am. J. Physiol. 253 (1987) H680–H689.
[7] J.E. Desmedt, Size principle of the recruitment and the calibration of the muscle force and speed in man, in: J.E. Desmedt (Ed.), Motor Control Mechanism in Health and Disease, Advances in Neurology, Raven Press, NY, 1983, pp. 227–251.
[8] R.R. Diehl, D. Linden, D. Lücke, P. Berlit, Spontaneous blood pressure oscillations and cerebral autoregulation, Clin. Auton. Res. 8 (1998) 7–12.
[9] G. Florian, A. Stancak, G. Pfurtscheller, Cardiac response induced by voluntary self-paced finger movement, Int. J. Psychophysiol. 28 (1998) 273–283.
[10] C. Julien, The enigma of Mayer waves: facts and models, Cardiovasc. Res. 70 (2006) 12–21.
[11] T.A. Kuusela, T.J. Kaila, M. Kähönen, Fine structure of the low-frequency spectra of heart rate and blood pressure, BMC Physiol. 13 (2003) 3–11.
[12] V.V. Le, T. Mitiku, G. Sungar, J. Myers, V. Froelicher, The blood pressure response to dynamic exercise testing: a systematic review, Prog. Cardiovasc. Dis. 51 (2008) 135–160.
[13] N. Lundberg, Continuous recording and control of ventricular fluid pressure in neurosurgical practice, Acta Psychiatr. Scand. Suppl. 36 (1960) 1–193.
[14] P.A. Obrist, R.A. Webb, J.R. Sutter, Heart rate and somatic changes during aversive conditioning and a simple reaction time task, Psychophysiology 5 (1969) 696–723.
[15] R.C. Oldfield, The assessment and analysis of handedness: the Edinburgh inventory, Neuropsychologia 9 (1971) 97–113.
[16] G. Pfurtscheller, R. Leeb, M. Slater, Cardiac responses induced during thought-based control of virtual environments, Int. J. Psychophysiol. 62 (2006) 134–140.
[17] G. Pfurtscheller, R. Leeb, D. Friedman, M. Slater, Centrally controlled heart rate changes during mental practice in immersive virtual environment: a case study with a tetraplegic, Int. J. Psychophysiol. 68 (2008) 1–5.
[18] G. Pfurtscheller, R. Ortner, G. Bauernfeind, P. Linortner, C. Neuper, Does conscious intention to perform a motor act depend on slow cardiovascular rhythms? Neurosci. Lett. 468 (2010) 46–50.
[19] G. Pfurtscheller, B.Z. Allison, C. Brunner, G. Bauernfeind, T. Solis-Escalante, R. Scherer, T.O. Zander, G.M. Mueller-Putz, C. Neuper, N. Birbaumer, The hybrid BCI, Front. Neurosci. (2010), doi:10.3389/fnpro.2010.00003.
[20] M.L. Schroeter, M.M. Bücheler, C. Preul, R. Scheid, O. Schmiedel, T. Guthke, D. Yves von Cramonet, Spontaneous slow hemodynamic oscillations are impaired in cerebral microangiopathy, J. Cereb. Blood Flow Metab. 25 (2005) 1675–1684.
[21] H. Seidel, H. Herzel, Bifurcations in a nonlinear model of the baroreceptorcardiac reflex, Physica D 115 (1998) 145–160.
[22] H.S. Smyth, P. Sleight, G.W. Pickering, Reflex regulation of arterial pressure during sleep in man. A quantitative method of assessing baroreflex sensitivity, Circ. Res. 24 (1969) 109–121.
[23] J.F. Spear, K.D. Kronhaus, E.N. Moore, R.P. Kline, The effect of brief vagal stimulation on the isolated rabbit sinus node, Circ. Res. 44 (1979) 75–88.
[24] Y.C. Tzeng, S.J.E. Lucas, G. Atkinson, C.K. Willie, P.N. Ainslie, Fundamental relationships between arterial baroreflex sensitivity and dynamic cerebral autoregulation in humans, J. Appl. Physiol. 108 (2010) 1162–1168.
[25] A.M. Van Roon, L.J.M. Mulder, M. Althaus, G. Mulder, Introducing a baroreflex model for studying cardiovascular effects of mental workload, Psychophysiology 41 (2004) 961–981.
[26] K.H. Wesseling, J.J. Settels, Baromodulation explains short term blood pressure Variability, in: J.F. Orlebeke, G. Mulder, L.P.J. Van Doornen (Eds.), The Psychophysiology of Cardiovascular Control, Plenum Press, New York, 1985, pp. 69–97.
[27] H. Witte, P. Putsche, K. Schwab, M. Eiselt, M. Helbig, T. Suesse, On the spatiotemporal organisation of quadratic phase-couplings in 'tracé alternant' EEG pattern in full-term newborns, Clin. Neurophysiol. 115 (2004) 2308–2315.
[28] B.J. Yates, S.D. Stocker, Integration of somatic and visceral inputs by the brainstem: functional considerations, Exp. Brain Res. 119 (1998) 269–275.
[29] R. Zhang, J.H. Zuckerman, C.A. Giller, B.D. Levine, Transfer function analysis of dynamic cerebral autoregulation in humans, Am. J. Physiol. Heart Circ. Physiol. 274 (1998) 233–241.

frontiers in
NEUROSCIENCE

PERSPECTIVE ARTICLE
published: 16 April 2010
doi: 10.3389/fnpro.2010.00003

# The hybrid BCI

**Gert Pfurtscheller[1]*, Brendan Z. Allison[1], Clemens Brunner[1], Gunther Bauernfeind[1], Teodoro Solis-Escalante[1], Reinhold Scherer[2], Thorsten O. Zander[3], Gernot Mueller-Putz[1], Christa Neuper[1] and Niels Birbaumer[4,5]**

[1] *Laboratory of Brain-Computer Interfaces, Institute for Knowledge Discovery, Graz University of Technology, Graz, Austria*
[2] *Computer Science and Engineering, University of Washington, Seattle, WA, USA*
[3] *Team PhyPA, Department of Human-Machine Systems, Berlin University of Technology, Berlin, Germany*
[4] *Institute of Medical Psychology and Behavioral Neurobiology, Eberhard-Karls-University, Tübingen, Germany*
[5] *Istituto di Ricovero e Cura a Carattere Scientifico, Ospedale San Camillo, Venezia, Italy*

***Edited by:***
*José del R. Millán,*
*Ecole Polytechnique Fédérale de Lausanne, Switzerland*

***Reviewed by:***
*Dario Farina,*
*Aalborg University, Denmark*
*Shangkai Gao,*
*Tsinghua University, China*

***Correspondence:**
*Gert Pfurtscheller, Laboratory of Brain-Computer Interfaces, Institute for Knowledge Discovery, Graz University of Technology, Krenngasse 37, Graz 8010, Austria.*
*e-mail: pfurtscheller@tugraz.at*

Nowadays, everybody knows what a hybrid car is. A hybrid car normally has two engines to enhance energy efficiency and reduce CO2 output. Similarly, a hybrid brain-computer interface (BCI) is composed of two BCIs, or at least one BCI and another system. A hybrid BCI, like any BCI, must fulfill the following four criteria: (i) the device must rely on signals recorded directly from the brain; (ii) there must be at least one recordable brain signal that the user can intentionally modulate to effect goal-directed behaviour; (iii) real time processing; and (iv) the user must obtain feedback. This paper introduces hybrid BCIs that have already been published or are in development. We also introduce concepts for future work. We describe BCIs that classify two EEG patterns: one is the event-related (de)synchronisation (ERD, ERS) of sensorimotor rhythms, and the other is the steady-state visual evoked potential (SSVEP). Hybrid BCIs can either process their inputs simultaneously, or operate two systems sequentially, where the first system can act as a "brain switch". For example, we describe a hybrid BCI that simultaneously combines ERD and SSVEP BCIs. We also describe a sequential hybrid BCI, in which subjects could use a brain switch to control an SSVEP-based hand orthosis. Subjects who used this hybrid BCI exhibited about half the false positives encountered while using the SSVEP BCI alone. A brain switch can also rely on hemodynamic changes measured through near-infrared spectroscopy (NIRS). Hybrid BCIs can also use one brain signal and a different type of input. This additional input can be an electrophysiological signal such as the heart rate, or a signal from an external device such as an eye tracking system.

**Keywords: brain–computer interface, hybrid BCI, motor imagery, event-related desynchronization, SSVEP**

## INTRODUCTION

Brain–computer interface (BCI) research is advancing very rapidly. Most BCI research still focuses on restoring communication and control in severely paralysed patients (Birbaumer et al., 1999; Wolpaw et al., 2002; Pfurtscheller et al., 2008a), but BCIs are quickly becoming useful to healthy people too (Allison et al., 2007; Nijholt et al., 2008). Modern BCIs may use invasive and non-invasive recording techniques, and non-invasive BCIs may rely on electrical potentials, magnetic fields, and hemodynamic changes (Wolpaw et al., 2006; Vaadia and Birbaumer, 2009). Non-invasive BCIs utilize changes in the dynamics of brain oscillations such as event-related (de)synchronization (ERD, ERS), steady-state evoked potentials (SSEPs), P300 evoked potentials and related components, real-time fMRI BOLD signals or near-infrared spectroscopy (NIRS)-measured oxyhemoglobin signals (Pfurtscheller et al., 2005a; Birbaumer and Cohen, 2007; Sitaram et al., 2007). Each of these BCIs has advantages and disadvantages.

Conventional "simple" BCIs rely on only one of these signals. Here, we describe ways to combine different approaches to create a "hybrid" BCI that exploits the advantages of different approaches. We also describe "hybrid" BCIs that combine a BCI with another interface.

A hybrid car usually has two engines, which rely on electricity and gasoline. The major goals of such a hybrid car are to enhance their energy efficiency and to reduce their $CO_2$ output. Similarly, a typical hybrid BCI is also composed of one BCI and another system (which might be another BCI), and must also achieve specific goals better than a conventional system. For example, a hybrid BCI might infer user intent more accurately during imagery-based and/or visual attention-based experimental paradigms, improve the overall performance of the system, or reduce the rate of false positives during resting periods of i.e. steady-state visual evoked potential (SSVEP)-based BCI applications. The hybrid BCI can either have more than one input whereby the inputs are typically processed simultaneously (**Figures 1B,C**) or operate two systems sequentially, whereby the first system can act as a "brain switch" (**Figures 1A,D,E**) or as "selector" (**Figures 1F,G**). There are other types of sequential BCIs possible, which could go beyond these switch/selector concepts and/or incorporate P300-based or other types or BCIs. We use the terms "simultaneous" and "sequential" to refer to these two types of hybrid BCIs. In both cases, as in any BCI, at least one of the input signals must be a signal recorded directly from the brain.

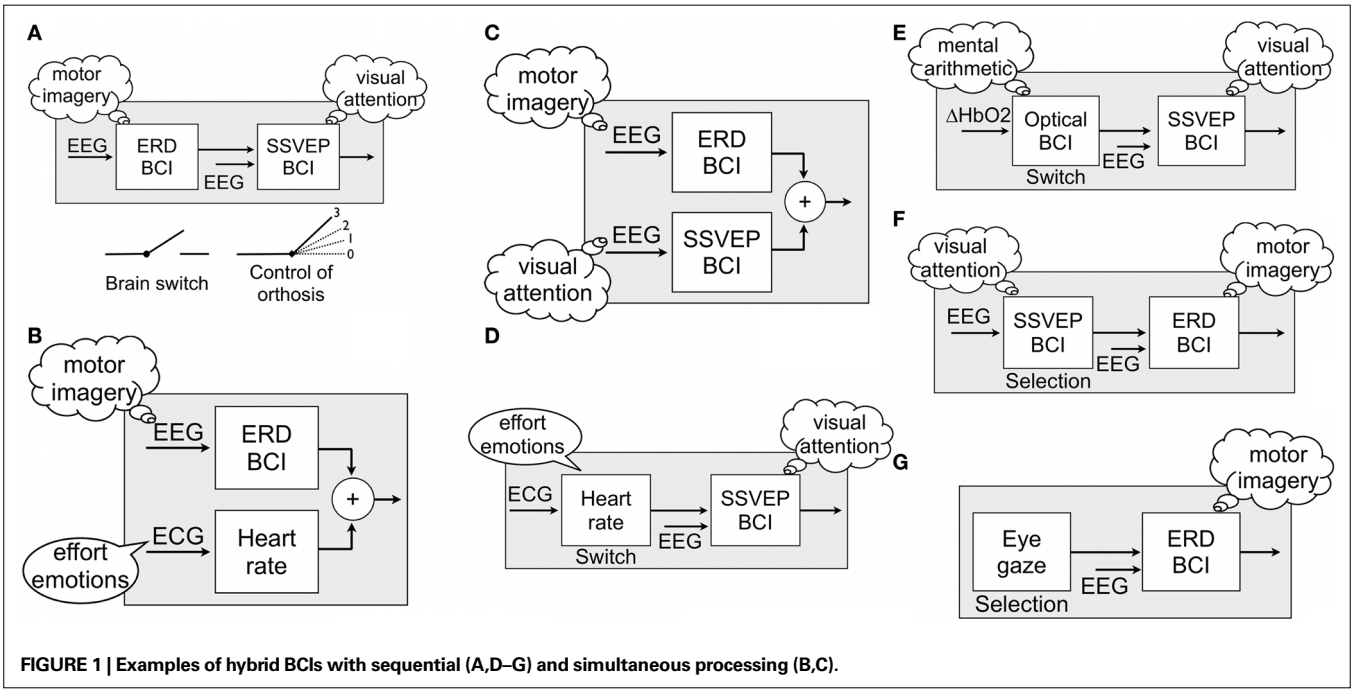


**FIGURE 1 | Examples of hybrid BCIs with sequential (A,D–G) and simultaneous processing (B,C).**

A brain switch is a BCI system designed to detect only one brain state (brain pattern) in the ongoing brain activity. A brain switch, like any communication system, should not produce any output when the user does not intend to communicate. In other words, the false positive rate should be as low as possible. Mason and Birch (2000) were the first to develop a brain switch based on EEG. They proposed a low-frequency asynchronous switch design able to automatically recognize single-trial, voluntary motor related potentials from ongoing EEG activity in bipolar channels. Recent work demonstrated that a single channel brain switch can also be realized when the post-imagery beta ERS is detected in the EEG during motor imagery (Pfurtscheller et al., 2005b; Pfurtscheller and Solis-Escalante, 2009; Solis-Escalante et al., 2010). A brain switch can also rely on SSVEPs with a high amplitude threshold (Cheng et al., 2002) or hemodynamic changes measured through NIRS (Coyle et al., 2007).

A simultaneous hybrid BCI can either use two different brain signals (e.g. electrical and hemodynamic signals), one brain signal (e.g. EEG) associated with two mental strategies (motor imagery and spatial visual attention; **Figure 1C**), or one brain signal and another input. Such an additional input can be a physiological signal like the electrocardiogram (ECG, **Figure 1B**) or a signal from an external device such as an eye gaze control system (Zander et al., in press).

Hybrid BCIs, like any BCI, must fulfil four criteria to function as BCI:

1. Direct: The system must rely on activity recorded directly from the brain.
2. Intentional control: At least one recordable brain signal, which can be intentionally modulated, must provide input to the BCI (electrical potentials, magnetic fields or hemodynamic changes).
3. Real time processing: The signal processing must occur online and yield a communication or control signal.
4. Feedback: The user must obtain feedback about the success or failure of his/her efforts to communicate or control.

## HYBRID BCI SYSTEMS

### SIMULTANEOUS ERD/SSVEP BCI TO IMPROVE ACCURACY

In a recent study, we evaluated the feasibility of combining two mental tasks that simulated a simultaneous hybrid BCI (**Figure 1C**). Fourteen subjects participated in three conditions that simulated a binary BCI (a BCI that allows two choices). In all conditions, each trial began with an arrow pointing to the left or right, which indicated that the subject should perform a left or right motor imagery task. In the first condition (the ERD condition), the left task was imagined left hand movement, and the right task was imagined right hand movement. In the second condition (the SSVEP condition), a left arrow cued the subject to focus attention on a left LED that flickered at 8 Hz, and the right arrow cued the subject to focus on a right LED that flickered at 13 Hz. In the third condition (the hybrid condition), a left arrow cued the subject to both imagine left hand movement and attend to the left LED, while the right arrow cued the subject to both imagine right hand movement and attend to the right LED. Performance was measured by classification accuracy (that is, whether a classifier could correctly distinguish left versus right tasks from the EEG) and subjective report (based on questionnaires). **Table 1** summarizes the resulting classification accuracies as well as the number of illiterates (subjects whose classification accuracy was below 70%). More details can be found elsewhere (Allison et al., 2010; Brunner et al., 2010).

There were four noteworthy results. First, classification accuracy was highest in the hybrid condition, although this effect did not reach statistical significance. Second, in both the ERD and SSVEP conditions, some subjects could not attain proficiency, meaning that their classification accuracy was too low for effective communication.

**Table 1 | Mean and standard deviation of the classification accuracy of 14 subjects in each condition.**

| | ERD | SSVEP | Hybrid |
|---|---|---|---|
| Mean accuracy (%) | 69.4 | 82.8 | 84.5 |
| Standard deviation (%) | 8.6 | 12.2 | 10.2 |
| Number of illiterates | 11 | 3 | 1 |

*The bottom row shows the number of illiterates, corresponding to subjects with a classification accuracy below 70%.*

This phenomenon has been called "BCI illiteracy" by some authors (Kübler and Müller, 2007; Nijholt et al., 2008). However, when a subject was not proficient with either the ERD or SSVEP approach, s/he was usually proficient with the other approach. This result implies that people who could not use an ERD BCI might attain proficiency with an SSVEP BCI, and vice versa. Third, the number of illiterates in the hybrid condition was significantly lower than in the ERD condition, while there was no significant difference in illiteracy in the SSVEP-hybrid comparison or the ERD-SSVEP comparison. This implies that subjects who could not use an ERD or SSVEP BCI could use a hybrid BCI. Fourth, the questionnaire responses revealed that subjects generally did not consider the hybrid condition more difficult than the other two conditions. Hence, a hybrid BCI might yield improved performance without taxing the user any more than a conventional simple BCI.

## SEQUENTIAL ERS-BASED BRAIN SWITCH TO TURN ON/OFF AN SSVEP BCI

The sequential hybrid BCI approach was inspired by earlier work that showed that SSVEP BCIs often send signals when the user did not intend to convey anything (called false positives), which can be especially problematic during breaks or resting periods. We recorded SSVEPs bipolarly from electrodes placed over the occipital area (electrode position O1, 2.5 cm inter-electrode distance). Subjects could focus on one of two LEDs mounted on an orthosis to open or close the orthosis whenever they wanted (Otto Bock Healthcare Products GmbH, Vienna, Austria). That is, we implemented a self-paced or asynchronous BCI, rather than a cue-paced or synchronous BCI. Subjects received real-time feedback by watching the orthosis open or close, and could hence correct errors. Our paradigm included some resting periods (breaks), during which the subjects were asked to avoid sending any commands. The LEDs continued to flicker during breaks, and the SSVEP detection algorithm remained active.

**Figure 2** summarizes the results in 10 able-bodied subjects (Linortner et al., 2009). The main findings were that most subjects could perform the task without training, but produced many false positives. Interestingly, good and bad performers displayed about the same rate of false positives during all resting periods, which collectively lasted several minutes. The rate of false non-intended commands in resting periods (FPr) was between 4 and 5/min, while the rate of false commands during orthosis control (FPa) was between 0.1 and 0.4/min. Hence, we wanted to find a way to improve this system by reducing the false positive rate.

The ERS-based brain switch detects brisk imagined foot movements in one Laplacian EEG channel recorded at the vertex (Cz) (Solis-Escalante et al., 2008, 2010; Pfurtscheller and Solis-Escalante, 2009), and can be seen as a special type of ERD BCI. Foot motor imagery induces a relatively stable pattern, known as post-imagery ERS or beta rebound, which can be easily recorded with electrodes overlaying the foot representation area close to the vertex (Pfurtscheller et al., 2005b; Pfurtscheller and Lopes da Silva, 1999). A post-imagery beta ERS-based brain switch has three appealing features: minimal training time for both the user and the classifier; effective communication with only one EEG channel; and few false positives.

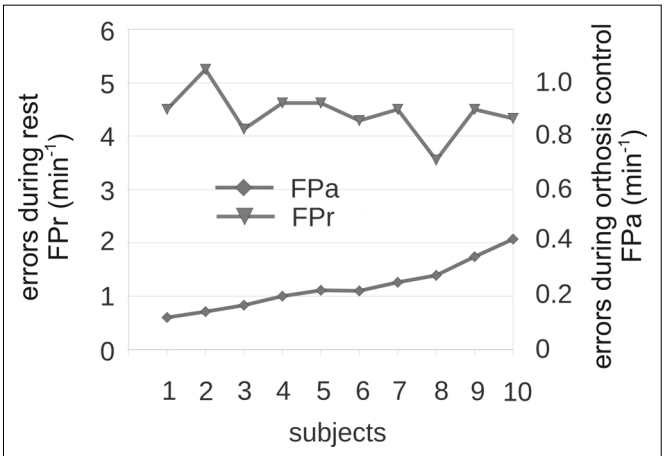


**FIGURE 2 | Performance measures of hand orthosis control in 10 subjects.** This figure displays the errors during orthosis control (FPa; right *y*-axis: scale 0–1.0) and during rest (FPr; left *y*-axis: 0–6). The *x*-axis presents subjects organized from low to high FPa. Subjects' FPas did not affect their FPrs.

We hypothesized that FPs during SSVEP conditions might be reduced by allowing subjects to deactivate the LEDs and SSVEP detection via the brain switch when they do not want to send commands. **Figure 1A** illustrates this concept of using a hybrid BCI that uses a brain switch to turn on/off an SSVEP BCI. We developed an ERS-based switch to activate or deactivate a four-step SSVEP-based orthosis. Users operate the SSVEP part of the BCI by gazing at an 8-Hz LED to open it, and gazing at a 13-Hz LED to close it. The brain switch ensures that the LEDs and SSVEP detection algorithms (Müller-Putz et al., 2008) only operate when needed for control; the user can deactivate the LEDs and SSVEP detection algorithm during resting periods.

**Figure 3** shows additional examples of self-paced switch control and orthosis operation in a healthy subject. Data from two runs (each lasting about 400 s) are displayed separately for the brain switch and the SSVEP orthosis control. In the first run four errors (FP) occurred with the switch during the total experiment. The orthosis control was erroneous in the first orthosis activity period, but nearly perfect thereafter. The situation improved in the second run, since no error occurred during switch control (FP = 0). This example shows a benefit of learning the dual task paradigm in this hybrid BCI, as documented by the improvements in run#2, and also shows that such a hybrid BCI is feasible (Pfurtscheller et al., 2010b).

This hybrid approach requires shifting between motor and visual tasks. Imagined movement induced the post-imagery ERS (beta rebound, used in switch), whereas visual attention modulates SSVEPs. Throughout the self-paced task, the user always obtained feedback

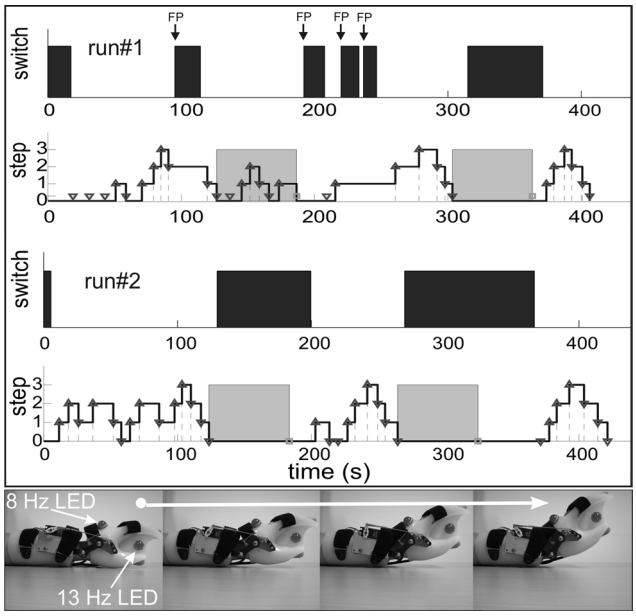


**FIGURE 3 | Examples of two runs (runs #1 and #2) in one able-bodied subject (s3) over several minutes each.** The lower traces of runs #1 and #2 display the four-step sequence of opening/closing the SSVEP-based orthosis with two 60-s breaks (grey shaded). The upper traces of runs #1 and #2 show the ERS-based switch operation (black bars indicate switch opened). The four-steps of orthosis opening (from left to right) are displayed in the bottom panel.

about success or failure of BCI operation, and could therefore adapt his or her mental strategy if necessary. **Table 2** shows the positive prediction value PPV [PPV = TP/(TP + FP)] for the brain switch (called PPVb) and for the SSVEP BCI (called PPVa) over six runs. The PPVb was 0.77 ± 0.19 (mean ± SD), and the PPVa was 0.73 ± 20.

## NIRS-BASED BCI AS A BRAIN SWITCH

In preliminary work, we explored an asynchronous hybrid BCI that combines a NIRS BCI with SSVEP orthosis control (**Figure 1E**). The optical BCI is based on NIRS and measures mentally modulated oxyhemoglobin ($HbO_2$) changes at closely spaced optodes placed over a predefined cortical area (for examples see Coyle et al., 2007; Bauernfeind et al., 2008).

One healthy subject performed four runs with the hybrid BCI system. In each run, the subject had to open and close (one activation block) the orthosis three times (for details see Sequential ERS-based Brain Switch to Turn On/Off an SSVEP BCI and Pfurtscheller et al., 2010b), each at self paced intervals, with 60 s breaks between the blocks (resting periods). Prior to the first block, the subject had to initiate the SSVEP orthosis control using the optical BCI. The brain switch was activated if the relative oxyhemoglobin concentration change (measured with two closely spaced optodes over position Fp1, see **Figure 4**), normalized to a 4-s baseline interval, exceeded a subject-specific value. During the resting period and after the last activation block, the subject was instructed to switch off the SSVEP orthosis control system to avoid FPs.

During the first two runs, FPs were detected in the activation as well as in the resting period. **Figure 4** shows that the subject displayed perfect performance in the third run using the NIRS switch, and only one FP occurred during the SSVEP orthosis control. In the last run, the subject displayed perfect performance with 100% accuracy, meaning no FPs occurred in the NIRS and SSVEP control, respectively.

Like the EEG, NIRS is well suited to BCI applications outside the lab. NIRS requires a simple optode montage, is relatively resistant to artefacts, and can be combined with EEG recording to

**Table 2 | Results from our study involving a brain switch to turn on/off an SSVEP based orthosis.**

| Subject/run | Brain switch | | | SSVEP | |
|---|---|---|---|---|---|
| | TP | FP | PPVb | PPVa | FPr ($min^{-1}$) |
| S11 | 5 | 0 | 1.00 | 0.47 | 0.00 |
| S12 | 5 | 2 | 0.71 | 0.52 | 0.50 |
| S21 | 11 | 9 | 0.55 | 0.82 | 2.50 |
| S22 | 8 | 3 | 0.73 | 1.00 | 1.00 |
| S31 | 7 | 4 | 0.64 | 0.79 | 3.00 |
| S32 | 5 | 0 | 1.00 | 0.76 | 0.00 |
| Mean | 6.83 | 3.00 | 0.77 | 0.73 | 1.17 |
| SD | 2.40 | 3.35 | 0.19 | 0.2 | 1.29 |

*The six runs reflect two runs each from three subjects. We show the rates of TPs, FPs and PPVb of the ERD BCI (switch) and PPVa and rate of errors/minute during resting periods (FPr) of the SSVEP BCI.*

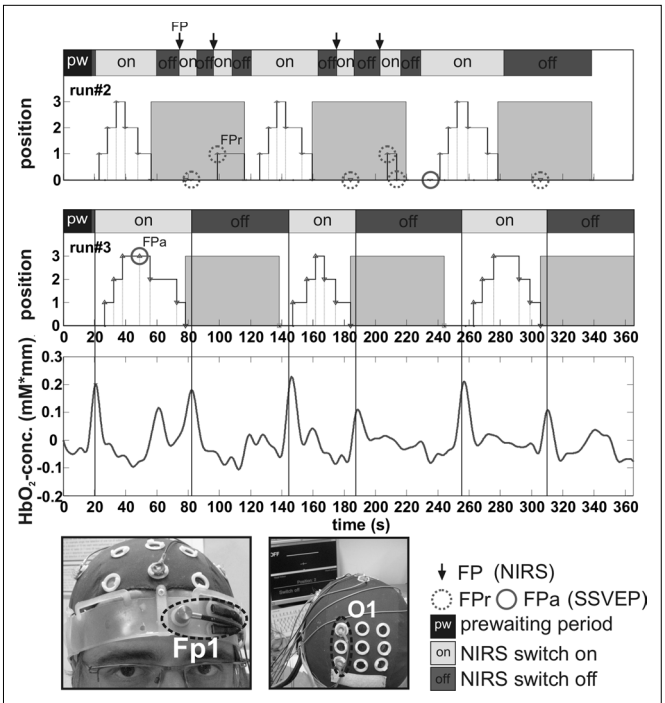


**FIGURE4 | From top to bottom: Position trace of the switch (grey areas mark closed switch position) and four-step SSVEP-based orthosis control trace (grey areas indicate 60-s resting periods) of run#2; position trace of brain switch and orthosis control of run#3; level of oxyhemoglobin ($HbO_2$) concentration of run#3; views of prefrontal optodes and bipolar occipital EEG electrode placements.** FPs of switch (FP) and SSVEP-based orthosis control (FPa, FPr) are indicated. Note the $HbO_2$ peaks associated with the intended mental tasks.

allow simultaneous measurement of electrical and hemodynamic changes. Both imaging approaches can detect specific brain states with a minimum of sensors (one bipolar EEG channel and two optodes). However, EEG can detect brain changes instantly, whereas NIRS entails a delay of a few seconds (Coyle et al., 2007). Further research is necessary to identify better training strategies, new experimental paradigms, and optimal optode positions to reliably classify data from a one or two NIRS channel BCI systems.

Spatio-temporal differences in brain oxygenation during movement execution and imagery were reported by Wriessnegger et al. (2008). They used a 24-channel NIRS system and explored the topographical distribution of the NIRS responses in a movement task. Their work showed that optode location selection and/or optimization is very important when developing a one-channel optical BCI suitable within a hybrid BCI.

## ENHANCEMENT OF BCI ACCURACY WITH BOTH EEG AND HEART RATE EVALUATION

Neocortical structures and the cardiovascular nuclei in the brain stem communicate intensively (Verberne and Owens, 1998). Central commands can activate cardiovascular nuclei in the brainstem and modify the heart rate (HR). Hence, motor imagery produces changes not only in characteristic EEG patterns (Pfurtscheller and Neuper, 2001), but also in the HR (Pfurtscheller et al., 2006, 2008b).

The HR can display either an event-related HR deceleration or acceleration. Two responses can be distinguished with HR deceleration: an early response related to stimulus anticipation and registration; and a second response related to motor preparation (Lacey and Lacey, 1980; Damen and Brunia, 1987; Papakostopoulos et al., 1990). One characteristic and stable HR response is its deceleration prior to internally (self)-paced finger movements (Florian et al., 1998; Pfurtscheller et al., 2010a). HR acceleration is also a common response to many situations; HR acceleration was reported during mental simulation of movement (Decety et al., 1991; Oishi et al., 2000) and during motor imagery (Papadelis et al., 2007; Pfurtscheller et al., 2008b).

Preparation of a specific movement and imagination of the same movement involve similar cortical networks (Porro et al., 1996; Lotze et al., 1999). Execution of movement is generally accompanied by a biphasic HR response starting with a preparatory decrease, followed by a fast increase and a decrease to the baseline (Brunia and Damen, 1985; Papakostopoulos et al., 1990; Florian et al., 1998). In training sessions with an EEG-based BCI (hand versus foot motor imagery), the HR usually decelerates (see Fig. 2 in Pfurtscheller et al., 2006). However, during EEG-based control of "walking" in a virtual street, the same mental strategy can induce HR acceleration (see Fig. 3 in Pfurtscheller et al., 2006). This suggests that the increased somatomotor effort and emotional processing ("walking" in virtual reality) are driving forces behind the HR acceleration. During a similar walking experiment in a virtual street, a tetraplegic patient revealed a significant HR increases in parallel with the mentally induced beta bursts (**Figure 5**).

The HR changes in the order of 10–20 bpm during effortful mental activity suggest that the BCI performance could be improved when a hybrid BCI uses both the EEG and the HR

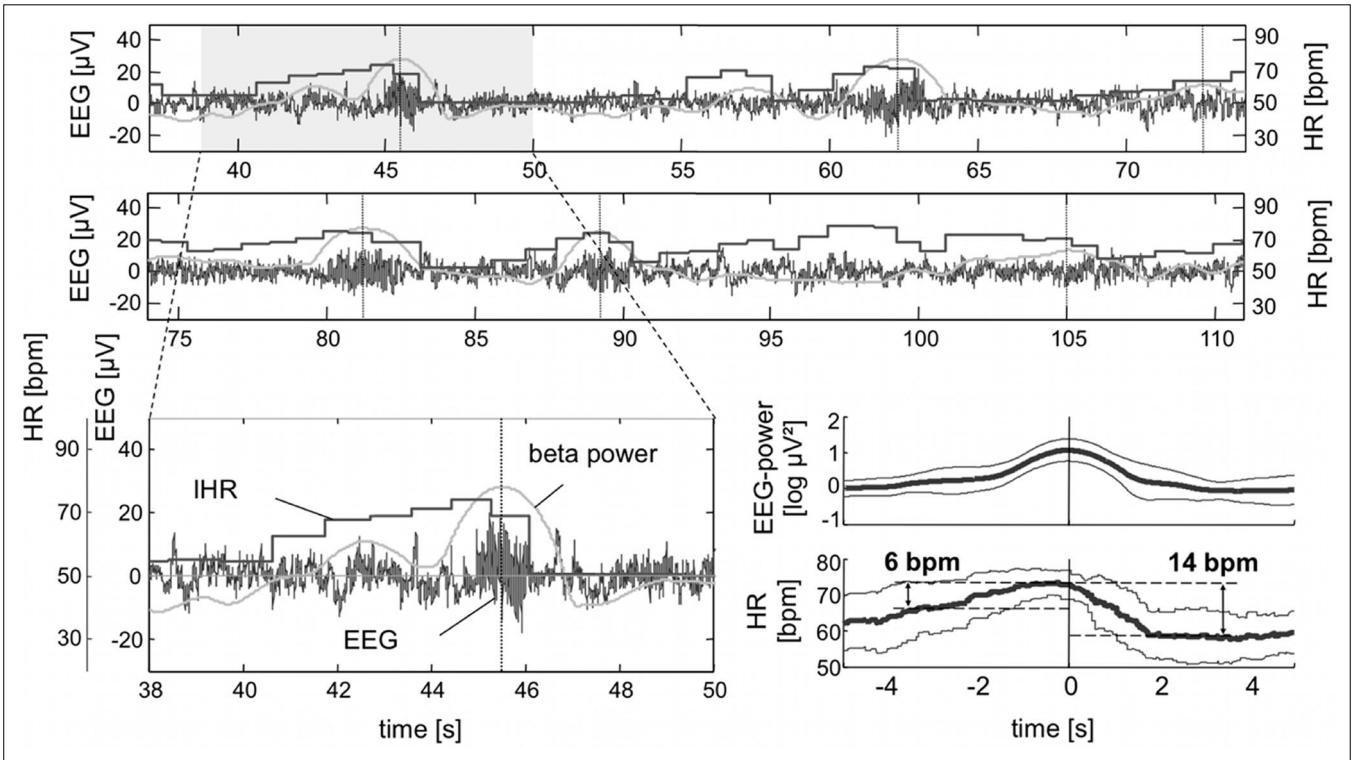


**FIGURE 5 | Raw EEG, heart rate and time course of the logarithmic band power (15–19 Hz), enlarged from a 10-s time window (lower panel, left), and averaged logarithmic beta power (mean ± SD) together with synchronous averaged HR response (mean ± SD, lower panel, right).** Remarkably, the HR increase starts some seconds before the band power enhancement. Modified from Pfurtscheller et al. (2008b).

response simultaneously for control purposes (**Figure 1B**). **Figure 6** presents offline analyses of the HR changes in the tetraplegic patient, which revealed that changes in the differentiated HR (dHR) can be detected in parallel with the motor imagery-induced EEG bursts used for online control.

#### INDUCED HR CHANGES FOR ON/OFF SWITCHES IN A SSVEP BCI

The previous section explored hybridizing a BCI with HR activity to increase accuracy. However, transient HR changes could also be used in a switch that is hybridized with a BCI, like a brain switch based on the ERD (see Sequential ERS-based Brain Switch to Turn On/Off an SSVEP BCI) or the hemodynamic response (see NIRS-based BCI as a Brain Switch). Respiration and blood pressure waves usually modulate the constant intrinsic rhythm of the heart. However, HR changes can also be modulated by central commands. Therefore, individuals may modulate their own HR by mental activity correlated with somatomotor processes (see Brunia and Damen, 1985; Papakostopoulos et al., 1990). Behaviourally triggered HR changes can be used in a switch (**Figure 1D**).

In an initial feasibility study to explore this prospect, we used brisk inspiration to modulate the HR. The HR-triggered switch could turn the SSVEP-operated prosthetic hand on and off. We recorded the ECG and computed the HR. Changes of the HR measured in beat-to-beat intervals (RRI) were computed and used to initiate the SSVEP BCI control. An on/off event was generated each time the relative change (dRRI), induced by brisk inspiration, exceeded the subject-specific threshold (see **Figure 7B**). The relative RRI change with the highest true positive rates during the cue-guided inspiration, and the lowest false positive detections during the remaining tasks, were selected through receiver operating analysis and used as basis for the online experiments.

Four light emitting diodes were affixed on the hand prosthesis (see **Figure 7A**), each flickering at a different frequency between 6.3 and 17.3 Hz (stimulation frequency). The EEG was recorded bipolarly from EEG electrodes placed 2.5 cm anterior and posterior to electrode position O2. The harmonic sum decision algorithm (Müller-Putz et al., 2005) was used for the SSVEP classification. The flickering light source with the highest harmonic sum within a given time period triggered the prosthetic hand movement. A typical selection time period of about 1.5 s was estimated empirically for each subject (see Scherer et al., 2007).

The online experiment used to evaluate the performance of the HR-switch lasted about 30 min. Subjects were verbally instructed to turn on the SSVEP BCI, perform a pre-defined motion sequence with the prosthetic hand, then turn the BCI off. The motion sequence to be performed was:

(i) O: open the hand;
(ii) L: rotate the hand 90° to the left;
(iii) R: rotate the hand 90° to the right;

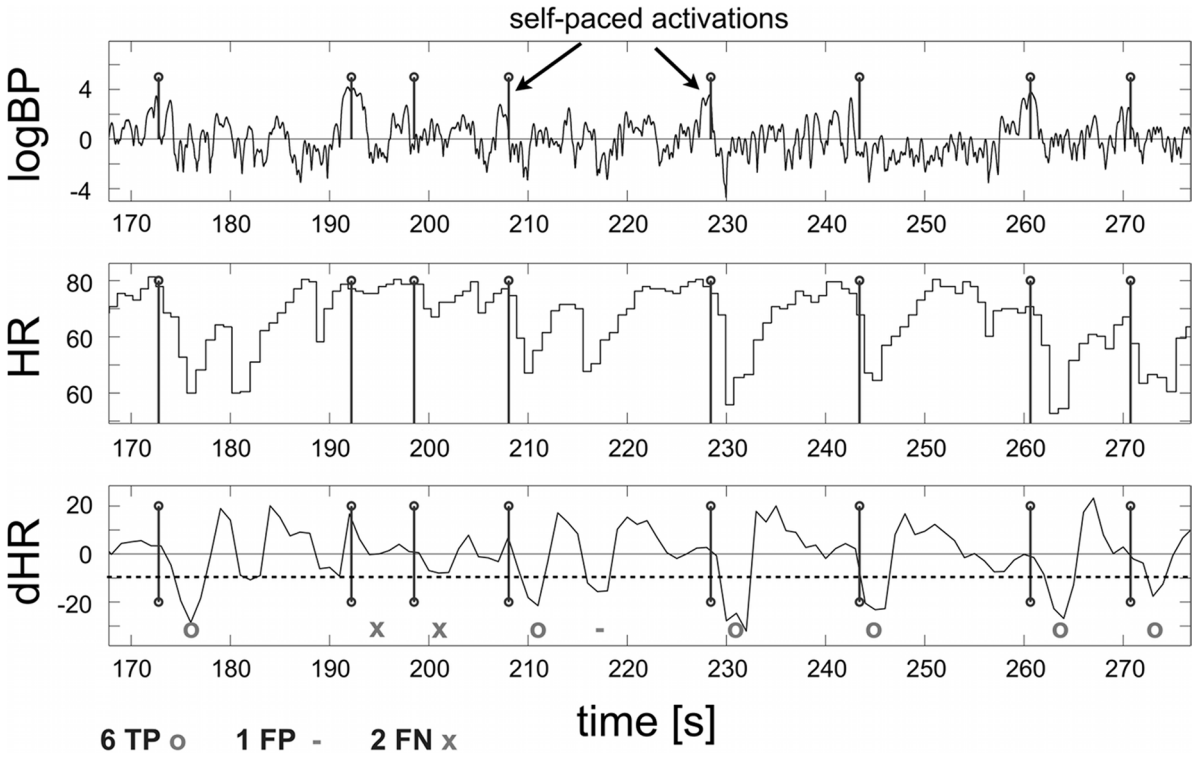


**FIGURE 6 | Beta power and HR changes during self-paced motor imagery.** This Figure shows logarithmic beta power with online detected output signals (vertical lines) during mental practice in virtual environment (for details see Pfurtscheller et al., 2008b), HR and first derivative of HR (dHR). The dHR time course shows that the detection of foot motor imagery with the HR correlates well with EEG detection and revealed six TPs, one FP and two FNs.

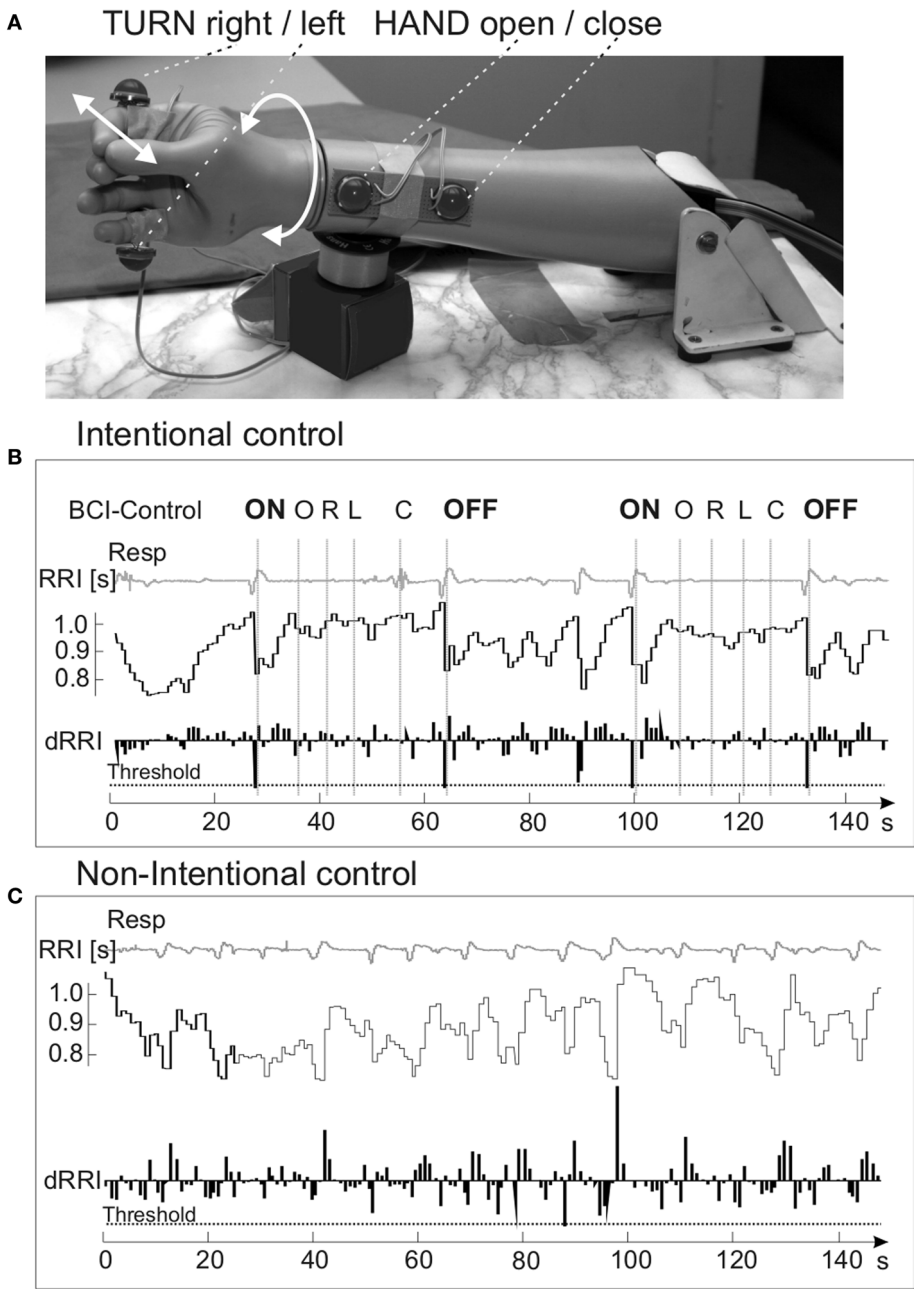


**FIGURE 7 | Prosthetic hand with four mounted LEDs (A), examples of respiratory signals (Resp), heart beat-to-beat intervals (RRI) measured in seconds and first derivative of RRI (dRRI) during intentional (B) and non-intentional control (C).** Two motion sequences (O, R, L, C) and the threshold are indicated. Modified from Scherer et al. (2007).

(iv) C: close the hand;
(v) R: rotate the hand 90° to the right;
(vi) O: open the hand;
(vii) C: close the hand; and
(viii) L: rotate 90° left, back to the original position.

The whole sequence had to be performed four times within 30 min. The start time of each sequence was randomly chosen by the experimenter, who talked to the subjects between the motor sequences. Subjects succeeded in switching on and off the BCI by brisk inspiration and operating the SSVEP-actuated hand prosthesis. Eight true positive HR switches were required to turn the BCI on and off for the four movement trials. The average number of false positive RRI detections was 2.9. The average number of erroneous (true negative) RRI detections was 4.9. The average selection speed for one out of the four SSVEP classes was about 9.5 s (6.3 commands per minute). On average, one SSVEP detection per minute was erroneous. These results, based on ten able-bodied subjects, suggest that transient HR changes, induced by brisk inspiration, are feasible signals in a hybrid BCI.

**Figure 7** shows examples of two sequences with respiratory and RRI signals, during intentional prosthesis control (**Figure 7B**) and non-intentional control (**Figure 7C**). The motion sequence was performed during the time between "ON" and "OFF".

### COMBINING EYE GAZE AND ERD BCI

This study, conducted in cooperation among Team PhyPA, TU Berlin, and Siemens Corporate Technology in Munich, Germany[1], explored an ERD-based BCI (ERD BCI) and eye gaze cursor control. If patients can control parts of their peripheral nervous system (PNS), then physiological signals from the PNS could provide control in a hybrid BCI. For example, if users can control eye movements, then they could select an item on the screen by fixating on it (Bolt, 1982; Jacob et al., 1993). The difficulty is the definition of an appropriate time window for the response (dwell time). It should be longer than the time needed to read the information encoded in the stimulus. Otherwise, items might be accidentally selected when a user simply looks at them, before s/he decided whether to select it. The dwell time should be as short as possible to avoid frustration and unnecessarily slow communication. It is difficult, and maybe impossible, to establish the optimal dwell time without an additional communication channel. Until now there is no adequate solution that deals appropriately with different stimulus complexities. One reason for this is the utilization of human gaze for two tasks – searching and selecting. While searching is a natural action within gaze behaviour, human beings are not used to triggering commands with their eyes.

One approach for solving this problem could be the addition of a second communication channel. This extra channel should be independent of eye movements, but still under voluntary control of the user. Both requirements might be fulfilled by an ERD BCI. Hence, an eye gaze system might be hybridized with an ERD BCI, as proposed in **Figure 1G**. Ten participants took part in this study, ranging from 19 to 36 years old. All participants reported normal or corrected-to-normal vision. The participants had to perform a search-and-select task. A reference string presented in the centre of the screen had to be found in a set of 12 strings, consisting of 11 distractors and one target. These strings were presented in a circular arrangement around the reference string to ensure a constant spatial distance. To emulate changes in the complexity of information encoded in items, two types of conditions have been defined. The "easy" condition used strings with four letters, and the "difficult" condition used strings with seven letters. All strings used only consonants to avoid similarities to known words. The distractors shared characters in some positions with the target string, and differed in other positions. The stimuli were chosen to avoid taxing working memory in the "easy" condition, and to push the limits of working memory in the "difficult" condition. Indeed, classic work in cognitive psychology has shown that most people's working memory is limited to about seven items (Miller, 1994).

In one condition, subjects had to select the target stimulus by fixating it for two different given dwell times. In the other condition, subjects instead used ERD to select targets. This approach shows that defining hybrid BCIs with two inputs from different physiological measures is feasible, similar to the example in **Figure 1D**. To ensure that the dwell times match stimulus complexity, different variants were evaluated in pilot experiments (1000 ms "easy"/1300 ms "difficult"). Details can be found in Vilimek and Zander (2009).

The comparison of dwell time based approaches (eye gaze input) versus the ERD-based approach shows that the ERD BCI is statistically significantly more accurate when selecting items of different complexity (see **Figure 8**). For both search conditions, task completion was fastest with short dwell times (easy: 4.0 s; difficult: 5.4 s), next was dwell time long, with BCI solution as the slowest activation method (5.9 s; 8.8 s), over both conditions.

A strong user preference (90%) and significantly lower frustration ratings (NASA TLX, frustration scale) resulted from subjective measures. Since subjects selected items more slowly and were less frustrated with an ERD approach, we infer that the subjects appreciated selecting items at their own pace. Taken together, these findings show that an ERD BCI could be an effective tool for supplementing eye gaze. Our results also suggest that a hybrid BCI based on eye gaze and ERD might be particularly useful in environments with rapid stimulus complexity changes.

## DISCUSSION

The described work shows that a hybrid BCI could successfully combine two different mental strategies, namely imagined hand movement and spatial visual attention. The mean accuracy of the reported cue-paced ERD study (see Simultaneous ERD/SSVEP BCI to Improve Accuracy; Allison et al., 2010; Brunner et al., 2010) was relatively poor (69.1 ± 8.6%, mean ± SD; 14 subjects). The low accuracy probably had two causes: the group consisted of naïve subjects without any BCI experience or training; and only two bipolar EEG channels over C3 and C4 were used. In a similar ERD study (Pfurtscheller et al., 2008c) with experienced subjects, 30 EEG recordings and processing with the common spatial pattern method the corresponding mean accuracy was 80 ± 10% (10 subjects) for the discrimination between left and right hand imagery.

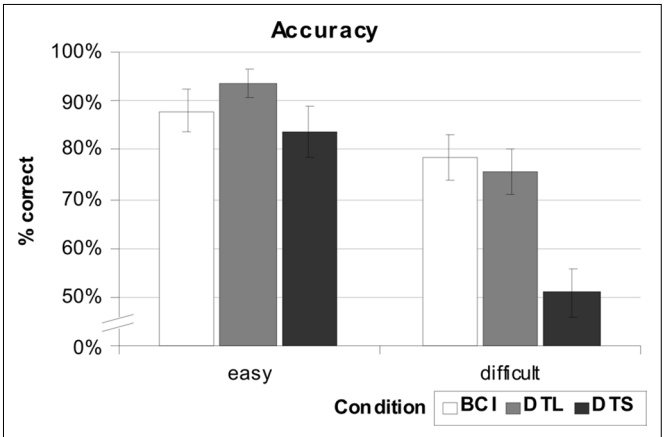


**FIGURE 8 | For condition "easy", accuracy of the BCI based solution was only slightly lower (88%) compared to the long dwell times (DTL, 93%).** Short dwell times (DTS) resulted in the lowest mean accuracy (83.3%). Remarkably, the BCI achieves the best results in accuracy for the condition "difficult" (78.7%), but only the difference to the short dwell time (51.1%) was significant.

[1]We thank Christian Kothe and Matti Gaertner (Team PhyPA) and Roman Vilimek (Siemens AG) for their support and help with this study.

However, in both of these studies, the maximum of the discrimination peak was present relatively early, namely ~1 s after visual cue onset. Examples for two subjects out of Pfurtscheller's study (**Figures 9A,B**) and five subjects out of Allison and Brunner's study (**Figure 9C**) document this early discrimination peak. This suggests that the discrimination between left and right motor imagery was strongest in a small time window after cue presentation. Other studies support this interpretation. Müller-Gerking et al. (2000) already reported such an initial recognition peak after visual cue presentation when subjects had to execute a real movement 1.5 s after cue-offset. They inferred that this result reflected a very short-lived brain state lasting about 300 ms after visual cue presentation. These findings with two different tasks, a memorized delayed movement execution task (Müller-Gerking et al., 2000) and a motor imagery task (Pfurtscheller et al., 2008c; Allison et al., 2010; Brunner et al., 2010), suggest that the visual cue acts as a trigger and activates visual specific cortical motor areas. Naito et al. (2002) suggested that "motor memories" are stored in cortical motor areas and cerebellar motor systems, and are important when memories related to previous actions are retrieved. However, this cue-triggered motor cortex activation starting about 300 ms after cue-onset is not necessarily a conscious process. This supports our view that a hybrid BCI that combines simultaneous ERD- and SSVEP-processing could yield better performance than an ERD- or SSVEP BCI alone because only the visual attention task requires fully conscious effort.

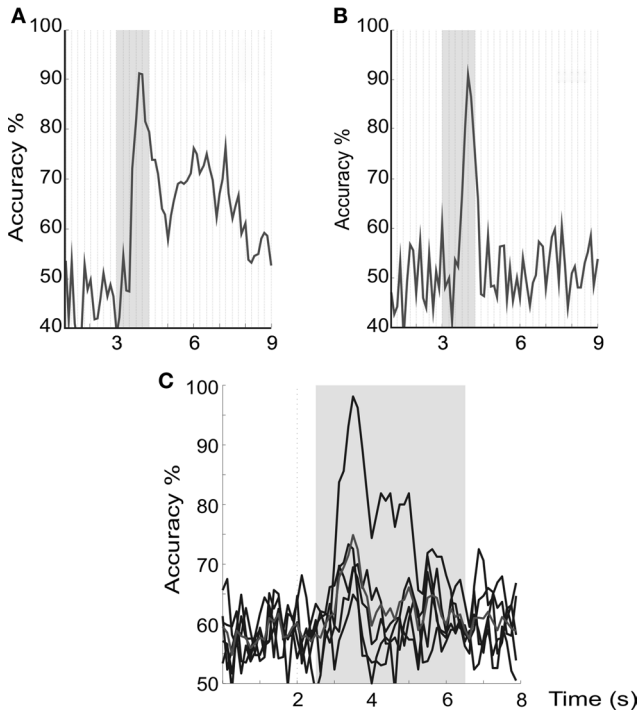


**FIGURE 9 | Example of discrimination time courses (off-line classification accuracy) from two different studies with visual cue-based right and left hand motor imagery.** In one study (Pfurtscheller et al., 2008c) subjects with BCI experience took part, whereas the other study used naïve subjects (for details see "Simultaneous ERD/SSVEP BCI to Improve Accuracy"; Allison et al., 2010). **(A,B)** Display the discrimination accuracy of two subjects from the group of BCI experienced subjects, and **(C)** displays superimposed accuracy time courses of five subjects of the naïve group. In all examples an early discrimination peak ~1 s after visual cue onset is visible. Cue duration is indicated by the grey area.

The switch concept we introduced, which uses only two EEG channels (one over motor cortex and one over occipital cortex) to combine ERD and SSVEP BCIs to realize orthosis control, demonstrates the usefulness of the hybrid BCI concept. In the six runs reported (**Table 2**), the false positive rate in resting periods was $1.2 \pm 1.3$/min (mean ± SD). This rate is clearly lower than the false positive rate reported during SSVEP-based orthosis control without brain switch (Linortner et al., 2009; Pfurtscheller et al., 2010b), which shows that the brain switch concept could substantially reduce false positives.

The ECG could also be used as second input for a hybrid BCI to enhance classification accuracy. This is only feasible with a paradigm that produces a large HR change. Cardiac and respiratory activity during imagined movement is proportional to mental effort (Decety et al., 1991). Subjects who vividly imagined a speed skating sprint displayed a significant HR increase (Oishi et al., 2000). Large HR responses may also occur when the user performs BCI experiments in an immersive virtual environment (VE). Pfurtscheller et al. (2008b) reported HR changes in the order of 10 bpm associated with foot motor imagery-based wheelchair movement in a multi-projection based stereo VE system commonly known as CAVE (Cave Automatic Virtual Environment). In such a hybrid BCI, it is fairly easy to classify such changes in the HR, and combine the results with the EEG classifications. Also, the imagery induced HR response is not always the same, and can differ between labs and CAVE applications (Pfurtscheller et al., 2006). The HR decreased during cue-paced motor imagery in the order of 3–5%, while the HR increased during immersive CAVE conditions by about the same amount.

When the HR is used as additional input signal for a hybrid BCI, the great variability of this signal must be considered. The HR is not only modified by the respiration and blood pressure waves of higher order (see e.g. Pfurtscheller et al., 2010a), but is also affected by fear, feelings, stress, mood or other psychological states. The major source for HR changes, namely the impact of respiration on the HR can be reduced, e.g. by an adaptive autoregressive filter algorithm (Florian et al., 1998). For the reduction of slow blood pressure waves on the HR the same algorithm can be used. Rapid changes in the HR are mediated by only the parasympathetic system, whereas slower variations are mediated beside others by the sympathetic system (Levy, 1977). Furthermore, it is vital that a BCI function when the user is under stress. These could be times when the user needs to communicate most. In stressful situations, the baroreflex vagal component is suppressed and the HR increases (Nosaka et al., 1991). Hybrid BCIs that use HR activity must account for stress-related changes in the HR.

Some of the studies reported used a limited number of subjects. More subjects should be run to assess effects across different people. However, the studies do validate different hybrid BCI concepts, and demonstrate the great variety of possible hybrid BCIs. In some cases (see Enhancement of BCI Accuracy With Both EEG and Heart Rate Evaluation), we started with offline simulations using data from "old" experiments. In other cases (see NIRS-based BCI as a Brain Switch) online studies are planned with feedback. Section

"Simultaneous ERD/SSVEP BCI to Improve Accuracy" describes offline simulations of a hybrid BCI, and we have just developed an online version of this study to explore this simultaneous hybrid approach. Promising results from one pilot subject are reported in Allison et al. (2010).

The large scale integrated project TOBI (Tools for Brain–Computer Interaction, EU Project FP 7 224631) aims to develop hybrid BCIs using a different definition. The TOBI project uses the same definition of a hybrid BCI as in the introduction, with the exception that a BCI should be available only if the user needs it. That is, a TOBI hybrid BCI might effectively use only one type of signal. Such a hybrid system might decide which input channel(s) offer the most reliable signal(s), and/or switch between input channels to improve information transfer rate, usability, or other factors.

### CONCLUSION AND OUTLOOK

Summarizing, different hybrid BCIs could expand a conventional "simple" BCI in different ways. Hybrid BCIs could involve a second type of input operating sequentially and/or simultaneously. The second input might be another BCI, which might require the user to perform additional mental tasks. The second input might use on other physiological signals (Wolpaw et al., 2002), or could be a conventional input such as a keyboard or mouse (Nijholt et al., 2008). Examples of sequentially operating hybrid BCIs include systems where the first BCI acts as simple switch to turn on/off the second BCI. This approach has been validated with two BCIs that use electrical brain signals, modified by different mental strategies (see Sequential ERS-based Brain Switch to Turn On/Off an SSVEP BCI), and two BCIs based on hemodynamic and electrical signals (see NIRS-based BCI as a Brain Switch), and a system that combines a BCI with HR changes (see Enhancement of BCI Accuracy With Both EEG and Heart Rate Evaluation and Induced HR Changes for On/Off Switches in a SSVEP BCI). Instead of serving as a switch, the second input might instead improve accuracy. This concept was validated in a study that combined ERD and SSVEP tasks (see Simultaneous ERD/SSVEP BCI to Improve Accuracy), and a different study that could lead to an ERD BCI combined with an eye tracker (see Combining Eye Gaze and ERD BCI).

Future work should assess different combinations of input signals, possibly involving three or more signals. One of the great challenges in hybrid BCI research is identifying the best combinations of signals to accomplish desired goals. The optimal combination probably differs considerably across users, and in some situations, a BCI might not be the best input mechanism. For a more comprehensive evaluation of hybrid BCIs, factors including system complexity, cost, user workload have to be evaluated. In the TOBI definition of a hybrid BCI, a BCI has to be available, and not necessarily used.

## ACKNOWLEDGMENTS

This work was partially supported by the EU project PRESENCCIA (IST-2006-27731), the European Community's Seventh Framework Programme FP7/2007-2013, BrainAble project, under grant agreement n°247447, the Wings for Life – Spinal Cord Research Foundation, the Austrian Allgemeine Unfallversicherung (AUVA), the Lorenz-Böhler Gesellschaft the Deutsche Forschungsgemeinschaft (DFS), the Land Steiermark (project A3-22.N-13/2009-8), the Neuro Center Styria (NCS), the BMBF-Computational Neuroscience Bernstein-Project and a grant from the European Research Council (ERC). We would like to thank Rupert Ortner and Patricia Linortner for assistance during the data collection of different experiments and the support of Otto Bock Healthcare Products GmbH, Vienna, Austria for providing the orthosis.

## REFERENCES

Allison, B. Z., Brunner, C., Kaiser, V., Müller-Putz, G. R., Neuper, C., and Pfurtscheller, G. (2010). Toward a hybrid brain–computer interface based on imagined movement and visual attention. *J. Neural Eng.* (in press).

Allison, B. Z., Wolpaw, E. W., and Wolpaw, J. R. (2007). Brain–computer interface systems: progress and prospects. *Expert Rev. Med. Devices* 4, 463–474.

Bauernfeind, G., Leeb, R., Wriessnegger, S. C., and Pfurtscheller, G. (2008). Development, set-up and first results for a one-channel near-infrared spectroscopy system. *Biomed. Tech. (Berl.)* 53, 36–43.

Birbaumer, N., and Cohen, L. G. (2007). Brain–computer interfaces: communication and restoration of movement in paralysis. *J. Physiol.* 579(Pt. 3), 621–636.

Birbaumer, N., Ghanayim, N., Hinterberger, T., Iversen, I., Kotchoubey, B., Kübler, A., Perelmouter, J., Taub, E., and Flor, H. (1999). A spelling device for the paralysed. *Nature* 398, 297–298.

Bolt, R. A. (1982). "Eyes at the interface," in *Proceedings of the 1982 Conference on Human Factors in Computing Systems* (New York: ACM Press), 360—362.

Brunia, C. H. M., and Damen, E. J. P. (1985). "Evoked cardiac responses during a fixed 4 sec foreperiod preceding four different responses," in *Psychophysiology of Cardiovascular Control*, eds J. F. Orlebeke, G. Mulder and L. J. P. van Doornen (New York: Plenum Publishing Corporation), 613–619.

Brunner, C., Allison, B. Z., Krusienski, D. J., Kaiser, V., Müller-Putz, G. R., Neuper, C., and Pfurtscheller, G. (2010). Improved signal processing approaches in an offline simulation of a hybrid brain–computer interface. *J. Neurosci. Methods* (in press).

Cheng, M., Gao, X., Gao, S., and Xu, D. (2002). Design and implementation of a brain–computer interface with high transfer rates. *IEEE Trans. Biomed. Eng.* 49, 1181–1186.

Coyle, S. M., Ward, T. E., and Markham, C. M. (2007). Brain–computer interface using a simplified functional near-infrared spectroscopy system. *J. Neural Eng.* 4, 219–226.

Damen, E. J. P., and Brunia, C. H. M. (1987). Changes in heart rate and slow brain potentials related to motor preparation and stimulus anticipation in a time estimation task. *Psychophysiology* 24, 700–713.

Decety, J., Jeannerod, M., Germain M., and Pastene, J. (1991). Vegetative response during imagined movement is proportional to mental effort. *Behav. Brain Res.* 42, 1–5.

Florian, G., Stancak, A., and Pfurtscheller, G. (1998). Cardiac response induced by voluntary self-paced finger movement. *Int. J. Psychophysiol.* 28, 273–283.

Jacob, R. J. K., Legett, J. J., Myers, B. A., and Pausch, R. (1993). Interaction styles and input/output devices. *Behav. Inf. Technol.* 12, 69–79.

Kübler, A., and Müller K. R. (2007). "An introduction to brain computer interfacing," in *Toward Brain–Computer Interfacing*, eds G. Dornhege, J. R. Millán, T. Hinterberger, D. McFarland and K. R. Müller (Cambridge, MA: MIT press), 1–25.

Lacey, B. C., and Lacey, J. I. (1980). Cognitive modulation of time-dependent primary bradycardia. *Psychophysiology* 17, 209–222.

Levy, M. N. (1977). "Parasympathetic control of the heart," in *Neural Regulation of the Heart*, eds W. C. Randall (New York: Oxford University Press), 95–129.

Linortner, P., Ortner, R., Müller-Putz, G. R., Neuper, C., and Pfurtscheller, G. (2009). "Self -paced control of a hand orthosis using SSVEP-based BCI," in *Proceedings of the13th International Conference on Human–Computer Interaction 2009* (Heidelberg: Springer), 716–720.

Lotze, M., Montoya, P., Erb, M., Hulsmann, E., Flor, H., Klose, U., Birbaumer, N., and Grodd, W. (1999). Activation of cortical and cerebellar motor areas during executed and imagined hand movements: an fMRI study. *J. Cogn. Neurosci.* 11, 491–501.

Mason, S. G., and Birch, G. E. (2000). A brain-controlled switch for asynchronous control applications. *IEEE Trans. Biomed. Eng.* 47, 1297–1307.

Miller, G. A. (1994). The magical number seven, plus or minus two: Some limits on our capacity for processing information. *Psychol. Rev.* 101, 343–352.

Müller-Gerking, J., Pfurtscheller, G., and Flyvbjerg, H. (2000). Classification of movement-related EEG in a memorized delay task experiment. *Clin. Neurophysiol.* 111, 1353–1365.

Müller-Putz, G. R., Eder, E., Wriessnegger, S. C., and Pfurtscheller, G. (2008). Comparison of DFT and lock-in amplifier features and search for optimal electrode positions in SSVEP-based BCI. *J. Neurosci. Methods* 168, 174–181.

Müller-Putz, G. R., Scherer, R., Brauneis, C., and Pfurtscheller, G. (2005). Steady-state visual evoked potential (SSVEP)-based communication: impact of harmonic frequency components. *J. Neural Eng.* 2, 1–8.

Naito, E., Kochiyama, T., Kitada, R., Nakamura, S., Matsumura, M., Yonekura, Y., and Sadato, N. (2002). Internally simulated movement sensations during motor imagery activate cortical motor areas and the cerebellum. *J. Neurosci.* 22, 3683–3691.

Nijholt, A., Tan, D., Pfurtscheller, G., Brunner, C., Millan, J. R., Allison, B., Graimann, B., Popescu, F., Blankertz, B., and Müller K. R. (2008). Brain–computer interfacing for intelligent systems. *IEEE Intell. Syst.* 23, 72–79.

Nosaka, S., Murase, S., and Murata, K. (1991). Arterial baroreflex inhibition by gastric distension in rats: mediation by splanchnic afferents. *Am. J. Physiol.* 260, R985–R994.

Oishi, K., Kasai T., and Maeshima, T. (2000). Autonomic response specificity during motor imagery. *J. Physiol. Anthropol. Appl. Hum. Sci.* 19, 255–261.

Papadelis, C., Kourtidou-Papadeli, C., Bamidis, P., and Albani, M. (2007). Effects of imagery training on cognitive performance and use of physiological measures as an assessment tool of mental effort. *Brain Cogn.* 64, 74–85.

Papakostopoulos, D., Banerji, N. K., and Pocock, P. V. (1990). Performance, EMG, brain electrical potentials and heart rate change during a self-paced skilled motor task in Parkinson's disease. *J. Psychophysiol.* 4, 163.

Pfurtscheller, G., Leeb, R., and Slater, M. (2006). Cardiac responses induced during thought-based control of a virtual environment. *Int. J. Psychophysiol.* 62, 134–140.

Pfurtscheller G., and Lopes da Silva F. H. (1999). Event-related EEG/MEG synchronization and desynchronization: basic principles. *Clin. Neurophysiol.* 110, 1842–1857.

Pfurtscheller, G., Müller-Putz, G., Scherer, R., and Neuper, C. (2008a). Rehabilitation with brain–computer interface systems. *IEEE Comp. Mag.* 41, 58–65.

Pfurtscheller, G., Leeb, R., Friedman, D., and Slater, M. (2008b). Centrally controlled heart rate changes during mental practice in immersive virtual environment: a case study with a tetraplegic. *Int. J. Psychophysiol.* 68, 1–5.

Pfurtscheller, G., Scherer, R., Müller-Putz, G. R., and Lopes da Silva, F. H. (2008c). Short-lived brain state after cued motor imagery in naive subjects. *Eur. J. Neurosci.* 28, 1419–1426.

Pfurtscheller, G., and Neuper, C. (2001). Motor imagery and direct brain–computer communication. *Proc. IEEE* 89, 1123–1134.

Pfurtscheller, G., Neuper, C., and Birbaumer, N. (2005a). "Human brain–computer interface," in *Motor Cortex in Voluntary Movements: A Distributed System for Distributed Functions. Series: Methods and New Frontiers in Neuroscience*, eds E. Vaadia and A. Riehle (Boca Raton: CRC Press), 367–401.

Pfurtscheller, G., Neuper, C., Brunner, C., and Lopes da Silva, F. H. (2005b). Beta rebound after different types of motor imagery in man. *Neurosci. Lett.* 378, 156–159.

Pfurtscheller G., Ortner R., Bauernfeind G., Linortner P., and Neuper C. (2010a). Does conscious intention to perform a motor act depend on slow cardiovascular rhythms? *Neurosci. Lett.* 468, 46–50.

Pfurtscheller, G., Solis-Escalante, T., Ortner, R., Linortner, P., and Müller-Putz, G. R. (2010b). Self-paced operation of an SSVEP-based orthosis with and without an imagery-based "brain switch": a feasibility study towards a hybrid BCI. *IEEE Trans. Neural Syst. Rehabil. Eng.* (in press).

Pfurtscheller, G., and Solis-Escalante, T. (2009). Could the beta rebound in the EEG be suitable to realize a "brain switch"? *Clin. Neurophysiol.* 120, 24–29.

Porro, C. A., Francescato, M. P., Cettolo, V., Diamond, M. E., Baraldi, P., Zuiani, C., Bazzocchi, M.,, and di Prampero, P. E. (1996). Primary motor and sensory cortex activation during motor performance and motor imagery: a functional magnetic resonance imaging study. *J. Neurosci.* 16, 7688–7698.

Scherer, R., Müller-Putz, G. R., and Pfurtscheller, G. (2007). Self-initiation of EEG-based brain–computer communication using the heart rate response. *J. Neural Eng.* 4, L23–L29.

Sitaram R., Zhang H., Guan C, Thulasidas M., Hoshi Y., Ishikawa A., Shimizu K., and Birbaumer N. (2007). Temporal classification of multichannel near-infrared spectroscopy signals of motor imagery for developing a brain–computer interface. *Neuroimage* 34, 1416–1427.

Solis-Escalante, T., Müller-Putz, G. R., Brunner, C., Kaiser V., and Pfurtscheller, G. (2010). Analysis of sensorimotor rhythms for the implementation of a brain switch for healthy subjects. *Biomed. Signal Process. Control* 5, 15–20.

Solis-Escalante, T., Müller-Putz, G. R., and Pfurtscheller, G. (2008). Overt foot movement detection in one single Laplacian EEG derivation. *J. Neurosci. Methods* 175, 148–153.

Vaadia, E., and Birbaumer, N. (2009). Grand challenges of brain computer interfaces in the years to come. *Front. Neurosci.* 3, 151–154.

Verberne, A. J., and Owens, N. C. (1998). Cortical modulation of the cardiovascular system. *Prog. Neurobiol.* 54, 149–168.

Vilimek, R., and Zander, T.O. (2009). "BC(eye): combining eye-gaze input with brain–computer interaction," in *Lecture Notes In Computer Science, Vol. 5615: Proceedings of the 5th International on Conference on Universal Access in Human–Computer Interaction. Part II: Intelligent and Ubiquitous Interaction Environments, HCI International San Diego* (Berlin/Heidelberg: Springer-Verlag).

Wolpaw, J. R., Birbaumer, N., McFarland, D. J., Pfurtscheller, G., and Vaughan, T. M. (2002). Brain–computer interfaces for communication and control. *Clin. Neurophysiol.* 113, 767–791.

Wolpaw, J. R., Loeb, G. E., Allison, B. Z., Donchin, E., do Nascimento, O. F., Heetderks, W. J., Nijboer, F., Shain,W. G., and Turner, J. N. (2006). BCI meeting 2005 – workshop on signals and recording methods. *IEEE Trans. Neural Syst. Rehabil. Eng.* 14, 138–141.

Wriessnegger, S. C., Kurzmann, J., and Neuper, C. (2008). Spatio-temporal differences in brain oxygenation between movement execution and imagery: a multichannel near-infrared spectroscopy study. *Int. J. Psychophysiol.* 67, 54–63.

Zander, T. O., Kothe, C., Jatzev S., and Gaertner M. (in press). "Enhancing human–computer interaction with input from active and passive brain–computer interfaces," in *The Human in Brain–Computer Interfaces and the Brain in Human–Computer Interaction*, eds D. S. Tan and A. Nijholt (Berlin: Springer).

**Conflict of Interest Statement:** The authors declare that the research was conducted in the absence of any commercial or financial relationships that could be construed as a potential conflict of interest.

*Received: 18 December 2009; paper pending published: 22 February 2010; accepted: 15 March 2010; published online: 16 April 2010.*

*Citation: Pfurtscheller G, Allison BZ, Brunner C, Bauernfeind G, Solis-Escalante T, Scherer R, Zander TO, Mueller-Putz G, Neuper C and Birbaumer N (2010) The hybrid BCI. Front. Neurosci.* ***4****:30. doi: 10.3389/fnpro.2010.00003*

*This article was submitted to Frontiers in Neuroprosthetics, a specialty of Frontiers in Neuroscience.*

International Journal of Psychophysiology 76 (2010) 186–192

Contents lists available at ScienceDirect

International Journal of Psychophysiology

journal homepage: www.elsevier.com/locate/ijpsycho

# Focal frontal (de)oxyhemoglobin responses during simple arithmetic

Gert Pfurtscheller [a,*], Günther Bauernfeind [a], Selina Christin Wriessnegger [a], Christa Neuper [a,b]

[a] Laboratory of Brain-Computer Interfaces, Institute for Knowledge Discovery, Graz University of Technology, A-8010 Graz, Austria
[b] Department of Psychology, University of Graz, A-8010 Graz, Austria

ARTICLE INFO

*Article history:*
Received 23 November 2009
Received in revised form 23 March 2010
Accepted 30 March 2010
Available online 8 April 2010

*Keywords:*
Hemodynamic response
Prefrontal cortex
Mental arithmetic
(De)oxyhemoglobin change
Near-infrared spectroscopy (NIRS)
Multi-channel NIRS

ABSTRACT

Near-infrared spectroscopy (NIRS) is a functional brain imaging method able to study hemodynamic changes during cortical activation. We studied the changes of oxy- and deoxyhemoglobin ([oxy-Hb], [deoxy-Hb]) with a 52-channel NIRS system during simple mental arithmetic in ten healthy volunteers over the prefrontal cortex. We found that eight of the ten subjects showed a relative focal bilateral increase of [oxy-Hb] in the dorsolateral prefrontal cortex (DLPFC) in parallel with a decrease in the medial area of the anterior prefrontal cortex (APFC). The [oxy-Hb] response in left DLPFC and APFC was significant, while the [deoxy-Hb] response was clearly smaller and not significant. These observations were discussed within the context of "focal activation/surround deactivation".



## 1. Introduction

Near-infrared spectroscopy (NIRS) is a recently developed technique that can reveal hemodynamic and metabolic changes during cortical activation. NIRS has been used to study hemodynamic responses (changes of oxy- and deoxyhemoglobin ([oxy-Hb], [deoxy-Hb])) to cognitive, visual, visuomotor and motor tasks (Franceschini et al., 2003; Herrmann et al., 2005; Herrmann et al., 2008; Hofmann et al., 2008; Shimada et al., 2004; Tanida et al., 2004; Wriessnegger et al., 2008). It is widely accepted that increases in [oxy-Hb] and slight decreases in [deoxy-Hb] are typical for activation (Buxton et al., 2004; Obrig et al., 1996; Strangman et al., 2002). Especially the PET study of Fox and Raichle (1986) could show that such a pattern of increasing [oxy-Hb] and decreasing [deoxy-Hb] is considered to reflect brain activation.

It is known that the frontal cortex plays a major role in solving a mental arithmetic (MA) task. Previous neuroimaging studies using functional magnetic resonance imaging (fMRI) exploring arithmetic tasks revealed left-sided and/or bilateral activation of the ventrolateral (VLPFC) and dorsolateral (DLPFC) prefrontal cortex (Kawashima et al., 2004; Menon et al., 2000; Rickard et al., 2000) during simple arithmetic operations like one-digit addition, subtraction and multiplication tasks.

Indeed, several NIRS studies have demonstrated the implication of the prefrontal cortex (PFC) during MA (Tanida et al., 2004; Bauernfeind et al., 2008; Hock et al., 1995; Hoshi et al., 1994; Hoshi and Tamura, 1993) but most of them used either only one or two NIRS channels. For example Tanida et al. (2004) investigated the relationship between asymmetry of the prefrontal cortex activity and the automatic nervous system (ANS) response during a mental arithmetic (MA) task. They found increases of [oxy-Hb] and total hemoglobin (=[oxy-Hb]+[deoxy-Hb]) associated with decreases of [deoxy-Hb] in the bilateral PFC. In contrast, Bauernfeind et al. (2008) performed a one-channel NIRS-study on MA tasks resulting in a prefrontal decrease of [oxy-Hb]. These different results might be due to the different type and duration of the MA tasks, the positioning of the optodes and the limited number of channels.

In recent years, NIRS technology was used alternatively to the electroencephalography (EEG) as a sensor technology for a non-invasive Brain-Computer Interface (BCI; Coyle et al., 2007; Sitaram et al., 2007; Luu and Chau, 2009; Bauernfeind et al., 2008; Pfurtscheller et al., in press). In the case of a NIRS-based (optical) BCI the user performs a mental task (e.g. motor imagery, mental calculation, and auditory imagery) and induces herewith hemodynamic changes recordable over the prefrontal or motor cortex areas. The optode placement especially over the prefrontal cortex is useful, because such a NIRS system is more practical and user-friendly and so suitable for application out of the lab. Furthermore online signal detection with an optical BCI could be relatively easier with antagonistic activation patterns, which means Hb responses displaying an opposite polarity (e.g. [oxy-Hb] increase and decrease) at different optode locations. Taken these into account the aim of the present study was to determine whether a simple arithmetic task can elicit focal changes of [oxy-Hb] and [deoxy-Hb] over prefrontal optode locations which can be used for future optical BCI systems.

* Corresponding author: Laboratory of Brain-Computer Interfaces, Institute for Knowledge Discovery, Graz University of Technology, Krenngasse 37, A-8010 Graz, Austria. Tel.: +43 316 873 5300; fax: +43 316 873 5349.
*E-mail address:* pfurtscheller@tugraz.at (G. Pfurtscheller).

0167-8760/$ – see front matter © 2010 Elsevier B.V. All rights reserved.
doi:10.1016/j.ijpsycho.2010.03.013

## 2. Material and methods

### 2.1. Subjects and experimental procedure

The investigations were carried out on a group of ten paid University students (five males and five females, all right-handed) aged 26.1 ± 2.7 years (mean ± SD). The subjects abstained from caffeine before recording, were seated in a comfortable armchair, and gave written informed consent before the experiment. The study was approved by the ethics committee of the Medical University of Graz.

The subjects were asked to serially subtract a one-digit number from a two-digit number (e.g. 97 − 4) as quickly as possible for 12 s. The numbers were presented visually on the monitor at the beginning of each trial. There was a 28 s pause at the end of each trial, so each trial lasted 40 s. During the pause, the subjects were instructed not to move and to stay relaxed by just looking at the black screen. In sum 24 trials were collected. To avoid enhancement of 3rd order blood pressure waves (De Boer et al., 1986) or their sub-harmonics an experimental paradigm with 12 s activity phase and 28 s pause was chosen. It is very important to control this type of waves since they have large magnitudes and can mask task-related changes (Bauernfeind et al., 2008; Coyle et al., 2004; Elwell et al., 1999).

### 2.2. Data acquisition and processing

A continuous wave system (ETG-4000, Hitachi Medical Co., Japan) was used to record brain oxygenation. The multi-channel system measures the change of [oxy-Hb] and [deoxy-Hb] in the unit of mM mm and consists of 16 photo-detectors and 17 light emitters (3 × 11 grid), resulting in a total of 52 channels. The sampling rate was set to 10 Hz. The distance between source and detector was 3 cm. The lowest line of channels was arranged along the FP1–FP2 line of the international EEG 10–20 system, with channel 48 exactly at the FP1 position (Fig. 1). In order to allow a probabilistic reference to cortical areas underlying the measurement channels and to make the results comparable to results provided by similar fMRI studies (e.g. Kawashima et al., 2004; Menon et al., 2000; Rickard et al., 2000) we used a procedure which projects topographical data based on skull landmarks into a 3D reference frame (MNI-space, Montreal Neurological Institute) optimized for NIRS analysis (Singh et al., 2005). So for each NIRS channel position (Fig. 1), a set of MNI coordinates (*x*, *y*, and *z*) with an error estimated (SD) was calculated. For further details on the corresponding anatomical structures see Okamoto et al. (2004).

After a visual inspection of the raw NIRS data, channels with poor signal quality were marked (in three subjects; two, four and nine channels respectively). Afterwards, a common average reference (CAR) spatial filter was used to remove global influences (e.g. changes in heart rate or respiratory influences). Therefore, for every time point, the mean of all non-marked channels was calculated and subtracted from each channel. For artifact reduction, a 0.09 Hz low pass Butterworth filter of order 4 with 60 dB in the stop band was designed. Additionally, a 0.01 Hz high pass filter was used to remove baseline drifts. For further details, see Bauernfeind et al. (2008). The subject with nine marked channels displayed too many artifacts and was removed from further analysis and a second subject showed no reliable pattern and was also omitted.

### 2.3. Calculation of task-related changes and topographic distribution

The mean task-related concentration changes of [oxy-Hb] and [deoxy-Hb] referred to a 10 s baseline interval prior to the task (seconds − 10 to 0) were calculated for each non-marked channel. For the marked channels, the changes were calculated by interpolating the surrounding channels.

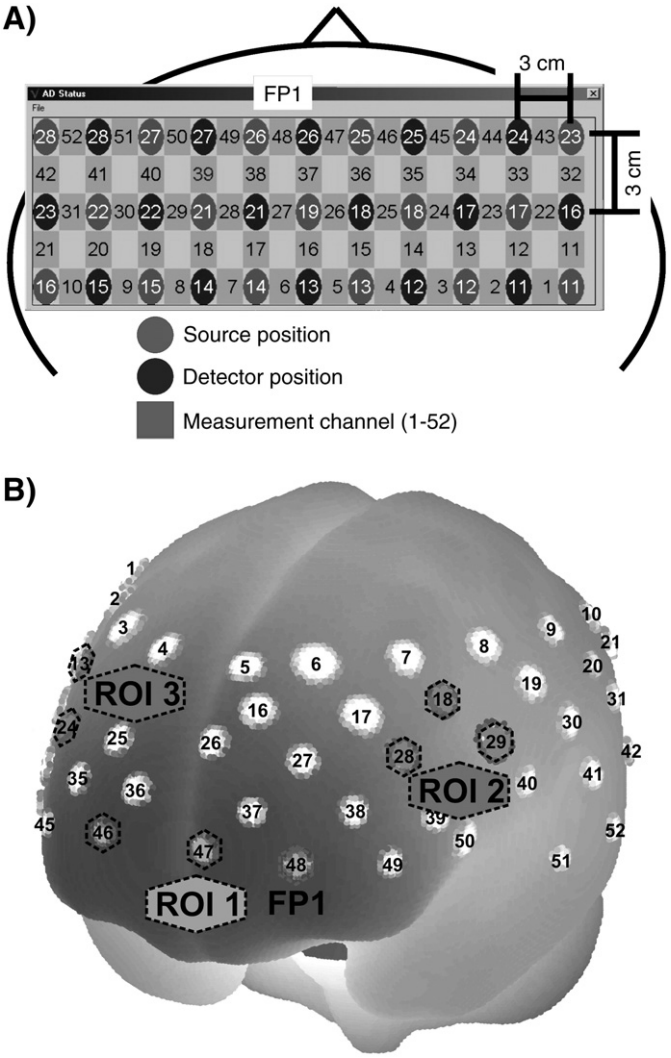


**Fig. 1.** A) Schematic illustration of the multi-channel array (52 channels, 3 × 11 grid). B) Projections of the NIRS channel positions on the cortical surface. Positions are overlaid on a MNI-152 compatible canonical brain which is optimized for NIRS analysis (Singh et al., 2005). The lowest line of channels was arranged along the FP1–FP2 line of the international EEG 10–20 system, with channel 48 exactly at the FP1 position. The centers of the circle regions represent the locations of the most likely MNI coordinates for the NIRS channel projected on the cortical surface. The edges represent the boundaries defined by the standard deviation.

The topographic distributions during the tasks are further visualized by plotting the [oxy-Hb] and [deoxy-Hb] values at their corresponding spatial position. A 2-D interpolation on a fine Cartesian grid was used to generate a scalp distribution. Two different points in time are illustrated. The first point between 0 and 2 s corresponds to the cue presentation and start of the task; the second point between 10 and 12 s corresponds to the end of the task. [oxy-Hb] and [deoxy-Hb] are visualized in different plots, but use the same scale. Increases are plotted in blue and decreases in red (no activation is plotted in white).

Examples of the hemodynamic responses at all 52 channels are displayed in Figs. 2 and 3.

### 2.4. Statistical analysis

Two 3 × 5 repeated measures of analyses (ANOVA) on the data were performed separately for [oxy-Hb] and [deoxy-Hb]. The two factors, "regions of interest" (ROI: frontal, left, right), and "time" (baseline, seconds 8–10, seconds 10–12, seconds 12–14, and seconds

14–16), were used as within-subject variables. The MNI coordinates and anatomical locations of the included channels are given in Table 1 and Fig. 1B. Additionally we calculated effect size measures ($\eta^2$) to obtain information on how strong the effects are (Cohen, 1988) and checked our data for outliers (Stevens, 2002). No outliers were found.

## 3. Results

Eight out of ten subjects displayed a relative focal bilateral increase of [oxy-Hb] accompanied by a [deoxy-Hb] decrease in the DLPFC (marked by gray broken line ellipses in the right upper panel of Fig. 2B). In parallel, they showed a decrease of [oxy-Hb], accompanied by a [deoxy-Hb] increase, in most channels overlaying the medial area of the anterior prefrontal cortex (APFC) (Fig. 2B, marked by a black broken line ellipsis).

Fig. 2 presents the grand average hemodynamic responses ([oxy-Hb], [deoxy-Hb]) during the task. The largest and thus most stable [oxy-Hb] decreases in the map are localized at channels 48 (FP1 position) and 37 (~3 cm posterior to FP1). The largest [oxy-Hb] increases can be found on the left hemisphere at channel 28 and on the right hemisphere at channel 24. The peak latency of the hemodynamic responses in the MA task at second 15, and the delay of the onset of the [oxy-Hb] decrease in the order of 2 s, is both clearly visible.

For statistical analysis, the averages of 3 channels of each ROI (ROI1: APFC, channels 46, 47 and 48; ROI2: left DLPFC, channels 18, 28 and 29; ROI3: right DLPFC, channels 13, 23 and 24) were calculated. The results of the 3×5 analysis of variance (ANOVA) revealed the following significant findings: For [oxy-Hb] the main effect of ROI revealed significance ($F(2,14)=27.93$; $p<0.01$; $\eta^2=0.80$). Furthermore the interaction ROI×time showed significance ($F(8,56)=24.37$; $p<0.01$; $\eta^2=0.78$). The Bonferroni posttest showed a significant change of [oxy-Hb] over left and frontal sites for all time periods compared to the baseline (Fig. 2A, lower panels). For [deoxy-Hb] no significant main effect of ROI: ($F(2,14)=2.61$; $p<0.11$; $\eta^2=0.27$) could be found. Although the interaction ROI×time showed significance ($F(8,56)=3.29$; $p<0.01$; $\eta^2=0.32$) the Bonferroni posttest showed no significant changes of [deoxy-Hb] compared to the baseline. Only in the later time

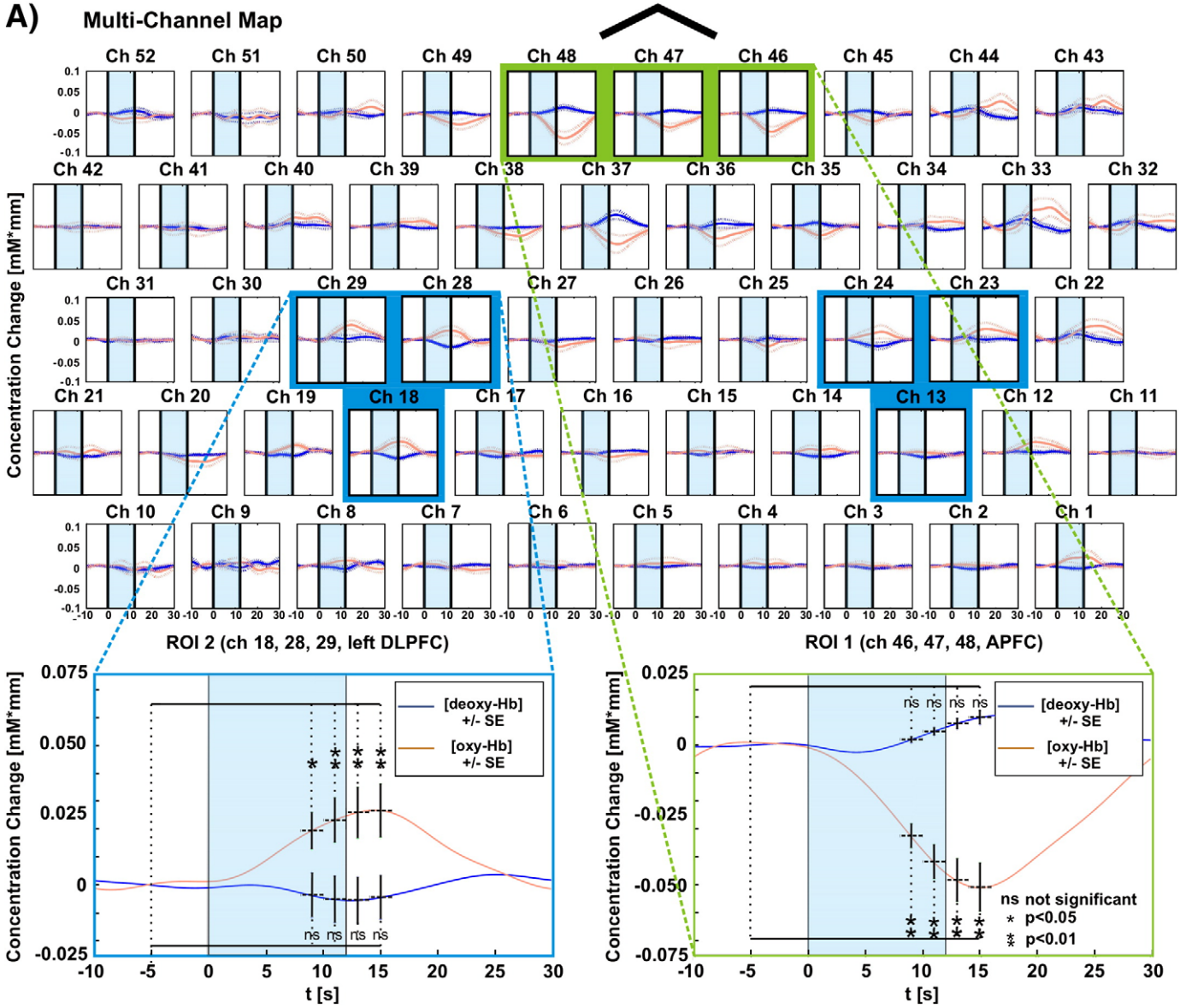


**Fig. 2.** A) Grand average (8 subjects) concentration changes (mean ± SE) of [oxy-Hb] and [deoxy-Hb] (upper panel) and averaged responses with significant changes for ROI2 and ROI1 (lower panels). B) Topographic distributions during the tasks at two different points in time (seconds 0–2; seconds 10–12). The focal bilateral increase of [oxy-Hb] in the DLPFC in parallel with the decrease of [oxy-Hb] in the medial area of the APFC are marked by gray and black broken line ellipses, respectively.

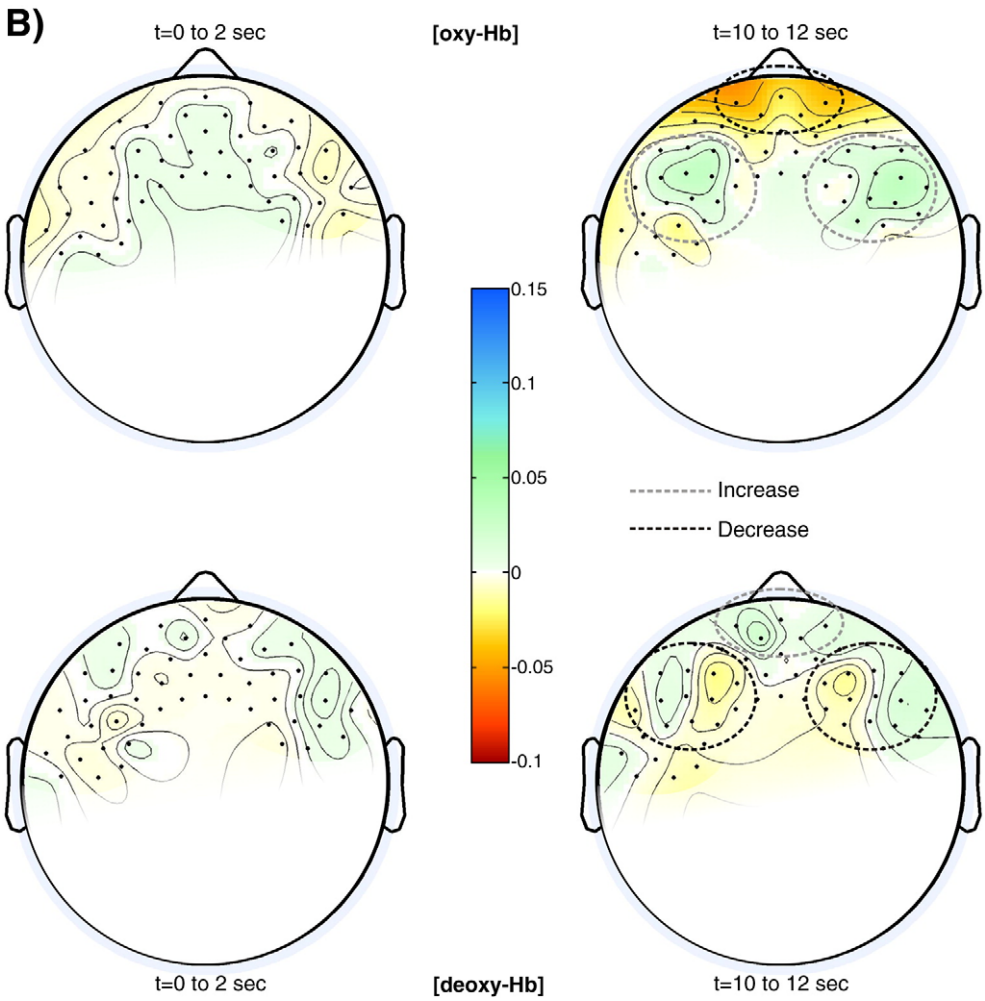


**Fig. 2** (*continued*).

periods significant differences between the frontal and the left and right ROI could be found.

Fig. 3 shows the hemodynamic responses for a representative subject. This subject also shows a relative focal bilateral increase of [oxy-Hb] in the DLPFC in parallel with a decrease of [oxy-Hb] in the medial area of the APFC. The largest [oxy-Hb] decrease is localized at channel 37 (~3 cm posterior to FP1, Fig. 3, lower panel left), the largest [oxy-Hb] increases can be found on the right hemisphere at channel 24 (Fig. 3, lower panel right). Note that neighboring channels (channels 27 and 28; channels 24 and 25, marked by broken line ellipses) display significant [oxy-Hb] responses with opposite polarity, which underlines the focal increase/decrease of [oxy-Hb] and [deoxy-Hb] in frontal areas.

## 4. Discussion

The purpose of the study was to investigate the spatio-temporal patterns of hemodynamic responses during a simple MA task in prefrontal brain regions. We found a relative focal bilateral increase (with a left hemispheric dominance) of [oxy-Hb] accompanied by a [deoxy-Hb] decrease in the DLPFC. In parallel, we found a decrease of [oxy-Hb] accompanied by a [deoxy-Hb] increase in most channels overlaying the medial area of the APFC. While the [oxy-Hb] changes revealed significance in both areas, the [deoxy-Hb] changes were not significant. The reason for the latter could be the small amplitude of the [deoxy-Hb] response. Theories of the hemodynamic response (e.g. Buxton et al., 2004) predict the [oxy-Hb] response to be larger than [deoxy-Hb], usually by a factor of 2 or more. Missing significant [deoxy-Hb] effects might be simply explained by the smaller amplitude of [deoxy-Hb]-responses, even when [deoxy-Hb] is better for localizing functions, and may correspond more closely to the BOLD response (Steinbrink et al., 2006). Therefore, it is not surprising that no significant [deoxy-Hb] responses were observed. For example, Hofmann et al. (2008) recently reported large [oxy-Hb] and small [deoxy-Hb] responses in a visual word recognition task and (Herrmann et al., 2008) large [oxy-Hb] and small [deoxy-Hb] responses during enhanced alertness.

First, the interesting finding of a significant simultaneous [oxy-Hb] increase and [oxy-Hb] decrease in different prefrontal areas during simple MA could be explained in the context of "focal activation/surround deactivation". Antagonistic activation patterns have been already described by brain activation studies using fMRI and EEG. For example Ehrsson et al. (2003) reported, in a foot movement execution and imagination task, a positive BOLD signal in the foot area and a negative BOLD in the hand area with slightly greater magnitude during real movements. This can be interpreted as "focal activation (positive BOLD)/surround deactivation (negative BOLD)". Furthermore Pfurtscheller and Neuper (1994) observed in their EEG study that the event-related desynchronisation (ERD) of alpha band activity does not occur in isolation, but is often accompanied by an increase in synchronization (ERS) in neighboring areas that correspond to the same or other modalities of information processing (Pfurtscheller and

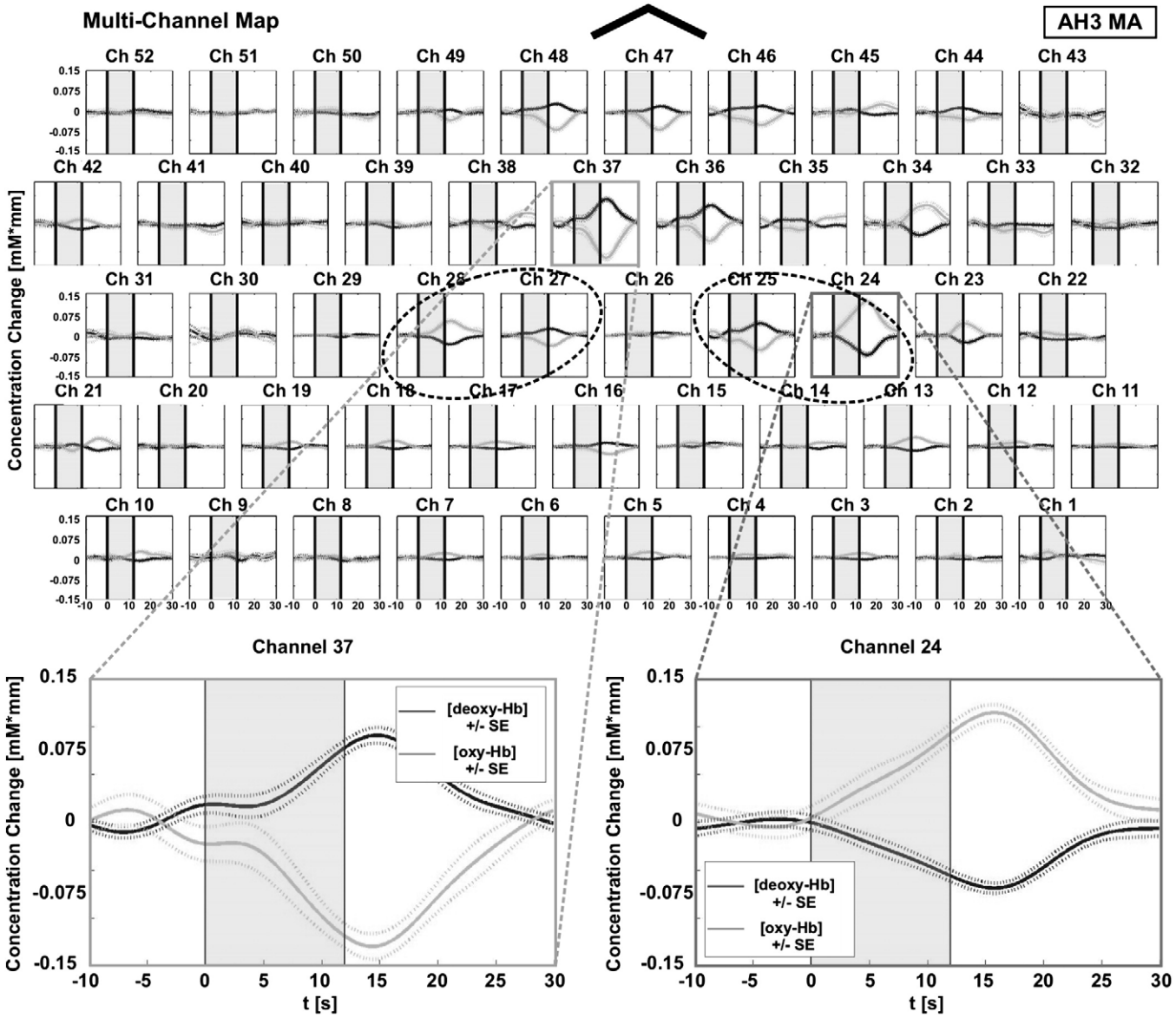


**Fig. 3.** Mean concentration changes (mean ± SE) during MA of a representative subject (AH3).

da Silva, 1999). This phenomenon was called "focal ERD/surround ERS" (Suffczynski et al., 1999). So, for example, foot movement or foot motor imagery results in a focal ERD at electrodes overlaying the foot representation area and/or the supplementary motor area, and in an ERS at electrodes overlaying the hand representation area.

How can such focal EEG and BOLD changes be interpreted? A study on inhibitory control of learned motor programs by Hummel and colleagues may give an answer (Hummel et al., 2002; Hummel et al., 2004). They found increased motor evoked potentials (MEPs) amplitudes, an amplitude decrease (ERD) of sensorimotor oscillations and a positive BOLD in the hand area during active retrieval of an acquired motor task. For the inhibition condition (the learned movement sequence was not executed) a significant reduction of MEPs together with an amplitude increase (ERS) of central 11–13 Hz oscillations and a negative BOLD was characteristic. Therefore we can conclude that a focal ERD and a positive BOLD characterize an activated neural structure, while an ERS of alpha band rhythms and a negative BOLD may characterize a deactivated or inhibited neural structure. Since recent fMRI–NIRS simultaneous measurements have documented that changes in the hemoglobin concentration are strongly correlated with the fMRI–BOLD signal (Strangman et al., 2002; Steinbrink et al., 2006) the reported antagonistic [oxy-Hb] response could be interpreted as another manifestation of a "focal activation/surround deactivation". While it is widely accepted that increases in [oxy-Hb] are typical for activation (Tanida et al., 2004; Obrig et al., 1996; Strangman et al., 2002) the interpretation of an [oxy-Hb] decrease is not so clear. Shimada et al. (2004) reported a significant decrease in prefrontal [oxy-Hb] during visual feedback of the moving hand in a reaching task and interpreted this decrease in terms of prefrontal "deactivation". Further Hofmann et al. (2008) reported on hemodynamic responses during lexical decisions on words and pseudowords using also a 52-channel Hitachi system. In the lexicality condition they found focal [oxy-Hb] increases in the superior frontal gyrus and left inferior parietal gyrus. Inspection of their corresponding topographic maps (Hofmann et al., 2008; Fig. 1A) gives evidence that optodes placed between these two activated areas show a deactivation ([oxy-Hb] decrease). Similarly results can be found for the second condition (word frequency, Fig. 1B) investigated there. Additionally antagonistic hemodynamic responses were also reported by Franceschini et al. (2003). They investigated the contra- and ipsilateral hemodynamic response of the sensorimotor cortex to unilateral voluntary movements, tactile, and electrical stimulation. For electrical stimulation, but not for voluntary movements and tactile

**Table 1**
Channel numbers, MNI coordinates, composite standard deviations for the estimation on the cortical surface (SD) and related Brodmann and anatomical areas of each ROI.

| ROI | Channel | MNI-space correspondence | | | | Cortical areas | |
|---|---|---|---|---|---|---|---|
| | | *x* | *y* | *z* | SD | BA | |
| 1 APFC | 46 | 23 | 72 | 8 | 4 | 10 | SFG |
| | 47 | −8 | 73 | 6 | 5 | 10 | MeFG |
| | 48 | −31 | 66 | 3 | 5 | 10 | MFG |
| 2 Left DLPFC | 18 | −51 | 23 | 41 | 5 | 9 | MFG |
| | 28 | −47 | 39 | 28 | 6 | 46 | MFG |
| | 29 | −61 | 11 | 28 | 6 | 9 | IFG |
| 3 Right DLPFC | 13 | 48 | 31 | 42 | 5 | 9 | MFG |
| | 23 | 57 | 26 | 29 | 5 | 46 | MFG |
| | 24 | 45 | 62 | 29 | 5 | 46 | MFG |

BA, Brodmann area; SFG, superior frontal gyrus; MFG, middle frontal gyrus; IFG, inferior frontal gyrus; MeFG, medial frontal gyrus.

stimulation they observed an ipsilateral deactivation pattern in parallel with a contralateral activation pattern. They interpreted the absent deactivation in the ipsilateral side during voluntary movement and tactile stimulation by the insufficient subtraction of systemic changes due to the increase of heart rate. So the deactivation pattern caused by inhibition or decrease in activity of certain brain areas that do not pertain to the attended process may sometimes be canceled out by systemic changes. For that reason it is appropriate to remove these systemic influences by different signal processing approaches (for example using a CAR spatial filter as done in our study) to uncover the deactivation pattern. In addition, assuming that not every cognitive process must necessarily lead to an increase in heart rate and therewith resulting in higher [oxy-Hb] concentration in the brain, an alternative explanation might be the fact that [oxy-Hb] must be drained from one part of the brain (deactivation) to be delivered to another region (activation).

Second, the results reported are in line with fMRI studies that found bilateral activation of the VLPFC and DLPFC and the inferior and superior parietal cortex, primarily in the left hemisphere, during the performance of different arithmetic tasks (Kawashima et al., 2004; Menon et al., 2000; Rickard et al., 2000).

Furthermore spontaneous activity, as measured with fMRI in the resting awake brain, is organized in multiple highly specific functional anatomical networks, named "resting state networks" (RSNs) (Mantini et al., 2007). "Deactivation" in such RSNs may be interpreted as a reallocation of resources from default functions to goal directed functional states (Damoiseaux et al., 2006; Raichle and Snyder, 2007). This RSNs concept could explain the activations of bilateral DLPFC areas and simultaneous deactivation of medial areas of the APFC that we observed, supporting the "focal activation/surround deactivation" concept. This means that similar focal activation patterns can be observed with fMRI and NIRS. Although the study revealed interesting results concerning hemodynamic changes in the prefrontal cortex during MA, some limitations should also be mentioned. First of all, the small sample of subjects. Although we found statistically significant [oxy-Hb] changes in 8 out of 10 subjects, a bigger sample is needed to clarify some individual changes of [oxy-Hb] increase/decrease during MA. It has to be taken into consideration that all optodes were placed over the PFC which is the most elaborated neocortical structure of the human brain and receives and sends commands to many cortical as well as sub cortical structures (for review see e.g. Miller and Cohen, 2001). It has been demonstrated that the PFC is strongly involved in conscious intention (Haggard, 2005) and attentional processes, response selection and response inhibition (Hummel et al., 2004; Koechlin et al., 2003; Rubia et al., 2003). This complex structure of the PFC could be one reason that, in the multi-channel NIRS recordings, the individual channels displayed some variable responses in a few subjects (see Fig. 3).The variability in the hemodynamic patterns may be related to slow (<0.1 Hz) fluctuations of ongoing neuronal activity, as reported recently with fMRI (Logothetis et al., 2009).

In summary, the study demonstrates that significant [oxy-Hb] increases and [oxy-Hb] decreases can be found at optodes placed over the prefrontal cortex even during simple MA. This finding demonstrates for the first time that the phenomenon of "focal activation/surround deactivation" is not only found in EEG and fMRI data but also with multi-channel NIRS. Furthermore, there is evidence that the antagonistic hemodynamic response pattern during MA may be suitable in an optical BCI with good performance, and that only 2 prefrontal NIRS channels may be necessary to realize such BCI system.

## Acknowledgements

The authors' BCI research has been supported by the EU project PRESENCCIA (IST-2006-27731), "Land Steiermark" (project A3-22. N-13/2009-8) and the Neuro Center Styria (NCS) in Graz, Austria. We would like to thank S. Kober for performing statistical analysis, B. Allison for proofreading the manuscript and the unknown reviewers for their important and helpful comments.

## References

Bauernfeind, G., Leeb, R., Wriessnegger, S.C., Pfurtscheller, G., 2008. Development, set-up and first results for a one-channel near-infrared spectroscopy system. Biomed. Tech. (Berl) 53 (1), 36–43.
Buxton, R.B., Uludağ, K., Dubowitz, D.J., Liu, T.T., 2004. Modeling the hemodynamic response to brain activation. Neuroimage 23 (Suppl 1), S220–S233.
Cohen, J., 1988. Statistical Power Analysis for the Behavioral Sciences. Lawrence Erlbaum Associates, Hillsdale, NJ.
Coyle, S., Ward, T., Markham, C., 2004. Physiological noise in near-infrared spectroscopy: implications for optical brain computer interfacing. Conf. Proc. IEEE Eng. Med. Biol. 6, 4540–4543.
Coyle, S.M., Ward, T.E., Markham, C.M., 2007. Brain-computer interface using a simplified functional near-infrared spectroscopy system. J. Neural. Eng. 4 (3), 219–226.
Damoiseaux, J.S., Rombouts, S.A., Barkhof, F., Scheltens, P., Stam, C.J., Smith, S.M., Beckmann, C.F., 2006. Consistent resting-state networks across healthy subjects. Proc. Natl Acad. Sci. USA 103 (37), 13848–13853.
De Boer, R.W., Karemaker, J.M., Strackee, J., 1986. On the spectral analysis of blood pressure variability. Am. J. Physiol. Heart Circ. Physiol. 251, H685–H687.
Ehrsson, H.H., Geyer, S., Naito, E., 2003. Imagery of voluntary movement of fingers, toes, and tongue activates corresponding body-part-specific motor representations. J. Neurophysiol. 90 (5), 3304–3316.
Elwell, C.E., Springett, R., Hillman, E., 1999. Oscillations in cerebral haemodynamics — implications for functional activation studies. Adv. Exp. Med. Biol. 471, 57–65.
Fox, P.T., Raichle, M.E., 1986. Focal physiological uncoupling of cerebral blood flow and oxidative metabolism during somatosensory stimulation in human subjects. Proc. Natl Acad. Sci. USA 83 (4), 1140–1144.
Franceschini, M.A., Fantini, S., Thompson, J.H., Culver, J.P., Boas, D.A., 2003. Hemodynamic evoked response of the sensorimotor cortex measured noninvasively with near-infrared optical imaging. Psychophysiol. 40 (4), 548–560.
Haggard, P., 2005. Conscious intention and motor cognition. Trends Cogn. Sci. 9 (6), 290–295.
Herrmann, M.J., Ehlis, A.C., Wagener, A., Jacob, C.P., Fallgatter, A.J., 2005. Near-infrared optical topography to assess activation of the parietal cortex during a visuo-spatial task. Neuropsychologia 43 (12), 1713–1720.
Herrmann, M.J., Huter, T., Plichta, M.M., Ehlis, A.C., Alpers, G.W., Mühlberger, A., Fallgatter, A.J., 2008. Enhancement of activity of the primary visual cortex during processing of emotional stimuli as measured with event-related functional near-infrared spectroscopy and event-related potentials. Hum. Brain Mapp. 29 (1), 28–35.
Hofmann, M.J., Herrmann, M.J., Dan, I., Obrig, H., Conrad, M., Kuchinke, L., Jacobs, A.M., Fallgatter, A.J., 2008. Differential activation of frontal and parietal regions during visual word recognition: an optical topography study. Neuroimage 40 (3), 1340–1349.
Hock, C., Müller-Spahn, F., Schuh-Hofer, S., Hofmann, M., Dirnagl, U., Villringer, A., 1995. Age dependency of changes in cerebral hemoglobin oxygenation during brain activation: a near-infrared spectroscopy study. J. Cereb. Blood Flow Metab. 15 (6), 1103–1108.
Hoshi, Y., Tamura, M., 1993. Detection of dynamic changes in cerebral oxygenation coupled to neuronal function during mental work in man. Neurosci. Lett. 150 (1), 5–8.
Hoshi, Y., Onoe, H., Watanabe, Y., Andersson, J., Bergström, M., Lilja, A., Långström, B., Tamura, M., 1994. Non-synchronous behaviour of neuronal activity, oxidative metabolism and blood supply during mental tasks in man. Neurosci. Lett. 172, 129–133.
Hummel, F., Saur, R., Lasogga, S., Plewnia, C., Erb, M., Wildgruber, D., Grodd, W., Gerloff, C., 2004. To act or not to act. Neural correlates of executive control of learned motor behavior. Neuroimage 23 (4), 1391–1401.
Hummel, F., Andres, F., Altenmüller, E., Dichgans, J., Gerlof, C., 2002. Inhibitory control of acquired motor programmes in the human brain. Brain 125, 404–420.
Kawashima, R., Taira, M., Okita, K., Inoue, K., Tajima, N., Yoshida, H., Sasaki, T., Sugiura, M., Watanabe, J., Fukuda, H., 2004. A functional MRI study of simple arithmetic — a comparison between children and adults. Brain Res. Cogn. Brain Res. 18 (3), 227–233.

Koechlin, E., Ody, C., Kouneiher, F., 2003. The architecture of cognitive control in the human prefrontal cortex. Science 302 (5648), 1181–1185.
Logothetis, N.K., Murayama, Y., Augath, M., Steffen, T., Werner, J., Oeltermann, A., 2009. How not to study spontaneous activity. Neuroimage 45 (4), 1080–1089.
Luu, S., Chau, T., 2009. Decoding subjective preference from single-trial near-infrared spectroscopy signals. J. Neural. Eng. 6 (1), 016003.
Mantini, D., Perrucci, M.G., Del Gratta, C., Romani, G.L., Corbetta, M., 2007. Electrophysiological signatures of resting state networks in the human brain. Proc. Natl Acad. Sci. USA 104 (32), 13170–13175.
Miller, E.K., Cohen, J.D., 2001. An integrative theory of prefrontal cortex function. Annu. Rev. Neurosci. 24, 167–202.
Menon, V., Rivera, S.M., White, C.D., Glover, G.H., Reiss, A.L., 2000. Dissociating prefrontal and parietal cortex activation during arithmetic processing. Neuroimage 12 (4), 357–365.
Obrig, H., Hirth, C., Junge-Hülsing, J.G., Döge, C., Wolf, T., Dirnagl, U., 1996. Cerebral oxygenation changes in response to motor stimulation. J. Appl. Physiol. 81 (3), 1174–1183.
Okamoto, M., Dan, H., Sakamoto, K., Takeo, K., Shimizu, K., Kohno, S., Oda, I., Isobe, S., Suzuki, T., Kohyama, K., Dan, I., 2004. Three-dimensional probabilistic anatomical cranio-cerebral correlation via the international 10–20 system oriented for transcranial functional brain mapping. Neuroimage 21 (1), 99–111.
Pfurtscheller G., Allison B., Brunner C., Bauernfeind G., Solis-Escalante T., Scherer R., Zander T., Müller-Putz G., Neuper C., Birbaumer N., in press. The hybrid BCI. Front. Neuropro. doi:10.3389/fnpro.2010.00003.
Pfurtscheller, G., da Silva, F.H.L., 1999. Event-related EEG/MEG synchronization and desynchronization: basic principles. Clin. Neurophys. 110, 1842–1857.
Pfurtscheller, G., Neuper, C., 1994. Event-related synchronization of mu rhythm in the EEG over the cortical hand area in man. Neurosci. Lett. 174, 93–96.
Raichle, M.E., Snyder, A.Z., 2007. A default mode of brain function: a brief history of an evolving idea. Neuroimage 37 (4), 1083–1090.
Rickard, T.C., Romero, S.G., Basso, G., Wharton, C., Flitman, S., Grafman, J., 2000. The calculating brain: an fMRI study. Neuropsychologia 38 (3), 325–335.
Rubia, K., Smith, A.B., Brammer, M.J., Taylor, E., 2003. Right inferior prefrontal cortex mediates response inhibition while mesial prefrontal cortex is responsible for error detection. Neuroimage 20 (1), 351–358.
Shimada, S., Hiraki, K., Matsuda, G., Oda, I., 2004. Decrease in prefrontal hemoglobin oxygenation during reaching tasks with delayed visual feedback: a near-infrared spectroscopy study. Brain Res. Cogn. Brain Res. 20 (3), 480–490.
Sitaram, R., Zhang, H., Guan, C., Thulasidas, M., Hoshi, Y., Ishikawa, A., Shimizu, K., Birbaumer, N., 2007. Temporal classification of multichannel near-infrared spectroscopy signals of motor imagery for developing a brain-computer interface. Neuroimage 34 (4), 1416–1427.
Singh, A.K., Okamoto, M., Dan, H., Jurcak, V., Dan, I., 2005. Spatial registration of multichannel multi-subject fNIRS data to MNI space without MRI. Neuroimage 27 (4), 842–851.
Steinbrink, J., Villringer, A., Kempf, F., Haux, D., Boden, S., Obrig, H., 2006. Illuminating the BOLD signal: combined fMRI–fNIRS studies. Magn. Reson. Imaging 24 (4), 495–505.
Stevens, J., 2002. Applied Multivariate Statistics for the Social Sciences. Erlbaum, Mahwah, New Jersey.
Strangman, G., Culver, J.P., Thompson, J.H., Boas, D.A., 2002. A quantitative comparison of simultaneous BOLD fMRI and NIRS recordings during functional brain activation. Neuroimage 17 (2), 719–731.
Suffczynski, P., Pijn, J.P., Pfurtscheller, G., da Silva, F.H.L., 1999. Event-related dynamics of alpha band rhythm: a neuronal network model of focal ERD/surrounded ERS, In: Pfurtscheller, G., Lopes da Silva, F.H.L. (Eds.), Event-related Desynchronization, Revised ed: Handbook of Electroenceph. and Clin. Neurophysiol, 6. Elsevier, Amsterdam, pp. 67–85.
Tanida, M., Sakatani, K., Takano, R., Tagai, K., 2004. Relation between asymmetry of prefrontal cortex activities and the autonomic nervous system during a mental arithmetic task: near infrared spectroscopy study. Neurosci. Lett. 369 (1), 69–74.
Wriessnegger, S.C., Kurzmann, J., Neuper, C., 2008. Spatio-temporal differences in brain oxygenation between movement execution and imagery: a multichannel near-infrared spectroscopy study. Int. J. Psychophysiol. 67, 54–63.

# On the removal of physiolgical artifacts from fNIRS

**G. Bauernfeind[1], I. Daly[1], G.R. Müller-Putz[1]**

[1] *Institute for Knowledge Discovery, Laboratory of Brain-Computer Interfaces, Graz University of Technology, Graz, Austria*

Correspondence: G. Bauernfeind, Institute for Knowledge Discovery, Laboratory of Brain-Computer Interfaces, Graz University of Technology, Krenngasse 37/III, 8010 Graz, Austria. E-mail: g.bauernfeind@tugraz.at

***Abstract.*** In the present study we report on the reduction of physiological rhythms in hemodynamic signals recorded with functional near-infrared spectroscopy (fNIRS). We investigated the use of two different signal processing approaches (independent component analysis [ICA] and transfer function models [TFs]) to reduce the influence of respiratory and blood pressure rhythms (Mayer waves) on the hemodynamic responses. The results show that both approaches reduce the artifactual influences equivalently well. However, TFs do so with significantly lower impact ($p < 0.01$) on none artifactual signal components then ICA.

*Keywords:* Functional near infrared spectroscopy, artifact removal, transfer function, independent component analysis

## 1. Introduction

Functional near-infrared spectroscopy (fNIRS) is a noninvasive optical technique that can be used for neuroscientific studies and optical brain–computer interfaces (oBCIs) systems [Coyle et al., 2004]. With fNIRS characteristic cerebral hemodynamic responses (changes in oxy- (oxy-Hb) and deoxyhemoglobin (deoxy-Hb) concentration) during different types of tasks can be measured. A common challenge, not only for oBCIs, is stable and reliable investigation and classification of spatio-temporal patterns. For this it is essential to reduce the influence of physiological noise. A spectral analysis of the optical signal reveals various quasi-periodic physiological rhythms, such as cardiovascular, vascular, respiratory and 3$^{rd}$ order blood pressure (BP) rhythms (Mayer waves; [Koepchen, 1991]), which may influence the recorded signals [Coyle et al., 2004; Elwell et al., 1991] and superimpose the changes caused by cerebral activation. The aim of this work is to investigate and compare two signal processing approaches (independent component analysis (ICA) and transfer function (TF) models) which reduce the systemic influences (respiration and Mayer waves) in the recorded fNIRS signals.

## 2. Material and Methods

### 2.1. Subjects, experimental design and data aquisition

The investigations were carried out on a group of 10 subjects (6 female, aged 24.2 ± 4.2 years) who participated in an fNIRS study on the cortical effects of BCI training [Bauernfeind et al., 2011]. In the framework of this study the subjects performed three sessions of cue-guided right hand or feet motor imagery. For fNIRS recordings a 52-channel continuous wave system (ETG-4000, Hitachi Medical Co.) measuring changes of oxy-Hb and deoxy-Hb in the cortex was used. Only channels covering the motor cortex (34 channels) were used for further analysis. Additionally, in two of the three sessions (2 and 3) the continuous BP signal (CNAP$^{TM}$ Monitor 500, CNSystems Medizintechnik AG) and the respiration (resp) were recorded and used in the present study. From the BP signal the diastolic BP (BPdia) was extracted. These two signals (BPdia and resp) were band-pass filtered between 0.07-0.13 Hz and 0.2-0.4 Hz, respectively, and used in the following approaches to reduce the systemic influences in the recorded oxy-Hb signal.

### 2.2. Signal processing and analysis

**ICA approach:** The oxy-Hb signal is decomposed into independent components (ICs) via SOBI ICA [Belouchrani et. al., 1997]. The coherence between each IC and the BPdia and resp signals is then calculated. ICs for which the coherence with one of the artifact signals is higher than the mean of all the coherence scores with that artifact signal plus 1 standard deviation are flagged for removal. The choice of this threshold is based upon a compromise between removal of the components with the largest coherence with artifact signals and the desire to retain components with small or zero artifact contamination. The remaining ICs not flagged for removal are used to reconstruct the cleaned signals.

**TF approach:** By using the BPdia and resp signals, TF models were applied to remove the related influences. These models are of the form of $N\ \mathrm{n}\ = X\ n\ -\ \sum_{u=0}^{m} g_u Y\ n-u$ where $X[n]$ (n=1,2,3,…) denotes the time series of the recorded signal, $g_u$ (u=1,2,..,m) the model parameters, $Y$ the systemic influence and $N$ the signal without the influence. For further information see [Florian et al., 1998].

**Comparison:** To compare both approaches the oxy-Hb power reduction (averaged over the used channels) in the frequency bands between 0.07 and 0.13 Hz, for BP influence, and 0.2 and 0.4 Hz, for the respiration, were calculated (Figure 1A). Additionally, the power reduction in the non-influenced bands (0 - 0.06, 0.14 - 0.19 and 0.41 - 0.8 Hz), denoted as stability, was investigated. Good artifact removal will reduce the power in the BP and respiration bands while making no significant changes to the power in the rest of the spectrum. Hence, the lower the stability measure the more accurate the removal of artifacts.

## 3. Results

Combining both sessions, with TFs a mean reduction of 54% (BP influence) and 28% (respiration influence) was possible. No significant difference (for details see Figure 1B) was found between TF and ICA (43% (BP influence), 16% (respiration influence)). Comparing the stability a significant difference ($p < 0.001$) between ICA (25%) and TFs (3%) can be found.

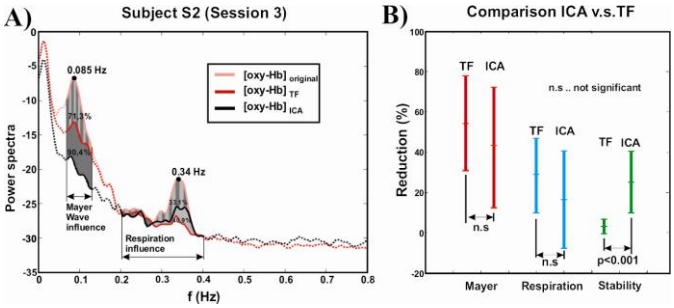


***Figure 1.*** *A) Example power spectrum (averaged over all channels) illustrating percentage reduction in Mayer wave and respiratory rhythms via ICA and TFs. B) General comparison between ICA and TF.*

## 4. Discussion

Both, ICA and TFs, are seen to produce large reductions in Mayer wave and respiration influences on the oxy-Hb signals. However, while TFs induce only small changes in none-artifactual signal components ICA induces much larger changes. This suggests that TFs are the most suitable choice for artifact reduction.

TFs require a large amount (~60s) of data with which to estimate the coefficients before they can begin to be applied. By contrast ICA does not require any previous measures of the signal. Hence, while TFs are more suitable for offline analysis in neuroscientific studies ICA is potentially much more suitable for online artifact removal and use in an oBCI. Finally, the influence on classification performance of both methods remains to be investigated.


### Acknowledgements

The authors' BCI research has been supported by the European ICT Programme Project FP7-224631 and the ''Land Steiermark''(project A3-22. N-13/2009-8).


### References


Bauernfeind G, Kaiser V, Kaufmann T, Kreilinger A, Kübler A, Neuper C. Cortical effects of BCI training measured with fNIRS. *International Journal of Bioelectromagnetism*, 13(2): 66-67, 2011.

Belouchrani A, Abed-Meraim K, Cardoso J, Moulines E. A blind source seperation technique using second-order statistics. IEEE Transactions on signal processing, 45(2): 434-444, 1997

Coyle S, Ward T, Markham C. Physiological noise in near-infrared spectroscopy: implications for optical brain computer interfacing. In proceedings of the 26th Annual International Conference of the IEEE/EMBS, 2004, 4540-4543.

Elwell CE, Springett R, Hillman E. Oscillations in cerebral haemodynamics – Implications for functional activation studies. *Advances in experimental medicine and biology*, 471: 57-65, 1999.

Florian G, Stancak A, Pfurtscheller G. Cardiac response induced by voluntary selfpaced finger movement. *International Journal of Psychophysiology*, 28: 273-283, 1998.

Koepchen HP. Physiology of rhythms and control systems: An integrative approach, in Rhythms, in physiological systems: An integrative approach. Haken H and Koepchen HP, Editors. Springer, 1991, 3-20.

# Classification of Focal Frontal Oxyhemoglobin Responses During Mental Arithmetic

G. Bauernfeind[1], R. Scherer[1], G. Pfurtscheller[1], C. Neuper[1,2]

[1]Institute for Knowledge Discovery, Laboratory of Brain-Computer Interfaces, Graz University of Technology, Graz, Austria
[2]Department of Psychology, University of Graz, Graz, Austria

g.bauernfeind@tugraz.at

**Abstract**

Near-infrared spectroscopy (NIRS) is a non-invasive optical technique for the assessment of functional activity in the human brain. Task-specific hemodynamic responses, i.e., concentration changes of oxy- and deoxyhemoglobin (oxy-Hb, deoxy-Hb) during cognitive, visual, visuo-motor, and motor tasks can be detected and used for brain-computer interfacing (BCI). For this study we used the data of a previous investigation on simple mental arithmetic (MA) tasks where we found antagonistic activation patterns (focal bilateral increase of oxy-Hb in the dorsolateral prefrontal cortex (DLPFC) in parallel with a decrease in the medial area of the anterior prefrontal cortex (APFC)) in eight of ten subjects. The oxy-Hb responses from the eight subjects were used to perform a cue-paced BCI off-line simulation. Therefore we searched for the best antagonistic feature combination from the left or right DLPFC and the APFC and compared it to individual features from the same regions. Our results indicate that the use of antagonistic features significantly increases the classification accuracy compared to individual features, that a mean classification accuracy of around 80 % by using antagonistic hemodynamic response patterns is possible, and that the use of these patterns may be a suitable control strategy for optical BCIs.

## 1 Introduction

Brain-computer interface (BCI) systems give users the possibility to communicate or interact through thought processes alone [1, 2]. The required methods are normaly based on the detection of neural activity by electroencephalography (EEG), magnetoencephalography (MEG), and recently, with functional magnetic resonance imaging (fMRI) [3, 4]. However, the use of these techniques may be restricted due to system size, ambient requirements, and user preparation (conductive gel, sensor placement, ...). As a more promising method the near-infrared spectroscopy (NIRS) technique can also be used for BCI systems [5]. However, there are some drawbacks to using NIRS for optical BCI applications. Beside the temporal resolution of the hemodynamic response - in the range of several seconds - a robust single-trial classification is essential. The identification of brain patterns that most naïve users can reliably generate and that are stable over time may significantly counteract this issue.

In [6] we investigated changes of oxy- and deoxyhemoglobin (oxy-Hb, deoxy-Hb) during the performance of simple mental arithmetic (MA) tasks in ten subjects. We found that eight out of ten subjects displayed a significant focal bilateral increase of oxy-Hb accompanied by a deoxy-Hb decrease in the dorsolateral prefrontal cortex (DLPFC). In parallel, they showed a significant decrease of oxy-Hb, accompanied by a deoxy-Hb increase, in most channels (the largest and most stable decreases are localized around the FP1 position) overlaying the medial area of the anterior prefrontal cortex (APFC). Such hemodynamic responses could be explained in the context of "focal activation/surround deactivation" and can be seen as antagonistic activation patterns [6]. We

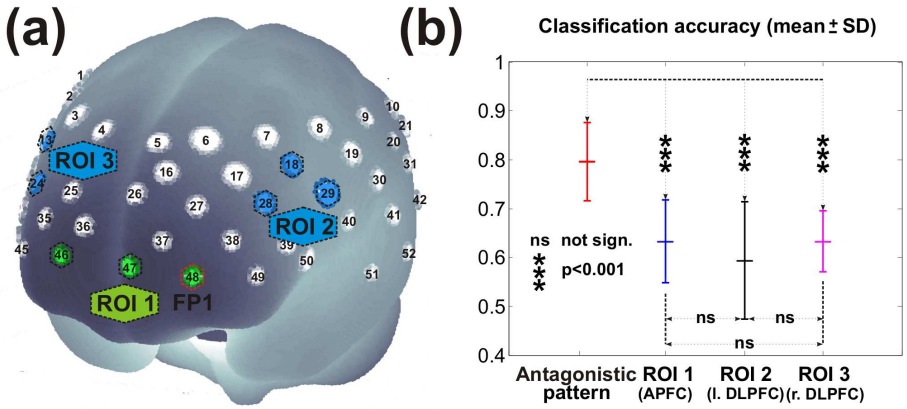


Figure 1: (a) Projections of the 52 NIRS channel positions (3x11 grid) on the cortical surface. Positions are overlaid on an MNI-152 compatible canonical brain which is optimized for NIRS analysis [7]. Also indicated are the regions of interest (ROI). (b) Significant contrasts of the classification accuracy between the antagonistic and individual features

hypothesized that these focal antagonistic hemodynamic response patterns during MA may be reliably detected by placing only two NIRS sensors over the prefrontal cortex. Here we evaluate the above hypothesis by means of cue-based BCI off-line simulations.

# 2 Methods

## 2.1 Subjects, Experimental Paradigm and Data Collection

The investigations were carried out on a group of eight healthy subjects (three males and five females, all right-handed) aged 26.0 ± 2.8 years (mean ± SD). The subjects were asked to perform a series of MA tasks. During the task they had to sequentially subtract a one-digit number from a two-digit number (e.g., 97-4=93, 93-4=89, ...; the initial subtraction was presented visually on a monitor) as quickly as possible for 12 seconds, afterwards a 28 s resting period was given. Subjects performed 3 or 4 runs resulting in 18 or 24 trials per class, respectively.
A continuous wave system (ETG-4000, Hitachi Medical Co., Japan) was used to record brain oxygenation. The multi-channel system measures the change of oxy-Hb and deoxy-Hb in the unit of mM*mm and consists of 16 photo-detectors and 17 light emitters (3x11 grid), resulting in a total of 52 channels. The lowest line of channels was arranged along the FP1- FP2 line of the international EEG 10-20 system, thus the grid covered the whole frontal lobe (for further details see [6]).

## 2.2 Data Analysis

The mean task-related concentration changes of oxy-Hb and deoxy-Hb, referenced to a 10 s baseline interval prior to the task (seconds -10 to 0) were calculated for each channel after removing baseline drifts by using a 0.01 Hz high-pass filter (for further details see [8]). To capture the antagonistic oxy-Hb patterns three regions of interest (ROI): $ROI_1$ over APFC, $ROI_2$ over the left DLPFC, and $ROI_3$ over right the DLPFC (see Figure 1a)) were defined according to the results of [6].
For classification a Fisher's linear discriminant analysis (LDA) classifier was used. To evaluate the LDA generalization, data recorded from each subject was split into a training and evaluation set. The former, consisting of trials 1 to 10 (16), was used to train and test the discriminative power of oxy-Hb feature combinations selected from the different ROIs. The best performing features were selected and used to train the LDA. The evaluation set, composed of the last eight trials, was then used to assess the performance of the trained LDA.

| Subj. | Anta. oxy-Hb feature | $ROI_1$ oxy-Hb feature | $ROI_2$ oxy-Hb feature | $ROI_3$ oxy-Hb feature |
|---|---|---|---|---|
| AG1 | 68.75 | 62.50 | 56.25 | 56.25 |
| AH3 | **87.50** | 62.50 | 50.00 | 62.50 |
| AK4 | **75.00** | 62.50 | 50.00 | 68.75 |
| AK8 | **87.50** | **81.25** | 50.00 | 62.50 |
| AL2 | **81.25** | 50.00 | 68.75 | 56.25 |
| AL6 | 68.75 | 62.50 | 50.00 | 62.50 |
| AM4 | **87.50** | 62.50 | **81.25** | 62.50 |
| AL2 | **81.25** | 62.50 | 68.75 | **75.00** |
| mean | 79.69 | 63.28 | 59.38 | 63.28 |
| SD | 8.01 | 8.48 | 12.05 | 6.19 |

Table 1: Classification accuracies (in %) for the antagonistic (Anta.) and individual features for all subjects. Bold numbers indicate classification accuracies above the chance level (71.9 % for 8 trials) [9].

Concentration changes (1-s mean) of the oxy-Hb response in the time windows from second 10 to 14 were labeled as class MA. Samples at seconds 26 to 30 were labeled as class REST. Features consist of an individual oxy-Hb value of one channel at a fixed time. For each subject, independent classifiers were trained and tested (leave-one-out cross validation) with individual oxy-Hb responses for each possible combination. Exhaustive Search, i.e., all possible feature combinations were evaluated, was used in the above procedure to identify the best performing antagonistic feature combination ($ROI_1$, $ROI_2$) or ($ROI_1$, $ROI_3$).

# 3 Results

The best performing classifiers calculated from the training set were used to compute an off-line simulation with the evaluation set (8 trials per class, see Table 1). Six out of the 8 subjects (75 %) performed better than the chance level (71.9 % for 8 trials) [9] using antagonistic patterns. In contrast only one subject performed better than random when using individual features from $ROI_1$, $ROI_2$, or $ROI_3$, respectively. An analysis of variance (ANOVA) and the Newman-Keuls posttest revealed that antagonistic features performed significantly better than individual features ($F_{(3/21)} = 8.74$; $p < 0.001$; Figure 1b).

# 4 Discussion

The aim of the study was to underpin the hypothesis of the usefulness of antagonistic oxy-Hb patterns (found in eight of ten subjects in [6]) in the context of single trial classification for optical BCIs. The given results state that only two NIRS sensors placed over predefined brain areas, i.e., left or right DLPFC and APFC, respectively, may significantly increase the performance of optical BCIs compared to the more common approach to use only one sensor (e.g., [10, 11]). By using the best antagonistic oxy-Hb features 75 % of the subjects reached accuracies above the chance level and a mean ± SD classification accuracy of 79.69 ± 8.01 % (Table 1) was computed. In contrast, individual features performed worse (classification accuracies of 63.28 ± 8.48 % ($ROI_1$), 59.38 ± 12.05 % ($ROI_2$) and 63.28 ± 6.19 % ($ROI_3$), Table 1). In each case only one subject reached accuracies above chance level.

# 5 Conclusion

The results of our study suggest that the use of antagonistic hemodynamic features may significantly increase the classification accuracy compared to individual features from the same regions. The off-line simulation results confirmed our hypothesis that two prefrontal NIRS channels can capture antagonistic hemodynamic patterns during a mental arithmetic task that can be detected reasonably well without the need of time consuming user-adaptation. In combination with a self paced paradigm the use of antagonistic pattern may be an important contribution for optical BCIs.

# 6 Acknowledgements

The authors' BCI research has been supported by the EU project PRESENCCIA (IST-2006-27731), "Land Steiermark" (project A3-22. N-13/2009-8) and the Neuro Center Styria (NCS) in Graz, Austria.

# References

[1] J. R. Wolpaw, N. Birbaumer, D. J. McFarland, G. Pfurtscheller, and T. M. Vaughan. Brain-computer interfaces for communication and control. *Clin Neurophysiol*, 113(6):94–109, 2002.

[2] N. Birbaumer. Breaking the silence: brain-computer interfaces (BCI) for communication and motor control. *Psychophysiology*, 43(6):517–532, 2006.

[3] N. Birbaumer, C. Weber, C. Neuper, E. Buch, K. Haapen, and L. Cohen. Physiological regulation of thinking: brain-computer interface (BCI) research. *Prog Brain Res*, 159:369–391, 2006.

[4] R. Sitaram, A. Caria, and N. Birbaumer. Hemodynamic brain-computer interfaces for communication and rehabilitation. *Neural Netw*, 22(9):1320–1329, 2009.

[5] S. Coyle, T. Ward, C. Markham, and G. McDarby. On the suitability of near-infrared (NIR) systems for next-generation brain-computer interfaces. *Physiol Meas*, 25(4):815–822, 2004.

[6] G. Pfurtscheller, G. Bauernfeind, S. C. Wriessnegger, and C. Neuper. Focal frontal (de)oxyhemoglobin responses during simple arithmetic. *Int J Psychophysiol*, 76:186–192, 2010.

[7] A. K. Singh, M. Okamoto, H. Dan, V. Jurcak, and I Dan. Spatial registration of multichannel multi-subject fNIRS data to MNI space without mri. *Neuroimage*, 27:842–841, 2005.

[8] G. Bauernfeind, R. Leeb, S. C. Wriessnegger, and G. Pfurtscheller. Development, set-up and first results for a one-channel near-infrared spectroscopy system. *Biomed Tech (Berl.)*, 53:36–43, 2007.

[9] G. R. Müller-Putz, R. Scherer, C. Brunner, R. Leeb, and G. Pfurtscheller. Better than random? A closer look on bci results. *Int J Bioelectromagn*, 10:52–55, 2008.

[10] M. Naito, Y. Michioka, K. Ozawa, Y. Ito, M. Kiguchi, and T. Kanazawa. A communication means for totally locked-in als patients based on changes in cerebral blood volume measured with near-infrared light. *IEICE Trans Inf Syst*, E90-D:1028–1037, 2007.

[11] K. Sagara, K. Kido, and K. Ozawa. Portable single-channel NIRS-based BMI system for motor disabilities' communication tools. *Conf Proc IEEE Eng Med Biol Soc*, 10:602–605, 2009.

# Slow Phase-related Oscillations of Prefrontal (De)oxyhemoglobin and Central EEG Alpha and Beta Power in the Resting Brain

G. Pfurtscheller[1], G. Bauernfeind[1], C. Neuper[1,2]

[1]Institute for Knowledge Discovery, Laboratory of Brain-Computer Interfaces, Graz University of Technology, Graz, Austria
[2]Department of Psychology, University of Graz, Graz, Austria

pfurtscheller@tugraz.at

**Abstract**

The present work examines the close interaction between brain and heart and shows that slow (de)oxyhemoglobin oscillations in the prefrontal cortex and changes in blood pressure and heart rate are coupled with a cyclic EEG alpha and beta power decrease in motor areas in the resting brain.

## 1 General Overview

Important features of biological systems are slow and ultraslow oscillations, particularly cyclic fluctuations around 0.1 Hz. Large-scale infraslow oscillations in the human cortex ranging from 0.02 to 0.2 Hz were reported by Vanhatalo and colleagues [1] in full-band EEG recordings. In this respect the study of Monto et al. [2] is particular of interest, because they demonstrated that the phase but not the amplitude of such slow oscillations correlated strongly with the subject's psychophysical performance. These results, and the observation that combined fMRI-EEG studies have demonstrated slow (<0.1 Hz) baseline fluctuations during resting wakefulness [3], strongly support the idea that slow EEG fluctuations are associated with fluctuations of the excitability of large-scale cortical networks (resting state networks, RSNs). Slow oscillations have not only been observed in cerebral oxyhemoglobin concentrations, oxygen availability of cortical tissue, cerebral blood flow velocity, and cerebral blood flow, but also in the cardiovascular system (so-called Mayer waves around 0.1 Hz; [4]).

Of interest is the mutual interaction between brain and heart. From non-human animal research, we have evidence that cortical systems, especially including the medial-prefrontal cortex, act as a network together with subcortical systems (known as "central autonomic network") to initiate and represent cardiac autonomic adjustments (Figure 1). This cooperative behavior of the two most important organs of the body is not unexpected, because the great French physiologist Claude Bernard intimated the connection between brain and heart (for a review see [5]). It is well documented that the prefrontal cortex is linked to autonomic motor circuits responsible for sympathoexcitatory and parasympathoinhibitory control of the heart. This means cortical activity controls cardiac activity, not only during movement execution and motor imagery, but also in the resting brain.

Prior to self-paced movement, the Bereitschaftspotential is generated and the EEG desynchronized, and also the heart rate decelerates and the heart rate intervals (RRIs) increase, respectively. All these changes in brain and heart activity start at least 1-3 seconds before the motor act, are unconscious and enter consciousness around 250 ms before movement. These observations can be seen as an example of the close interaction between brain and heart and the relatively long time durations of the individual phenomena in the order of some seconds.

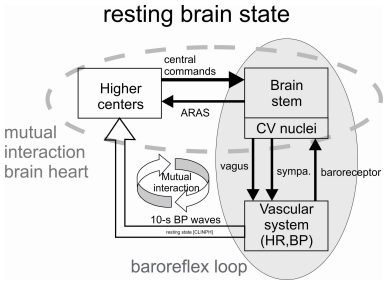


Figure 1: Simplified scheme of interactions between brain and heart during rest.

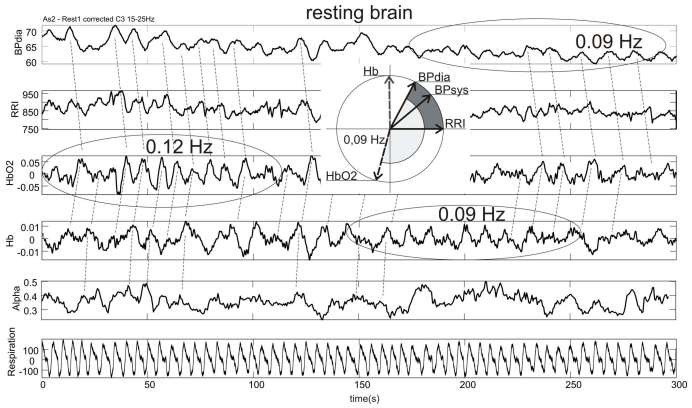


Figure 2: Time courses of BPdia, RRI, $HbO_2$, Hb, respiration and EEG beta power recorded during 5 minutes of rest. Dominant in all traces are the varying oscillations around 0.1 Hz. The phase relationships between slow waves at 0.09 Hz are indicated by stippled lines and in the phase plot. Note the instability of slow cyclic oscillations especially in the (de)oxyhemoglobin concentration

## 2 Methods

We continuously measured blood pressure (BP), heart rate intervals (RRI), prefrontal oxyhemoglobin ($HbO_2$) and deoxyhemoglobin (Hb) with the near-infrared spectroscopy (NIRS) method [4] and central EEG signals during 5 minutes of rest. 19 healthy subjects were investigated, about 60% of whom had slow $HbO_2$/Hb oscillations around 0.1 Hz in the resting brain.

## 3 Results and Discussion

During 5 minutes of rest, the BP, RRI and $HbO_2$/Hb exhibited slow oscillations around 0.1 Hz, which were non-stationary. Examples of one characteristic subjects are shown in Figure 2. The average phase shift between diastolic BP and RRI oscillations was 81 $\pm$ 21$^o$ (mean $\pm$ SD) with BP leading. The phase shift between BP and HbO2 was varying between 0 and 200$^o$ with BP also leding. Some subject displayed a clear phase relationship between prefrontal $HbO_2$/Hb oscillations and central EEG alpha or beta power changes during rest.

In summary, slow out-of-phase $HbO_2$ - Hb oscillations in prefrontal cortex are coupled with a cyclic EEG alpha and beta power decrease in motor areas in the resting brain. Hence, the timing of movement execution or imagery at free will appears to be modulated by fluctuations of brain excitability in the prefrontal cortex coupled to motor cortex activity.

# 4 Conclusion

Three points are of interest for BCI research and new developments in the near future:

- First, oscillations around 0.1 Hz have to be considered as physiological noise when an optical BCI is realized. They can be removed, e.g. by the use of a transfer function model. The prefrontal cortex is of special interest because the optodes can be easily attached there and because the user‘s intent is accompanied by the activation of prefrontal network. Such optical BCIs with optodes placed over the prefrontal cortex are especially suitable for use at home or work.
- Second, rhythmic cortical excitability changes around 0.1 Hz can be used to present the cue-stimuli phase-related to slow prefrontal oxyhemoglobin, blood pressure or heart rate oscillations during e.g. ERD-based BCI training. It can be expected that such an experimental paradigm can shorten the trainings time and improve the BCI performance.
- Third, pathways originating in the prefronal cortex can activate cardiovascular neurons in the brain stem and result in cardiac changes. Such heart rate changes can be on the order of 10 beats/min during foot motor imagery, and easily be detected in the ongoing ECG signal [6]. Parallel processing of EEG and ECG signals in a hybrid BCI can improve the BCI performance.

# 5 Acknowledgements

The authors' BCI research has been supported by the EU project PRESENCCIA (IST-2006-27731), "Land Steiermark" (project A3-22. N-13/2009-8) and the Neuro Center Styria (NCS) in Graz, Austria.

# References

[1] S. Vanhatalo, J. M. Palva, M. D. Holmes, J. W. Miller, J. Voipio, and K. Kaila. Infraslow oscillations modulate excitability and interictal epileptic activity in the human cortex during sleep. *Proc Natl Acad Sci U S A*, 101(14):5053–5057, 2004.

[2] S. Monto, S. Palva, and J. Voipioand J. M. Palva. Very slow EEG fluctuations predict the dynamics of stimulus detection and oscillation amplitudes in humans. *J Neurosci*, 28(33):8268–8272, 2008.

[3] D. Mantini, M. G. Perrucciand C. Del Gratta, G. L. Romani, and M. Corbetta. Electrophysiological signatures of resting state networks in the human brain. *Proc Natl Acad Sci U S A*, 104(32):13170–13175, 2007.

[4] G. Pfurtscheller, D. Klobassa, C. Altstätter, G. Bauernfeind, and C. Neuper. About the stability of phase-shifts between slow oscillations around 0.1 hz in cardiovascular and cerebral systems. *IEEE Trans Biomed Eng*, PP(99):1, 2011.

[5] J. F. Thayer and R. D. Lane. Claude bernard and the heart-brain connection: further elaboration of a model of neurovisceral integration. *Neurosci Biobehav Rev*, 33(2):81–88, 2008.

[6] G. Pfurtscheller, B. Z. Allison, C. Brunner, G. Bauernfeind, T. Solis-Escalante, R. Scherer, T. O. Zander, G. R. Müller-Putz, C. Neuper, and N. Birbaumer. The hybrid BCI. *Front Neurosci*, 4:30, 2010.

# Neural correlates of the execution and inhibition of well learned foot and finger movements: an NIRS study.

G. Bauernfeind[1], K. Schweizer[2], S. Kober[2], G. Pfurtscheller[1], C. Neuper[1,2]
E-mail: g.bauernfeind@tugraz.at
[1]Institute for Knowledge Discovery, Graz University of Technology, Graz, Austria;
[2]Department of Psychology, University of Graz, Graz, Austria

## INTRODUCTION

Adequate behaviour requires the control (execution/inhibition) of learned programs in a situational context. Inspired by the fMRI-work of Hummel [1] the aim of this study was to investigate the appropriate control of acquired and memorized motor programs (to our knowledge the first time) with the NIRS method.

## METHODS

Investigations were carried out with a group of 16 subjects (7 males, 9 females) aged 26.9 ± 3.4 years (mean ± SD). The experiment consisted of three blocks in the following order: Hand movement block (indicated by showing the picture of a hand); foot movement block (indicated by showing the picture of a foot) and a block with randomized hand and foot movements. In each block the subjects had to execute/inhibit sequences (8 movements, duration 10 sec) of right hand finger or foot movements of two different task complexities in a random order. In order to indicate if execution or inhibition was required a green (execution) or a red (inhibition) frame was shown around the picture. A commercial NIRS system (ETG-4000, Hitachi Medical Co., Japan, 46 channels) was used to record brain oxygenation (oxy-Hb and deoxy-Hb). After a visual inspection of the raw NIRS data, trials containing motion artefacts were removed manually. Afterwards a common average reference (CAR) spatial filter was used. Hereafter, the mean task related (de)oxy-Hb changes were calculated and a statistical analysis was performed.

## RESULTS

The execution of finger/foot movements caused an increase of oxy-Hb and a decrease of deoxy-Hb in the hand or foot representation area (left or medial somatosensory cortex) which is typical for an activation pattern. The inhibition of finger/foot movements caused a decrease of oxy-Hb and an increase of deoxy-Hb in the hand or foot representation area. An additional general observation was the finding of an oxy-Hb increase and a decrease in the deoxy-Hb in the medial area of the anterior prefrontal cortex during the inhibition of finger/foot movements.

## DISCUSSION

All these (preliminary) findings (investigation is in progress) are in line with the findings of Hummel [1] and provide the importance of doing research not only in activation but also in inhibition conditions with NIRS. Additionally these results may be useful in therapeutic strategies to enhance functional recovery.

## References

[1] Hummel F, Saur R, Lasogga S, et al. To act or not to act. Neural correlates of executive control of learned motor behavior. Neuroimage 2004; 23(4):1391-401.

**Poster Nr. 2**

# Fokale frontale (De)oxyhämoglobin-Änderungen während einfacher arithmetischer Aufgaben: Anmerkungen zur Verwendung als Steuersignal für optische Gehirn-Computer-Interface (oBCI)-Anwendungen

Günther Bauernfeind[1], Selina Wriessnegger[1], Gert Pfurtscheller[1], Christa Neuper[1,2]

[1]Institut für Semantische Datenanalyse, Technische Universität Graz, Österreich; [2]Institut für Psychologie, Karl-Franzens-Universität Graz, Österreich

Verschiedene Forschungsgruppen haben im Laufe der letzten Jahrzehnte ihren Schwerpunkt auf Kommunikations- bzw. Ansteuerungshilfe für schwerst gelähmte PatientInnen gelegt. Die dazu notwendigen Methoden der Brain-Computer-Interface (BCI)-Technologie basieren üblicherweise auf der Detektion kognitiver Prozesse aus mittels Elektroenzephalographie (EEG) gemessenen Signalen. Neben der Verwendung des EEG ist eine Realisierung solcher Systeme auch auf Basis der funktionellen Magnetresonanztomographie (fMRI) oder der Magnetoenzephalographie (MEG) möglich. Zusätzlich zu diesen bereits gut etablierten Methoden bietet sich die Nah-Infrarot-Spektroskopie (NIRS) als eine weitere vielversprechende Methode an. Gegenüber EEG, fMRI und MEG bietet die NIRS den Vorteil einer einfacheren Applikation. Weitere Vorteile gegenüber fMRI und MEG bestehen in einer kostengünstigeren Anschaffung sowie der Mobilität des Messgerätes. Als Steuersignale können dabei die sensomotorischen Aktivierungsmuster während einer Bewegungsvorstellung herangezogen werden. Neben diesen ist auch eine Verwendung von Aktivierungsmustern während kognitiver Aufgaben, hier im Speziellen bei Durchführung einer einfachen arithmetischen Aufgabe, möglich. In den letzten Jahren konnte in vielen NIRS-Studien eine starke Beteiligung des präfrontalen Cortex (PFC) gezeigt werden. Dabei wurden jedoch nur wenige Messpositionen (meist ein oder zwei) für die NIRS-Messung herangezogen. Um einen genaueren Einblick in Bildung und Verteilung der Aktivierungsmuster zu erhalten, wurde in dieser Studie ein Vielkanal-NIRS-System verwendet.

Die Untersuchungen wurden an einer Gruppe von zehn gesunden ProbandInnen durchgeführt. Bei acht dieser zehn TeilnehmerInnen konnte über dem dorsolateralen PFC ein fokaler bilateraler Anstieg in der Oxyhämoglobinkonzentration, begleitet von einem Abfall der Deoxyhämoglobin-Konzentration, gemessen werden. Parallel zu dieser dorsolateralen Aktivierung ist auch ein Anstieg in der Deoxyhämoglobinkonzentration bei gleichzeitigem Abfall der Oxyhämoglobin-Konzentration über dem mittleren Bereich des anterioren PFC messbar. Diese antagonistischen Muster lassen sich als Steuersignale für oBCI-Systeme verwenden, wobei mittels der Multikanalmessung die entsprechenden Messpositionen zu bestimmen sind.

# Classification of Focal Frontal Oxyhemoglobin Responses During Mental Arithmetic

G. Bauernfeind[1], R. Scherer[1], G. Pfurtscheller[1], C. Neuper[1,2]

[1]*Institute for Knowledge Discovery, BCI Lab, Graz University of Technology, Austria*

[2]*Department of Psychology, University of Graz, Austria*

## Introduction

For near-infrared spectroscopy (NIRS) based optical brain-computer interface (BCI) systems [1] a robust single-trial classification of task-specific hemodynamic responses, i.e., concentration changes of oxy- and deoxy-hemoglobin ([oxy-Hb], [deoxy-Hb]), is essential [2]. The identification of brain patterns that the majority of naïve users can reliably generate and that are stable over time may significantly support this issue.
For this investigation [2] we used the data of a previous study on simple mental arithmetic (MA) tasks [3] where we found antagonistic activation patterns (Fig. 1) in eight of ten subjects.

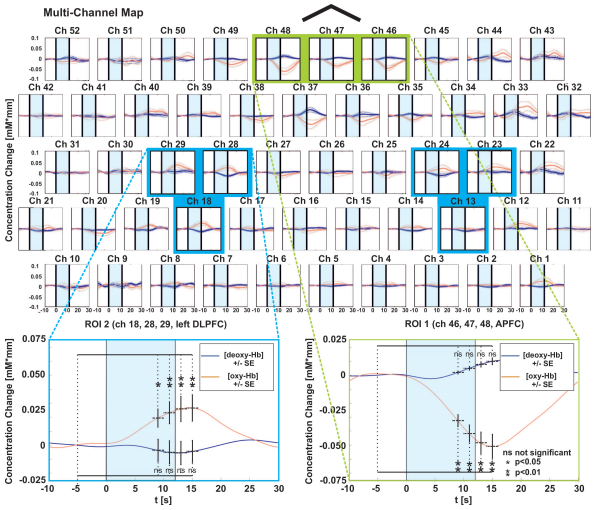


**Figure 1:** Grand average (8 subjects) concentration changes (mean ± SE) showing an focal bilateral increase of [oxy-Hb] in the dorsolateral prefrontal cortex (DLPFC) in parallel with a decrease in the medial area of the anterior prefrontal cortex (APFC) and averaged responses. For further details see [3].

## Methods

We used the [oxy-Hb] responses to search for the best antagonistic feature combination and compared it to individual features from the same regions. Additionally we investigated the use of antagonistic [deoxy-Hb], total hemoglobin [Hbtot] and pairs of [oxy-Hb] and [deoxy-Hb] features as well as the existence of a group-related feature set.

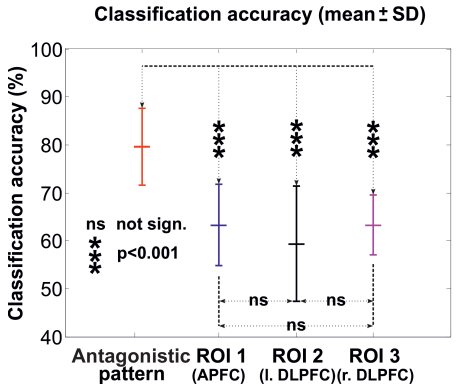


**Figure 2:** Significant contrasts of the classification accuracy between the antagonistic and individual features.

## Subjects, Experimental Paradigm and Data Collection

- Subjects: Three males and five females 26.0 ± 2.8 years
- Task: Series of MA tasks. Sequentially subtraction of a one-digit from a two-digit number (e.g., 97-4=93, 93-4=89, ...) for 12 seconds followed by a 28 s resting period (18 or 24 trials per class) [3].
- Data Collection: 52-channel continuous wave system (ETG-4000, Hitachi Medical Co., Japan). For further details see [3].

## Data Analysis

- Baseline drifts removed by a 0.01 Hz high-pass filter [4]
- Calculation of task-related concentration change referenced to a 10 s baseline interval prior the task (seconds -10 to 0)
- Definition of three regions of interest (ROI): Figure 1; [3]
- Data splitted into training and evaluation set [2]
- Fetures: Concentration changes (1-s window mean) from second 10 to 14 (class MA); from seconds 26 to 30 (class REST)
- Independent classifiers trained and tested (leave-one-out cross validation)
- Identification of best performing antagonistic feature combination by Exhaustive Search

## Results

- Antagonistic [oxy-Hb] features perform significantly better than individual features ($F_{(3/21)} = 8.74$; $p < 0.001$; Fig. 2, Table 1).
- Antagonistic [oxy-Hb] features perform significantly better than antagonistic [deoxy-Hb] features ($F_{(4/28)} = 2.81$; $p < 0.05$). No significant differences were found between antagonistic [oxy-Hb], antagonistic [Hbtot] as well as ([oxy-Hb], [deoxy-Hb]) tuples (Table 1).
- The group-related [oxy-Hb] features set (most commonly selected features (Ch. 47 and 28; $t_{MA} = 12$s, $t_{REST} = 28$s) of all subjects) achieved a classification accuracy of 70.3 % over all subjects (Table 1). No significant differences were found between the use of subject-specific antagonistic features and the group-related feature set.

**Table 1:** Classification accuracies (in %) for the antagonistic and individual features as well as for antagonistic [deoxy-Hb], [Hbtot] and tuples of [oxy-Hb] and [deoxy-Hb] and the group-related set of antagonistic [oxy-Hb] features.

| | Anta. | $ROI_1$ | $ROI_2$ | $ROI_3$ | Antagonistic pattern | | | |
|---|---|---|---|---|---|---|---|---|
| Subj. | [oxy-Hb] feature | [oxy-Hb] feature | [oxy-Hb] feature | [oxy-Hb] feature | [deoxy-Hb] | [Hbtot] | [deoxy-Hb] and [oxy-Hb] | group-related |
| AG1 | 68.75 | 62.50 | 56.25 | 56.25 | 68.75 | 50.00 | 68.75 | 68.75 |
| AH3 | **87.50** | 62.50 | 50.00 | 62.50 | 62.50 | **81.25** | 68.75 | **75.00** |
| AK4 | **75.00** | 62.50 | 50.00 | 68.75 | 62.50 | 56.30 | **75.00** | 68.75 |
| AK8 | **87.50** | **81.25** | 50.00 | 62.50 | **81.25** | **93.75** | **81.25** | **87.50** |
| AL2 | **81.25** | 50.00 | 68.75 | 56.25 | 50.00 | 68.75 | 68.75 | 62.50 |
| AL6 | 68.75 | 62.50 | 50.00 | 62.50 | 56.25 | 56.25 | 62.50 | 50.00 |
| AM4 | **87.50** | 62.50 | **81.25** | 62.50 | 62.25 | **93.75** | 68.75 | **75.00** |
| AN5 | **81.25** | 62.50 | 68.75 | **75.00** | **87.50** | **81.25** | **93.75** | **75.00** |
| mean | 79.69 | 63.28 | 59.38 | 63.28 | 66.38 | 72.66 | 73.44 | 70.31 |
| SD | 8.01 | 8.48 | 12.05 | 6.19 | 12.48 | 17.33 | 9.88 | 10.95 |

## Discussion

Our results indicate that the use of the antagonistic [oxy-Hb] features significantly increases the classification accuracy from 63.3 % to 79.7 %. These results support the hypothesis that antagonistic hemodynamic response patterns are a suitable control strategy for optical BCI, and that only two prefrontal NIRS channels are needed for good performance.

## References

1. S. Coyle and T. Ward and C. Markham and G. McDarby, *Physiological Measurement*, 25(4):815–822, 2004.
2. G. Bauernfeind and R. Scherer and G. Pfurtscheller and C. Neuper, *Medical and Biological Engineering and Computing*, 49(9):979–984, 2011.
3. G. Pfurtscheller and G. Bauernfeind and S. C. Wriessnegger and C. Neuper, *International Journal of Psychophysiology*, 76:186–192, 2010.
4. G. Bauernfeind and R. Leeb and S.C. Wriessnegger and G. Pfurtscheller, *Biomedizinische Technik (Berl.)* 53:36-43, 2008.

## Acknowledgments

*The authors' BCI research has been supported by the "Land Steiermark" (project A3-22. N-13/2009-8) and the Neuro Center Styria (NCS) in Graz, Austria.*

# Cortical Effects of BCI Training Measured with fNIRS

G. Bauernfeind[1], V. Kaiser[1], T. Kaufmann[2], A. Kreilinger[1], A. Kübler [2], C. Neuper[1,3]

[1] Institute for Knowledge Discovery, Graz University of Technology, Graz, Austria
[2] Department of Psychology I, University of Würzburg, Würzburg, Germany
[3] Department of Psychology, University of Graz, Graz, Austria

## Introduction

As a result of feedback training, for example motor imagery (MI) based BCI training, and non-stationarity of the measured EEG signals, relevant EEG patterns usually change and require the adjustment of classifier and feedback [1, 2]. To evaluate which areas are involved in such changes and how the activity of these areas changes over time, the present study investigates cortical effects of BCI training with multichannel fNIRS measurements.

## Methods

**Participants:** The investigations were carried out on a group of 15 subjects (8 male, 7 female, all right-handed, aged 24 ± 2.3).

**Experiment:** Ten experimental sessions: one screening, six BCI-training and three fNIRS sessions without feedback (Figure 1A). In the fNIRS sessions the participants had to imagine cue-guided right hand (RH) or feet (FE) MI (Figure 1B). In the training sessions the subjects received feedback in form of a cursor on a computer screen.

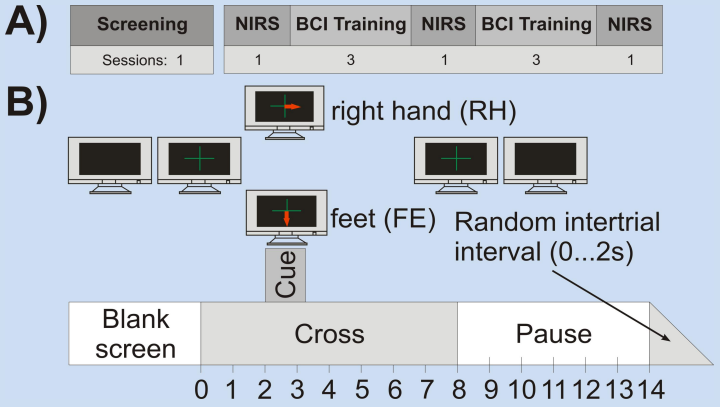


*Figure 1: A) Experimental sessions B)Timing of the fNIRS paradigm.*

**Data acquisition and processing:** EEG was recorded bipolarly from electrodes placed over C3, Cz and C4. For fNIRS recording a multichannel continuous wave system was used. The system measured the change of [oxy-Hb] and [deoxy-Hb] in (mM mm) and consisted of 16 detectors and 17 emitters (3×11 grid, 52 Ch.). The grid was arranged above the motor cortex (Figure 2). For the subsequent analysis only the [oxy-Hb] data of channels covering functional involved areas were used.
Averages of three regions of interest (ROI; ROI1 over C3; ROI2 over Cz and ROI3 over C4; Figure 2) were computed. For statistical analysis the subjects were split into two equal groups (n=5) according to their mean classification accuracy of the EEG sessions (accuracy < or > 70 %).

## Results

The ANOVA revealed a significant interaction "GROUP" x "CHANNEL" x "SESSION" ($F(4, 32) = 3.68$, $p<0.05$). For bad performer (< 70 %) significant differences between C3 and C4 during session one (.0063 ± 0.0039; -.0058 ± .0044) and two (.0001 ± .0062; -.0082 ± .0048) and between Cz and C4 during session two (.0021 ± .0042; -.0082 ± .0048) and three (.0035 ± .0032; -.0056 ± .0044) could be found. For the good performers (> 70 %) significant differences between C3 (.0044 ± .0077) and Cz (-.0048 ± .0032) could be found in session three.

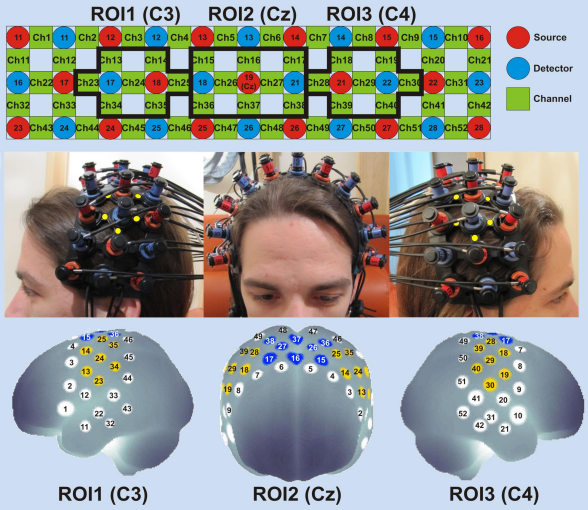


*Figure 2: A) Schematic illustration of the multi-channel array. B) Array mounted on a subjects head. C) Projections of the NIRS channel positions on the cortical surface.*

## Discussion and Conclusion

According to the group membership, significant differences in the course of the BCI training could be found. The subjects below 70 % accuracy showed significant cortical activation differences between C3 and C4 (strong lateralization effect) as well as between Cz and C4, but no significant difference between C3 and Cz in the course of the training.
These findings could be interpreted as a co-activation of C3 and Cz during both tasks, which may explain that these subjects performed worse in the EEG sessions (< 70 %). In contrast, the subjects above 70 % showed no significant differences between C3 and C4 as well as between Cz and C4 in the course of the training, but according to the trainings task (hand vs. feet MI) significant differences between C3 and Cz at the end of the feedback training.
In summary, the study demonstrates that significant activity changes in functionally involved areas in the course of the training could be found and that these changes occur accordingly to the training task.

**References:**
[1] Neuper C, Müller-Putz GR, Scherer R, Pfurtscheller G. Motor imagery and EEG-based control of spelling devices and neuroprostheses. Prog Brain Res, 159: 393-409, 2006.
[2] Vidaurre C, Schlögl A, Scherer R, Cabeza R, Pfurtscheller G. Study of on-line adaptive discriminant analysis for EEG-based brain computer interfaces. IEEE Trans on Biomed Eng, 54:550-556, 2007.

**Acknowledgements:** This work is supported by the European ICT Programme Project FP7-224631, the "Land Steiermark" (project A3-22. N-13/2009-8) and the Neuro Center Styria (NCS) in Graz, Austria. This paper only reflects the authors' views and funding agencies are not liable for any use that may be made of the information contained herein.

# Single trial classification of focal frontal (de)oxyhemoglobin responses during simple arithmetic

G. Bauernfeind[1], R. Scherer[1], S.C. Wriessnegger[1], G. Pfurtscheller[1], C. Neuper[1,2]

[1]Laboratory of Brain-Computer Interfaces, Institute for Knowledge Discovery, Graz University of Technology, Graz, Austria

[2]Department of Psychology, University of Graz, Graz, Austria

## Introduction

Brain-computer interface (BCI) systems allow paralysed patients control of computers or external devices. Such systems are normally based on the electroencephalography (EEG) [1]. Beside EEG, such systems have also been realized with magnetoencephalography and recently with functional magnetic resonance imaging (fMRI) methods [1, 2]. However, the use of these techniques is restricted due to system size and ambient requirements. As a more promising method the near-infrared spectroscopy (NIRS) technique can also be used for future BCIs based on hemodynamic responses [2, 3, 4]. Besides motor tasks mainly cognitive tasks, in particular mental arithmetic (MA) operations are used. Several NIRS studies have demonstrated the implication of the prefrontal cortex (PFC) during MA, and found characteristic hemodynamic responses, but most of them used only one or two NIRS channels.

In this work, we studied PFC activation pattern during MA with a multichannel NIRS system and examined their usefullness for BCI applications (single trial classification) [5].

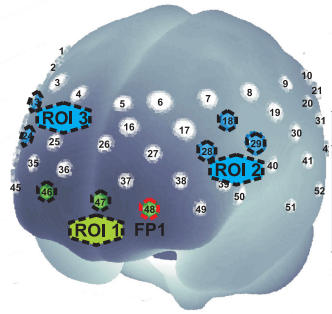


**Figure 1:** Projections of the NIRS channel positions on the cortical surface. Positions are overlaid on a MNI-152 compatible canonical brain which is optimized for NIRS analysis. The lowest line of channels was arranged along the FP1–FP2 line of the international EEG 10–20 system, with channel 48 exactly at the FP1 position. The centers of the circle regions represent the locations of the most likely MNI coordinates for the NIRS channel projected on the cortical surface. The edges represent the boundaries defined by the standard deviation. Modified from [5].

**Table 1:** Channel numbers, MNI coordinates, composite standard deviations for the estimation on the cortical surface (SD) and related Brodmann and anatomical areas of each ROI.

| ROI | Channel | MNI-space correspondence | | | | Cortical areas |
|---|---|---|---|---|---|---|
| | | *x* | *y* | *z* | SD | BA | |
| 1 APFC | 46 | 23 | 72 | 8 | 4 | 10 | SFG |
| | 47 | −8 | 73 | 6 | 5 | 10 | MeFG |
| | 48 | −31 | 66 | 3 | 5 | 10 | MFG |
| 2 Left DLPFC | 18 | −51 | 23 | 41 | 5 | 9 | MFG |
| | 28 | −47 | 39 | 28 | 6 | 46 | MFG |
| | 29 | −61 | 11 | 28 | 6 | 9 | IFG |
| 3 Right DLPFC | 13 | 48 | 31 | 42 | 5 | 9 | MFG |
| | 23 | 57 | 26 | 29 | 5 | 46 | MFG |
| | 24 | 45 | 62 | 29 | 5 | 46 | MFG |

BA, Brodmann area: SFG, superior frontal gyrus; MFG, middle frontal gyrus; IFG, inferior frontal gyrus; MeFG, medial frontal gyrus.

## Methods

Ten subjects (five males/ five females, all right-handed, aged 26.1 ± 2.7 years) were asked to repitively subtract a one-digit number from a two-digit number (e.g. 97-4=93, 93-4=89, …) as quickly as possible for 12 seconds.

To record brain oxygenation a continuous wave system (ETG-4000, Hitachi Medical Co., Japan) was used. The multi-channel system measures the change of [oxy-Hb] and [deoxy-Hb] in the unit of mM mm and consists of 16 photo-detectors and 17 light emitters (3×11 grid), resulting in a total of 52 channels. The lowest line of channels was arranged along the Fp1- Fp2 line of the international EEG 10-20 system, so the grid covers the whole frontal lobe (Fig. 1).

The mean task related concentration changes of oxy-Hb and deoxy-Hb referred to a 10 second baseline interval prior to the task (seconds -10 to 0) were calculated for each channel.

## Results

*Characteristic hemodynamic responses*

Fig. 2 presents the grand average hemodynamic responses ([oxy-Hb], [deoxy-Hb]) during the mental task. Eight out of ten subjects displayed a relative focal bilateral increase of [oxy-Hb] accompanied by a [deoxy-Hb] decrease in the dorsolateral PFC (DLPFC). In parallel, they showed an antagonistic decrease of [oxy-Hb], accompanied by a [deoxy-Hb] increase, in most channels overlaying the medial area of the anterior PFC (APFC).

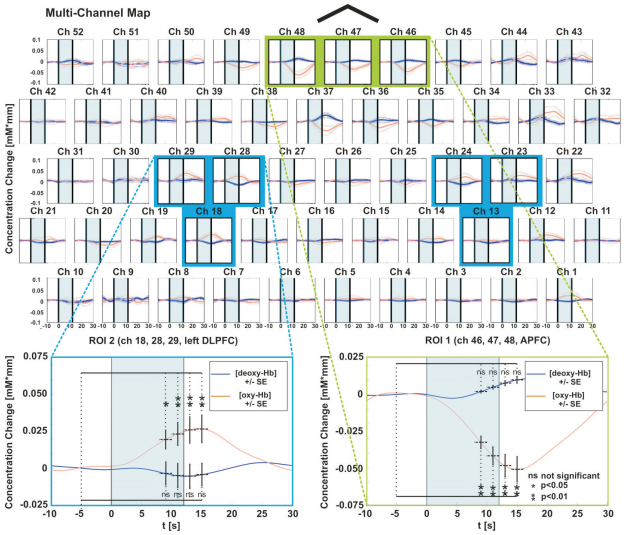


**Figure 2:** Grand average (8 subjects) concentration changes (mean±SE) of [oxy-Hb] and [deoxy-Hb] (upper panel) and averaged responses with significant changes for ROI2 and ROI1 (lower panels).

*Single trial classification*

According to these findings we hypnotized that there is evidence that the antagonistic response pattern during MA may be suitable in an optical BCI with good performance, and that only two NIRS channels over the PFC may be necessary to realize such a BCI system.We used the characteristic [oxy-Hb] responses from the eight subjects to search for the best antagonistic feature combination from the left or right DLPFC and the APFC and compared it to individual features from the same regions (Table 2 and Fig. 3).

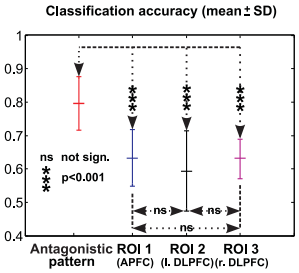


**Figure 3:** Significant contrasts of the classification accuracy between the antagonistic and individual features.

**Table 2:** Classification accuracies (in %, bold numbers indicate classification accuracies above the chance level) for all subjects using best antagonistic feature combination and individual feature.

| | Anta | ROI1 | ROI2 | ROI3 |
|---|---|---|---|---|
| AG1 | 68.75 | 62.50 | 56.25 | 56.25 |
| AH3 | **87.50** | 62.50 | 50.00 | 62.50 |
| AK4 | **75.00** | 62.50 | 50.00 | 68.75 |
| AK8 | **87.50** | **81.25** | 50.00 | 62.50 |
| AL2 | **81.25** | 50.00 | 68.75 | 56.25 |
| AL6 | 68.75 | 62.50 | 50.00 | 62.50 |
| AM4 | **87.50** | 62.50 | **81.25** | 62.50 |
| AN5 | **81.25** | 62.50 | 68.75 | **75.00** |
| | | | | |
| mean | 79.69 | 63.28 | 59.38 | 63.28 |
| SD | 8.01 | 8.48 | 12.05 | 6.19 |

## Conclusion

First, the results reported are in line with fMRI studies that found bilateral activation of the ventrolateral PFC and DLPFC and the inferior and superior parietal cortex, primarily in the left hemisphere, during the performance of different arithmetic task [8]. Second, the antagonistic [oxy-Hb] response can be interpreted as another manifestation of a "focal activation/surround deactivation". Such antagonistic activation patterns have been already described by brain activation studies using fMRI and EEG [6,7] but for the first time with multi-channel NIRS [5]. Finally, by using the antagonistic features the MA tasks were classified with an average accuracy of 80% and the use of the antagonistic features improved the classification accuracy significantly compared to individual features. Furthermore our finding demonstrates that only two prefrontal NIRS channels are necessary to realize an optical BCI system, based on antagonistic hemodynamic response pattern, with good performance.

[1] Birbaumer, N., Weber, C., Neuper, C., Buch, E., Haapen, K. & Cohen, L. (2006) Physiological regulation of thinking: brain-computer interface (BCI) research. Progress in Brain Research, 159, 369–391.
[2] Sitaram, R., Caria, A. & Birbaumer, N. (2009). Hemodynamic brain-computer interfaces for communication and rehabilitation. Neural Networks, 22(9), 1320-1328.
[3] Coyle, S., Ward, T., Markham, C. & McDarby, G. (2004a) On the Suitability of Near-Infrared Systems for Next Generation Brain Computer Interfaces. Physiological Measurement, 25, 815-822.
[4] Bauernfeind, G., Leeb, R., Wriessnegger, S.C. & Pfurtscheller, G., (2008). Development, set-up and first results for a one-channel near-infrared spectroscopy system. Biomedizinische Technik/ Biomedical engineering, 53(1), 36-43.
[5] Pfurtscheller G., Bauernfeind G., Wriessnegger S.C. & Neuper C., (2010). Focal frontal (de)oxyhemoglobin responses during simple arithmetic. Int J Psychophysiol. 76(3), 186-192.
[6] Pfurtscheller, G. & Neuper, C., (1994). Event-related synchronization of mu rhythmin the EEG over the cortical hand area in man. Neurosci. Lett. 174, 93–96.
[7] Ehrsson, H.H., Geyer, S., Naito, E., (2003). Imagery of voluntary movement of fingers, toes, and tongue activates corresponding body-part-specific motor representations. J. Neurophysiol. 90 (5), 3304–3316.
[8] Menon, V., Rivera, S.M., White, C.D., Glover, G.H. & Reiss, A.L. (2000). Dissociating prefrontal and parietal cortex activation during arithmetic processing. Neuroimage 12(4), 357-365.

This work was supported by:

- PRESENCCIA IST-27731
- Neuro Center Styria
- Land Steiermark A3-22.N-13/2009-8

# Anhang B

## BioSig Files

Die angeführten Files wurden der Open-Soure Software-Bibliothek "BioSig"(`http://biosig.sourceforge.net/`) übermittelt und der BioSig-Toolbox hinzugefügt.

# Übersicht t320 Paket:

```
% ------------------------------------------------------------------------
% T320: Removal of Physiolgical Artifacts from NIRS
% ------------------------------------------------------------------------
%   adaptPulseremove.m    removes the Pulse influence from NIRS signals using
%                         calcInfluence.m
%   calcInfluence.m       calculates the unknown influence of the Pulse-Noise
%                         using the LMS algorithm
%   remNoiseTF.m          removes respiration and MayerWave artefacts by the
%                         transfer function approach
%   remNoiseICA.m         removes respiration and MayerWave artefacts by ICA
%                         approach
%   remNoiseCAR.m         removes respiration and MayerWave artefacts by CAR
%                         approach
%
% ------------------------------------------------------------------------
% Additional files
% ------------------------------------------------------------------------
%   calcNIRSspectra.m     calculates the Spectrum of the NIRS signal
%   calcBPlin.m           calculates the linear interpolated BPdia or BPsys
%                         signal using
%   sysdetect.m           calculates fiducially points of systolic BP
%   diadetect.m           calculates fiducially points of diastolic BP
%   Illustration_multichannel_spectra.m   uses the calcNIRSspectra function
%                         to calculate and illustrates the [(de)oxy-Hb]
%                         spectra of each used NIRS channel from a 3*11
%                         measurement grid
%   DEMO_t320_nirs.m      demonstrates different approaches for the
%                         removal of physiological artefacts from NIRS
%                         signals
```

## adaptPulseremove.m:

```
function [cleanSignal]=adaptPulseremove(dirtySignal,Noise,fs)
%
% adaptPulseremove removes the influence of the Pulse-Signal from the
% [(de)oxy-Hb] signal
%
% [cleanSignal]=adaptPulsremove(dirtySignal,Noise,fs)
%
% Input:
%   dirtySignal     ... dirty signal (either [oxy-Hb] or [deoxy-Hb]) with
%                       pulse influence
%   Noise           ... artificial Noise signal (either BP signal or signal
%                       from a fingerpulse sensor
%   fs              ... Sampling frequency
%
% Output:
%   cleanSignal     ... clean signal without influence


% Copyright (C) 2012 by the Institute for Knowledge Discovery, Graz
% University of Technology
% Guenther Bauernfeind <g.bauernfeind@tugraz.at>
% WWW: http://bci.tugraz.at/
% $Id: adaptPulseremove.m v0.1 2012-02-13 10:00:00 ISD$
%
% This software was implemented in the framework of the Styrian government
% project "Einfluss von Herz-Kreislauf-Parametern auf das Nah-Infrarot-
% Spektroskopie (NIRS) Signal" (A3-22.N-13/2009-8)and is part of the BIOSIG-
% toolbox http://biosig.sf.net/
%
% LICENSE:
%
%   This program is free software: you can redistribute it and/or modify
%   it under the terms of the GNU General Public License as published by
%   the Free Software Foundation, either version 3 of the License, or
%   (at your option) any later version.
%
%   This program is distributed in the hope that it will be useful,
%   but WITHOUT ANY WARRANTY; without even the implied warranty of
%   MERCHANTABILITY or FITNESS FOR A PARTICULAR PURPOSE.  See the
%   GNU General Public License for more details.
%
%   You should have received a copy of the GNU General Public License
%   along with this program.  If not, see <http://www.gnu.org/licenses/>.

% Pre-processing (band-pass filtering) of the Noise-Signal to get only the
% Pulse influence
    Wnpulse=[0.8 1.8];                    %Borders of the filter
    N=200;
    b = fir1(N,Wnpuls/(fs/2),'bandpass');
    Noise=filtfilt(b,1,Noise);

    Noise=Noise/max(Noise); %Normalise
```

```
% Definition/calculation of the unknown influence (using LMS algorithm)
    calcPulseNoise = calcInfluence(dirtySignal, Noise);


% Post processing (high pass filtering) to avoid removements below 0.8 Hz
    Wn=0.8;
    N=200;
    b = fir1(N,Wn/(fs/2),'high');
    calcPulseNoise=filtfilt(b,1,calcPulseNoise);

% Calculation of the cleaned signal
    cleanSignal=dirtySignal-calcPulseNoise;

end
```

## calcInfluence.m:

```
function [influence] = calcInfluence(dirtySignal, Noise)
% calcInfluence calculates the unknown influence of the Pulse-Noise using
% the LMS algorithm
%
% [influence] = calcInfluence(dirtySignal, Noise)
%
% Input:
%   dirtySignal     ... dirty signal (either [oxy-Hb] or [deoxy-Hb]) with
%                       puls influence
%   Noise           ... preprocessed artificial Noise signal (either BP
%                       signal or signal from a fingerpulse sensor
%
% Output:
%   influence       ... calculated unknown influence

% Copyright (C) 2012 by the Institute for Knowledge Discovery, Graz
% University of Technology
% Guenther Bauernfeind <g.bauernfeind@tugraz.at>
% WWW: http://bci.tugraz.at/
% $Id: calcInfluence.m v0.1 2012-02-13 10:00:00 ISD$
%
% This software was implemented in the framework of the Styrian government
% project "Einfluss von Herz-Kreislauf-Parametern auf das Nah-Infrarot-
% Spektroskopie (NIRS) Signal" (A3-22.N-13/2009-8)and is part of the BIOSIG-
% toolbox http://biosig.sf.net/%
% LICENSE:
%
%   This program is free software: you can redistribute it and/or modify
%   it under the terms of the GNU General Public License as published by
%   the Free Software Foundation, either version 3 of the License, or
%   (at your option) any later version.
%
%   This program is distributed in the hope that it will be useful,
%   but WITHOUT ANY WARRANTY; without even the implied warranty of
%   MERCHANTABILITY or FITNESS FOR A PARTICULAR PURPOSE.  See the
%   GNU General Public License for more details.
%
%   You should have received a copy of the GNU General Public License
%   along with this program.  If not, see <http://www.gnu.org/licenses/>.

M=length(dirtySignal);

% Parameters
N=50;
y=zeros(M,1);
w = zeros(N,1);
u1 = zeros(N,1);

for i=1:1:M
    if i<N
        u1(N:-1:N-i+1)=Noise(i:-1:1);
    else
        u1(N:-1:1) = Noise(i:-1:i-N+1);
```

```
    end
    y(i) = w'*u1;

    %LMS
    k = 0.05*u1;
    E = dirtySignal(i) - w'*u1;
    w = w + k*E;


end

influence=y;
```

## remNoiseTF.m:

```
function corrSignal=remNoiseTF(signal,noise,fs,windowlength)
%
% remNoiseTF removes respiration an blood pressure related noise from
% [(de)oxy-Hb] signals by using a transfer function model [1,2]. For a
% detailed description of the model see [3].
%
%   [corrSignal]=remNoiseTF(signal,noise,fs,shift)
%
% Input:
%   signal     ... signal with noise (either [oxy-Hb] or [deoxy-Hb])
%   noise      ... noise signal from a different source (respiration, BPdia,
%                  HR, ...
%   fs         ... sampling frequency
%
% Optional input parameter:
%   windowlength ... length of one segment for the correction, default=240
%                    seconds
%
% Output:
%   corrSignal:  ... corrected signal without influence of noise
%
% [1] Priestley, M.B., 1981. Spectral Analysis and Time Series. Vol. 1 and 2.
%     Academic Press, London, pp. 671.
% [2] Wei, W.W.S., 1990. Time Series Analysis; Univariate and Multivariate
%     Methods. Addison Wesley, New York, pp. 289.
% [3] Florian G, Stancak A, Pfurtscheller G. Cardiac response induced by
%     voluntary selfpaced finger movement. International Journal of
%     Psychophysiology, 28: 273-283, 1998.


% Copyright (C) 2012 by the Institute for Knowledge Discovery, Graz
% University of Technology
% Rupert Ortner and Guenther Bauernfeind <g.bauernfeind@tugraz.at>
% WWW: http://bci.tugraz.at/
% $Id: remNoiseTF.m v0.1 2012-02-13 10:00:00 ISD$
%
% This software was implemented in the framework of the Styrian government
% project "Einfluss von Herz-Kreislauf-Parametern auf das Nah-Infrarot-
% Spektroskopie (NIRS) Signal" (A3-22.N-13/2009-8)and is part of the BIOSIG-
% toolbox http://biosig.sf.net/%
%
% LICENSE:
%
%   This program is free software: you can redistribute it and/or modify
%   it under the terms of the GNU General Public License as published by
%   the Free Software Foundation, either version 3 of the License, or
%   (at your option) any later version.
%
%   This program is distributed in the hope that it will be useful,
%   but WITHOUT ANY WARRANTY; without even the implied warranty of
%   MERCHANTABILITY or FITNESS FOR A PARTICULAR PURPOSE.  See the
%   GNU General Public License for more details.
%
```

```
%   You should have received a copy of the GNU General Public License
%   along with this program.  If not, see <http://www.gnu.org/licenses/>.

if nargin==3
    windowlength=240; %240
end


global mmax;
mmax=15;     %maximum filter order in function Korr_p (for details see [3])

seq=(fs*windowlength);
partn=ceil(length(signal)/seq);
Corr=zeros(length(signal),1); %pre-allocation of the correction term
endact=0;                      % end of actual part of signal
for i=1:partn
    onset=(i-1)*seq+1;
    ending=i*seq;

    if ending > length(signal)
        ending=length(signal);
    end

    if onset==1
        noise_e=[ones(mmax,1)*noise(1);noise(onset:ending)];
    else
        noise_e=noise(onset-mmax:ending);
    end

    %Calculation of the correction term using partTF
    Corr_p=partTF(noise_e,signal(onset:ending));
    Corr(endact+1:endact+length(Corr_p))=Corr_p;
    endact=endact+length(Corr_p);
end

endsignal=length(signal);
Corr(end+1:endsignal)=Corr(end);


corrSignal=signal-Corr;      % Corrected Signal
%--------------------------------------------------------------------------
%--------------------------------------------------------------------------
function Corr_p=partTF(noise_e,signal_p)
% partTF is the implementation of the transfer function equations from [3].
%
% Input
%     noise_e       ...  noise
%     signal_p      ...  signal
%
%
% Output:
%      Corr_p       ... Correction term

% Copyright (C) 2012 by the Institute for Knowledge Discovery, Graz
% University of Technology
```

```
% Rupert Ortner and Guenther Bauernfeind <g.bauernfeind@tugraz.at>
% WWW: http://bci.tugraz.at/
% $Id: partTF.m v0.1 2012-02-13 10:00:00 ISD$
%
% This software was implemented in the framework of the Styrian government
% project "Einfluss von Herz-Kreislauf-Parametern auf das Nah-Infrarot-
% Spektroskopie (NIRS) Signal" (A3-22.N-13/2009-8)and is part of the BIOSIG-
% toolbox http://biosig.sf.net/%%
% LICENSE:
%
%   This program is free software: you can redistribute it and/or modify
%   it under the terms of the GNU General Public License as published by
%   the Free Software Foundation, either version 3 of the License, or
%   (at your option) any later version.
%
%   This program is distributed in the hope that it will be useful,
%   but WITHOUT ANY WARRANTY; without even the implied warranty of
%   MERCHANTABILITY or FITNESS FOR A PARTICULAR PURPOSE.  See the
%   GNU General Public License for more details.
%
%   You should have received a copy of the GNU General Public License
%   along with this program.  If not, see <http://www.gnu.org/licenses/>.


global mmax;
noise_p=noise_e(mmax+1:end);
mmin=5;
g_yy=xcov(noise_p,mmax,'biased');
g_xy = xcov(signal_p,noise_p,mmax,'biased');%cross-cov. of signal and noise
g_xx0 = xcov(signal_p,0,'biased');          %Autocov. of signal_p

index=mmax+1;   %tau=0
lambda=zeros(1,mmax-mmin+1);
gu=cell(mmax,1);
for m=mmin:mmax
    g_xy_pj=g_xy(index:index+m);         %Gamma_xy from 0 to m
    g_yy_uj=g_yy(index:index+m);         %Gamma_yy from 0 to m
    G=toeplitz(g_yy_uj);
    gu{m}=inv(G)*g_xy_pj;
    Snn=g_xx0-gu{m}'*g_xy_pj;
    lambda(m-mmin+1)=length(noise_p)*log(Snn)+2*(m+1);
end
[minm,minind]=min(lambda);       %minimizing lambda
mind=mmin+minind-1;
b=gu{mind};

S=filter(b,1,noise_e);
Corr_p=S(mmax+1:end);
```

## remNoiseICA.m:

```
function [cleanSignals] = remNoiseICA( Signals,bpNoise,respNoise,fs,ExCh)
%
% remNoiseICA removes respiration an blood pressure related noise from
% [(de)oxy-Hb] signals by using ICA. The [(de)oxy-Hb] signal is decomposed
% into independent components (ICs) via SOBI ICA [1]. The coherence between
% each IC and the noise signals is then calculated. ICs for which the
% coherence with one of the artefact signals is higher than the mean of all
% the coherence scores with that artefact signal plus 1 standard deviation
% are flagged for removal.
%
% The code uses the runica function from:
% Makeig, Scott et al. "EEGLAB: ICA Toolbox for Psychophysiological
% Research". WWW Site, Swartz Center for Computational Neuroscience,
% Institute of Neural Computation, University of San Diego California
% <www.sccn.ucsd.edu/eeglab/>, 2000.
%
% Please be sure to have included
%
%   [cleanSignals]=remNoiseICA( Signals,bpNoise,respNoise,fs,ExCh)
%
% Input:
%   Signals    ... Signals with noise (either [oxy-Hb] or [deoxy-Hb])
%   bpNoise    ... Noise signal BP
%   respNoise  ... Noise signal respiration
%   fs         ... Sampling frequency
%   ExCh       ... Channels not used
%
%
% Output:
%   cleanSignals  ... corrected signal without influence of noise
%
%[1] Belouchrani A, Abed-Meraim K, Cardoso J, Moulines E. A blind source
%    seperation technique using second-order statistics. IEEE Transactions
%    on signal processing, 45(2): 434-444, 1997


% Copyright (C) 2012 by the Institute for Knowledge Discovery, Graz
% University of Technology
% Ian Daly <ian.daly@tugraz.at> and Guenther Bauernfeind
% <g.bauernfeind@tugraz.at>
% WWW: http://bci.tugraz.at/
% $Id: remNoiseICA.m v0.1 2012-02-13 10:00:00 ISD$
%
% This software was implemented in the framework of the Styrian government
% project "Einfluss von Herz-Kreislauf-Parametern auf das Nah-Infrarot-
% Spektroskopie (NIRS) Signal" (A3-22.N-13/2009-8)and is part of the BIOSIG-
% toolbox http://biosig.sf.net/%%
% LICENSE:
%
%   This program is free software: you can redistribute it and/or modify
%   it under the terms of the GNU General Public License as published by
%   the Free Software Foundation, either version 3 of the License, or
%   (at your option) any later version.
```

```
%
%   This program is distributed in the hope that it will be useful,
%   but WITHOUT ANY WARRANTY; without even the implied warranty of
%   MERCHANTABILITY or FITNESS FOR A PARTICULAR PURPOSE.  See the
%   GNU General Public License for more details.
%
%   You should have received a copy of the GNU General Public License
%   along with this program.  If not, see <http://www.gnu.org/licenses/>.

    artSig(1,:) = bpNoise;
    artSig(2,:) = respNoise;

    chsUse=[1:1:size(Signals,2)];
    chsUse(ExCh{1,1})=[];

    dirtySignals = Signals(:,chsUse);


    [ICweights ICsphere,compvars,bias,signs,lrates,S] = runica(
dirtySignals','maxsteps',40 );

    % 2. Get activations.
    S = ICweights * ICsphere * dirtySignals(1:size(artSig,2),:)';

    allICsArt = [S; artSig];
    % Normalise signals.
    for i = 1:size( allICsArt,1 ),
        allICsArt(i,:) = allICsArt(i,:) - mean( allICsArt(i,:) );
        allICsArt(i,:) = allICsArt(i,:) ./ std( allICsArt(i,:) );
    end


    %artIndex  = [zeros(1,size(S,1)) ones(1,size(artSig,1))];

    % Get coherence.
    for k = 1:size(allICsArt,1)-3,
        [a b] =
mscohere(allICsArt(end,:),allICsArt(k,:),[],[],fs);%hanning(fs),fs/2,fs);

        cohVal(1,k)=mean( a );
    end

    for k = 1:size(allICsArt,1)-3,
        [a b] =  mscohere(allICsArt(end-
1,:),allICsArt(k,:),[],[],fs);%hanning(fs),fs/2,fs);

        cohVal(2,k)=mean( a );
    end
    for k = 1:size(allICsArt,1)-3,
        [a b] =  mscohere(allICsArt(end-
2,:),allICsArt(k,:),[],[],fs);%hanning(fs),fs/2,fs);

        cohVal(3,k)=mean( a );
    end
```

```
    indI = mean( cohVal(1,:) ) + std( cohVal(1,:) );
    [removeICs1] = find( cohVal(1,:) > indI );
    indI = mean( cohVal(2,:) ) + (std(cohVal(2,:)).*0.5);
    [removeICs2] = find( cohVal(2,:) > indI );
    removeICs = unique( [removeICs1 removeICs2] );
    removeICs = removeICs( find(removeICs <= size(ICweights,1) ) );

    %noRemovedICs = length( removeICs );

    % RunICA.
    ICweights2 = ICweights;
    ICsphere2 = ICsphere;
    S(removeICs,:) = 0;

    % 5. Translate from ICs back to original data.
    data = (ICweights2*ICsphere2)^-1 * S;

    cleanSignals = zeros(size(Signals));

    cleanSignals(1:size(data,2),chsUse) = data';


end
```

## remNoiseCAR.m:

```
function [cleanOxysignals, cleanDeoxysignals]=
remNoiseCAR(oxy_signals,deoxy_signals,ExCh)
%
% remNoiseCAR removes respiration an blood pressure related noise from
% [(de)oxy-Hb] signals by using CAR.
%
%   [cleanSignals] = remNoiseCAR(Signals,fs,ExCh)
%
% Input:
%   oxy_signals      ... Oxy-Signals with noise
%   deoxy_signals    ... Deoxy-Signals with noise
%   ExCh             ... Channels not used
%
%
% Output:
%   cleanOxysignals    ... corrected Oxy-signal without influence of noise
%   cleanDeoxysignals  ... corrected Deoxy-signal without influence of noise

% Copyright (C) 2012 by the Institute for Knowledge Discovery, Graz
% University of Technology
% Guenther Bauernfeind <g.bauernfeind@tugraz.at>
% WWW: http://bci.tugraz.at/
% $Id: remNoiseCAR.m v0.1 2012-02-13 10:00:00 ISD$
%
% This software was implemented in the framework of the Styrian government
% project "Einfluss von Herz-Kreislauf-Parametern auf das Nah-Infrarot-
% Spektroskopie (NIRS) Signal" (A3-22.N-13/2009-8)and is part of the BIOSIG-
% toolbox http://biosig.sf.net/%
%
% LICENSE:
%
%   This program is free software: you can redistribute it and/or modify
%   it under the terms of the GNU General Public License as published by
%   the Free Software Foundation, either version 3 of the License, or
%   (at your option) any later version.
%
%   This program is distributed in the hope that it will be useful,
%   but WITHOUT ANY WARRANTY; without even the implied warranty of
%   MERCHANTABILITY or FITNESS FOR A PARTICULAR PURPOSE.  See the
%   GNU General Public License for more details.
%
%   You should have received a copy of the GNU General Public License
%   along with this program.  If not, see <http://www.gnu.org/licenses/>.

        CAR_ch_f=ExCh{1,1};
        CAR_ch=[1:1:size(oxy_signals,2)];
        CAR_ch(CAR_ch_f)=[];

        mean_oxy_signal=mean(oxy_signals(:,CAR_ch),2);
        mean_deoxy_signal=mean(deoxy_signals(:,CAR_ch),2);

        for tt=1:size(oxy_signals,2)
        cleanOxysignals(:,tt)=oxy_signals(:,tt)-mean_oxy_signal(:,1);
```

```
        cleanDeoxysignals(:,tt)=deoxy_signals(:,tt)-mean_deoxy_signal(:,1);
        end
end
```

## calcNIRSspectra.m:

```
function r=calcNIRSspectra(signal,fs)
% calcNIRSspectra calculates the Spectrum of the NIRS signal
%
% r=calcNIRSspectra(signal,fs)
%
% Input:
%   signal  ... NIRS signal (either [oxy-Hb] or [deoxy-Hb]
%   fs      ... Sampling frequency
%
% Output:
%   r       ... structure containing the spectrum.


% Copyright (C) 2012 by the Institute for Knowledge Discovery, Graz
% University of Technology
% Guenther Bauernfeind <g.bauernfeind@tugraz.at>
% WWW: http://bci.tugraz.at/
% $Id: calcNIRSspectra.m v0.1 2012-02-13 10:00:00 ISD$
%
% This software was implemented in the framework of the Styrian government
% project "Einfluss von Herz-Kreislauf-Parametern auf das Nah-Infrarot-
% Spektroskopie (NIRS) Signal" (A3-22.N-13/2009-8)and is part of the BIOSIG-
% toolbox http://biosig.sf.net/%
%
% LICENSE:
%
%   This program is free software: you can redistribute it and/or modify
%   it under the terms of the GNU General Public License as published by
%   the Free Software Foundation, either version 3 of the License, or
%   (at your option) any later version.
%
%   This program is distributed in the hope that it will be useful,
%   but WITHOUT ANY WARRANTY; without even the implied warranty of
%   MERCHANTABILITY or FITNESS FOR A PARTICULAR PURPOSE.  See the
%   GNU General Public License for more details.
%
%   You should have received a copy of the GNU General Public License
%   along with this program.  If not, see <http://www.gnu.org/licenses/>.

% Used setting
windowtyp= 'Hanning';    % Window typ
window_length = 100;     % Windowlength in [s]
window_overlap = 50;     % Define Overlap in [s]
fft_length     = 200;



    if strcmp(windowtyp, 'Hamming') == 1
        window = hamming(window_length*fs);
    elseif strcmp(windowtyp, 'Hanning') == 1
        window = hann(window_length*fs);
    elseif strcmp(windowtyp, 'Triang') == 1
```

```
        window = triang(window_length*fs);
    elseif strcmp(windowtyp, 'Bartlett') == 1
        window = bartlett(window_length*fs);
    end




[p, f] = psd(signal-mean(signal), fft_length*fs, fs, window,
window_overlap*fs,'linear');


r{1}.p = p;
r{1}.f = f;
r{1}.fs = fs;




end
```

## calcBPlin.m:

```
function linBP = calcBPlin(signal,fs,typ)
% calcBPlin calculates the linear interpolated BPdia or BPsys signal and is
partially based
% on the calcHR function written by Clemens Brunner.
%
%
% [linBP] = calcBPlin(signal,fs,typ)
%
% Input:
%   signal   ... Raw continuous BP signal
%   fs       ... Sampling frequency
%   typ      ... [1] systolic BP
%            ... [2] diastolic BP
%
%
% Output:
%   linBP    ... linear interpolated BPdia or BPsys signal
%

% Copyright (C) 2012 by the Institute for Knowledge Discovery, Graz
% University of Technology
% Guenther Bauernfeind <g.bauernfeind@tugraz.at>
% WWW: http://bci.tugraz.at/
% $Id: calcBPlin.m v0.1 2012-02-13 10:00:00 ISD$
%
% This software was implemented in the framework of the Styrian government
% project "Einfluss von Herz-Kreislauf-Parametern auf das Nah-Infrarot-
% Spektroskopie (NIRS) Signal" (A3-22.N-13/2009-8)and is part of the BIOSIG-
% toolbox http://biosig.sf.net/%
% LICENSE:
%
%   This program is free software: you can redistribute it and/or modify
%   it under the terms of the GNU General Public License as published by
%   the Free Software Foundation, either version 3 of the License, or
%   (at your option) any later version.
%
%   This program is distributed in the hope that it will be useful,
%   but WITHOUT ANY WARRANTY; without even the implied warranty of
%   MERCHANTABILITY or FITNESS FOR A PARTICULAR PURPOSE.  See the
%   GNU General Public License for more details.
%
%   You should have received a copy of the GNU General Public License
%   along with this program.  If not, see <http://www.gnu.org/licenses/>.


% Calculate BPsys or BPdia

if typ==1
    h_BP = sysdetect(signal, fs);
end
if typ==2
    h_BP = diadetect(signal, fs);
end
```

```
time = h_BP.EVENT.POS;

timesec=time./fs;

bp=signal(time);

%%%%%%linear interpolation%%%%%%
X=timesec;                                  %old time axis
XI = (timesec(1):1/fs:timesec(end))';       %new time axis for interpolation
linBP = interp1(X,bp,XI,'linear');          %HR linear interpolated
linBP=[linBP(1)*ones(time(1)-1,1);linBP;linBP(end)*ones(length(signal)-
time(end),1)];
```

## sysdetect.m:

```
function [HDR] = sysdetect(signal,fs)
% SYSDETECT - detection of SYS_BP_points
%
%   [HDR] = sysdetect(signal,fs)
%
% Input:
%   signal          ... BP signal data
%   fs              ... Sampling frequency
%
% Output:
%   HDR.EVENT.pos   ... fiducially points of systolic BP
%


% Copyright (C) 2012 by the Institute for Knowledge Discovery, Graz
% University of Technology
% Guenther Bauernfeind <g.bauernfeind@tugraz.at>
% WWW: http://bci.tugraz.at/
% $Id: sysdetect.m v0.1 2012-02-13 10:00:00 ISD$
%
% This software was implemented in the framework of the Styrian government
% project "Einfluss von Herz-Kreislauf-Parametern auf das Nah-Infrarot-
% Spektroskopie (NIRS) Signal" (A3-22.N-13/2009-8)and is part of the BIOSIG-
% toolbox http://biosig.sf.net/%
% LICENSE:
%
% LICENSE:
%
%   This program is free software: you can redistribute it and/or modify
%   it under the terms of the GNU General Public License as published by
%   the Free Software Foundation, either version 3 of the License, or
%   (at your option) any later version.
%
%   This program is distributed in the hope that it will be useful,
%   but WITHOUT ANY WARRANTY; without even the implied warranty of
%   MERCHANTABILITY or FITNESS FOR A PARTICULAR PURPOSE.  See the
%   GNU General Public License for more details.
%
%   You should have received a copy of the GNU General Public License
%   along with this program.  If not, see <http://www.gnu.org/licenses/>.



%Remove of the trend
signal=detrend(signal,1);

%Reduction of noise, LP filtering 10 Hz
[N,Wn]=buttord(10/(fs/2),30/(fs/2),3,60);
[b,a]=butter(N,Wn,'low');
signal=filtfilt(b,a,signal);

%smooth
signal=smooth(signal);
```

```
%1st derivation
d_signal=diff(signal);
%tresholding
TH=std(d_signal);
k=find(d_signal>TH);
%seperation
sep=fs/3; %Puls lies below 180 bpm
% Detection
kpp(1)=k(1);
kpn=[];
for i=1:length(k)-1
    if k(i+1)-k(i)>sep     %To wave must be separated at least by sep
        kpp=[kpp,k(i+1)]; %The point before sep is the last one of the wave
        kpn=[kpn,k(i)];   %the next one is the starting point of the next
                          %wave
    end
end
kpn=[kpn,k(length(k))];   %the last point of k is the last one of the last
                          %wave

for i=1:length(kpp)
    [m,n(i)]=max(d_signal(kpp(i):kpn(i)));
    pos_detect(i)=kpp(i)+n(i)-1;
end
if pos_detect(1)<=40
    pos_detect=pos_detect(2:end);
end
if pos_detect(end)>=length(signal)-40
    pos_detect=pos_detect(1:end-1);
end
for i=1:length(pos_detect)
    [m1,n1(i)]=max(signal(pos_detect(i):pos_detect(i)+40));
    pos(i)=pos_detect(i)+n1(i)-1;
end

HDR.EVENT.POS=pos;
```

## diadetect.m:

```
function [HDR] = diadetect(signal,fs)
% diadetect - detection of Diastolic_BP points
%
%   HDR = diasysdetect(signal,Fs)
%
% Input:
%   signal      ... BP signal data
%   fs          ... Sampling frequency
%
% Output:
%   HDR.EVENT   ... fiducially points of diastolic BP
%
%


% Copyright (C) 2012 by the Institute for Knowledge Discovery, Graz
% University of Technology
% Guenther Bauernfeind <g.bauernfeind@tugraz.at>
% WWW: http://bci.tugraz.at/
% $Id: diadetect.m v0.1 2012-02-13 10:00:00 ISD$
%
% This software was implemented in the framework of the Styrian government
% project "Einfluss von Herz-Kreislauf-Parametern auf das Nah-Infrarot-
% Spektroskopie (NIRS) Signal" (A3-22.N-13/2009-8)and is part of the BIOSIG-
% toolbox http://biosig.sf.net/%
%
% LICENSE:
%
%   This program is free software: you can redistribute it and/or modify
%   it under the terms of the GNU General Public License as published by
%   the Free Software Foundation, either version 3 of the License, or
%   (at your option) any later version.
%
%   This program is distributed in the hope that it will be useful,
%   but WITHOUT ANY WARRANTY; without even the implied warranty of
%   MERCHANTABILITY or FITNESS FOR A PARTICULAR PURPOSE.  See the
%   GNU General Public License for more details.
%
%   You should have received a copy of the GNU General Public License
%   along with this program.  If not, see <http://www.gnu.org/licenses/>.

%Remove of the trend
signal=detrend(signal,1);

%Reduction of noise, LP filtering 10 Hz
[N,Wn]=buttord(10/(fs/2),30/(fs/2),3,60);
[b,a]=butter(N,Wn,'low');
signal=filtfilt(b,a,signal);

%Smoothing
signal=smooth(signal);
%1st derivation
d_signal=diff(signal);
%tresholding
```

```
TH=std(d_signal);
k=find(d_signal>TH);
%seperation
sep=fs/3; %Puls lies below 180 bpm
% Detektion
kpp(1)=k(1);
kpn=[];
for i=1:length(k)-1
    if k(i+1)-k(i)>sep    %To wave must be separated at least by sep
        kpp=[kpp,k(i+1)]; %The point before sep is the last one of the wave
        kpn=[kpn,k(i)];   %the next one is the starting point of the next
                          %wave
    end
end
kpn=[kpn,k(length(k))];   %the last point of k is the last one of the last
                          %wave

for i=1:length(kpp)
    [m,n(i)]=max(d_signal(kpp(i):kpn(i)));
    pos_detect(i)=kpp(i)+n(i)-1;
end

if pos_detect(1)<=40
    pos_detect=pos_detect(2:end);
end

for i=1:length(pos_detect)
    [m1,n1(i)]=min(signal(pos_detect(i)-40:pos_detect(i)));
    pos(i)=pos_detect(i)-40+n1(i)-1;
end

HDR.EVENT.POS=pos;
```

## Illustration_multichannel_spectra.m:

```
function [rOxy rDeoxy]=Illustration_multichannel_spectra(ChNr, oxy_Data,
deoxy_Data, fs, dispFreq, ExCh)
% Illustration_multichannel_spectra
% uses the calcNIRSspectra function to calculate and illustrates the
% [(de)oxy-Hb]spectra of each used NIRS channel from a 3*11 measurement grid
%
% [rOxy rDeoxy]=Illustration_multichannel_spectra(ChNr, oxy_Data, deoxy_Data,
%              fs, dispFreq, ExCh)
%
% Input:
%   ChNr           ... Number of the current channel
%   oxy_Data       ... Oxy data of the current channel
%   deoxy_Data     ... Deoxy data of the current channel
%   fs             ... Sampling frequency
%   dispFreq       ... Frequencies up to this value are plotted
%   ExCh           ... Channels not used
%
% Output:
%   rOxy           ... Structure containing the [oxy-Hb] spectrum
%   rDeoxy         ... Calculated [deoxy-Hb] spectrum

% Copyright (C) 2012 by the Institute for Knowledge Discovery, Graz
% University of Technology
% Guenther Bauernfeind <g.bauernfeind@tugraz.at>
% WWW: http://bci.tugraz.at/
% $Id: Illustration_multichannel_spectra.m v0.1 2012-02-13 10:00:00 ISD$
%
% This software was implemented in the framework of the Styrian government
% project "Einfluss von Herz-Kreislauf-Parametern auf das Nah-Infrarot-
% Spektroskopie (NIRS) Signal" (A3-22.N-13/2009-8)and is part of the BIOSIG-
% toolbox http://biosig.sf.net/%
%
% LICENSE:
%
%   This program is free software: you can redistribute it and/or modify
%   it under the terms of the GNU General Public License as published by
%   the Free Software Foundation, either version 3 of the License, or
%   (at your option) any later version.
%
%   This program is distributed in the hope that it will be useful,
%   but WITHOUT ANY WARRANTY; without even the implied warranty of
%   MERCHANTABILITY or FITNESS FOR A PARTICULAR PURPOSE.  See the
%   GNU General Public License for more details.
%
%   You should have received a copy of the GNU General Public License
%   along with this program.  If not, see <http://www.gnu.org/licenses/>.


   % check if current channel is used

        for i=1:1:size(ExCh{1,1},2)
            if ChNr==ExCh{1,1}(i)
                rOxy =[];
```

```
                rDeoxy=[];
                return
            end
        end



  %% Illustration definition for 3*11 grid
                    %first row
                    if ChNr==1
                        %set(gca,'Visible','off')
                        g1=axes('position',[0.05300 0.76667 0.07576
0.125]);axes(g1);
                    end
                    if ChNr==2
                        g2=axes('position',[0.14394 0.76667 0.07576
0.125]);axes(g2);end
                    if ChNr==3
                        g3=axes('position',[0.23485 0.76667 0.07576
0.125]);axes(g3);end
                    if ChNr==4
                        g4=axes('position',[0.32576 0.76667 0.07576
0.125]);axes(g4);end
                    if ChNr==5
                        g5=axes('position',[0.41667 0.76667 0.07576
0.125]);axes(g5);end
                    if ChNr==6
                        g6=axes('position',[0.50758 0.76667 0.07576
0.125]);axes(g6);end
                    if ChNr==7
                        g7=axes('position',[0.59848 0.76667 0.07576
0.125]);axes(g7);end
                    if ChNr==8
                        g8=axes('position',[0.68939 0.76667 0.07576
0.125]);axes(g8);end
                    if ChNr==9
                        g9=axes('position',[0.78030 0.76667 0.07576
0.125]);axes(g9);end
                    if ChNr==10
                        g10=axes('position',[0.87121 0.76667 0.07576
0.125]);axes(g10);end

                    %second row
                    if ChNr==11
                        g11=axes('position',[0.00758 0.60000 0.07576
0.125]);axes(g11);end
                    if ChNr==12
                        g12=axes('position',[0.09848 0.60000 0.07576
0.125]);axes(g12);end
                    if ChNr==13
                        g13=axes('position',[0.18939 0.60000 0.07576
0.125]);axes(g13);end
                    if ChNr==14
                        g14=axes('position',[0.28030 0.60000 0.07576
0.125]);axes(g14);end
```

```
                    if ChNr==15
                        g15=axes('position',[0.37121 0.60000 0.07576
0.125]);axes(g15);end
                    if ChNr==16
                        g16=axes('position',[0.46212 0.60000 0.07576
0.125]);axes(g16);end
                    if ChNr==17
                        g17=axes('position',[0.55303 0.60000 0.07576
0.125]);axes(g17);end
                    if ChNr==18
                        g18=axes('position',[0.64394 0.60000 0.07576
0.125]);axes(g18);end
                    if ChNr==19
                        g19=axes('position',[0.73485 0.60000 0.07576
0.125]);axes(g19);end
                    if ChNr==20
                        g20=axes('position',[0.82575 0.60000 0.07576
0.125]);axes(g20);end
                    if ChNr==21
                        g21=axes('position',[0.91667 0.60000 0.07576
0.125]);axes(g21);end

                    %third row
                    if ChNr==22
                        g22=axes('position',[0.05300 0.43334 0.07576
0.125]);axes(g22);end
                    if ChNr==23
                        g23=axes('position',[0.14394 0.43334 0.07576
0.125]);axes(g23);end
                    if ChNr==24
                        g24=axes('position',[0.23485 0.43334 0.07576
0.125]);axes(g24);end
                    if ChNr==25
                        g25=axes('position',[0.32576 0.43334 0.07576
0.125]);axes(g25);end
                    if ChNr==26
                        g26=axes('position',[0.41667 0.43334 0.07576
0.125]);axes(g26);end
                    if ChNr==27
                        g27=axes('position',[0.50758 0.43334 0.07576
0.125]);axes(g27);end
                    if ChNr==28
                        g28=axes('position',[0.59848 0.43334 0.07576
0.125]);axes(g28);end
                    if ChNr==29
                        g29=axes('position',[0.68939 0.43334 0.07576
0.125]);axes(g29);end
                    if ChNr==30
                        g30=axes('position',[0.78030 0.43334 0.07576
0.125]);axes(g30);end
                    if ChNr==31
                        g31=axes('position',[0.87121 0.43334 0.07576
0.125]);axes(g31);end

                    %fourth row
                    if ChNr==32
```

```
                        g32=axes('position',[0.00758 0.26667 0.07576
0.125]);axes(g32);end
                    if ChNr==33
                        g33=axes('position',[0.09848 0.26667 0.07576
0.125]);axes(g33);end
                    if ChNr==34
                        g34=axes('position',[0.18939 0.26667 0.07576
0.125]);axes(g34);end
                    if ChNr==35
                        g35=axes('position',[0.28030 0.26667 0.07576
0.125]);axes(g35);end
                    if ChNr==36
                        g36=axes('position',[0.37121 0.26667 0.07576
0.125]);axes(g36);end
                    if ChNr==37
                        g37=axes('position',[0.46212 0.26667 0.07576
0.125]);axes(g37);end
                    if ChNr==38
                        g38=axes('position',[0.55303 0.26667 0.07576
0.125]);axes(g38);end
                    if ChNr==39
                        g39=axes('position',[0.64394 0.26667 0.07576
0.125]);axes(g39);end
                    if ChNr==40
                        g40=axes('position',[0.73485 0.26667 0.07576
0.125]);axes(g40);end
                    if ChNr==41
                        g41=axes('position',[0.82575 0.26667 0.07576
0.125]);axes(g41);end
                    if ChNr==42
                        g42=axes('position',[0.91667 0.26667 0.07576
0.125]);axes(g42);end

                    %fifth row
                    if ChNr==43
                        g43=axes('position',[0.05300 0.10000 0.07576
0.125]);axes(g43);end
                    if ChNr==44
                        g44=axes('position',[0.14394 0.10000 0.07576
0.125]);axes(g44);end
                    if ChNr==45
                        g45=axes('position',[0.23485 0.10000 0.07576
0.125]);axes(g45);end
                    if ChNr==46
                        g46=axes('position',[0.32576 0.10000 0.07576
0.125]);axes(g46);end
                    if ChNr==47
                        g47=axes('position',[0.41667 0.10000 0.07576
0.125]);axes(g47);end
                    if ChNr==48
                        g48=axes('position',[0.50758 0.10000 0.07576
0.125]);axes(g48);end
                    if ChNr==49
                        g49=axes('position',[0.59848 0.10000 0.07576
0.125]);axes(g49);end
                    if ChNr==50
```

```
                        g50=axes('position',[0.68939 0.10000 0.07576
0.125]);axes(g50);end
                    if ChNr==51
                        g51=axes('position',[0.78030 0.10000 0.07576
0.125]);axes(g51);end
                    if ChNr==52
                        g52=axes('position',[0.87121 0.10000 0.07576
0.125]);axes(g52);end


%%   Calculate and display the [(de)oxy-Hb] spectra


        %calculate [(de)oxy-Hb] spectra

        rOxy=calcNIRSspectra(oxy_Data,fs);
        rDeoxy=calcNIRSspectra(deoxy_Data,fs);

        %display [oxy-Hb] spectra
        p1 = rOxy{1}.p;
        f1 = rOxy{1}.f;
        Color='r';
        idx = find(f1<=dispFreq);
        plot(f1(idx), 10*log10(p1(idx)),'Color', Color,'LineWidth',1.5);
        hold on

        %display [deoxy-Hb] spectra
        p1 = rDeoxy{1}.p;
        f1 = rDeoxy{1}.f;
        Color='b';
        idx = find(f1<=dispFreq);
        plot(f1(idx), 10*log10(p1(idx)),'Color', Color,'LineWidth',1.5);
        xlabel('f [Hz]','FontSize',6);
end
```

# demo_t320_nirs.m:

```
% DEMO_t320_nirs
% Demonstrates Different Approaches for the
% Removal of Physiological Artefacts from NIRS Signals

% Copyright (C) 2012 by the Institute for Knowledge Discovery, Graz
% University of Technology
% Guenther Bauernfeind <g.bauernfeind@tugraz.at>
% WWW: http://bci.tugraz.at/
% $Id: demo_t320_nirs.m v0.1 2012-02-13 10:00:00 ISD$
%
% This software was implemented in the framework of the Styrian government
% project "Einfluss von Herz-Kreislauf-Parametern auf das Nah-Infrarot-
% Spektroskopie (NIRS) Signal" (A3-22.N-13/2009-8)and is part of the BIOSIG-
% toolbox http://biosig.sf.net/
%
% LICENSE:
%
%   This program is free software: you can redistribute it and/or modify
%   it under the terms of the GNU General Public License as published by
%   the Free Software Foundation, either version 3 of the License, or
%   (at your option) any later version.
%
%   This program is distributed in the hope that it will be useful,
%   but WITHOUT ANY WARRANTY; without even the implied warranty of
%   MERCHANTABILITY or FITNESS FOR A PARTICULAR PURPOSE.  See the
%   GNU General Public License for more details.
%
%   You should have received a copy of the GNU General Public License
%   along with this program.  If not, see <http://www.gnu.org/licenses/>.




clear all
close all

% load file

load('Demo_Daten_t320.mat')

%% Settings
dispFreq=2;                                     %Display frequency for
spectra calculation
fs=Demo.Setting.fs_NIRS;                        %Sampling frequency NIRS data
fs_Physio=Demo.Setting.fs_Physio;               %Sampling frequency Physio
data
ExCh=Demo.Setting.ExcludedSurroundingChannels;  %Channels not used for
analysis
%% Signals
Oxy_signals=Demo.Data.oxy_signals;              %Oxy-Signals
Deoxy_signals=Demo.Data.deoxy_signals;          %Deoxy-Signals
BP_high=Demo.Data.bp;                           %BP signal
```

```
Resp_high=Demo.Data.resp;                          %Respiration Signal
ECG_high=Demo.Data.ecg;                            %ECG Signal
BPsys_high = calcBPlin(BP_high,fs_Physio,1);          %BPsys calculation
BPdia_high = calcBPlin(BP_high,fs_Physio,2);          %BPdia calculation

% Downsampling to 10Hz (Necessary for elimination of the physiolgical
% artifacts)
BP= resample(BP_high,fs,fs_Physio);
BPsys= resample(BPsys_high,fs,fs_Physio);
BPdia= resample(BPdia_high,fs,fs_Physio);
Resp= resample(Resp_high,fs,fs_Physio);
ECG= resample(ECG_high,fs,fs_Physio);

%% Raw [(de)oxy-Hb] data for comparison

% Illustration of [(de)oxy-Hb] raw spectra and
% calculation of averaged raw spectra

spect=[];
count=1;

for ChNr=1:1:size(Oxy_signals,2)
    figure(1);
    orient landscape
    [rOxy rDeoxy]=Illustration_multichannel_spectra(ChNr,
Oxy_signals(:,ChNr), ...
        Deoxy_signals(:,ChNr),fs, dispFreq, ExCh);

    if ~isempty(rOxy)
        spect(:,1,count)=rOxy{1}.p;
        spect(:,2,count)=rDeoxy{1}.p;
        count=count+1;
        Base=rOxy{1}.f;
    end

end

close

%Average [(de)oxy-Hb] spectra over all used channels

dat_spec_raw=[];

    for k = 1 : size(spect,2)
        dat_spec_raw(:,k)=mean(spect(:,k,:),3);
    end



%% adaptPulsremove

% In this implementation the BP signal is used to define the puls inluence.
% Beside the BP signal also the signal from a fingerpuls sensor is applicable
```

```
for  ChNr=1:1:size(Oxy_signals,2) %beginn der Kanalschleife

Data.oxy_signals_withoutputs(:,ChNr)=adaptPulsremove(Oxy_signals(:,ChNr),BP,f
s);

Data.deoxy_signals_withoutputs(:,ChNr)=adaptPulsremove(Deoxy_signals(:,ChNr),
BP,fs);
end

% Illustration of [(de)oxy-Hb] puls cleaned spectra and
% calculation of averaged puls cleaned spectra

spect=[];
count=1;

for ChNr=1:1:size(Oxy_signals,2)
    figure(2);
    orient landscape
    [rOxy rDeoxy]=Illustration_multichannel_spectra(ChNr,
Data.oxy_signals_withoutputs(:,ChNr), ...
        Data.deoxy_signals_withoutputs(:,ChNr),fs, dispFreq, ExCh);

    if ~isempty(rOxy)
        spect(:,1,count)=rOxy{1}.p;
        spect(:,2,count)=rDeoxy{1}.p;
        count=count+1;
        Base=rOxy{1}.f;
    end

end

close

%Average [(de)oxy-Hb] spectra over all used channels

dat_spec_pulscleaned=[];

    for k = 1 : size(spect,2)
        dat_spec_pulscleaned(:,k)=mean(spect(:,k,:),3);
    end


% Comparison raw and cleaned
                    figure(3)
                    % [oxy-Hb] raw
                    p1 = dat_spec_raw(:,1);
                    f1 = Base;
                    Color=[1 0.6 0.6];
                    idx = find(f1<=dispFreq);
                    plot(f1(idx), 10*log10(p1(idx)),'Color',
Color,'LineWidth',1.5);
                    hold on
                    % [deoxy-Hb] raw
                    p1 = dat_spec_raw(:,2);
                    Color=[0.8 0.8 1];
```

```
                    plot(f1(idx), 10*log10(p1(idx)),'Color',
Color,'LineWidth',1.5);
                    % [oxy-Hb] puls clean
                    p1 = dat_spec_pulscleaned(:,1);
                    Color='r';
                    idx = find(f1<=dispFreq);
                    plot(f1(idx), 10*log10(p1(idx)),'Color',
Color,'LineWidth',1.5);
                    % [deoxy-Hb] puls clean
                    p1 = dat_spec_pulscleaned(:,2);
                    Color='b';
                    plot(f1(idx), 10*log10(p1(idx)),'Color',
Color,'LineWidth',1.5);
                    ylabel('Power spectrum
','FontSize',16,'FontWeight','bold')
                    xlabel('f (Hz)','FontSize',16,'FontWeight','bold')
                    title('Avg. Spectrum [(de)oxy-Hb] before and after puls
removal' ,'FontSize',12,'FontWeight','demi','Interpreter','none')
                    legend('[oxy-Hb]_r_a_w','[deoxy-Hb]_r_a_w','[oxy-
Hb]_c_l_e_a_n','[deoxy-Hb]_c_l_e_a_n')

%% Respiration and Mayerwave (BP influence) removed by remNoiseTF

dispFreq=0.8;

%preprocessing Mayer wave influence
Wnmayer=[0.07 0.13];
N=200;
b = fir1(N,Wnmayer/(fs/2),'bandpass');
Mayer=filtfilt(b,1,BPdia);  %Beside the BPdia also the BPsys or the HR signal
is applicable

Mayer=Mayer-mean(Mayer);



for  ChNr=1:1:size(Oxy_signals,2)

Data.oxy_signals_withoutmayer(:,ChNr)=remNoiseTF(Oxy_signals(:,ChNr),Mayer,fs
);

Data.deoxy_signals_withoutmayer(:,ChNr)=remNoiseTF(Deoxy_signals(:,ChNr),Maye
r,fs);
end



%preprocessing respiratory influence
 Wnresp=[0.20 0.40];
 N=200;
 b = fir1(N,Wnresp/(fs/2),'bandpass');
 Resp=filtfilt(b,1,Resp);

 Resp=Resp-mean(Resp);

for  ChNr=1:1:size(Oxy_signals,2)
```

```
Data.oxy_signals_withoutmayer_resp(:,ChNr)=remNoiseTF(Data.oxy_signals_withou
tmayer(:,ChNr),Resp,fs);

Data.deoxy_signals_withoutmayer_resp(:,ChNr)=remNoiseTF(Data.deoxy_signals_wi
thoutmayer(:,ChNr),Resp,fs);
end


% Illustration of [(de)oxy-Hb] Mayer and respiration cleaned spectra and
% calculation of averaged cleaned spectra

spect=[];
count=1;

for ChNr=1:1:size(Oxy_signals,2)
    figure(4);
    orient landscape
    [rOxy rDeoxy]=Illustration_multichannel_spectra(ChNr,
Data.oxy_signals_withoutmayer_resp(:,ChNr), ...
        Data.deoxy_signals_withoutmayer_resp(:,ChNr),fs, dispFreq, ExCh);

    if ~isempty(rOxy)
        spect(:,1,count)=rOxy{1}.p;
        spect(:,2,count)=rDeoxy{1}.p;
        count=count+1;
        Base=rOxy{1}.f;
    end

end

close

%Average [(de)oxy-Hb] spectra over all used channels

dat_spec_mayer_respcleaned=[];

    for k = 1 : size(spect,2)
        dat_spec_mayer_respcleaned(:,k)=mean(spect(:,k,:),3);
    end


% Comparison raw and cleaned
                    figure(5)
                    % [oxy-Hb] raw
                    p1 = dat_spec_raw(:,1);
                    f1 = Base;
                    Color=[1 0.6 0.6];
                    idx = find(f1<=dispFreq);
                    plot(f1(idx), 10*log10(p1(idx)),'Color',
Color,'LineWidth',1.5);
                    hold on
                    % [deoxy-Hb] raw
                    p1 = dat_spec_raw(:,2);
```

```
                    Color=[0.8 0.8 1];
                    plot(f1(idx), 10*log10(p1(idx)),'Color',
Color,'LineWidth',1.5);
                    % [oxy-Hb] puls clean
                    p1 = dat_spec_mayer_respcleaned(:,1);
                    Color='r';
                    idx = find(f1<=dispFreq);
                    plot(f1(idx), 10*log10(p1(idx)),'Color',
Color,'LineWidth',1.5);
                    % [deoxy-Hb] puls clean
                    p1 = dat_spec_mayer_respcleaned(:,2);
                    Color='b';
                    plot(f1(idx), 10*log10(p1(idx)),'Color',
Color,'LineWidth',1.5);
                    ylabel('Power spectrum
','FontSize',16,'FontWeight','bold')
                    xlabel('f (Hz)','FontSize',16,'FontWeight','bold')
                    title('Avg. Spectrum [(de)oxy-Hb] before and after BP
(Mayer wave) and Respiration removement with TF'
,'FontSize',12,'FontWeight','demi','Interpreter','none')
                    legend('[oxy-Hb]_r_a_w','[deoxy-Hb]_r_a_w','[oxy-
Hb]_c_l_e_a_n','[deoxy-Hb]_c_l_e_a_n')

%% Respiration and Mayerwave (BP influence) removed by remNoiseICA

%preprocessing Mayer wave influence
Wnmayer=[0.07 0.13];
N=200;
b = fir1(N,Wnmayer/(fs/2),'bandpass');
Mayer=filtfilt(b,1,BPdia);  %Beside the BPdia also the BPsys or the HR signal
is applicable

Mayer=Mayer-mean(Mayer);

%preprocessing respiratory influence
Wnresp=[0.20 0.40];
N=200;
b = fir1(N,Wnresp/(fs/2),'bandpass');
Resp=filtfilt(b,1,Resp);



Data.oxy_signals_ICA=remNoiseICA(Oxy_signals,Mayer,Resp,fs,ExCh);
Data.deoxy_signals_ICA=remNoiseICA(Deoxy_signals,Mayer,Resp,fs,ExCh);

% Illustration of [(de)oxy-Hb] Mayer and respiration cleaned spectra and
% calculation of averaged cleaned spectra

spect=[];
count=1;

for ChNr=1:1:size(Oxy_signals,2)
    figure(6);
    orient landscape
```

```
    [rOxy rDeoxy]=Illustration_multichannel_spectra(ChNr,
Data.oxy_signals_ICA(:,ChNr), ...
        Data.deoxy_signals_ICA(:,ChNr),fs, dispFreq, ExCh);

    if ~isempty(rOxy)
        spect(:,1,count)=rOxy{1}.p;
        spect(:,2,count)=rDeoxy{1}.p;
        count=count+1;
        Base=rOxy{1}.f;
    end

end

close

%Average [(de)oxy-Hb] spectra over all used channels

dat_spec_ICA=[];

    for k = 1 : size(spect,2)
        dat_spec_ICA(:,k)=mean(spect(:,k,:),3);
    end


% Comparison raw and cleaned
                    figure(7)
                    % [oxy-Hb] raw
                    p1 = dat_spec_raw(:,1);
                    f1 = Base;
                    Color=[1 0.6 0.6];
                    idx = find(f1<=dispFreq);
                    plot(f1(idx), 10*log10(p1(idx)),'Color',
Color,'LineWidth',1.5);
                    hold on
                    % [deoxy-Hb] raw
                    p1 = dat_spec_raw(:,2);
                    Color=[0.8 0.8 1];
                    plot(f1(idx), 10*log10(p1(idx)),'Color',
Color,'LineWidth',1.5);
                    % [oxy-Hb] puls clean
                    p1 = dat_spec_ICA(:,1);
                    Color='r';
                    idx = find(f1<=dispFreq);
                    plot(f1(idx), 10*log10(p1(idx)),'Color',
Color,'LineWidth',1.5);
                    % [deoxy-Hb] puls clean
                    p1 = dat_spec_ICA(:,2);
                    Color='b';
                    plot(f1(idx), 10*log10(p1(idx)),'Color',
Color,'LineWidth',1.5);
                    ylabel('Power spectrum
','FontSize',16,'FontWeight','bold')
                    xlabel('f (Hz)','FontSize',16,'FontWeight','bold')
```

```
                    title('Avg. Spectrum [(de)oxy-Hb] before and after BP
(Mayer wave) and Respiration removement with ICA'
,'FontSize',12,'FontWeight','demi','Interpreter','none')
                    legend('[oxy-Hb]_r_a_w','[deoxy-Hb]_r_a_w','[oxy-
Hb]_c_l_e_a_n','[deoxy-Hb]_c_l_e_a_n')
%% Respiration and Mayerwave (BP influence) removed by remNoiseCAR

[Data.oxy_signals_CAR, Data.deoxy_signals_CAR] =
remNoiseCAR(Oxy_signals,Deoxy_signals,ExCh);

% Illustration of [(de)oxy-Hb] Mayer and respiration cleaned spectra and
% calculation of averaged cleaned spectra

spect=[];
count=1;

for ChNr=1:1:size(Oxy_signals,2)
    figure(8);
    orient landscape
    [rOxy rDeoxy]=Illustration_multichannel_spectra(ChNr,
Data.oxy_signals_CAR(:,ChNr), ...
        Data.deoxy_signals_CAR(:,ChNr),fs, dispFreq, ExCh);

    if ~isempty(rOxy)
        spect(:,1,count)=rOxy{1}.p;
        spect(:,2,count)=rDeoxy{1}.p;
        count=count+1;
        Base=rOxy{1}.f;
    end

end

close

%Average [(de)oxy-Hb] spectra over all used channels

dat_spec_ICA=[];

    for k = 1 : size(spect,2)
        dat_spec_CAR(:,k)=mean(spect(:,k,:),3);
    end


% Comparison raw and cleaned
                    figure(9)
                    % [oxy-Hb] raw
                    p1 = dat_spec_raw(:,1);
                    f1 = Base;
                    Color=[1 0.6 0.6];
                    idx = find(f1<=dispFreq);
                    plot(f1(idx), 10*log10(p1(idx)),'Color',
Color,'LineWidth',1.5);
                    hold on
                    % [deoxy-Hb] raw
```

```
                    p1 = dat_spec_raw(:,2);
                    Color=[0.8 0.8 1];
                    plot(f1(idx), 10*log10(p1(idx)),'Color',
Color,'LineWidth',1.5);
                    % [oxy-Hb] puls clean
                    p1 = dat_spec_CAR(:,1);
                    Color='r';
                    idx = find(f1<=dispFreq);
                    plot(f1(idx), 10*log10(p1(idx)),'Color',
Color,'LineWidth',1.5);
                    % [deoxy-Hb] puls clean
                    p1 = dat_spec_CAR(:,2);
                    Color='b';
                    plot(f1(idx), 10*log10(p1(idx)),'Color',
Color,'LineWidth',1.5);
                    ylabel('Power spectrum
','FontSize',16,'FontWeight','bold')
                    xlabel('f (Hz)','FontSize',16,'FontWeight','bold')
                    title('Avg. Spectrum [(de)oxy-Hb] before and after BP
(Mayer wave) and Respiration removement with CAR'
,'FontSize',12,'FontWeight','demi','Interpreter','none')
                    legend('[oxy-Hb]_r_a_w','[deoxy-Hb]_r_a_w','[oxy-
Hb]_c_l_e_a_n','[deoxy-Hb]_c_l_e_a_n')
```